Physiol Rev 88: 919–982, 2008;
doi:10.1152/physrev.00018.2007.

Genesis and Regulation of the Heart Automaticity

MATTEO E. MANGONI AND JOËL NARGEOT

Institute of Functional Genomics, Department of Physiology, Centre National de la Recherche Scientifique UMR5203, Institut National de la Santé et de la Recherche Médicale U661, University of Montpellier I and II, Montpellier, France

Downloaded from physrev.physiology.org on October 4, 2011

0031-9333/08 $18.00 Copyright © 2008 the American Physiological Society

Mangoni ME, Nargeot J. Genesis and Regulation of the Heart Automaticity. *Physiol Rev* 88: 919-982, 2008; doi:10.1152/physrev.00018.2007.—The heart automaticity is a fundamental physiological function in higher organisms. The spontaneous activity is initiated by specialized populations of cardiac cells generating periodical electrical oscillations. The exact cascade of steps initiating the pacemaker cycle in automatic cells has not yet been entirely elucidated. Nevertheless, ion channels and intracellular Ca^{2+} signaling are necessary for the proper setting of the pacemaker mechanism. Here, we review the current knowledge on the cellular mechanisms underlying the generation and regulation of cardiac automaticity. We discuss evidence on the functional role of different families of ion channels in cardiac pacemaking and review recent results obtained on genetically engineered mouse strains displaying dysfunction in heart automaticity. Beside ion channels, intracellular Ca^{2+} release has been indicated as an important mechanism for promoting automaticity at rest as well as for acceleration of the heart rate under sympathetic nerve input. The potential links between the activity of ion channels and Ca^{2+} release will be discussed with the aim to propose an integrated framework of the mechanism of automaticity.

I. INTRODUCTION

The heart pacemaker activity sets the rhythm and rate of cardiac chamber contraction. Autonomic regulation of heart rate plays a fundamental role in the integration of vital functions and influences animal behavior and capability to respond to changing environmental conditions. Heart rate has also been recently linked to the overall risk of cardiovascular mortality and morbidity (232).

In the adult heart of higher vertebrates, pacemaking is generated by specialized "pacemaker" cells having low contractility and generating a periodical electrical oscillation (Fig. 1). Gene expression in cardiac pacemaker cells seems to be qualitatively similar to that of working myocytes, yet a quantitatively different level of expression of some ion channels, connexins (Cx), and transcription factors generates the distinctive phenotype of spontaneously active myocytes (179, 317, 477). In spite of the physiological importance of cardiac automaticity, some aspects of the pacemaker mechanism have not been elucidated and are still under debate. Indeed, different views of the ionic and cellular basis of the pacemaker mechanism and its regulation by the autonomic nervous system have been proposed [see previous articles in this Journal (63, 215) and Refs. 74, 120, 307].

Unraveling the mechanisms of pacemaking in spontaneously active cells is a fascinating and complex task. Experimental and theoretical approaches, such as in vitro and in vivo electrophysiology, pharmacology, and genetics, as well as numerical modeling of pacemaking are necessary. Automatic cells of the adult heart are characterized by the presence of the diastolic depolarization, a depolarizing phase that drives the membrane voltage at the end of repolarization to the following action potential threshold (Fig. 1*B*).

The pacemaker mechanism has been intensively studied for more than 40 years. The diastolic depolarization is an electrical phenomenon, so pacemaking has been first interpreted in terms of activation of specific ionic currents (see Refs. 63, 215). Between 1960 and 1980, pacemaker activity has been investigated by intracellular recording of automaticity and ionic currents on spontaneously active tissue strips coming from the Purkinje fiber network (118, 192, 485, 495) and the sinoatrial node (SAN) (62, 364, 533). During these pioneering years, some ionic currents involved in the generation of automaticity have been described. Key breakthroughs were the discovery of the hyperpolarization activated current (I_f) in SAN (64) and Purkinje fibers (118, 122) and the description of the role of dihydropyridine (DHP)-sensitive Ca^{2+} current (I_{Ca}) in the SAN action potential generation (364). Very low inward rectifier current (I_{K1}) density is found in the rabbit SAN. In contrast, automatic tissue expresses strong I_f (366). The SAN action potential is predominantly controlled by I_{Ca} so that the action potential upstroke velocity is much lower in the SAN than in the ventricle. The SAN repolarization phase also differs from that of the working myocardium. Indeed, as the SAN expresses low levels of the transient outward current (I_{to}), the repolarization phase is predominantly controlled by the delayed rectifier current (I_K) (62). Finally, the SAN action potential also lacks the plateau phase. These electrophysiological properties confer to the SAN action potential its typical form (Fig. 1*B*).

The patch-clamp technique has become popular for studying the ionic basis of pacemaker activity on individual pacemaker cells (215). Different families of ion channels have been described (58). Two distinct I_{Ca} components have been identified (172): the L-type Ca^{2+} current ($I_{Ca,L}$) and the T-type current ($I_{Ca,T}$). A fast (I_{Kr}) (451) and a slow (I_{Ks}) (278) delayed rectifier has been reported. Furthermore, application of the patch-clamp technique has improved the study of the sensitivity of these channels to autonomic agonists. Two major insights into the physiological role of ion channels in the generation and

Downloaded from physrev.physiology.org on October 4, 2011

regulation of pacemaker activity have been obtained: the relevance of f-channels in the regulation of heart rate at low parasympathetic tone (124) and the physiological significance of the heterogeneity of ion channel expression in the SAN (58). The importance of the Na^+-Ca^{2+} exchanger (NCX) in pacemaking in the amphibian sinus venosus (227, 228) and mammalian SAN (44) has been recently highlighted, and the contribution of spontaneous intracellular Ca^{2+} release in the generation of automaticity has been emphasized (510).

New important insights into the pacemaker mechanism are now coming from the study of genetically modified mouse strains in which specific ion channels have been inactivated or modified. This genetic approach constitutes a necessary implementation to electrophysiological and pharmacological evidence, since selective inhibitors of ion channels are not always available. Gene targeting in the mouse has generated interesting models of dysfunction of pacemaker activity (393, 467, 522). The possibility to study pacemaker activity in mouse models is very recent (312, 313) and has provided exciting insights into the specific functional role of L-type $Ca_v1.3$ (309, 546) and T-type $Ca_v3.1$ (314) channels in the generation of SAN automaticity. Because of the tiny size of the dominant pacemaker region in the mouse heart (498), isolation of mouse SAN cells is technically challenging. Our group has been the first to obtain recordings of automaticity and ion channels from isolated mouse SAN cells (312, 313). Other groups have successfully employed this new preparation to study pacemaker activity in wild-type (86, 93, 279) and genetically modified mouse strains (196, 294, 309, 314, 546). Limitations of the use of the mouse for the study of cardiac automaticity are correlated with the very high basal heart rate of this species. We can thus expect that pacemaker mechanisms may assume a different role in mice than in larger mammals and humans. Nevertheless, the new possibility of isolating mouse SAN tissue and primary pacemaker cells has created a new interest into the study of the ionic basis of pacemaker activity generation and regulation.

Until the last decade, research on the physiology of heart automaticity was limited to the domain of basic science. However, there is currently a renewal of interest on cardiac pacemaking, and an increasing number of laboratories are now focusing their efforts on the regulation of heart rate. Indeed, the pharmacological control of cardiac automaticity is now becoming an important issue in the management of ischemic heart diseases (123). Iden-

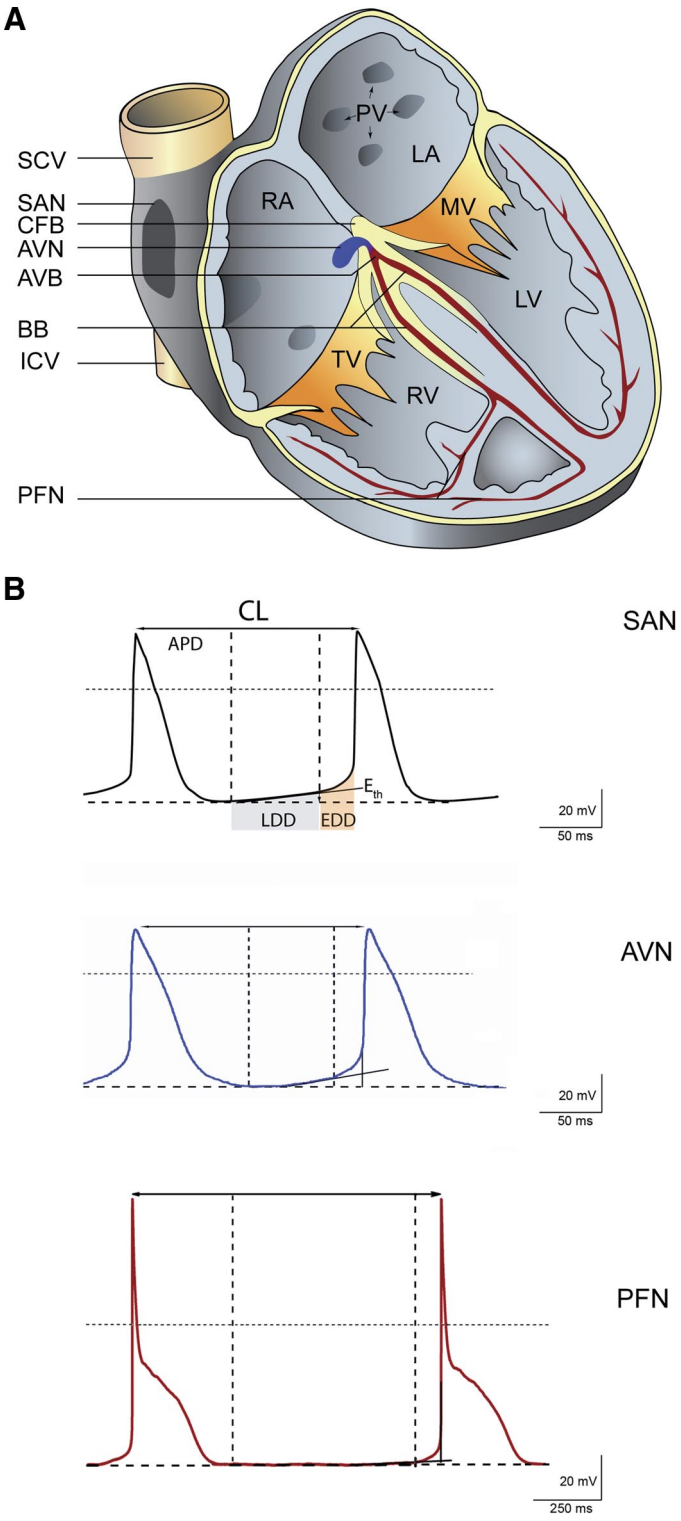

FIG. 1. *A*: the mammalian heart with the cardiac conduction system. The sinoatrial node (SAN) is located at the entry of the superior vena cava (SCV) in the right atrium (RA). The atrioventricular node (AVN) extends in a region delimited by the inferior vena cava (ICV), the central fibrous body (CFB), and the tricuspid valve (TV). The atrioventricular bundle (AVB) divides in the bundle branches (BB) and originates the left and right Purkinje fibers network (PFN). Other abbreviations are: LA, left atrium; PV, pulmonary veins; MV, mitral valve; RV, right ventricle; LV, left ventricle. [Adapted from Moorman and Christoffels (341).] *B*: recordings of automaticity and action potential waveforms of isolated mouse SAN, AVN, and PFN cells. Cl, cycle length; APD, action potential duration; E_{th}, action potential threshold; LDD, linear part of the diastolic depolarization; EDD, exponential part of the diastolic depolarization. (From Marger Nargeot and Matteo Mangoni, unpublished observations.)

Downloaded from physrev.physiology.org on October 4, 2011

tification of ion channels involved in the generation of automaticity also constitutes the basis for the development of putative genetic and cellular therapies for dysfunctions of pacemaking (94, 423, 424). Finally, knowledge of pacemaker mechanisms is fundamental for understanding the basis of inherited diseases of the heart rhythm.

In this review, we will focus on the cellular mechanisms underlying heart automaticity and its regulation by the autonomic nervous system in the adult heart. Different views of automaticity will be compared and commented. To this aim, we will try to give an overview of how ion channels and Ca^{2+} signaling can influence pacemaking under different physiological conditions. Finally, we will provide the reader with a short discussion on how ion channels involved in pacemaker activity are becoming useful targets in the development of new therapies for heart diseases.

II. AUTOMATICITY IN CARDIAC CELLS AND DISTRIBUTION OF PACEMAKER ACTIVITY IN THE HEART TISSUE

In the mammalian heart, three major structures are endowed with automaticity and are able to drive the heartbeat: the SAN, which constitutes the physiological pacemaker, the atrioventricular node (AVN), and the Purkinje fibers network (Fig. 1*A*). Functional evidence in favor of a supraventricular dominant pacemaker was obtained by Gaskell in the slowly beating tortoise heart (154, 155). Anatomically, the SAN was identified a century ago by Keith and Flack (237), shortly after Tawara's description of the atrioventricular junction (476; see Ref. 460 for review). The intrinsic SAN beating rate is normally faster than that of the cardiac conduction system and suppresses pacemaking in the AVN and Purkinje network. However, automaticity in AVN can become dominant in case of SAN block or failure (220). Purkinje fibers can also generate a viable rhythm in conditions of atrioventricular block. For these reasons, the SAN region is indicated as the primary pacemaker, while the AVN and Purkinje fibers are indicated as secondary (or accessory) pacemakers. In this section, we review basic principles of automaticity in primary and secondary pacemaking regions. Some aspects of the structure and function of SAN, AVN, and the His-Purkinje system are commented on.

A. Molecular Determinants of SAN Formation

In the early embryonic heart, all cardiomyocytes display automaticity. The embryonic myocardium of the primary heart tube is characterized by slow conduction velocity, and even if dominant pacemaker activity is present at the venous pole, automaticity can be originated at any point of the heart tube (341). The differentiation of the cardiac chambers (heart ballooning) and the maturation of myocytes forming the working myocardium of the late embryo are associated with the disappearance of this kind of "diffuse" automaticity. Working myocytes of the mature cardiac chambers have completely lost automaticity and display fast conduction velocity (see Refs. 341, 386 for review). In the adult heart, pacemaker activity is confined to the SAN and AVN, two regions in which the intercellular conduction velocity is relatively slow. The mechanisms underlying the confinement of pacemaker activity and the patterning of the SAN and AVN during development are mostly unresolved. However, progress has been recently obtaining in the identification of transcription factors involved in the differentiation of cell lineages contributing to the SAN formation (207, 208, 338, 341).

Mommersteeg et al. (338) reported that the SAN develops in the inflow tract region of the embryonic heart (Fig. 2). This region is characterized by expression of the T-box transcription factor *Tbx3* and the *Hcn4* ion channel gene (coding for f-channels). This SAN primordium is also devoid of Cx40, which is typical of fast-conducting working myocardium (Fig. 2). Mommersteeg et al. (338) have also provided evidence that the Nkx2–5 transcription factor (NK2 transcription factor related to locus 5 of *Drosophila*) may act as a repressor of the SAN lineage gene program, since mice lacking Nkx2–5 show ectopic expression of *Tbx3* and *Hcn4* throughout the heart tube. Intact activity of Nkx2–5 is also required to suppress *Tbx3* expression outside the developing SAN and to trigger the atrial gene expression program (338). If Nkx2–5 appears to suppress SAN formation through inhibition of *HCN4* expression and other markers, *Tbx3* constitutes an activator of the SAN gene expression program (208) and a repressor of heart chamber formation. Expression of *Tbx3* in the whole heart tube suppresses chamber formation (207). Mouse embryos in which *Tbx3* has been inactivated show that this gene is essential to activate the SAN related gene expression program, and to prevent expression of myocardial markers in the SAN region. Ectopic expression of *Tbx3* in the adult atria of transgenic mice is sufficient to reactivate focal automaticity and some SAN markers (208).

Hoogars et al. (208) have proposed that SAN formation (at least starting from E10) is due to proliferation of *Tbx3*-expressing cells rather than to recruitment of myocytes having initiated the atrial gene program. Also, labeling of cell lineages suggests that the SAN is to be considered as a remnant of cell populations that did not enter the myocardial expression program (338). Blaschke et al. (40) have reported that the homeodomain transcription factor *Shox2* is involved in the formation of the SAN region. Particularly, *Shox2* knockout mice die around E12 and show severe SAN hypoplasia. Furthermore, zebrafish embryos lacking Shox2 are bradycardic, an observation

Downloaded from physrev.physiology.org on October 4, 2011

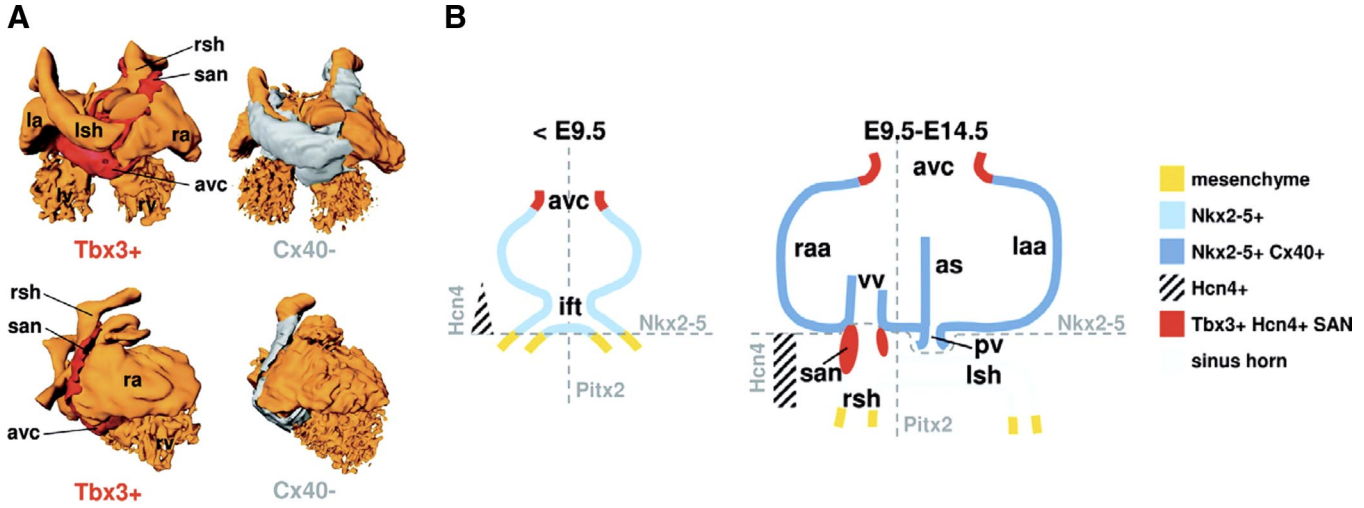

FIG. 2. *A*: computer-based 3-dimensional reconstructions (465) of the mouse embryonic heart at 14.5 post coitum (E14.5). In this reconstruction, the left ventricular myocardium has been removed to show the blood-filled lumen (orange), from the dorsal (*top panels*) and the right side (*bottom panels*). The Tbx3-positive myocardium is in red, and the Cx40-negative myocardium is in grey. Note that expression of *Tbx3* is restricted to areas in which Cx40 expression is absent. *B*: schematic representation which shows the patterns of expression of critical markers in the developing fast conducting myocardium or SAN primordia (see sect. IIA). *Left panel* delineates the expression pattern until E9.5, and *middle panel* shows the pattern between E9.5 and E14.5. Dotted lines identify borders of *Nkx2–5* expression domains. Except for the yellow-colored mesenchyme, only myocardium is depicted (see legend in *right panel*). Abbreviations are as follows: as, atrial septum; avc, atrioventricular canal; ift, inflow tract; la/ra, left and right atrium; laa/raa, left and right atrial appendage; lsh/rsh, left and right sinus horn; lv/rv, left and right ventricle; pv, pulmonary vein; san, sinoatrial node; vv, venous valves. [From Mommersteeg et al. (338).]

which is consistent with the involvement of *Shox2* in the determination of the pacemaker tissue (40).

B. Automaticity in the Sinoatrial Node

In this section, we aim to provide a concise overview of automaticity in the SAN. Some fundamental structural aspects of the SAN cellular and electrophysiological organization will be discussed. Because the rabbit has been extensively used as an animal model to study the mechanisms of pacemaking, we will focus on results obtained from the rabbit atrial-SAN preparation. Further discussion of the SAN structure and variations between species can be found in some excellent reviews by Opthof (374) and Boyett and co-workers (57, 58).

SAN pacemaker tissue is located in the intercaval region (Fig. 3*A*) and extends towards the endocardial side of the crista terminalis (Fig. 3, *B–D*). Spontaneously active cells are found in the area delimited by the crista terminalis, the left and right branch of the sinoatrial ring bundle and the interatrial septum (Fig. 3, *B–D*). Beside pacemaker cells, the SAN also contains atrial cells, fibroblasts, and adipocytes (130). The collagen content of the SAN region is relatively high (377). However, collagen does not seem to have an adverse effect on SAN conduction, because species having different SAN collagen content display similar conduction times (377). During aging, the size and position of SAN do not change, but its structure undergoes remodeling associated with an augmentation of collagen content (6).

The overall electrical coupling within the SAN is weak (see Ref. 58 for review). Two lines of evidence indicate that SAN automaticity is in fact partially suppressed by the electrotonic load imposed by the atrium. First, removal of the right atrium results in an acceleration of SAN pacing rate (241, 248). Second, direct coupling of a SAN cell to an atrial cell suppresses pacemaker activity (224, 482). However, a relatively low electrical coupling between pacemaker cells seems to be necessary for the SAN to be able to drive the atrium. Indeed, by employing numerical modeling, Joyner and van Cappele (225) have indicated that the SAN should have a minimal size to drive the atrium, but also that intranodal cellular coupling should be relatively weak to protect pacemaking from the hyperpolarizing electrical load imposed by the atrium. Watanabe et al. (514) have also used numerical modeling to show that stronger electrical coupling between SAN and atrium would stop pacemaking.

The SAN is structurally heterogeneous. Two views of the cellular organization of the SAN have been proposed. In the "gradient" model of SAN (58), there is a progressive transition in the size and electrical properties of pacemaker cells between the SAN center and the periphery. Cells in the center (labeled in red in Fig. 3) are small and have intrinsically slower pacing rate and upstroke velocity compared with that at the periphery (labeled in blue in Fig. 3), which have faster pacing rate, upstroke velocity, and intermediate properties between "pure" pacemaker and atrial cells. Verheijck et al. (499) have proposed that the SAN region is constituted by automatic cells having

Downloaded from physrev.physiology.org on October 4, 2011

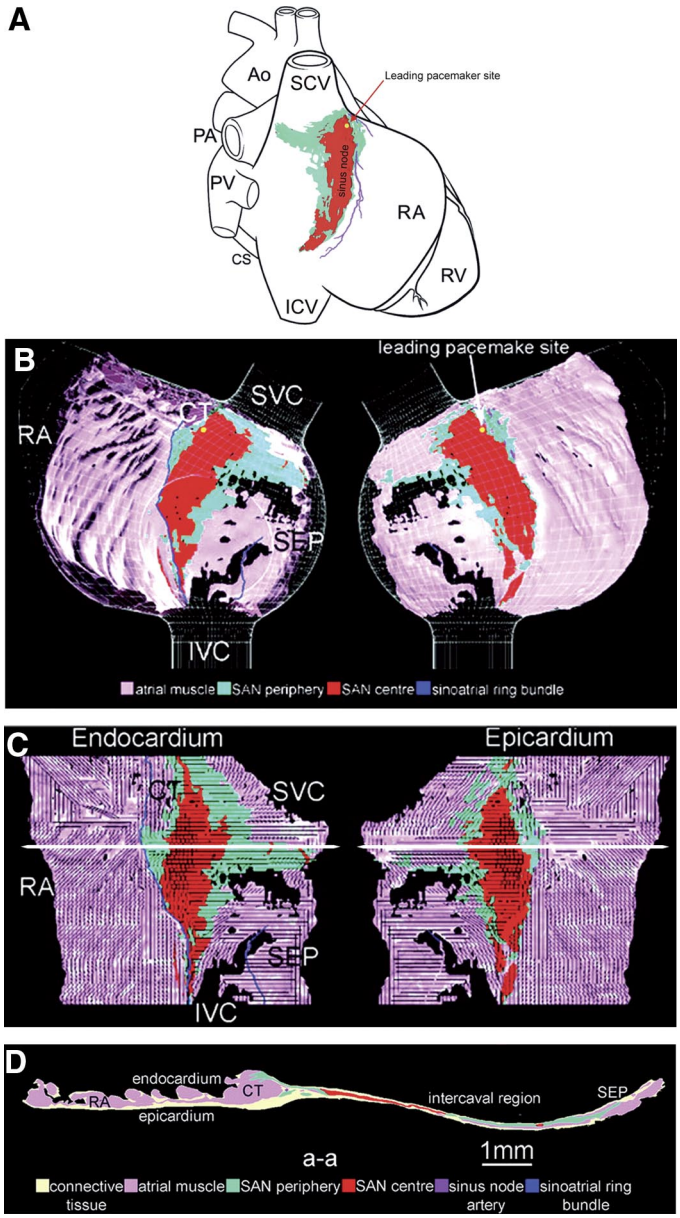

FIG. 3. A 3-dimensional computer model of the rabbit SAN as proposed by Dobrzynski et al. (130). In all panels, central SAN tissue is labeled in red, while peripheral SAN tissue is depicted in green. The yellow dot indicates the leading SAN pacemaking site, and the blue line indicates the SAN ring. *A*: topographical organization of the rabbit SAN, as viewed in an ideal intact heart diagram. Note the extension of peripheral SAN tissue around the superior vena cava (see also Fig. 6*C*). Ao, aorta; PA, pulmonary artery; CS, coronary sinus. Other abbreviations are as in Fig. 1. *B* and *C*: endocardial (*left*) and epicardial (*right*) view of SAN central and peripheral tissue. In *B*, SAN myocytes are shown in a simple framework model of the right atrium. In *C*, myocyte orientation is shown. Note the mesh organization of central SAN tissue. Peripheral SAN myocytes are predominantly oriented perpendicularly to the crista terminalis and extend toward the interatrial septum (SEP). *D*: model section of the SAN cut at the level of the white line in *C*. Note that peripheral SAN tissue extends onto the endocardial side of the crista terminalis. Central SAN myocytes are embedded in connective tissue. [From Dobrzynski et al. (130).]

variable intrinsic pacing rate and action potential configuration. Contrary to the "gradient" model, there would be no preferential distribution of small pacemaker cells in the SAN center. Indeed, pacemaker cells having different degrees of automaticity and action potential configuration are supposed to be uniformly distributed in the SAN region. Verheijck et al. (499) have indicated that atrial cells are present in the SAN, their density being maximal in the SAN periphery and minimal in the center. This latter view of the SAN structure has been called the "mosaic" model.

Consistent with the gradient model of SAN is the observation that tissue balls isolated from the rabbit SAN periphery display a distinct electrophysiological profile compared with that from the center (57, 60, 248, 250, 355, 370) (Fig. 4*A*). More importantly, a "central" and "peripheral" SAN can be defined by using electrophysiological and histochemical criteria (57, 130). Consistently with the mosaic model, atrial cells have been unambiguously identified in the peripheral SAN by using a $Cx40^{EGFP+/-}$ knock-in mouse line (331) and by direct staining with Cx40 antibodies (130). Verhejick et al. (498) have recorded atrial action potential activity in the intact mouse SAN (Fig. 4*B*). However, atrial cells seem to be absent in the rabbit central SAN. In conclusion, even if the gradient model seems to explain better SAN electrophysiological behavior, certain elements of the mosaic model are to be included in future structural SAN models.

Dobrzinsky et al. (130) have recently proposed the first comprehensive structural computer model of the rabbit SAN (see Fig. 3). In this model, peripheral SAN tissue constitutes the SAN impulse exit pathway. Peripheral cells can be defined by membrane expression of Cx43 and middle neurofilament (NF-M) protein. SAN peripheral cells are large and predominantly arranged in parallel. Cells in the SAN center are smaller and express the low-conductance Cx45 and NF-M. Central pacemakers are arranged in a mesh and wrapped around bundles of connective tissue. The mouse SAN seems to share some common features with the rabbit SAN (289). In the central mouse SAN, cells are packed in a compact structure (compact node) and are oriented perpendicularly to the crista terminalis (289). Cells at the periphery are loosely packed and are oriented parallel to the crista. Numerical simulations of impulse propagation from the leading pacemaker site to the atrium have indicated that the SAN could not sustain atrial beating if cellular coupling and conduction were uniformly low throughout the SAN (224). Expression of different connexins in the SAN center and periphery contributes to create a gradient in impulse conduction velocity from the leading pacemaker site to SAN periphery and exit zone, so that conduction velocity in central SAN is lower than that measured in the periphery (see Ref. 61 for review). Beside Cx45, expression of Cx30.2 has been also reported in the mouse SAN

Downloaded from physrev.physiology.org on October 4, 2011

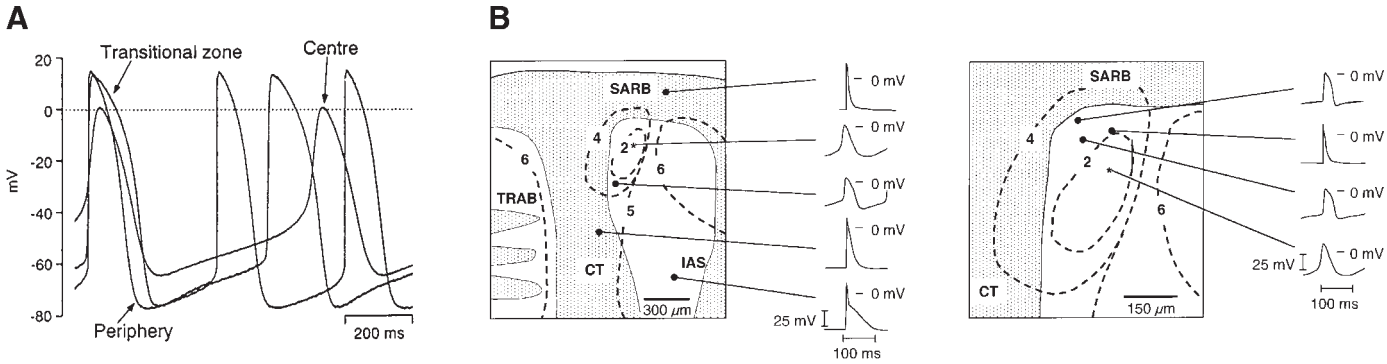

FIG. 4. *A*: pacemaker activity of isolated tissue balls from the SAN center, periphery and transitional zone. Tissue from the SAN center has intrinsically slower automaticity and more positive maximum diastolic potential, while peripheral and transitional tissues are intrinsically faster and have a more negative maximum diastolic potential. [Original recordings from Boyett et al. (59).] *B*: intracellular microelectrode recordings of automaticity in an isolated mouse SAN. The leading pacemaker site is indicated by asterisk. Note the presence of the diastolic depolarization phase in this recording site (*right panel*) and suppression of automaticity in a location in the vicinity of the leading site (*left panel*), and in the SAN periphery close to the interatrial septum (IAS). Atrial-type action potentials are recorded in the mouse SAN (*right panel*). Automaticity is not recorded in the crista terminalis (CT) and in the right branch of the sinoatrial ring (SARB). [Original recordings from Verheijck et al. (498), with permission from Elsevier.]

and AVN (257). Cx30.2 has smaller conductance than Cx45 (70). It has been proposed that Cx30.2 contributes to the intrinsically slow conduction velocity in the SAN and in the AVN (258). This view is supported by the observation that mice in which Cx30.2 has been inactivated have shortened P-Q intervals (256).

Expression of Cx43 in the SAN periphery enhances cell-to-cell electrical coupling thereby forming a "transitional" zone between the slow-conducting leading pacemaker site and the fast-conducting atrial tissue (130).

Kodama et al. (248) have shown that small tissue balls from the SAN periphery have intrinsically faster pacing rate than balls from the central SAN (Fig. 3*A*). However, as reported by Bleeker (41), the central SAN can lead pacemaker activity in spite of its lower beating rate, because cells at the periphery are electrotonically inhibited by the right atrium. Differences in intrinsic firing rates of central and peripheral SAN are due to heterogeneous expression of ion channels (60, 250, 355) and proteins involved in Ca^{2+} homeostasis (267, 349). Particularly, larger cells from SAN periphery express higher I_f and I_{Na} densities than small cells in the SAN center. Enhanced expression of I_f and I_{Na} can explain the faster pacing rate and upstroke velocity recorded in tissue from the SAN periphery. The stronger pacemaker activity in cells of the SAN periphery can help overcome the suppressive effect of the right atrium on the overall SAN automaticity (58). It would be important to develop a comprehensive model of SAN activity including both structural and electrophysiological data. Theoretically, such a model could be integrated in an anatomical and biophysically detailed three-dimensional model of the heart (102) and would be an important step for understanding some integrative properties of heart automaticity at the organ level.

The physiological role of fibroblasts in the SAN has not been completely elucidated. Fibroblasts form an extensive network in the SAN (73, 105). Camelliti et al. (73) have shown that fibroblasts can functionally connect with SAN myocytes, possibly by Cx45-mediated gap junctions. Apparently, SAN fibroblasts do not participate to intranodal conduction (105). However, they may act in the transduction of the atrial wall stress to SAN myocytes. In this respect, Kohl et al. (252) have proposed that fibroblasts participate in the mechanoelectrical regulation of SAN rate.

C. Properties of Isolated SAN Pacemaker Cells

Isolated SAN pacemaker cells are a widespread experimental model for studying the pacemaker mechanism. Several research groups have described the electrophysiological properties of enzymatically isolated calcium-tolerant (216) pacemaker cells from a variety of mammals including the rabbit (114, 125, 492), guinea pig (12, 333), pig (372), rat (457), and mouse (86, 313). The gross morphology of spontaneously active cells is conserved between species. Cells from the rabbit and mouse SAN have been empirically classified in three distinct morphologies, namely, "spindle," "elongated," and "spider" (125, 313, 499) (Fig. 5, *A* and *B*). In the rabbit and mouse, spindle-shaped cells are generally smaller than elongated and spider cells, their capacitance varying between ~15 and 30 pF. Under Nomarski optics, the cytoplasm of spindle cells appears transparent and poor in myofilaments. Elongated cells have a longer longitudinal axis and larger capacitance (between 35 and 50 pF) than spindle-shaped cells. In some elongated cells, the cytoplasm is darker than in spindle cells. This is possibly due

Downloaded from physrev.physiology.org on October 4, 2011

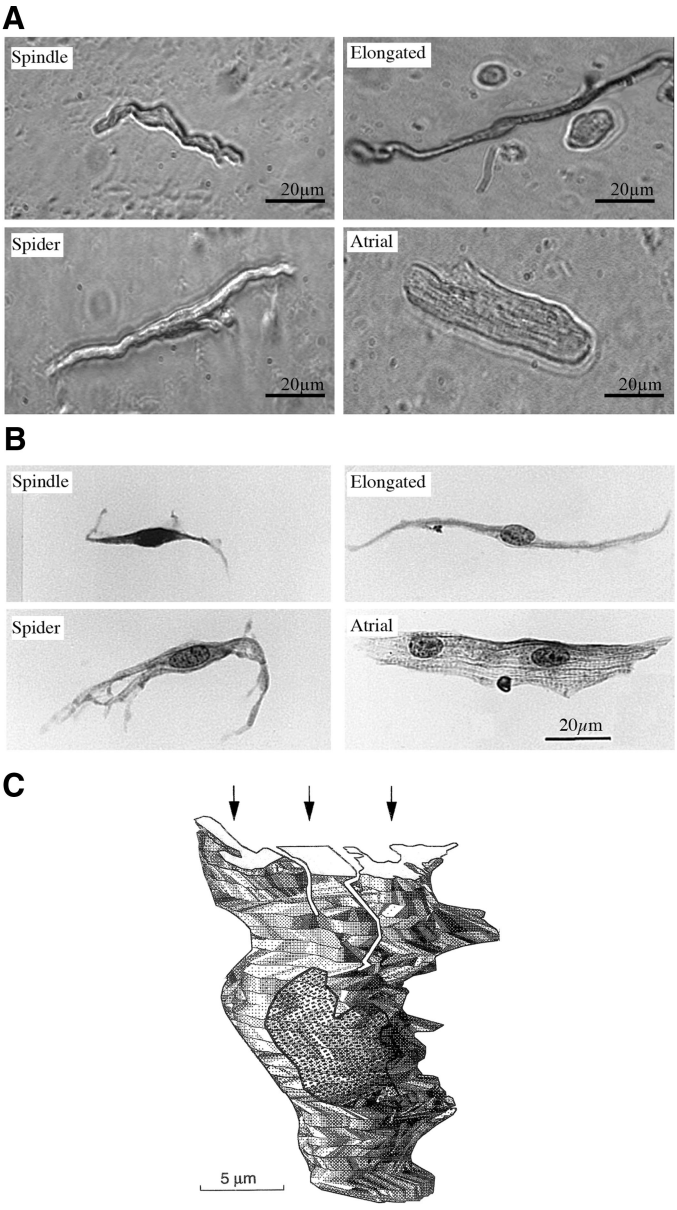

FIG. 5. Morphology of isolated mouse (*A*) and rabbit (*B*) SAN cells. Atrial cells can be isolated from the SAN in both species. *C*: a simple structural model of a rabbit SAN spider cell. These cells have branched cytoplasm (arrows) and are mononucleated. [Photographs in *A* from Mangoni and Nargeot (312), with permission from Elsevier; pictures in *B* and *C* from Verheijck et al. (499).]

to a higher myofilament density than in spindle cells (Fig. 5*A*). Spider cells have branched cytoplasm (see Fig. 5*C*). The functional significance of such a peculiar morphology is not known. In the rabbit, small spindle-shaped cells are considered to be leading pacemaker cells (presumably from the SAN center), while larger elongated cells come from the SAN periphery (204). However, this may not be an absolute rule, since small clusters of mouse SAN cells containing both spindle and elongated cells have been observed in the mouse SAN (499) (Mangoni and Nargeot, unpublished observations).

D. Pacemaker Shift and Extranodal Supraventricular Automaticity

The position of the leading pacemaker site is not fixed. The pacemaker initiation site can shift in different zones of the SAN. Pacemaker shifts can be induced by autonomic regulatory inputs, temperature, atrial stretch, as well as by pharmacological interventions (Fig. 6*A*) (58, 442). Experimentally, pacemaker shift has been studied in the rabbit SAN (374), but naturally occurs also in dogs (47) and humans. Variability in the position of the leading pacemaker site in human subjects has been shown by Boineau et al. (46). It is possible that pacemaker shift underlies dynamic changes in the morphology of the P-wave observed in ECG recordings (442). Schuessler et al. (442) have reported that pacemaking can be located at any point of the intercaval region as well as, in some cases, in the left atrium. Interestingly, cells from the sleeves of pulmonary veins have recently been shown to display spontaneous activity (83, 205).

The leading pacemaker site is situated where local automaticity is faster. We can thus expect that sympathetic input will shift the leading site where automaticity is most sensitive to adrenergic stimulation, while parasympathetic activity shifts pacemaking where automaticity is less inhibited by cholinergic transmitters (300). Boyett et al. (58) have attributed pacemaker shift to the heterogeneous expression of ion channels in the SAN center and periphery. Accordingly, a given channel blocker will shift pacemaking to a site where automaticity is less dependent from the targeted channel. This hypothesis has been experimentally verified by using Ca^{2+} (250), K^{+} (249), and f-channel inhibitors (355). In the rabbit, shifts induced by epinephrine and acetylcholine roughly correspond to SAN zones in which I_f block has very moderate effect on pacing rate, an observation that matches the framework proposed for channel blockers (58). Yamamoto et al. (531) have shown that application of isoproterenol to intact atria can shift the leading pacemaker site from the central SAN, to a location between the superior vena cava and the interatrial groove. Under basal conditions, automaticity in this site is less robust than in the SAN, but under isoproterenol, it can be as fast as in the SAN. These observations are indicative of the existence of multiple functional pacemaker sites outside the "classical" SAN region (Fig. 6*B*).

There is now substantial evidence indicating that myocytes capable to drive pacemaking are present outside the SAN. Indeed, spontaneously beating cells can be isolated from the right atrium (408, 427) and from the bundle branches of the mouse heart (Mangoni, unpublished observations). Automatic cells are also present around the tricuspid valve (11). These cells are very likely to be part of an extranodal extension of the atrial conduction system. Importantly, the existence of such an extension has been recently demonstrated by staining of

Downloaded from physrev.physiology.org on October 4, 2011

rabbit and rat atria with antibodies directed against Cx45 and HCN4 (Fig. 6*C*) (531). Particularly, it has been shown that cells having "nodal" phenotype extend from the rear of the superior vena cava to the interatrial groove. Nodal-like cells with high expression of both Cx45 and HCN4 are present around the atrioventricular valves (the atrioventricular ring bundles) and reach the AVN (531). The presence of an atrial conduction system extension may be due to common embryonic origin and/or development of these cells with that of SAN and AVN (411).

The physiological significance of automaticity in latent pacemaker cells of the right atrium is unclear. These cells have been shown to be capable of assuming the control of the heartbeat under conditions of SAN failure and to play a role in the generation of atrial arrhythmias (426). In the left atrium, cells generating focal discharge have been found at the boundary between the left atrium and the pulmonary veins in human subjects affected of paroxystic atrial fibrillation (532). The key role of these cells in triggering and sustaining atrial fibrillations has been clearly recognized (175, 176). Tissue sleeves from rabbit pulmonary veins display transient automaticity triggered by rapid pacing, application of ryanodine (205, 531), and stretch (83). A diastolic depolarization phase can be recorded in these cells, but automaticity is insensitive to I_f block by Cs^+ (531). The expression of ionic currents in these cells resembles much more that of non-automatic atrial than pacemaker cells (141). The ionic mechanism responsible for pacemaking will need investigation in the near future.

In conclusion, one can wonder why some automatic sites outside the SAN (e.g., the interatrial groove extension) can effectively sustain normal pacemaking while others can trigger atrial arrhythmias. In this respect, it is worth noting that pacemaking in these regions is intrinsically less robust than that of the SAN (or less sensitive to autonomic regulation). Consequently, in case of activation of these sites, atrial activation may not have the correct space- and frequency-dependent properties.

E. Automaticity in the Atrioventricular Node

The AVN sets the appropriate frequency-dependent conduction delay between the atria and ventricles. It also limits ventricular activation during atrial tachyarrhythmias, thereby protecting ventricular rhythm. The AVN has a dual electrical input from the atrium, namely, the "fast"

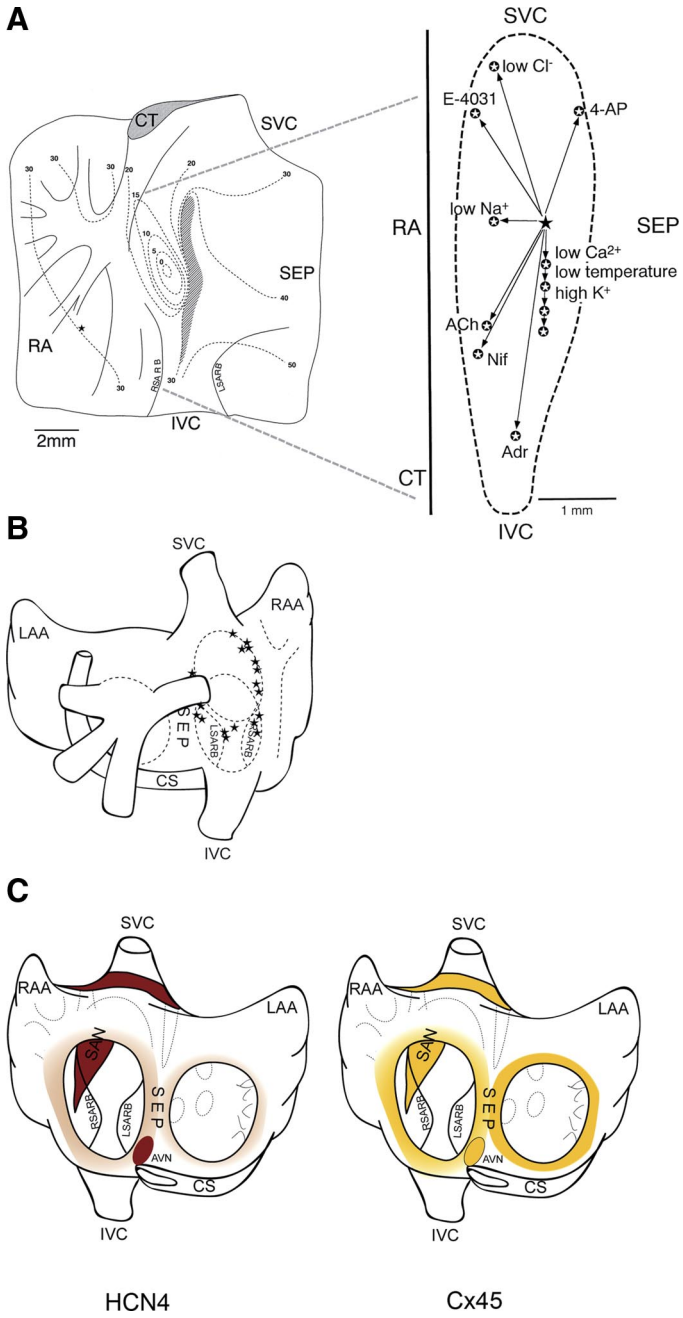

FIG. 6. Pacemaker shift and extranodal supraventricular automaticity in the rabbit heart. *A*: shift of the leading pacemaker site inside the rabbit SAN region. In the *left panel*, SAN activation after impulse generation in a central leading pacemaker site (marked as the point activating at zero time) is depicted. Isochronal curves indicate the spread of impulse conduction toward the crista terminalis. After activation of the crista terminalis, the impulse propagates in the right atrium (30 ms isochronal) and to the right and left branches of the SAN ring bundles (RBSARB and LBARB). Note the block of impulse conduction in the direction of the interatrial septum. [From Boyett et al. (59).] The *right panel* indicates the shift of the leading pacemaker site under the influence of different ionic and pharmacological agents. [From Boyett et al. (58).] *B*: variability of the position of the leading pacemaking site in isolated rabbit hearts. The leading site can be found inside and sometimes outside the "classical" SAN region. Asterisks indicate the position of the impulse origin in each of the 18 preparations tested. *C*: dorsal view of the left and right atria showing the extension of the atrial conduction system in the rabbit heart. Extension is defined according to extranodal distribution of HCN4 (red) and Cx45 (yellow) immunoreactivity (see text of sect. II*C*). Positively stained cells are found around the mitral and tricuspid valves, as well in the interatrial groove. [Modified from Yamamoto et al. (531).]

Downloaded from physrev.physiology.org on October 4, 2011

and "slow" pathways of conduction (336, 356). However, the AVN is also endowed of automaticity. AVN automaticity can effectively drive the heart after SAN failure or block.

The intact AVN is a complex and highly heterogeneous structure. For a recent review on the AVN structure and conduction, the reader is referred to Efimov et al. (140). Here, we will discuss the principal aspects of the atrioventricular junction and automaticity. In spite of a growing knowledge about the histology and electrophysiology of AVN, a detailed correlation between the different anatomical components and action potential configurations recorded from the AVN is not yet available. Debate still exists between morphologists and physiologists about which structures of the atrioventricular junction should be included in an ideal "true" AVN (140). In this review, we will endorse the physiological definition of the AVN, as indicated by Billette (39). This includes all structures contributing to the atrial-His conduction interval. We thus define the AVN as the region comprised in the Koch's triangle, with the heterogeneous structure included in the central fibrous body, as well as the posterior nodal extension (PNE) projecting in the isthmus below the coronary sinus (Fig. 7*A*). The central fibrous body contains the enclosed part of the AVN with the compact node (CN) and lies at the apex of the triangle. The action potential configuration and expression of ion channels in the AVN are heterogeneous. Three types of action potential waveforms have been identified in early studies (see Ref. 140 for review): atrionodal (AN), nodal (N), and nodo-His (NH). The N-type action potential is characterized by slow upstroke velocity and action potential amplitude, while AN and NH action potentials have intermediate properties between nodal and atrial or His action potentials, respectively. Billette (38) has presented a microelectrode mapping study of the AVN and defined six cell types based on action potential morphology and refractoriness. It would be very important to build a comprehensive model of the functioning of the AVN. However, it is still difficult to correlate action potential types with the structural organization of the atrioventricular tissue. Histologically, the AVN is composed by a "superficial" (subendocardial) layer and "middle" and "deep" innermost layers (37a). Based on simultaneous microelectrode recording and optical mapping of rabbit AVN activation under SAN rhythm, Efimov and Mazgalev (139) have supported the hypothesis that the superficial layer is predominantly composed by AN-type cells, while the middle layer is composed of cells having N-type properties. The AVN superficial layer is rich in Na^+ channels (391) and Cx43, while the intermediate layer forming the CN is essentially poor in Na^+ channels (391, 441). Furthermore, the intermediate layer expresses the low-conductance Cx45 rather than Cx43 or Cx40 (61, 140). Consistently, lower conduction velocities are recorded in the middle N-type layer than in the superficial AN-type layer (139).

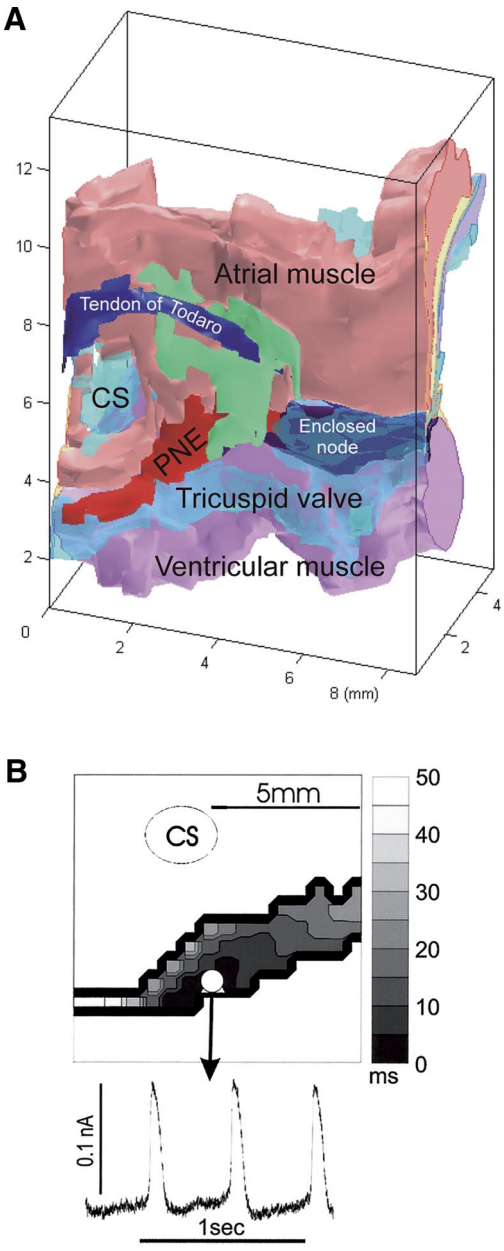

FIG. 7. *A*: a computer model of the rabbit atrioventricular junction shows the basic structural organization of the AVN. The AVN is a heterogeneous structure delimited by the tricuspid valve, the tendon of Todaro, and the coronary sinus. The posterior nodal extension (PNE) is depicted in red and constitutes a major site of origin of junctional AVN automaticity. It can also be part of the slow pathway of atrioventricular conduction. The enclosed node is shown in purple and is continuous to the PNE. The green zone corresponds to AVN tissue composed by loosely packed atrial cells. It is possible that these atrial cells are part of the fast AVN conduction pathway. [From Boyett et al. *J Electrocardiol* 38 *Suppl*: 113-120, 2005, with permission from Elsevier.] *B*: mapping of automaticity in the rabbit AVN. Pacemaking originates in the PNE and spreads to the atrial muscle and to the enclosed node (*top panel*). Optical recording of automaticity in the PNE is shown in the *bottom panel*.

Downloaded from physrev.physiology.org on October 4, 2011

The location of the leading AVN pacemaker site has been a matter of debate. Initiation of automaticity has been identified in the N-NH part of the node (140, 515). Recently, Dobrzynski et al. (131) attempted to locate the site of origin of pacemaker activity in isolated rabbit AVN preparations. These authors have employed optical mapping with voltage-sensitive dyes to study the spread of excitation from the automatic site to the fast and slow AVN conduction pathways. In 14 preparations studied, pacemaker activity originated in the PNE in 10 preparations (Fig. 7*B*). Pacemaking originated in the N/NH region of AVN in four other preparations. Dobrzynski et al. (131) also reported that the PNE pacemaker site expresses high density of neurofilament 160 (NF160), Cx45, and the HCN4 protein which codes for "pacemaker" f-channels. Finally, the PNE can constitute a region of slow conduction during AVN reentry and premature beats (131).

In conclusion, the PNE extension of AVN is able to generate pacemaking and can effectively pace the atrioventricular junction. It is thus possible that the leading pacemaker site in AVN more frequently originates in the PNE, which is also part of the slow AVN conduction pathway. It is possible that in vivo both the PNE and NH-CS region can generate junctional automaticity. It would be interesting to test if pacemaker shift exists in the AVN. Indeed, it cannot be excluded that the dominant site can shift between the PNE and the NH-CS region depending on the physiological conditions.

AVN cells have been successfully isolated from rabbit (187, 347), guinea pig (539), and mouse (314). Individual rabbit AVN cells display two different phenotypes: "ovoid" cells resembling spindle SAN cells and "rod-shaped" cells. Munk et al. (347) have reported action potential waveforms having AN, N, and NH properties in isolated rabbit AVN cells. These authors reported that N and NH action potential waveforms were typical for ovoid cells, while AN waveforms were associated with rod-shaped cellular morphology. It seems a consistent finding that the majority of ovoid cells are spontaneously active (347, 539). Some rod-shaped cells are also automatic (187), but pacemaker activity is present in a more negative diastolic range (347). As to ionic currents, ovoid cells express relatively high densities of I_f and $I_{Ca,L}$ (347, 539). However, rod-shaped cells seem to lack I_f (187, 347).

F. Automaticity in Purkinje Fibers

The intrinsic conduction velocity of ventricular myocardium is not sufficient to achieve synchronized contraction of the cardiac chambers. The Purkinje fiber network ensures a proper propagation of the cardiac impulse along the ventricular myocardium. Purkinje fibers are very fast conducting. The upstroke velocity in Purkinje fibers (429) and cells (72) can approach 1,000 V/s, a value at least threefold that of ventricular muscle (203). Quick conduction in Purkinje fibers is due to high expression of both Na^+ channels (101, 191) and Cxs (245). Furthermore, the intercellular resistance to impulse conduction in the Purkinje network of different mammals can be as low as 100 Ω/cm, approaching that of the intracellular milieu (72, 335).

The Purkinje fibers network can pace the heart, in case of complete atrioventricular block. Automaticity in Purkinje fibers can become important, because conduction in the AVN and bundle branches is prone to block under different genetic and physiopathological conditions. Automaticity in Purkinje fibers is slower than in the SAN and AVN. Depending on the species considered, pacemaking rate in Pukinje fibers varies between 25 and 40 beats/min, which is sufficient to set a viable cardiac output. Action potentials in Purkinje fibers are similar but not identical to those of ventricular myocardium and display longer action potential duration and a more negative diastolic potential than SAN and AVN cells (Fig. 8*B*) (13, 72, 331, 501). Verkerk et al. (501) have shown heterogeneity in the duration of repolarization in sheep Purkinje cells (PCs). According to these authors, sheep PCs can display either prominent phase I repolarization and short-lasting plateau phase or absence of phase I associated with longer plateau phase. Early afterdepolarizations (EADs) are often observed in intact Purkinje fibers (13) and isolated PCs (Fig. 8*D*) (331). Spontaneous EADs in the Purkinje network can constitute an important trigger of ventricular arrhythmias (13).

Compared with pacemaker cells from the SAN and AVN, spontaneously beating PCs have distinct morphology and electrophysiological properties (Fig. 8, *C* and *D*). After enzymatic isolation, PCs can be distinguished in vitro from ventricular and SAN cells by their shape and size (72, 331). PCs are mainly rod-shaped and larger than SAN and AVN cells, but generally smaller than ventricular myocytes (72, 331) (Fig. 8*C*). PCs have been successfully isolated from the mouse heart by using a transgenic mouse line in which the enhanced green fluorescent protein (EGFP) has been knocked in the gene coding for Cx40 ($Cx40^{EGFP+/-}$ mouse, see Fig. 8, *A* and *C*) (331). Similar to what is observed in intact fibers, spontaneously beating PFCs have a large action potential overshoot and a long-lasting plateau phase (Figs. 1*B* and 8*D*). EADs can also be recorded during repolarization (Fig. 8*D*), a phenomenon that has been observed also in paced intact fibers (13). The maximum diastolic potential can be close to −90 mV in calf Purkinje fibers (127). In contrast, mouse Purkinje fibers seem to have more positive diastolic potentials (−75 mV) (13). The negative diastolic potential in Purkinje fibers is attributed to I_{K1}. Indeed, in calf Purkinje fibers, I_{K1} density is high enough to drive the maximum diastolic potential close to the equilibrium of K^+ (72, 118).

Downloaded from physrev.physiology.org on October 4, 2011

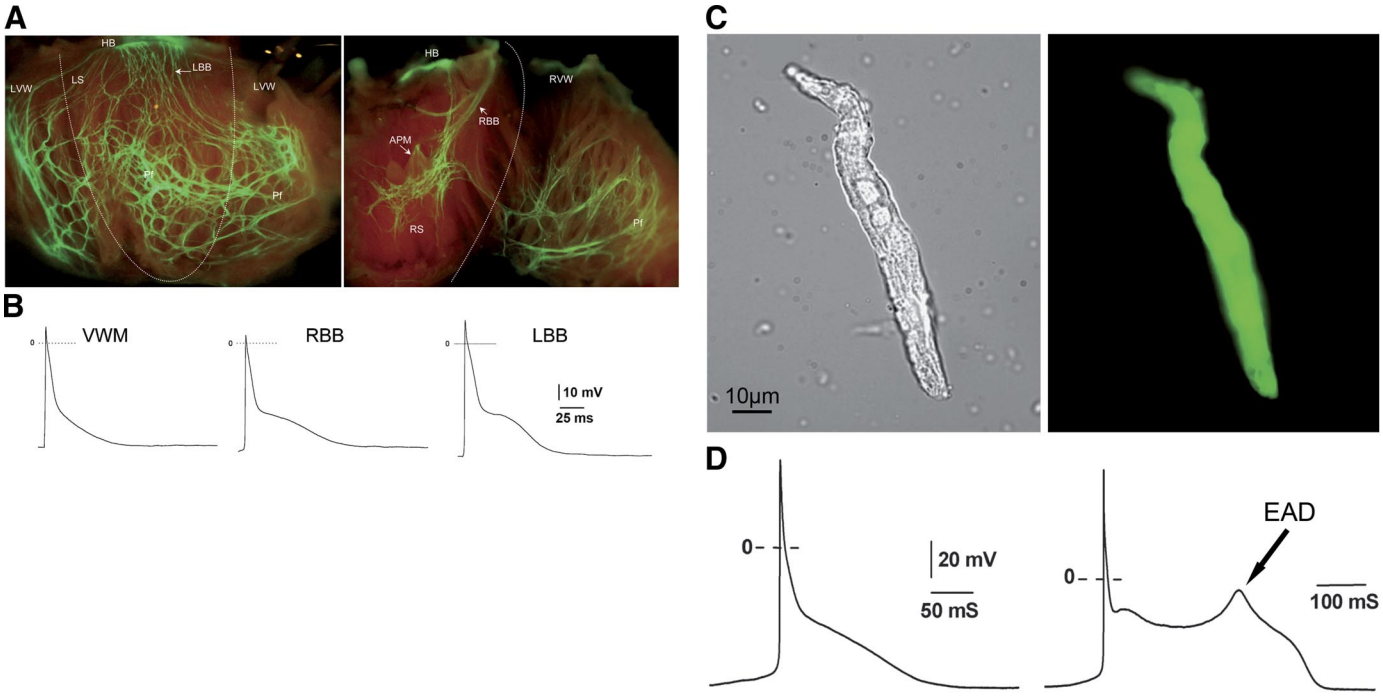

FIG. 8. *A*: structural organization of mouse Purkinje fibers (PF). In this mouse line, the EGFP has been knocked in the gene encoding for Cx40. Asymmetry of the PF network is then visualized by epifluorescence. In the right ventricle, PF originate from a common trunk (RBB) that ramificates in secondary branches, which laterally terminate in contact with papillary muscle (APM). PF in the left ventricle arise from the left bundle branches (LBB) in continuity with the His bundle (HB) and form a dense network on the left ventricular free wall (LVW). Dotted lines indicate the axis of cutting along the right (RS) and left (LS) ventricular septum to expose the ventricular free walls. *B*: evoked action potentials recorded using the same preparation as in *A*. Records are from the ventricular working myocardium (VWM), the right (RBB) and left (LBB) bundle branches. Note the longer action potential plateau phase in the bundle branches composed by Purkinje fibers. *C*: line shows the morphology of a spontaneously active mouse Purkinje cell under visible light (*right panel*) and EGFP epifluorescence (*left panel*). *D*: automaticity and action potential configuration in an isolated Purkinje cell as shown in *C*. Spontaneous early afterdepolarizations (EADs) are often observed during the action potential plateau phase. [From Miquerol et al. (331), with permission from Elsevier.]

Consequently, automaticity needs to be generated in a more negative voltage interval than in the SAN or AVN. However, automaticity of Purkinje fibers can be increased by stretch induced by ventricular filling (233). The presence of a large I_{K1} can partly explain the relatively slow intrinsic beating rate of Purkinje fibers. Ionic currents underlying SAN pacemaking have been found also in Purkinje fibers (72, 501, 502). The presence of I_f has been extensively described in isolated Purkinje fibers by DiFrancesco (118, 122) and others (72) as that of $I_{Ca,T}$. Other ionic mechanisms as the NCX can participate to automaticity in Purkinje fibers (307).

III. MOLECULAR DETERMINANTS OF ION CHANNELS IN AUTOMATIC HEART CELLS

A. f-Channels

Almost all spontaneously active cells coming from heart rhythmogenic centers express f-channels (21). DiFrancesco and co-workers (20, 120, 121) have proposed that I_f is the predominant ionic mechanism underlying cardiac automaticity. SAN pacemaker cells robustly express I_f (125, 313). In the rabbit, I_f density is higher in the SAN periphery than in the center (355). I_f can be recorded also in the myocardium, where it can be activated below the physiological resting potential (535). It has been shown that disease states such as atrial fibrillation and heart failure enhance I_f expression and shift positively the current voltage dependence (see Ref. 79 for review). I_f is a mixed cationic current carried by Na^+ and K^+ (2). Permeability to Na^+ is predominant, but K^+ activates I_f conductance (115, 122, 125). Ca^{2+} permeability of f-channels has been reported in HEK cells expressing recombinant HCN2 channels (538) and in rat ventricular cells (537). In the SAN and AVN, I_f activates upon membrane hyperpolarization with variable threshold between -50 and -65 mV (21). The threshold of I_f is substantially more negative in Purkinje fibers (118).

Several factors can influence the activation of f-channels. β-Adrenergic receptor activation stimulates (21) while muscarinic agonists inhibit I_f (129). This regulation is mediated by direct activation of f-channels by cAMP (50, 128), which facilitates channel opening (126). DiFrancesco and Tortora (128) failed to observe a direct regulation of SAN

Downloaded from physrev.physiology.org on October 4, 2011

f-channels by purified protein kinase A (PKA) (128). In SAN cells, direct regulation of voltage dependence by cAMP can quantitatively account for I_f regulation by autonomic agonists (126). The existence of a PKA-mediated regulation of I_f has been suggested by Chang et al. (80) in canine Purkinje cells and in murine stem cells derived from cardiomyocytes (1). Intracellular Ca^{2+} have been reported to positively regulate I_f by either increasing current conductance (171) or by positively shifting the current voltage dependence (416). The mechanisms by which Ca^{2+} regulate I_f has not been elucidated. Inside-out patch-clamp experiments seem to exclude a direct Ca^{2+} effect on f-channels (540).

Four gene isoforms, named HCN1–4, code for f-channels and have been cloned from the mouse (295, 435), rabbit (217), and human (296, 444). These isoforms display different activation threshold, kinetics, and sensitivity to cAMP (234). Particularly, HCN1 channels show the more positive threshold for activation, the fastest activation kinetics, and the lowest sensitivity to cAMP (295, 435), while HCN4 channels are slowly gating and strongly sensitive to cAMP (217, 296, 444). HCN2-mediated channels have intermediate properties between HCN1- and HCN4-mediated channels (234). It has been proposed that the transmembrane protein KCNE2 stimulates the surface expression and accelerates the kinetics of HCN channels in heterologous expression system (536) and in cardiomyocytes (404). It has also been proposed that KCNE2 can switch HCN2-mediated currents from time dependent to time independent (302).

HCN4 is the predominant f-channel isoform expressed in the SAN (317, 342, 450) and AVN (317). The HCN1 and HCN2 isoforms are also expressed in these rhythmogenic centers (317, 342, 344, 450).

However, the molecular composition of native cardiac f-channels has not been elucidated. The strong expression of HCN4 mRNA in the SAN and AVN and the high sensitivity of native f-channels to cAMP (126) suggest that HCN4 is a major determinant of native I_f. Remarkably, native I_f has faster activation kinetics than I_f mediated by HCN1-HCN4 heterotetramers. Such a difference cannot be accounted for the presence of basal cAMP or KCNE2 in intact SAN cells (7). Recent studies have described a "context-dependent" regulation of native f-channels. Qu et al. (403) overexpressed HCN2 channels in neonatal and adult ventricular myocytes and showed that I_f voltage dependence was dependent on the developmental state of the cells. Furthermore, transfection of HCN2 and HCN4 channels in HEK cells and neonatal ventricular myocytes yields I_f currents that activated more positively in cardiomyocytes than in HEK cells, irrespectively of the transfected isoform (402). These observations indicate that cellular factors other than cAMP and KCNE2 contribute to the native SAN I_f kinetics and voltage dependence. Barbuti et al. (19) have reported that in rabbit SAN cells, HCN4 channels interact with caveolin-3 and are concentrated in caveolar membrane lipid rafts. Chemical disorganization of caveolar structures positively shifted the I_f activation curve and slowed the current deactivation kinetics (19). In a follow-up study, the same group showed that β_2-receptors colocalize with f-channels in cavelolar structures and that β_2-dependent regulation of I_f also requires caveolar membrane compartimentalization (20). It thus seems very likely that cAMP-dependent regulation of f-channels takes place locally, in a subcellular space delimited by lipid rafts. Pian et al. (392) have reported that phosphatidylinositol 4,5-bisphosphate (PIP_2) prevents rundown of both recombinant HCN2-mediated and native rabbit SAN I_f. It is thus possible that a multiplicity of factors other than cAMP can participate in the regulation of I_f in the SAN. Regulation of HCN2 channels by stretch has been reported by Li et al. (287). These authors have studied HCN2-mediated I_f expressed in *Xenopus* oocytes. In this preparation, stretch accelerated both activation and deactivation kinetics of I_f (287).

B. Voltage-Dependent Ca^{2+} Channels

Voltage-dependent Ca^{2+} channels (VDCCs) are an important pathway of Ca^{2+} entry in pacemaker cells. L- and T-type VDCCs have been consistently recorded in spontaneously active SAN and AVN cells (145, 172, 314, 401, 539). L-type VDCCs are expressed throughout the myocardium, are sensitive to dihydropyridines (DHPs) such as nifedipine and BAY K 8644, and are stimulated by PKA-dependent phosphorylation (491). For further discussion on the physiology and pharmacology of cardiac L-type VDCCs, the reader is referred to some recent reviews (470, 491). In the heart, L-type VDCCs initiate contraction (475) and contribute to pacemaker activity (309, 497, 546).

$I_{Ca,L}$ in the SAN and AVN activates upon depolarization at a variable threshold between −50 and −30 mV (309, 314, 497, 539, 546) and displays Ca^{2+}- and voltage-dependent inactivation (172, 311). Expression of $I_{Ca,L}$ in the rabbit SAN is heterogeneous; larger cells (presumably from the SAN periphery) express less current density than smaller cells (349). In the SAN, $I_{Ca,L}$ is regulated by PKA (390) and by activated Ca^{2+}/calmodulin-dependent protein kinase II (CaMKII) (509), which regulates the current activation and reactivation kinetics (509). Similarly, in ventricular cells, CaMKII facilitates opening of L-type channels in response to Ca^{2+} permeation, with consequent stimulation of $I_{Ca,L}$ amplitude and slowing of current inactivation (135, 528).

L-type VDCCs are multisubunit complexes, constituted by a pore-forming $\alpha 1$ subunit in association with different accessory subunits ($\alpha 2$-δ, β, and γ) (470). Four L-type $\alpha 1$-subunits have been cloned and classified in the Ca_v1 gene family (78). The $Ca_v1.1$ $\alpha 1$-subunit is responsi-

Downloaded from physrev.physiology.org on October 4, 2011

ble for excitation-contraction coupling in skeletal muscle (474). $Ca_v1.4$ is expressed in the retina, spinal cord, and immune cells (324). $Ca_v1.2$ and $Ca_v1.3$ are expressed in neurons, as well as in cardiovascular and neuroendocrine cells (77). In the ventricle, the $Ca_v1.2$ α-subunit is the predominant molecular determinant of $I_{Ca,L}$. This α-subunit is expressed in the SAN, AVN, and the atria (45, 309, 317, 472). Recombinant and native $Ca_v1.3$-mediated $I_{Ca,L}$ displays a more negative activation threshold and slower inactivation kinetics than $Ca_v1.2$-mediatd $I_{Ca,L}$. $Ca_v1.3$ channels have also reduced sensitivity to DHPs (254). In contrast, SAN $Ca_v1.2$-mediated and $Ca_v1.3$-mediated $I_{Ca,L}$ seem to be similar as to their sensitivity to β-adrenergic agonists (309).

T-type VDCCs are activated at more negative voltages than L-type VDCCs. The kinetic hallmark of native and heterogously expressed $I_{Ca,T}$ is slow activation and fast voltage-dependent inactivation. The single-channel conductance of T-type VDCCs is also smaller than that of L-type VDCCs (388). Three genes coding for T-type α1-subunits have been cloned (103, 339, 340, 387) and named $Ca_v3.1$, $Ca_v3.2$, and $Ca_v3.3$. The $Ca_v3.1$ isoform is functionally expressed in neonatal rat atrial myocytes (282), in the AT-1 cell line (438), in the developing mouse heart (103), and in mouse SAN and AVN (314). In the adult SAN, expression of the $Ca_v3.1$ isoform is higher than that of $Ca_v3.2$ (45, 314). The $Ca_v3.2$ isoform has been cloned from a human heart library (103), and possibly constitutes the predominant $I_{Ca,T}$ isoform in the rat embryonic heart (146). In contrast, expression of $Ca_v3.1$ channels increases during the perinatal period and is maximal in adulthood (358). To date, expression of the $Ca_v3.3$ isoform has not been found in the myocardium, the SAN, and AVN (314, 340). No specific drugs able to discriminate between $Ca_v3.1$ and $Ca_v3.2$ channels are presently available. However, $Ca_v3.2$ channels are much more sensitive to Ni^{2+} than $Ca_v3.1$ channels, the concentration for half-block (EC_{50}) being ~5 and 150 μM for $Ca_v3.2$ and $Ca_v3.1$ channels, respectively (265).

C. St-Channels

The I_{st} current has been recorded by Guo et al. (166) in rabbit SAN and AVN (165). This current has also been found in SAN cells from guinea pig, rat, and mouse (86, 457). I_{st} activates at about −70 mV, peaks at about −50 mV, and is positively regulated by β-adrenergic agonists (166). I_{st} is carried by Na^+, but is clearly distinct from I_{Na}, since it is insensitive to tetrodotoxin (TTX), blocked by DHP antagonists, and inhibited by divalent cations such as Ca^{2+}, Mg^{2+}, and Ni^{2+} (166). Single st-channels have a unitary conductance similar to that of L-type VDCCs (~13 pS) and are facilitated by BAY K 8644 (333). Mitsuye et al. (334) have reported that I_{st} expression is restricted to spontaneously active SAN and AVN cells, since no I_{st} is recorded in quiescent cells from these two regions.

The molecular determinants of I_{st} have not yet been identified. I_{st} could be mediated by a new subtype of L-type VDCCs (166), or by a still unidentified splice variant. This hypothesis would be consistent with the pharmacological sensitivity of I_{st} to agonist and antagonist DHPs.

D. Voltage-Dependent Na^+ Channels

A significant fraction of rabbit SAN pacemaker cells expresses I_{Na} in culture (348, 351). I_{Na} is heterogeneously expressed in the adult rabbit SAN (204, 250). Honjo et al. (204) reported that I_{Na} expression is higher in large cells (presumably from the SAN periphery) than in small cells (from the SAN center). A high percentage of small cells is devoid of I_{Na} (204). Consistently, pacemaking in SAN periphery is sensitive to TTX, while automaticity in tissue balls from the SAN center is insensitive to TTX application (250, 255). In contrast, SAN cells of newborn rabbits show high I_{Na} expression (24). In the newborn, expression of I_{Na} is maximal during the first 3 wk after birth and then declines irrespectively of cell size (24). High expression of I_{Na} is present also in adult mouse SAN cells (279, 312, 313). The SAN I_{Na} is more sensitive to TTX than I_{Na} of the working myocardium. TTX-sensitive I_{Na} has been reported in rabbit neonatal (25) and in adult mouse SAN cells (279). TTX in the nanomolar range reduces the beating rate of isolated mouse hearts (304) and SAN pacemaker cells (279).

Na^+ channels are related to a large family of genes coding for 10 α-subunit isoforms (see Ref. 534 for review). The electrophysiological properties of the α-subunit can be modulated by accessory β1- and β2-subunits (534). By using in situ hybridization, Baruscotti et al. (25) have shown that the newborn SAN expresses the neuronal TTX-sensitive $Na_v1.1$ α-subunit isoform. Expression of both the TTX-sensitive $Na_v1.1$ and TTX-resistant "cardiac" Nav1. 5 isoforms has been reported in the mouse SAN at the protein level (279).

E. Voltage-Dependent K^+ Channels

Voltage-dependent K^+ channels (VDKCs) control the action potential repolarization phase in spontaneously active cells (58) and in the working myocardium (353, 422). In SAN and AVN, three VDKC-mediated currents have been recorded: the fast (I_{Kr}) and slow (I_{Ks}) delayed rectifiers and the transient outward current (I_{to}).

I_{Kr} is activated upon depolarization from a threshold of −50 mV. In voltage-clamp experiments, I_{Kr} fully activates at about −20 mV and displays strong inward rectification (93, 218, 496). At positive voltages, inactivation of

Downloaded from physrev.physiology.org on October 4, 2011

I_{Kr} counterbalances activation, thereby generating a region of negative slope conductance (93). When the membrane voltage is switched back to negative potentials, I_{Kr} slowly deactivates to generate tail currents, which contribute to set the maximum diastolic potential (see sect. VI). Tail currents are due to channel reopening followed by time-dependent closure at negative membrane potential (452). Shibasaki (452) has reported that the single-channel conductance of I_{Kr} channels in 150 mM K^+ is 11 pS, giving an estimate of ~1,000 channels in a typical rabbit SAN cell. I_{Kr} is sensitive to class III methanesulfonanilide compounds E-4031 and dofetilide (UK-68798), as well as to a plethora of unrelated compounds used in medical practice (473).

I_{Kr} channels are coded by the ERG gene family, which includes three members named ERG1-ERG3. The ERG1 gene is expressed in the heart (398). Mutations in the human ERG1 gene or in its accessory subunit KCNE2 can impair ventricular repolarization and lead to long-QT syndrome (92, 236). In the mouse SAN, mRNAs of the three known ERG1 splicing variants 1a, 1a′, and 1b have been found (93). However, the composition of native I_{Kr} channels in SAN, AVN, and Purkinje fibers has not yet been elucidated. Lees-Miller et al. (273) have proposed that both ERG1a and -1b are able to form recombinant channels with properties similar to those of native I_{Kr}, but to date, only ERG1a immunoreactivity has been identified in the ventricle (397).

The I_{Ks} current is kinetically and pharmacologically distinct from I_{Kr}. I_{Ks} has slower activation and faster deactivation kinetics than I_{Kr}. I_{Ks} is sensitive to the 293B channel blocker, which is currently employed for studying the physiological role of this current (275, 278). Expression of I_{Kr} and I_{Ks} in the rabbit SAN is heterogeneous. Indeed, high I_{Kr} and I_{Ks} densities have been recorded in large SAN cells, while smaller cells seem to express only I_{Kr} (278). Species-dependent differences in I_{Kr} and I_{Ks} expression seem to exist. I_{Kr} has not been recorded in isolated pig SAN cells, which express only I_{Ks} (372). I_{Ks} has not yet been directly recorded in mouse SAN cells (Mangoni, unpublished observations). However, Temple et al. (478) have reported expression in the mouse SAN of the KCNQ1 accessory subunit KCNE1. On the other hand, mice lacking KCNE1 have susceptibility to spontaneous atrial fibrillation, but do not show alterations in SAN pacemaker activity (478).

Three genes named *KCNQ1-KCNQ3* encode for I_{Ks}, but only KCNQ1-related expression is found in the heart (352). The sensitivity of I_{Kr} and I_{Ks} to β-adrenergic agonists in pacemaker cells would need further investigation. Voltage-clamp studies on intact SAN tissue preparations have reported stimulation of I_K by epinephrine (62). These observations have been confirmed in isolated rabbit SAN cells (277). Sensitivity of I_{Kr} to β-adrenergic agonists has been reported in ventricular myocytes (194), but this issue has not been addressed in SAN cells.

The I_{to} current is characterized by fast activation and inactivation kinetics (see, for example, Ref. 277). Pharmacologically, I_{to} can be identified thanks to its sensitivity to 4-aminopyridine (4-AP) (422). In working myocytes, at least two components of I_{to} have been identified and named $I_{to,f}$ and $I_{to,s}$, according to their fast and slow inactivation kinetics, respectively (353). Expression of I_{to} in rabbit SAN cells is heterogeneous (60, 206, 277). Indeed, pacemaker activity of SAN tissue balls isolated from the SAN periphery is more sensitive to block of I_{to} by 4-AP than that from the center of the SAN (60). In rabbit SAN cells, I_{to} density is positively correlated with the cell size (206, 277).

I_{to} channels are coded by the K_v1 and K_v4 gene family (354). The composition of native I_{to} channels in the SAN and conduction system is not yet known. In the mouse heart, inactivation of Kv1.4 channels abolishes $I_{to,s}$ (291). The channel complex mediating the $I_{to,f}$ component is formed by heteromultimers of $K_v4.2$ and $K_v4.3$ channel subunits (168). The KChIP2 protein is also associated with the I_{to} channel complex (8). KChIP2 regulates current inactivation and channel targeting to the cell membrane (8). Ventricular cells isolated from mice lacking KChiP2 have no I_{to} and display prolonged action potential duration. Episodes of ventricular tachyarrhythmias are recorded in KChiP2 knockout mice (260).

In conclusion, I_{to} appears to play a role in the action potential repolarization phase of peripheral SAN cells, but is probably less important in the SAN center. However, mice lacking both $I_{to,s}$ and $I_{to,f}$ have no apparent dysfunction of the SAN rhythm (290). Further studies will be needed to elucidate the subunit composition and the physiological role of I_{to} in spontaneously active cells.

F. G Protein-Activated, ATP-Dependent, and Inward Rectifier K^+ Channels

The acetylcholine-activated current (I_{KACh}) is strongly expressed in the SAN, atria, and AVN (124, 159, 367). In these tissues, I_{KACh} is activated by muscarinic and adenosine receptors by direct binding of G protein βγ-subunits to the I_{KACh} channel complex (for review, see Refs. 520, 521). Four genes named Kir3.1-Kir3.4 underlie I_{KACh} channels (520). Kir3.1 and Kir3.4 are expressed in the heart (521). Cardiac I_{KACh} channels are tetrameric complexes containing Kir3.1 and Kir3.4 channels (521). However, mice lacking Kir3.4 channels have no cardiac I_{KACh} (522), because Kir3.1 channels require Kir3.4 channels to be targeted at the cell membrane (238).

ATP-dependent K^+ channels have been described in rabbit SAN cells (184). These channels underlie $I_{K,ATP}$ and are open when the intracellular concentration of ATP is

Downloaded from physrev.physiology.org on October 4, 2011

lowered. Van Wagoner (493) has shown that $I_{K,ATP}$ channels are activated by stretch. Cell swelling by a hypotonic solution was used in this work to demonstrate that $I_{K,ATP}$ can generate a significant whole cell current under mechanical stress. Activation of $I_{K,ATP}$ by stretch has been reported also in ventricular cells (251), but these observations have not yet been confirmed in pacemaker tissue. In rabbit SAN cells, $I_{K,ATP}$ slows pacemaker activity and hyperpolarizes the cell maximum diastolic potential (184). Han et al. (184) have proposed that the slowing of heart rate induced by $I_{K,ATP}$ can be important for protecting the myocardium from ischemic damage or stunning. This interesting hypothesis has not yet been experimentally verified.

Rabbit SAN and AVN cells express very low densities of inward-rectifier K^+ current I_{K1} (62, 215, 350, 363, 366). In contrast, I_{K1} is present in the working myocardium (422) and in Purkinje fibers (118). I_{K1} is responsible for the negative diastolic potential of PFCs. However, I_{K1} can be moderately expressed in rat (457) and mouse (86) SAN cells, even if at a much lower density than the working myocardium. In the heart, I_{K1} channels are coded by the Kir2.1 and Kir2.2 channel subunits (352).

G. Cl^- Channels, Volume-Activated Channels, and Stretch-Activated Cationic Channels

The first evidence for the presence of chloride current (I_{Cl}) in spontaneously active cells came from Purkinje fibers. In this preparation, De Mello (106) reported that I_{Cl} represents a substantial fraction of the total membrane conductance during the action potential. I_{Cl} has been reported by Seyama who estimated that Cl^- are responsible for ~9% of the total membrane conductance and that I_{Cl} underlies a significant part of the membrane inward-going rectification in the SAN (449). Hagiwara et al. (174) have characterized a stretch-activated background I_{Cl} in rabbit SAN cells. This current is distinct from the voltage- and Ca^{2+}-dependent, cAMP-sensitive [$I_{Cl(Ca)}$] present in ventricular myocytes (16, 471), and probably belongs to the family of volume-activated anion-selective currents (VAC_{Cl}) (27), because the current was activated by cell inflation (174). Hagiwara et al. (174) reported that SAN background I_{Cl} is insensitive to intracellular Ca^{2+} depletion and cAMP. Bescond et al. (37) have reported that angiotensin II (ANG II) activates background I_{Cl} in SAN cells via a protein kinase C (PKC)-dependent signaling pathway. Verkerk et al. (504) have tested the possibility that $I_{Cl(Ca)}$ is present in SAN cells and its possible role in the action potential repolarization. They recorded $I_{Cl(Ca)}$ in about one-third of SAN cells tested. $I_{Cl(Ca)}$ activated from about −20 mV, peaked between +30 and +40 mV, and was augmented by norepinephrine. The kinetic behavior of SAN $I_{Cl(Ca)}$ (504) was similar to $I_{Cl(Ca)}$ in atrial, Purkinje, and ventricular myocytes (210). Verkerk et al. (504) have tested the role of $I_{Cl(Ca)}$ in SAN automaticity, by employing action potential clamp experiments and numerical modeling (504). They found that $I_{Cl(Ca)}$ activates late during the action potential upstroke phase and gives moderate contribution to the repolarization phase. No contribution of $I_{Cl(Ca)}$ to the maximum diastolic potential or diastolic depolarization rate was observed (504).

VAC_{Cl} are activated by an increase in cell volume or by agents that alter membrane tension and mechanical stretch (27). VAC_{Cl} open with a quite slow response to cell volume change (464). $I(VAC_{Cl})$ is time independent, outwardly rectifying, and reverses between the cell resting potentials and action potential plateau phase. Consequently, VAC_{Cl} shortens the action potential duration and depolarizes the membrane resting potential, thereby acting to decrease cell volume (27). In the heart, VAC_{Cl} play a role in the ischemic response and seem to be overexpressed in the hypertrophied myocardium (27). The existence of mechanosensitive VAC_{Cl} in SAN has been directly proposed firstly by Arai et al. (14), who showed that the positive chronotropic response induced by strong stretch stimuli in SAN tissue is inhibited by Cl^- channel blockers. However, Cooper and Kohl (99) have failed to observe an effect of a Cl^- channel blocker under conditions of moderate mechanical load.

SAC are cationic nonselective or K^+ selective. Compared with VAC_{Cl}, SAC activate fast upon mechanical stimulation. Kohl et al. (251) have suggested that fast activation of SAC can be involved in the beat-by-beat regulation of heart rate. SAC are inhibited by Gd^{3+} (383), streptomycin (151), and the spider toxin GsMTx-4 (42). Cooper and Kohl (99) reported that the chronotropic response of isolated pacemaker cells is inhibited by GsMTx-4, thus indicating functional expression of SAC in SAN cells.

IV. PUMPS AND EXCHANGE CURRENTS

A. The Na^+-K^+ Pump Current I_p

The electrogenic role of Na^+–K^+ pump is well established. Under physiological ionic concentrations, three Na^+ are extruded and two K^+ are transported in the intracellular milieu for each pump cycle. Consequently, the Na^+–K^+ pump generates a net outward current that influences cellular pacemaking. In Purkinje fibers, I_p stimulation hyperpolarizes the membrane potential and slows spontaneous activity (149). Noma and Irisawa (362) have recorded I_p-mediated membrane hyperpolarization in rabbit SAN multicellular preparations, by rapidly switching perfusion from K^+-free Tyrode's solution to one containing 5.4 mM K^+ (362). A similar hyperpolarization of the

Downloaded from physrev.physiology.org on October 4, 2011

membrane potential has been observed in atrioventricular cells (261). I_p properties can be studied by varying the intracellular K^+ concentration after block of time- and voltage-dependent currents, according to the protocol described by Gadsby et al. for ventricular cells (150). I_p can also be isolated pharmacologically by employing ouabain or strophantidine (261, 362, 431). Sakai et al. (431) have studied the properties of I_p in isolated rabbit SAN cells. They reported that I_p carries a significant steady-state outward current in physiological extracellular K^+ and 50 mM intracellular Na^+. Similarly to I_p recorded in ventricular cells (150), SAN I_p displays voltage-dependent behavior (431). I_p voltage dependence is evident in the pacemaker range with a relative half activation voltage of about −50 mV. Furthermore, I_p is very sensitive to changes in intracellular Na^+ so that the current doubles when changing Na^+ from about 15 to 25 mM Na^+ (431).

In SAN cells, I_p contributes to the setting of the maximum diastolic potential in the range of −60 mV (362). In this respect, Sakai et al. (431) have estimated that the net outward I_p-mediated current in intact SAN cells is ~14 pA in the experiments by Noma and Irisawa (362) and ~20 pA in their recordings. However, since automaticity is essentially a periodical process, it is also possible that I_p varies cyclically during the pacemaker cycle according to its intrinsic voltage and Na^+ dependency. Furthermore, one may wonder if I_p can respond to transient changes in intracellular Na^+ induced by activation of ion channels such as I_{Na} and I_f. Choi et al. (90) have measured changes in intracellular Na^+ activity (a^i_{Na}) in multicellular and isolated SAN cell preparations under application of isoproterenol, carbachol, and I_f blockers. These authors reported that isoproterenol-induced acceleration of the pacing rate was accompanied by an elevation of a^i_{Na}. Application of Cs^+ and ZD-7288 reduced (but did not completely abolished) the rise in a^i_{Na}, thus suggesting a link between I_f stimulation by isoproterenol and a^i_{Na}. In contrast, both carbachol and ZD-7288 reduced a^i_{Na} in spontaneously beating myocytes but had no effect on quiescent cells. These data are strongly suggestive of a significant influence of I_f on intracellular a^i_{Na}. It is thus tempting to speculate that f-channels can be functionally coupled to I_p in SAN pacemaker cells. This hypothesis can be particularly relevant when considering that f-channels are concentrated in membrane lipid rafts. It is possible that opening of f-channels induces a highly localized rise in intracellular Na^+ concentration. The presence of the Na^+–K^+ pump near f-channels is important for maintaining the ionic homeostasis.

B. The Na^+-Ca^{2+} Exchanger Current I_{NCX} and the Na^+-H^+ Exchanger

The NCX is a major actor intervening in cardiac cell Ca^{2+} homeostasis. Indeed, Ca^{2+} entry during the diastole and action potential upstroke increases intracellular Ca^{2+} concentration ($[Ca^{2+}]_i$) stimulating NCX activity. Stoichiometry of Na^+-Ca^{2+} transport through NCX is electrogenic, one Ca^{2+} is extruded for three Na^+ entering the cell (454). The result is a net inward current (I_{NCX}) which depolarizes the membrane voltage. In the working myocardium, NCX is responsible for Ca^{2+} efflux during action potential repolarization (35, 142). In the rabbit myocardium, I_{NCX} extrudes ~30% of the total Ca^{2+} required to activate contraction, while the sarcoplasmic reticulum Ca^{2+}-ATPase (SERCA) actively removes Ca^{2+} from the cytoplasm to replenish the SR (142). Regardless of the species considered, Ca^{2+} extrusion by NCX quantitatively matches Ca^{2+} influx triggering Ca^{2+}-induced Ca^{2+} release (CICR), while SERCA transport must match ryanodine receptor (RyR)-dependent Ca^{2+} release. The ventricular I_{NCX} contributes to action potential plateau as well as to contractile relaxation (35). Positive regulation of NCX activity by β-adrenergic receptor activation is linked to positive inotropism in ventricular and Purkinje myocytes (35).

Early evidence of the presence of I_{NCX} in pacemaker tissue was obtained by Brown et al. (65) using multicellular SAN preparations. These authors showed that the slow inward current had a second late component that could be attributed to Na^+-Ca^{2+} exchange. Similarly, Zhou and Lipsius (547) recorded I_{NCX} in cat latent atrial pacemaker cells by applying depolarizing voltage steps eliciting $I_{Ca,L}$ which, in turn, activated I_{NCX}. NCX activity closely follows changes in $[Ca^{2+}]_i$. For example, in cane toad (*Bufo marinus*) sinus venosus cells, an increase in I_{NCX} precedes the measured systolic Ca^{2+} transient, thus suggesting that I_{NCX} is significantly stimulated by an increase in subsarcolemmal $[Ca^{2+}]_i$ (228). Furthermore, inhibition of NCX activity by Ni^{2+} slows the decline of the caffeine-induced release, indicating that NCX is a major controller of $[Ca^{2+}]_i$ in toad sinus venosus cells (228). The physiological role of I_{NCX} in pacemaking can be tested by fast removal of extracellular Na^+ or substitution with Li^+. In these conditions, $[Ca^{2+}]_i$ quickly rises and pacemaker activity stops (44, 228, 433). Intact NCX activity is thus necessary for maintaining automaticity of pacemaker cells in both amphibians (228) and mammals (44, 433). The importance of NCX in the generation of cardiac automaticity will be discussed in a following section of this review.

The Na^+-H^+ exchanger (NHE) is a pH-regulatory protein present in the plasma membrane of all cardiac myocytes. In response to intracellular acidosis, the protein removes one intracellular H^+ in exchange for an extracellular Na^+ (305). NHE is regulated by several humoral factors including ANG II and endothelin (305). NHE1 is the predominant isoform expressed in cardiac myocytes (305). In isolated ferret hearts, NHE1 is responsible for ~50% of the total H^+ efflux (163). NHE1 has been

Downloaded from physrev.physiology.org on October 4, 2011

implicated in cardiac pathological states including ischemia (see Refs. 198, 305 for review). Indeed, strong activation of NHE1 following intracellular acidosis leads to increased intracellular Na^+ concentration and consequent $[Ca^{2+}]_i$ build up through activation of I_{NCX} (198). We can thus expect that NHE and, more generally, proteins involved in H^+ handling (198) can be involved in the SAN chronotropic response to ischemia and acidosis (see sects. IX*E* and X*B*). However, we currently lack a detailed characterization of NHE-mediated current in SAN.

V. PATTERNS OF GENE EXPRESSION IN ADULT PACEMAKER TISSUE

In this short section, we review evidence on the differential expression pattern of ion channels in the heart's rhythmogenic centers and in working myocardium. Han et al. (179) have studied the expression of ion channels potentially involved in automaticity in canine Purkinje fibers and compared it with ventricular myocardium. This study combined RT-PCR with Western blotting of membrane proteins. Results have shown that HCN4 is highly expressed in canine Purkinje fibers, while it seemed undetectable in ventricular muscle. HCN2 expression was comparable in Purkinje fibers and the ventricle. Expression of $Ca_v1.2$ and NCX was higher in the ventricle than in Purkinje fibers. Genes coding for $I_{Ca,T}$ ($Ca_v3.1$, $Ca_v3.2$, and $Ca_v3.1$) were all more expressed in Purkinje fibers. Similar peculiarities in the pattern of expression of Purkinje fibers have been recently reported by Gaborit et al. (148) in nondiseased human heart.

Marionneau et al. (317) have employed a high-throughput RT-PCR approach (112) to assess the ion channel expression pattern in the mouse SAN and AVN. Indeed, real-time RT-PCR array technology allows handling of small tissue samples that contain low quantities of mRNA. These authors have compared the expression of 71 channels and related genes in the SAN, AVN, right atrium, and left ventricle (Fig. 9*A*). Transcripts coding for HCN1 and HCN4 show the highest expression level in the SAN. The SAN and AVN are distinguished by high expression of $Ca_v1.3$ and $Ca_v3.1$ mRNAs. HCN2 mRNA is present in the SAN, but at lower levels than HCN1 and HCN4 mRNA. The AVN is characterized by expression of Nav1.7, Kv1.6, as well as the K^+ β-subunit Kvβ1. These transcripts appear to be specific of the AVN (317). Significant expression of Nav1.1 has been found in the AVN. The $Ca_v\alpha2\delta2$ may constitute a potential accessory subunit for VDCCs in the SAN and AVN, because mRNA encoding for this subunit is highly expressed in the nodes and in Purkinje fibers. Mouse pacemaker tissues show predominant expression of the Na^+ channel β-subunits Navβ1 and Navβ3. It is possible that the association of Navβ1 and Navβ3 to Nav α-subunits speeds up inactivation of I_{Na}. Finally,

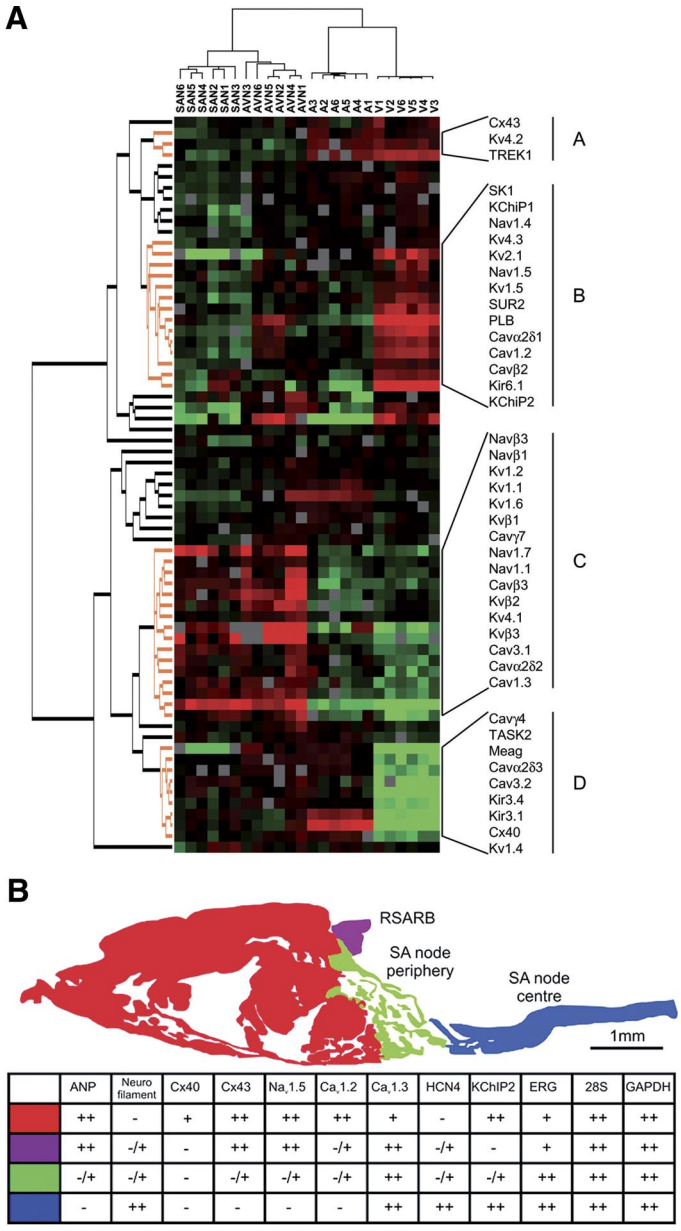

	ANP	Neuro filament	Cx40	Cx43	$Na_v1.5$	$Ca_v1.2$	$Ca_v1.3$	HCN4	KChIP2	ERG	28S	GAPDH
	++	-	+	++	++	++	+	-	++	+	++	++
	++	-/+	-	++	++	-/+	++	-/+	-	+	++	++
	-/+	-/+	-	-/+	-/+	-/+	++	-/+	-/+	++	++	++
	-	++	-	-	-	-	++	++	++	++	++	++

FIG. 9. *A*: a combined quantitative PCR and two-way hierarchical clustering approach is used to compare the expression pattern in six mouse SAN (SAN1–6), AVN (AVN1–6), atria (A1–6), and ventricles (V1–6). Seventy-one mRNAs encoding ion channel subunits and Ca^{2+} handling proteins are considered. The expression of each gene is represented by a colored row, and each column defines a tissue sample. A false color scale starting from dark green (lowest expression) to bright red is applied. Four gene clusters (*A–D*) are shown at the left of the panel. In the figure, *cluster B* identifies genes that are highly expressed in working myocardium, while *cluster C* identifies groups of genes that are highly expressed in the SAN and AVN. [From Marionneau et al. (317), with permission from Wiley-Blackwell.] *B*: quantitative RT-PCR analysis of 10 representative gene transcripts in rabbit central SAN (blue), peripheral SAN (green), right atrium (red), and SAN ring bundle (RSARB, purple). Symbol (++) stands for abundant expression, (+) stands for expression, (+/−) indicates expression in some cells, and (−) indicates absence of detectable expression. [From Tellez et al. (477).]

Downloaded from physrev.physiology.org on October 4, 2011

Kv1.1, Kv1.4, Kv1.6, Kvβ1, and Kvβ3 are highly expressed in the SAN and AVN (317). Electrophysiological investigation of mouse SAN and AVN cells will be needed to elucidate the functional role of these K^+ channels in pacemaking and conduction.

By combining quantitative RT-PCR and immunohistochemistry, Tellez et al. (477) have investigated the regional expression of genes involved in automaticity and conduction in the rabbit central and peripheral SAN. The atrial muscle was used as a reference of nonpacing myocardium (Fig. 9*B*). In this work, a quantitative switch between channel isoforms has been highlighted: moving from the atrium to the SAN center, $Ca_v1.2$ is substituted by $Ca_v1.3$, Nav1.5 by Nav1.1, and Kv1.4 by Kv4.2. As to RyRs, RyR2 is gradually downregulated, while expression of RyRs augmented in the SAN center. The SAN periphery shows an intermediate expression pattern between atrial muscle and central SAN (477).

In conclusion, cells endowed with automaticity are characterized by enhanced expression of some channels including HCN4, $Ca_v1.3$, and $Ca_v3.1$. Furthermore, the central rabbit and mouse SAN express the TTX-sensitive $Na_v1.1$ subunit. Differences in the expression pattern of ion channels in spontaneously active tissues versus the working myocardium are essentially quantitative, rather than qualitative. Numerical modeling work has suggested that quantitative changes in ionic channels can induce pacemaking (264). Overexpression of HCN (143) channels or silencing of I_{K1} (327) has been shown to induce automaticity in myocardial cells. However, pacemaker cells have also a peculiar morphological phenotype. It is thus likely that factors other than ion channels contribute to the specific phenotype of primary SAN pacemaker cells.

VI. GENESIS OF CARDIAC AUTOMATICITY: MECHANISMS OF PACEMAKING

A. Concepts

In the following sections, we will review the current knowledge on the ionic and intracellular signaling mechanisms underlying the generation of pacemaker activity. We aim to discuss published evidence on how different families of ion channels, pumps, exchangers, and intracellular Ca^{2+} signaling generate and regulate pacemaking. Many research groups have focused on primary SAN pacemaker activity so that the bulk of evidence discussed here is obtained from isolated pacemaker cells or intact SAN tissue. There is currently no general agreement as to which mechanism is necessary for initiating automaticity or, in other words, which ionic and/or cellular mechanism specifically confers automaticity to pacemaker cells.

Different groups have proposed alternative views of the mechanisms underlying pacemaker activity and emphasized the importance of in situ catecholamines production (136, 395, 396), ionic currents such as I_f (120, 121), I_{Ca} (172, 309), I_{Kr} (93, 371), I_{st} (334), or spontaneous diastolic Ca^{2+} release (307).

From a conceptual point of view, searching for pacemaker mechanisms requires the description of the electrophysiological, signaling, and transcriptional processes that are active (or specifically inactive) in pacemaker cells. These mechanisms underlie the morphological and functional differences between spontaneously active cells and contractile myocytes and/or would be responsible for the commitment of cardiac precursors toward the pacemaker function in the adult SAN and in the cardiac conduction system. Knowledge of the pacemaker mechanisms would help confer automaticity to target regions of the working myocardium or to undifferentiated cardiac precursors. Such a concept has now been applied with the aim to create "biological pacemakers" in stem cells or in the cardiac conduction system by in situ gene transfer (see sect. XI). We will first discuss evidence involving ion channels in the generation of automaticity and then review recent work showing that pacemaking also involves the activity of NCX and spontaneous diastolic Ca^{2+} release. I_f is considered as a key ion channel underlying automaticity. The relevance of I_f in the genesis of pacemaker activity is supported by different lines of electrophysiological, pharmacological, and genetic evidence. The importance of spontaneous Ca^{2+} release in the generation of pacemaker activity is indicated in experiments involving pharmacological inhibition of RyRs in rabbit SAN cells. When reviewing the current knowledge of the I_f-based pacemaking and that mediated by spontaneous Ca^{2+} release, we will try to highlight differences as well as similarities between these two proposals. Particularly, these views are not mutually exclusive and, more importantly, experiments performed in other laboratories (including ours) from genetically modified mouse strains lacking $Ca_v1.3$, $Ca_v3.1$, and HCN channels indicate that the generation of automaticity requires the intervention of more than one individual mechanism. Also, it has been shown that the influence of a given ion channel or RyRs on pacemaker activity can vary regionally in the SAN.

B. Ion Channels and Cardiac Automaticity: General Considerations

Automaticity in pacemaker cells of the adult heart stops when the cell membrane potential is depolarized by addition of KCl in the extracellular solution. Automaticity in adult pacemaker cells thus differs from that of early embryonic myocytes which maintain spontaneous con-

Downloaded from physrev.physiology.org on October 4, 2011

tractions even at depolarized membrane potentials (326, 505). This observation demonstrates that mature pacemaker cells require voltage-dependent ion channels to generate automaticity. From a theoretical point of view, pacemaker activity can be considered as an oscillator generated by a time-varying outward current with a constant or voltage-dependent inward current activated during the repolarization phase. The generation of the diastolic depolarization requires the flow of a net inward current at the end of the repolarization phase. Several ion channels with distinct biophysical and pharmacological properties are potentially involved in the diastolic depolarization phase. I_{Kr} and I_{Ks} are activated during the upstroke phase of the action potential and then deactivate quite slowly during the end of the repolarization and diastolic depolarization. As I_{Kr} and I_{Ks} drive outward currents, a net inward current must overcome outward components to initiate membrane depolarization. As to the relevance of membrane ion channels, we will base our discussion on the working hypothesis that, in isolated pacemaker cells, such an inward current is generated by the association of I_f with I_{st}, $I_{Ca,T}$, $I_{Ca,L}$, and I_{Na}. The importance of I_{NCX} will be reviewed in a separate section. A substantial amount of data on ion channels in SAN pacemaker activity comes from rabbit and guinea pig SAN. However, new insights have been obtained from genetically altered mouse strains.

C. Role of I_{Kr} and I_{Ks} in Automaticity

In rabbit SAN pacemaker cells, the cardiac I_{Kr} current sets the position of the maximum diastolic potential and controls action potential repolarization (371, 496). The physiological significance of I_{Kr} in rabbit SAN automaticity has been studied in spontaneously beating cells using E-4031. In spontaneously active cells, partial inhibition of I_{Kr} by nanomolar concentrations of E-4031 positively shifts the maximum diastolic potential and decreases the action potential amplitude and rate of rise. E-4031 also prolongs the action potential repolarization phase (371, 496). The overall physiological effect is a slowing of the pacing rate in isolated hearts and pacemaker cells (Fig. 10, *A* and *B*). Slowing of pacemaker activity is due to a reduction in the recruitment of other currents contributing to the diastolic depolarization, such as I_f, $I_{Ca,L}$, and $I_{Ca,T}$. Indeed, the positive shift of the maximum diastolic potential will reduce I_f activation and increase voltage-dependent inactivation of $I_{Ca,L}$ and $I_{Ca,T}$ during the diastolic depolarization (93). In isolated SAN cells of rabbit (371) and guinea pig (320), complete block of I_{Kr} by micromolar concentrations of E-4031 quickly terminates automaticity, and the cell resting potential settles between −30 and −40 mV. Similar effects of I_{Kr} block by E-4031 have been reported in mouse pacemaker cells by Clark et al. (93). Consistent with this pharmaco-

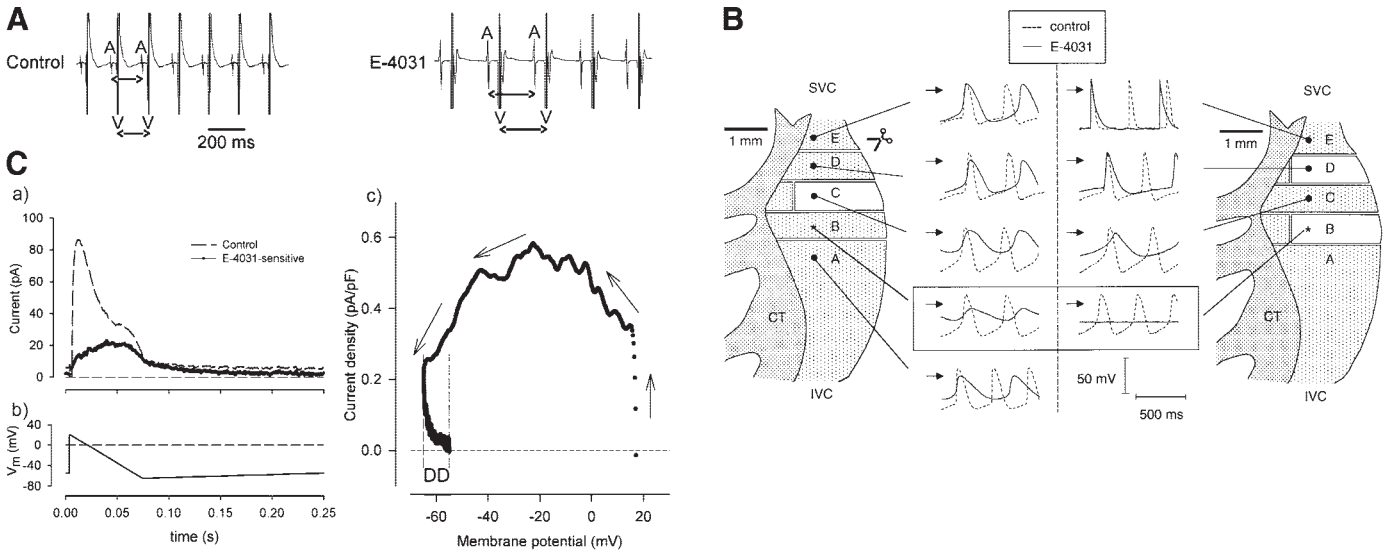

FIG. 10. *A*: I_{Kr} inhibition by 5 μM E-4031 slows the pacing rate of isolated Langendorff-perfused mouse hearts. [From Clark et al. (93).] *B*: atrio-sinus electrical interactions influence SAN pacemaking and action potential repolarization phase. Effect of 1 μM E-4031 on automaticity recorded from rabbit SAN tissue strips. Two independent experiments are shown. Asterisks indicate location of the leading pacemaking site. I_{Kr} inhibition depolarizes the maximum diastolic potential and slows pacemaking in all tissue strips connected to the crista terminalis. However, E-4031 abolishes pacemaker activity in *strip B* after that it has been cut off the crista terminalis. Filled circles indicate the site of action potential recording. [From Verheijck et al. (500).] *C*: currents from 20 consecutive action potential cycles are averaged before and after application of 2.5 μM E-4031. E-4031-sensitive difference current is obtained by subtraction. Cell has been voltage-clamped with a simulated ideal SAN action potential waveform (*b*). *c*: Current-to-voltage plot of mean E-4031-sensitive current from six different SAN cells voltage-clamped with the action potential waveform in *b*. Arrows show direction of current trajectory. The ideal diastolic interval (DD) of simulated action potential is indicated by shadowed grey vertical box at −65 and −55 mV. [From Clark et al. (93).]

Downloaded from physrev.physiology.org on October 4, 2011

logical evidence is the observation that mice lacking the ERG1b-mediated channels have no fast I_{Kr} component and are prone to develop episodes of bradycardia (272). It is interesting to note that I_{Kr} blockers induce negative chronotropism also in the zebrafish heart (329). This observation indicates that the function of ERG1/KCNH2 channels in pacemaking may be shared between fishes and mammals. Clark et al. (93) have studied I_{Kr} density and kinetics during pacemaking by pharmacological subtraction of the E-4031-sensitive current from the total systolic and diastolic current. These recordings have shown that I_{Kr} reaches a maximum during the repolarization phase at about −25 mV and then progressively declines throughout the diastolic interval to reach almost the zero level before the following action potential threshold (Fig. 10*C*). However, Zaza et al. (541) reported that I_{Kr} in rabbit SAN cells does not completely deactivate during the pacemaker cycle and can be present as a sustained current component throughout the diastolic depolarization phase.

The role of I_{Kr} in rabbit pacemaking has also been studied by a numerical modeling approach (369, 371). Calculation results are consistent with the view that I_{Kr} is the key repolarizing current in rabbit SAN cells. I_{Kr} inward rectification results in a decrease in the membrane resistance during the repolarization phase, relative to plateau phase (369). I_{Kr} deactivation contributes to the net current change during the early diastolic depolarization phase (369). Consequently, I_{Kr} activation and kinetics during the pacemaker cycle are critical factors for determining activation of ion channels during diastolic depolarization. It has also been suggested that I_{Kr} dependency from the extracellular K^+ concentration ($[K^+]_o$) in isolated pacemaker cells may account for the sensitivity of pacing rate to elevated $[K^+]_o$ in the intact SAN (369).

I_{Kr} thus plays an obligatory role in action potential repolarization of isolated rabbit and mouse (93) SAN cells. However, block of I_{Kr} by E-4031 significantly slows, but does not completely suppress, pacemaking in isolated Langendorff-perfused mouse hearts (93, 371) (Fig. 10*A*) or in intact rabbit right atrial preparations (500) (Fig. 10*B*). These observations may be explained by the presence of the electrotonic load imposed to the SAN by atrial tissue, which has a more negative diastolic potential. Atrial electrical influence partially compensates for I_{Kr} block to drive SAN repolarization (500). In conclusion, I_{Kr} also plays an important role in the way in which SAN automaticity is coupled to the surrounding atrial tissue. The regional distribution of I_{Kr} expression needs to be taken into consideration for understanding the physiological relevance of this current. As previously indicated, I_{Kr} is expressed regionally in the rabbit SAN (249). Small cells display a lower I_{Kr} density than larger cells (278). It has been proposed that low I_{Kr} expression is responsible for the less negative maximum diastolic potential in central SAN cells and could explain the enhanced sensitivity of pacemaking in the SAN center to E-4031 (278).

If I_{Kr} appears to be the predominant delayed rectifier current in the rabbit and rodents, primary SAN automaticity in pigs has been reported to depend from I_{Ks} (372). In this preparation, block of I_{Ks} by 293B stops automaticity the same way E-4031 does in rabbit SAN cells. As no detectable I_{Kr} has been found in pig SAN cells, we should conclude that I_{Ks} effectively replaces I_{Kr} for pacemaking in the pig. The presence of I_{Ks} rather than I_{Kr} in pig SAN can be a form of adaptation to a slower heart rate in large mammals compared with rodents (372). Inhibition of I_{Ks} has a significant effect on pacemaker activity in guinea pig (320) and peripheral rabbit (275) SAN cells. As these cells express both I_{Kr} and I_{Ks}, I_{Kr} can still drive pacemaking under inhibition of I_{Ks}.

D. Role of I_f in Automaticity

The physiological relevance of the I_f current in pacemaking has been a matter of debate for many years. However, a consistent amount of data now shows that I_f plays a key role in the generation of adult SAN pacemaker activity. For completeness, we will briefly summarize some useful aspects of the debate on the role of I_f in SAN pacemaking, because this point is still discussed in some recent reviews (2, 94, 121, 307).

In the SAN, I_f is the only voltage-dependent current to be activated upon membrane hyperpolarization. By the biophysical point of view, f-channels can open during the late phase of repolarization close to the maximum diastolic potential. According to the current view, I_f would initiate the first part of the diastolic depolarization until the activation threshold of T- and L-type channels is reached (94, 117). It has been questioned whether I_f size and kinetics at diastolic voltages would be compatible with the amount of inward current needed to initiate a depolarizing phase in the presence of an outward current (113, 173). Arguments for this were based on the observed variability of the I_f activation threshold in isolated SAN cells and on the relatively slow I_f activation kinetics at positive voltages (114). These kinds of uncertainties have led Denyer and Brown (114) and Hagiwara et al. (173) to propose an alternative view of the initiation of the diastolic depolarization in SAN. These authors have measured a voltage-independent, time-independent "background" current (I_b) carried by Na^+ (173). The size of this current would be theoretically sufficient to drive the diastolic depolarization upon I_{Kr} decay (173). According to this view, the diastolic depolarization is initiated by the decay of an outward current (I_{Kr}) which unmasks a voltage-independent constant depolarizing current (I_b) (173). These results have been directly challenged by DiFrancesco (116) who showed that, at least in some beat-

Downloaded from physrev.physiology.org on October 4, 2011

ing SAN cells, the instantaneous time-independent current on hyperpolarization flows in the outward direction (rather than inward) in the full range of the diastolic depolarization. This work has also shown that the I_f size at weak hyperpolarizing potentials can be substantially underestimated in patch-clamp experiments due to current run-down and wash-out phenomena of the cytosolic environment (116). However, the reversal potential of I_b can vary in preparations of isolated SAN cells as reported by different authors (114, 116, 173, 492, 496). Noble et al. (359) have used a numerical modeling approach to infer the effects of varying I_b and I_f densities on rabbit SAN pacemaking. These authors have suggested that I_b and I_f may play a reciprocal role in pacemaking, because an increase in one of these current induces a reduction in the amount of the other current. As for I_b, the size of I_f at voltages positive to the maximum diastolic potential would be sufficient to drive the diastolic depolarization. In this respect, Van Ginneken and Giles (492) and Zaza et al. (541) have also reported that the size of I_f can increase significantly in the diastolic depolarization range. Particularly, Zaza et al. (541) have shown that the net inward Cs^+-sensitive current during the diastolic depolarization is almost fourfold that theoretically necessary to drive this phase.

In conclusion, available electrophysiological data show that I_f is in fact activated during the diastolic depolarization. Both time-independent background currents and I_f may show variability between preparations and recording conditions employed (113, 116, 173, 496). At least part of SAN background currents can be attributed to either I_{Cl} (37) or TRPM4-mediated I_b described by Demion et al. (109) However, their relevance to pacemaking is not yet firmly established. Discussions on the role of I_f in pacemaking are now focused on whether this current is necessary for automaticity and on its relative contribution to the β-adrenergic modulation of heart rate (121, 307).

The relevance of I_f to pacemaker activity is now supported by pharmacological and genetic evidence. Indeed, pharmacological inhibition of f-channels slows pacemaker activity in vitro in isolated pacemaker cells and SAN tissue, as well as in vivo in experimental animal models.

Sensitivity of f-channels to Cs^+ has been used to infer the quantitative contribution of f-channels to SAN pacemaker activity (113, 365). When tested on spontaneously beating cells, 2–5 mM Cs^+ significantly slows the pacing rate (113). Cs^+ induces negative chronotropism even in the absence of any evident additional effect on I_{Kr} or $I_{Ca,L}$ (113). The fact that Cs^+ slows but does not stop pacemaker activity has been interpreted as an indication that I_f contributes to pacemaking without being an absolute prerequisite for automaticity (113, 365). This interpretation has been questioned by DiFrancesco (120), who highlighted that Cs^+ block would be partially relieved at positive voltages. According to DiFrancesco (120), unblocked f-channels would still be able to drive the diastolic depolarization at rest and to mediate control of pacemaking by autonomic agonists (420). In conclusion, the action of Cs^+ on pacemaker activity demonstrates that I_f participates to the generation of pacemaker activity. However, no definitive quantitative insights about the importance of f-channels can be obtained by using this ion.

The negative chronotropic action of organic f-channel blockers such UL-FS 49 (480, 488), ZD-7228 (53, 318), and ivabradine (480) provides further evidence on the relevance of I_f in the control of the diastolic depolarization rate. These inhibitors of native cardiac I_f are all open- and use-dependent f-channel blockers (see Ref. 21 for review). The mechanism of channel block is essentially similar for all these drugs. Indeed, the drug binds to the channel from the intracellular side and probably stays in its binding site when the channel shuts off during deactivation. When the channel opens during the following pacemaker cycle, current flow in the inward direction will promote channel unblock (66, 162, 489, 490).

The most specific organic blocker of I_f is ivabradine (21). When tested at concentrations that are selective for I_f, ivabradine slows pacemaker activity by specifically reducing the slope of the linear part of the diastolic depolarization (68, 479) (Fig. 11*A*). This drug blocks the native rabbit SAN I_f with an EC_{50} of ~2–3 μM (48). At these concentrations, ivabradine slows automaticity in isolated rabbit pacemaker cells by ~20% (479). Consistently, ivabradine reduces the heart rate in vivo in conscious dogs (461) and mice (132, 280) (Fig. 11*B*). The observation that ivabradine leads to heart rate slowing, but does not block pacemaking, suggests that pharmacological inhibition of f-channels in these conditions can regulate pacemaking without impairing automaticity per se. However, the relative fraction of I_f blocked during pacemaker activity in these experiments is difficult to estimate since, as previously discussed, the blocking action of ivabradine on f-channels is both use and current dependent (66). Consequently, current block will be more pronounced at positive potentials such as during action potential repolarization and late diastolic depolarization. The fraction of I_f blocked for a given concentration of ivabradine measured at potentials negative to the maximum diastolic potential is thus likely to represent an underestimation of the real current block during pacemaker activity. On the other hand, slowing of pacing rate induced by ivabradine will favor unblock of the channel. Reduction of heart rate by ivabradine at a given rate is thus the equilibrium between f-channel block and unblock aided by the reduced firing rate. Further investigation is needed to clarify the exact quantitative relationship between I_f block by heart rate reducing agents (as ivabradine) and the slowing of pacemaker activity. The heterogeneous distribution of I_f will also influence the sensitiv-

Downloaded from physrev.physiology.org on October 4, 2011

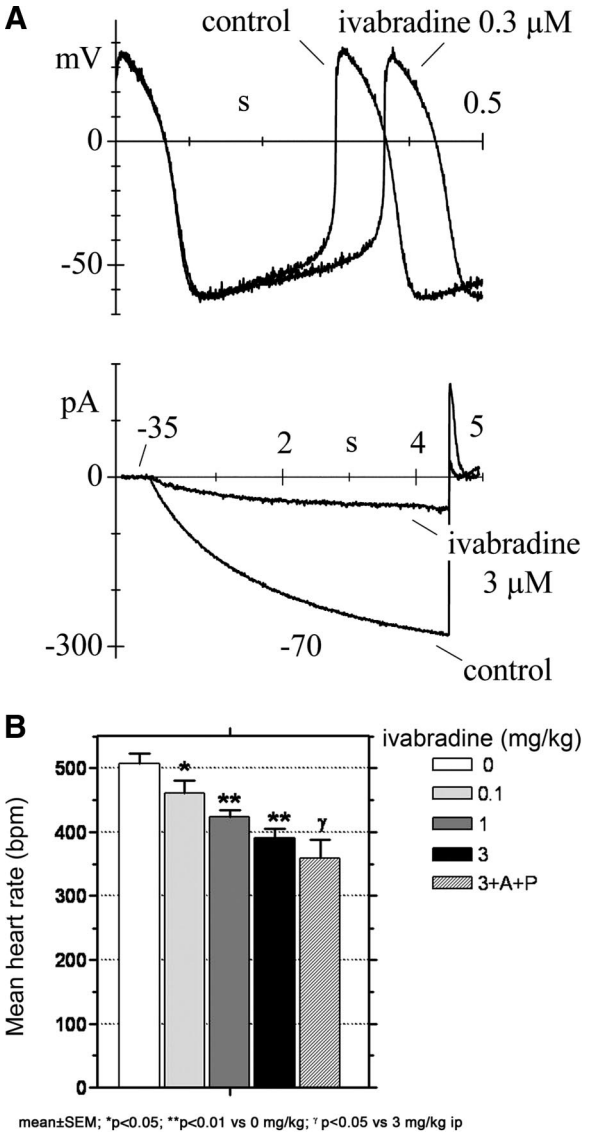

FIG. 11. *A*: pharmacological inhibition of I_f by 0.3 μM ivabradine slows pacemaker activity of a rabbit SAN pacemaker cell (*top panel*). Note that I_f inhibition reduces the cell pacing rate by selectively reducing the slope of the linear part of the diastolic depolarization, without affecting any other action potential parameter. Ivabradine block of I_f current is shown in the *bottom panel*. [From DiFrancesco (121).] *B*: in vivo heart rate reduction in mice treated by an intraperitoneal bolus of increasing doses of ivabradine. (A+P) indicate coinjection with ivabradine of atropine and propranolol to inhibit pharmacologically, the autonomic input (see sect. VII*A*). [Original data from Marger et al. (316).]

ity of pacemaker activity to different f-channel blockers in the center versus the periphery of the SAN. Indeed, the fractional slowing of pacemaker activity by Cs^+, UL-FS 49, and ZD-7228 is larger in the SAN periphery than in the center (355).

In addition to electrophysiological and pharmacological data, there is now substantial genetic evidence of the relevance of f-channels in the generation of automaticity. In animal models, insights are coming from a spontaneous zebrafish mutant (18) as well as from genetically modified mice lacking HCN2 and HCN4 channels in the heart (196, 294, 466). The first genetic evidence associating f-channels with the generation of cardiac pacemaking came from a large-scale random mutagenesis study aimed to identify new genes involved in zebrafish cardiovascular development (Fig. 12A). The mutant line *slow mo* is associated with a reduced heart rate in embryos (18) and adult (513) zebrafish. Isolated heart cells from *slow mo* embryos have no fast-activating I_f component and show strongly reduced I_f density (18) (Fig. 12*A*). Similarly, adult *slow mo* fishes have reduced heart rate and low I_f expression in the atrium and ventricle (513). The association between low I_f expression and bradycardia in *slow mo* mutants constitute strong evidence of the importance of f-channels for automaticity in zebrafish.

Inactivation of HCN2 channels in the mouse heart induces SAN dysrhythmia and a 30% reduction of I_f in isolated SAN cells (294) (Fig. 12*B*). HCN2 gene inactivation slows the kinetics of I_f activation, suggesting that HCN2 channels may contribute to the fast kinetic component of I_f. Interestingly, maximal I_f current stimulation by cAMP is not changed in SAN cells from HCN2 knockout mice (294) (Fig. 12*B*). HCN2 knockout mice do not show reduction of the mean heart rate (294). However, SAN dysrhythmia of HCN2 knockout mice indicates that these channels play a role in stabilizing the heart rate. Global or heart-specific inactivation of HCN4 channels provokes lethality in mouse embryos. Embryos lacking HCN4 channels die between day 9 and 12 post coitum (466). Younger embryos lacking HCN4 channels have slow heart rate and show almost complete suppression of I_f. Furthermore, cAMP regulation of heart rate is abolished in developing hearts (466). Stieber et al. (466) have also reported an absence of pacemaker cells having "mature" action potential characteristics in HCN4-deficient embryonic hearts. Indeed, only cells characterized by early "embryonic" pacemaker activity (308) are found in HCN4-deficient hearts. To overcome the problem of embryonic lethality in mice lacking HCN4 channels, Hermann et al. (196) have developed a temporally inducible deletion of *Hcn4* ($HCN4^C$ mouse). SAN cells from $HCN4^C$ mice show a 75% reduction of I_f with a depressed response to isoproterenol. Most $HCN4^C$ cells are quiescent, but normal automaticity can be restored to normal pacing rates by superfusion of saturating doses of isoproterenol (196). In vivo, $HCN4^C$ mice are characterized by the presence of SAN pauses, yet the maximal heart rate measured under exercise, or after administration of isoproterenol, does not differ from that of wild-type counterparts (196). Hermann et al. (196) reported that the frequency of SAN pauses is significantly increased during transitions for elevated to low heart rates. These authors have thus proposed that HCN4 channels are not required for acceleration of heart rate, but rather constitute a backup mechanism that is

Downloaded from physrev.physiology.org on October 4, 2011

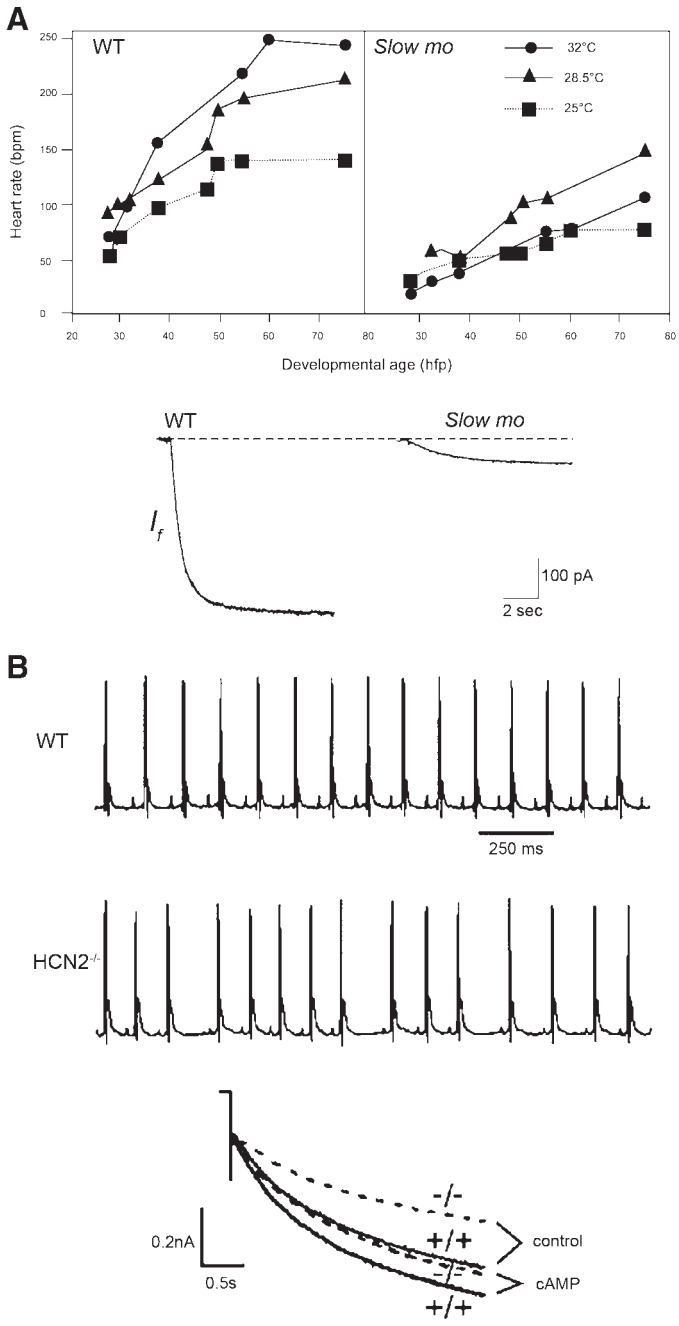

FIG. 12. *A*: *Slow mo* zebrafish mutant embryos have reduced heart rate and lack the fast kinetic component of I_f. Heart rate slowing is consistently found throughout the embryo development and is independent from the water temperature (*top panel*). I_f current density is strongly downregulated in cardiac myocytes isolated from *slow mo* embryos. Residual I_f in *Slow mo* hearts displays slower activation kinetics than in wild-type (WT) counterparts (*bottom panel*). [From Baker et al. (18), copyright National Academy of Science, USA.] *B*: telemetric electrocardiograms in freely-moving HCN2 knockout ($HCN2^{-/-}$) mice show SAN arrhythmia. Note that the basal heart rate is similar in WT and $HCN2^{-/-}$ mice, but the interbeat interval is more variable in knockout animals. The density of I_f is reduced by ~30% in $HCN2^{-/-}$ SAN cells, but current responsiveness to cAMP is unaltered. [From Ludwig et al. (294), with permission from Macmillan Publisher Ltd.]

important for stimulating and stabilizing pacemaker initiation in conditions of lowered heart rate.

In summary, results obtained in mice lacking HCN2 and HCN4 channels suggest a predominant role of HCN4 channels in mediating the adrenergic stimulation of I_f. However, results obtained from $HCN4^C$ mice (196) indicate that HCN4 channels are not the only mechanism involved in the β-adrenergic regulation of heart rate, at least in the adult mouse.

E. Role of $I_{Ca,L}$ in Automaticity

L-type Ca^{2+}channels are important contributors to the upstroke phase of the pacemaker action potential and play a role in the generation of the SAN diastolic depolarization (for a recent review, see Ref. 310). Block of $I_{Ca,L}$ by nifedipine stops pacemaker activity in primary central pacemaker cells (250). However, application of nifedipine to SAN tissue strips from the periphery of the node slows pacemaking but does not block automaticity. These observations have been accounted for by the presence in the SAN periphery of I_{Na} driving the action potential upstroke under $I_{Ca,L}$ blockade (250). The differential effect of $I_{Ca,L}$ inhibition in the center and in the periphery of the rabbit SAN underlines the problem of separating the possible contribution of $I_{Ca,L}$ to the diastolic depolarization from that of the upstroke phase of the action potential. This problem is particularly difficult to solve, since pharmacological block of $I_{Ca,L}$ during the action potential upstroke can have "knock on" effects on the recruitment of ionic currents during repolarization as well as the following diastolic depolarization. Furthermore, $I_{Ca,L}$ is regulated by PKA and CaMKII (390, 509). Consequently, the contribution of $I_{Ca,L}$ to automaticity can be influenced by the phosphorylation state of the channel. CaMKII activity is required for pacemaking, since CaMKII inhibitors terminate automaticity in isolated cells (509). The necessity of CaMKII in automaticity can be explained, in part, by the regulation of $I_{Ca,L}$ activation and reactivation kinetics by CaMKII (509). However, CaMKII can also have other unknown targets in pacemaker cells. Thus sensitivity of pacemaking to inhibition of CaMKII should not be taken as evidence of the importance of $I_{Ca,L}$ in the genesis of automaticity per se.

There is now substantial genetic and pharmacological data supporting the view that $I_{Ca,L}$ contributes to both the action potential upstroke and diastolic depolarization. Indeed, $Ca_v1.2$ channels seem to be involved in the action potential upstroke phase, while $Ca_v1.3$ channels substantially contribute to the diastolic depolarization (309, 310).

Verheijck et al. (497) have been the first to propose that the $I_{Ca,L}$ activation threshold is more negative in SAN than in the ventricle (497). These authors recorded the

Downloaded from physrev.physiology.org on October 4, 2011

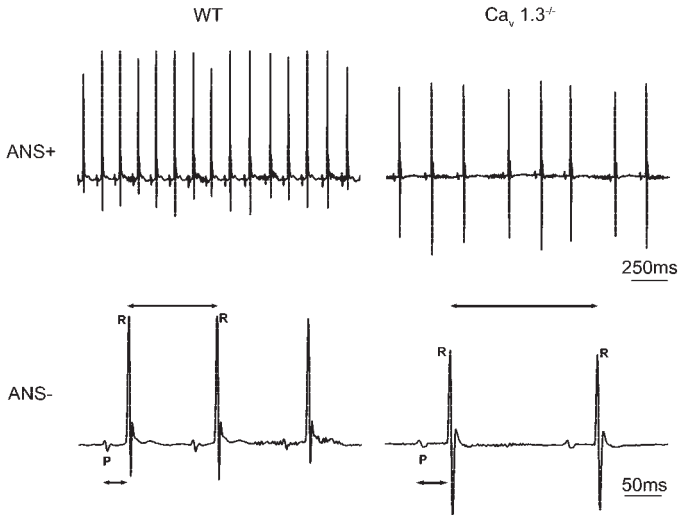

FIG. 13. Electrocardiograms of freely moving $Ca_v1.3^{-/-}$ mice show bradycardia and slowing of atrioventricular conduction. Note that in $Ca_v1.3^{-/-}$ mice, the interbeat interval is irregular and significantly longer than in WT mice (SAN arrhythmia, *top panel*). Association of bradycardia and arrhythmia is typical of resting $Ca_v1.3^{-/-}$ mice with unaltered autonomic regulation of heart rate (ANS+). When the input of the autonomic nervous system is blocked postsynaptically by combined administration of atropine and propranolol (ANS−), arrhythmia is in part compensated, but bradycardia and prolongation of the PR interval are still evident. (Mangoni and Nargeot, unpublished recordings.)

DHP-sensitive current during the diastolic depolarization and showed that $I_{Ca,L}$ is activated as early as in the linear part of the pacemaker potential. $I_{Ca,L}$ current density then increases at the action potential threshold and becomes fully activated during the upstroke. This work demonstrated that the kinetics of SAN $I_{Ca,L}$ do not behave as its ventricular counterpart but is activated at more negative voltages to support the pacemaker potential.

Involvement of L-type channels in pacemaking in vivo is also strongly suggested by in vivo ECG recordings showing that DHPs induce bradycardia in anesthetized mice (268). The unexpected observation that mice lacking L-type $Ca_v1.3$ channels had pronounced bradycardia and SAN arrhythmia was the first genetic indication of the importance of these channels in pacemaker activity (393). In these mice, bradycardia persists after pharmacological block of the autonomic nervous system, and intact atria from $Ca_v1.3^{-/-}$ mice have slower pacing rate than wild-type counterparts (393) (Fig. 13). Two studies have demonstrated that $Ca_v1.3$ channels play a major role in automaticity of isolated SAN (546) (Fig. 14*A*) and in pacemaker cells (309) (Fig. 14*B*). Indeed, pacemaker cells from $Ca_v1.3$ knock-out mice have erratic and intermittent pacemaking, leading to an overall lower degree of automaticity than that of wild-type cells (309) (Fig. 14*B*). These studies have also shown that $Ca_v1.3$ channels generate $I_{Ca,L}$ with different properties than that of $Ca_v1.2$-mediated $I_{Ca,L}$. Indeed, native $Ca_v1.3$ channels activate at negative potentials from about −50 mV (see Fig. 15*A*). Inactivation of $Ca_v1.3$ channels shifted the activation of $I_{Ca,L}$ to more positive potentials, thereby abolishing $I_{Ca,L}$ in the voltage range corresponding to

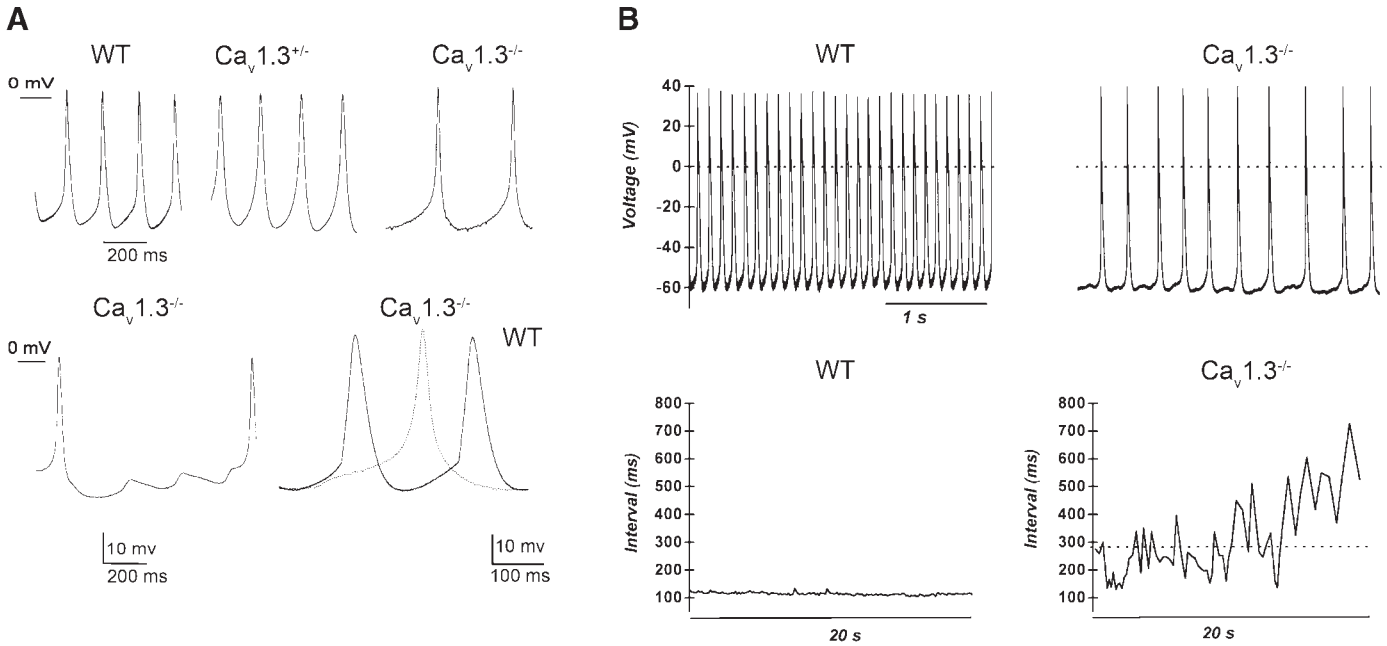

FIG. 14. *A*: intracellular microelectrode recordings of automaticity in isolated SANs from WT, $Ca_v1.3^{+/-}$, and $Ca_v1.3^{-/-}$ mice. Note slowing of automaticity and pauses in a SAN from $Ca_v1.3^{-/-}$ mouse. [Data from Zhang et al. (546).] *B*: isolated SAN pacemaker cells from $Ca_v1.3^{-/-}$ mice have slower pacemaker activity than WT cells (*top panel*). Slow pacemaking in cells lacking $Ca_v1.3$ channels is associated with irregular interbeat interval (bottom panel). [Data from Mangoni et al. (309).]

Downloaded from physrev.physiology.org on October 4, 2011

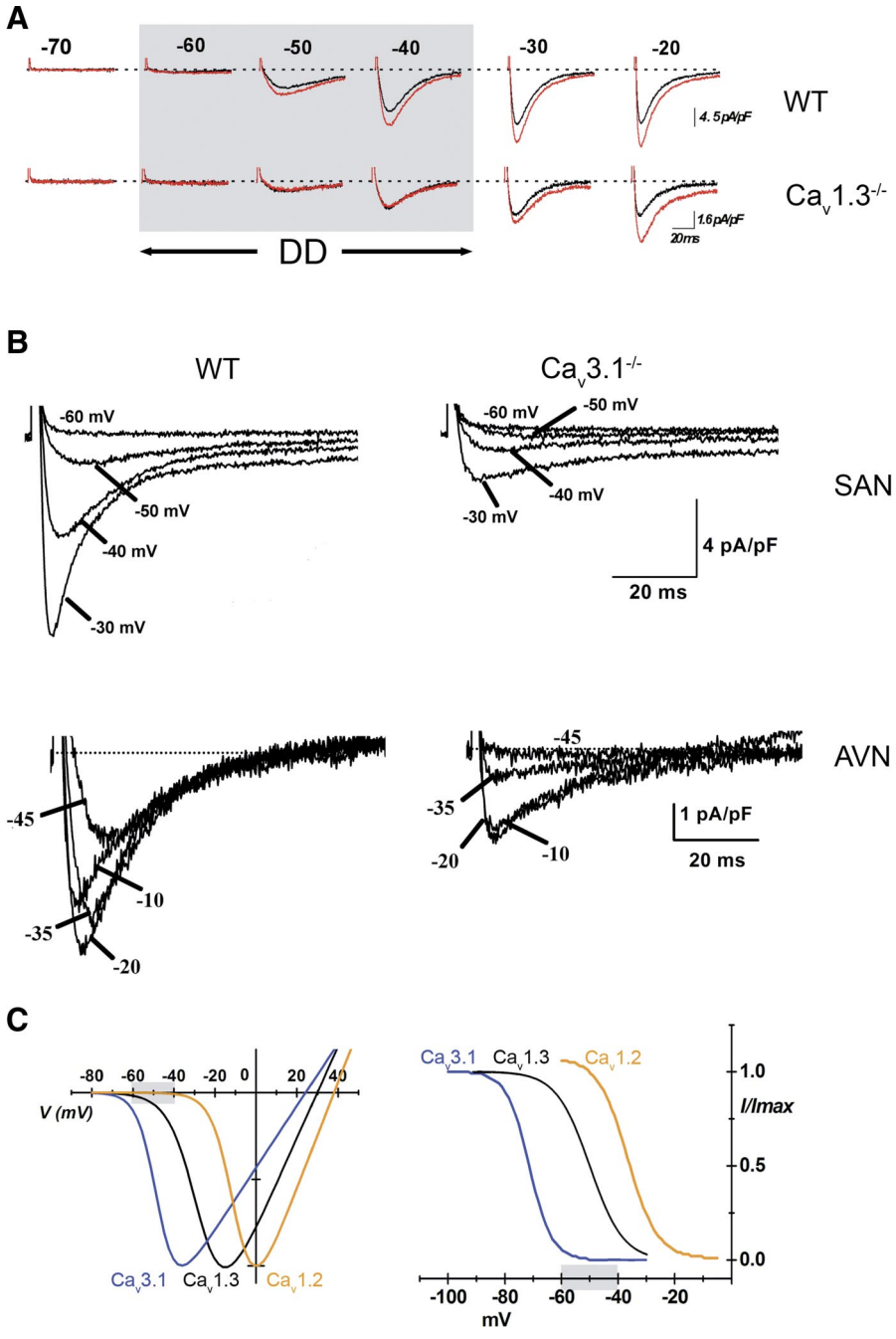

FIG. 15. *A*: voltage-dependent Ca^{2+} currents in pacemaker SAN cells from WT and $Ca_v1.3^{-/-}$ mice. Currents are evoked from a holding potential of −80 mV at the indicated test potentials. Current stimulation by BAK K 8644 is used to detect activation of $I_{Ca,L}$ at a given test voltage. In $Ca_v1.3^{-/-}$ SAN cells, BAY K 8644 has no effect at test potentials negative to −30 mV. This observation indicates that inactivation of $Ca_v1.3$ channels abolishes a $I_{Ca,L}$ component which has intermediate activation threshold between $I_{Ca,T}$, and the "classical" $I_{Ca,L}$. $Ca_v1.3$-mediated $I_{Ca,L}$ is activated in the diastolic depolarization range (DD, shaded gray box). [Data from Mangoni et al. (309).] *B*: inactivation of $Ca_v3.1$ channels suppresses $I_{Ca,T}$ in spontaneously active SAN and AVN cells isolated from $Ca_v3.1^{-/-}$ mice. Note reduction of the total Ca^{2+} current density and the slowing of the total I_{Ca} inactivation. The residual Ca^{2+} current is attributed to $Ca_v1.3$- and $Ca_v1.2$-mediated $I_{Ca,L}$. [Data from Mangoni et al. (314).] *C*: current-to-voltage relationships (*left*) and steady-state inactivation (*right*) of native SAN $Ca_v3.1$, $Ca_v1.3$, and $Ca_v1.2$ channels. [Adapted from Mangoni et al. (310).]

that of the diastolic depolarization. Inactivation of $Ca_v1.3$ channels reduces $I_{Ca,L}$ density by ~70% in pacemaker cells. Residual $I_{Ca,L}$ is attributable to $Ca_v1.2$-mediated $I_{Ca,L}$. Consistent with this hypothesis, $I_{Ca,L}$ in pacemaker cells from $Ca_v1.3$ knockout mice is more sensitive to DHPs (309) and has faster inactivation kinetics (546). Activation of β-adrenergic receptors by norepinephrine shifts negatively the threshold for activation of $Ca_v1.3$-mediated $I_{Ca,L}$, to about −55 mV (309). Interestingly, this threshold is comparable to that observed for the nifedipine-sensitive $I_{Ca,L}$ measured in spontaneously beating rabbit SAN cells (497). This suggests the existence of $Ca_v1.3$ channels also in rabbit SAN cells. The maximal pacing rate in $Ca_v1.3$ knockout hearts in the presence of isoproterenol is slightly slower than that of wild-type hearts (322). This observation can be explained by taking into consideration that stimulation of $I_{Ca,L}$ by saturating concentrations of norepinephrine cannot compensate for the lack of $I_{Ca,L}$ in the diastolic depolarization range (309).

In conclusion, insights gained from mice lacking $Ca_v1.3$ channels are indicative of a distinction in the func-

Downloaded from physrev.physiology.org on October 4, 2011

tional role of $Ca_v1.3$ channels contributing to automaticity and $Ca_v1.2$ channels triggering myocardial contraction. Indeed, suppression of $Ca_v1.3$-mediated $I_{Ca,L}$ impacts on cardiac automaticity and conduction, but has no effect on myocardial contractile performance (322). The differential roles of $Ca_v1.3$ and $Ca_v1.2$ channels in the heartbeat has also been shown pharmacologically by employing a knock-in mouse strain in which $Ca_v1.2$ channels are insensitive to DHPs ($Ca_v1.2DHP^{-/-}$ mouse) (462). The in vivo bradycardic effect induced by DHPs is not changed in $Ca_v1.2DHP^{-/-}$ mice, indicating that the dominant L-type VDCC isoform participating to automaticity is in fact $Ca_v1.3$ (462).

As stated above, $Ca_v1.3$ knockout mice also display a slowing of atrioventricular conduction (see Fig. 13) (322, 393, 546). Particularly, $Ca_v1.3$ knockout mice show I and II degree atrioventricular blocks, an observation which has been found in freely moving (393) and anesthetized mice (546), as well as in isolated $Ca_v1.3$ knockout hearts (322). It will be interesting to test the hypothesis that $Ca_v1.3$ channels are also involved in automaticity of the AVN.

Inactivation of the $Ca_v1.2$ α1-subunit induces lethality of the late mouse embryo. Heart development in early $Ca_v1.2$ knockout embryos is paralleled by overexpression of the $Ca_v1.3$ α1-subunit (529), as well as by upregulation of a distinct L-type Ca^{2+} current that is also present in $Ca_v1.3$ knockout embryonic hearts (445). Overexpression of $Ca_v1.3$ channels can be a compensatory mechanism for the loss of $Ca_v1.2$ channels, even if $Ca_v1.3$ channels cannot ensure viability of the late embryo. Embryonic hearts from a spontaneous zebrafish mutant strain lacking the $Ca_v1.2$ α1 subunit (*Isl* mutant) show depressed and erratic atrial beating (425). Consistent with the role of $Ca_v1.2$ in mediating cardiac contraction, hearts from *Isl* mutants have no ventricular contraction. It is not known whether $Ca_v1.2$ channels can contribute to automaticity in embryonic fish atria. Jones et al. (222) reported progressive loss of $Ca_v1.2$ protein in SAN tissue from aging guinea pigs, concomitantly with a reduction in automaticity and an augmentation of SAN rate sensitivity to DHPs. These data are suggestive of a participation of $Ca_v1.2$ channels in pacemaking, at least during the aging process.

F. Role of $I_{Ca,T}$ in Automaticity

$I_{Ca,T}$ is expressed in the SAN (145, 172), AVN (140), and Purkinje fibers (199, 484). T-channels can be found in the automatic mouse and zebrafish embryonic myocardium (18, 104). $I_{Ca,T}$ has also been described in the amphibian sinus venosus (49).

The role of $I_{Ca,T}$ in cardiac automaticity has long been uncertain. Native $I_{Ca,T}$ has low steady-state availability at diastolic membrane voltages typical of leading SAN pacemaker cells. However, it has long been known that $I_{Ca,T}$ inhibitors such as Ni^{2+} and tetrametrine slow pacemaker activity of SAN cells (172, 439).

The role of T-channels in automaticity has been recently investigated by targeted inactivation of the $Ca_v3.2$ (84) and $Ca_v3.1$ (314) α-subunit isoforms. Mice lacking $Ca_v3.2$ channels have no ECG alterations (84), indicating that the lack of this isoforms either has no impact on the generation and conduction of the cardiac impulse, or that a compensatory mechanism is established during heart development. It is not still possible to discriminate between these hypotheses, because SAN ionic currents and automaticity have not yet been studied in $Ca_v3.2^{-/-}$ mice. A striking finding coming from $Ca_v3.1^{-/-}$ mice is that $I_{Ca,T}$ cannot be detected in SAN and AVN cells (Fig. 15*B*). Indeed, as both $Ca_v3.1$ and $Ca_v3.2$ mRNA are expressed in mouse SAN, one would expect to find residual $I_{Ca,T}$ in $Ca_v3.1^{-/-}$ pacemaker cells. The absence of $Ca_v3.2$-mediated $I_{Ca,T}$ in $Ca_v3.1^{-/-}$ SAN cells has not yet been explained, but recent studies have reported that only $Ca_v3.1$-mediated $I_{Ca,T}$ is recorded in rat atria after birth (146, 358). These findings are suggestive of a developmental switch between $Ca_v3.2$ and $Ca_v3.1$ channels in the heart. According to this hypothesis, $Ca_v3.2$ channels are functionally expressed in the developing myocardium, while $Ca_v3.1$ channels are predominant in the adult heart. It would be important to investigate the differential role of $Ca_v3.1$ and $Ca_v3.2$ channels to automaticity during the cardiac development. Inactivation of $Ca_v3.1$ channels induces moderate bradycardia and slowing of atrioventricular conduction in $Ca_v3.1^{-/-}$ mice (314) (Fig. 16). Moderate bradycardia is observed in $Ca_v3.1^{-/-}$ mice even after pharmacological block of the autonomic nervous system, indicating slowing of SAN automaticity (Fig. 16*C*). Accordingly, spontaneous activity in isolated SAN pacemaker cells is slowed by ~30% (Fig. 16*D*).

Despite pharmacological and genetic data showing the involvement of $I_{Ca,T}$ in pacemaking, we presently lack a precise description of how T-channel activity contributes to the diastolic depolarization. The existence of a $I_{Ca,T}$-mediated "window" current component in the diastolic depolarization range has been proposed for rabbit SAN cells (401). However, this is not a consistent finding between different authors (see, for example, Ref. 172). The relatively negative threshold for activation of $Ca_v1.3$-mediated $I_{Ca,L}$ can possibly interfere with measurement of $I_{Ca,T}$, leading to the false impression of residually available $I_{Ca,T}$ at about −50 mV (M. Mangoni, unpublished observations; see also Fig. 15, *A* and *C*). As the absolute density of $I_{Ca,T}$ available at pacemaker potentials is low, one may wonder whether contribution of T-channels to pacemaking can be due to coupling with intracellular Ca^{2+} signaling. Such a mechanism has been proposed by Huser et al. (211) in cat latent atrial pacemaker cells.

Downloaded from physrev.physiology.org on October 4, 2011

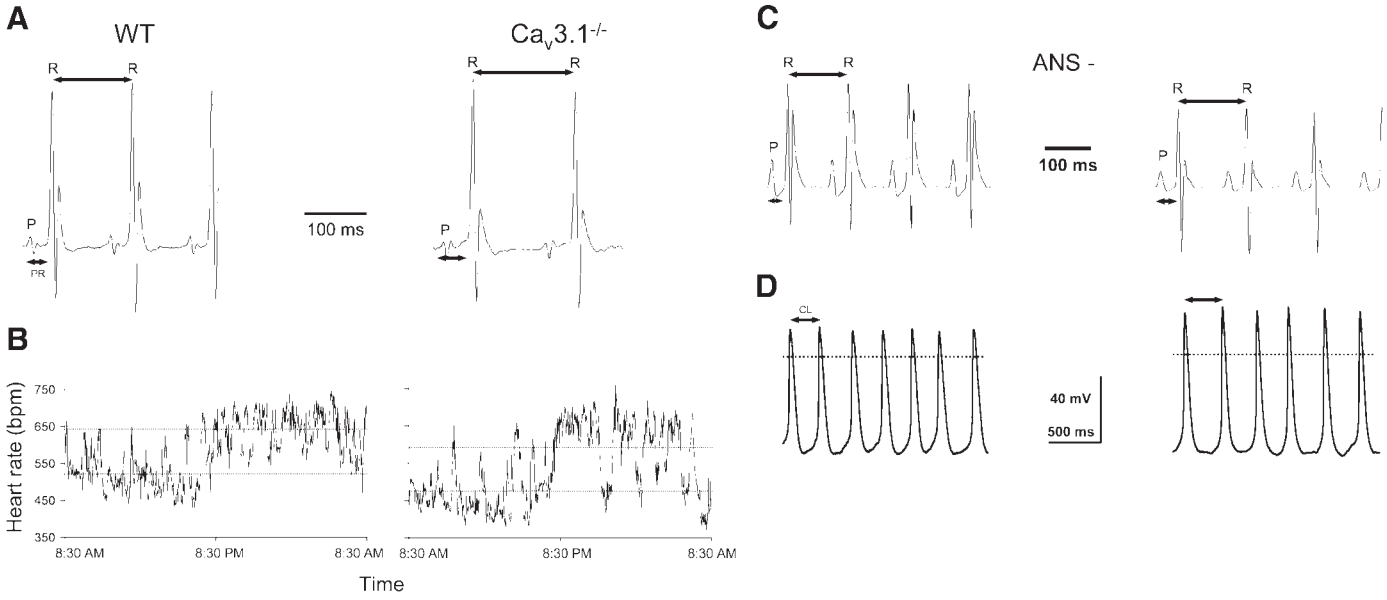

FIG. 16. $Ca_v3.1^{-/-}$ mice have moderate heart rate reduction and prolongation of the PR interval. *A*: telemetric electrocardiograms of WT and $Ca_v3.1^{-/-}$ mice. *B*: circadian variability of heart rate in WT and $Ca_v3.1^{-/-}$ mice. Continuous recordings lasting 24 h provide evidence that the mean heart rate is lowered in $Ca_v3.1^{-/-}$ mice (dotted lines). *C*: $Ca_v3.1^{-/-}$ mice have intrinsically slower heart rate than WT mice. *D*: pacemaker activity of isolated SAN cells is slower in $Ca_v3.1$ than in WT mice. [Data from Mangoni et al. (314).]

These authors have recorded intracellular Ca^{2+} release during pacemaking and found that 40 μM Ni^{2+} reduced Ca^{2+} release from the sarcoplasmic reticulum (SR) and the slope of the late phase of the diastolic depolarization. Ni^{2+} did not affect Ca^{2+} release during the action potential upstroke (systolic Ca^{2+}), but only Ca^{2+} released during the diastolic depolarization phase (diastolic Ca^{2+}). In latent pacemaker cells, $I_{Ca,T}$ activation during diastolic depolarization triggers local Ca^{2+} release, generating an inward current through stimulation of I_{NCX} (211). According to Lipsius et al. (288), there exists a local control of Ca^{2+} release involving T-type channels, RyRs of the SR, and NCX (288). Such a functional coupling between T-type channels and SR could explain earlier observations indicating that prevention of SR Ca^{2+} release with ryanodine reduces $I_{Ca,T}$ (285). No direct evidence for $I_{Ca,T}$-induced SR Ca^{2+} release in primary SAN pacemaker cells has yet been reported. Vinogradova et al. (506) have reported that 50 μM Ni^{2+} failed to inhibit subsarcolemmal diastolic Ca^{2+} release in spontaneously beating rabbit SAN cells, as well as spontaneous Ca^{2+} release in arrested pacemaker cells (510). However, these data do not exclude the possibility that $Ca_v3.1$-mediated T-channels can contribute to SR Ca^{2+} release since native SAN $Ca_v3.1$ channels are resistant to this concentration of Ni^{2+} (314). The more negative diastolic potential in latent pacemaker cells can favor T-channel opening during the diastolic depolarization. The role of $I_{Ca,T}$ in automaticity of the conduction system is still unknown. $Ca_v3.1^{-/-}$ mice have slowed atrioventricular conduction (314) (Fig. 16). Measurements of atrioventricular conduction times indicate that the AVN is the site where impulse propagation is slowed (314). It will be interesting to test if automaticity of AVN cells is affected by inactivation of $Ca_v3.1$ channels. $Ca_v3.1$ channels do not appear to be involved in conduction in mouse Purkinje fibers. Indeed, neither the intraventricular conduction time nor the QRS are changed in $Ca_v3.1^{-/-}$ mice (314).

G. Role of N- and R-type Channels in Heartbeat Regulation

Beside L- and T-type channels, an involvement of VDCCs belonging to the Ca_v2 gene family in the regulation of heart rhythm and rate has been recently proposed. Mouse lines lacking N-type $Ca_v2.2$ and R-type $Ca_v2.3$ channels have been developed (214, 293, 516). No expression of $Ca_v2.2$ channels in the heart has been reported. However, these channels contribute to the activity of sympathetic nerve terminals (214). $Ca_v2.2^{-/-}$ mice have increased heart rate and mean blood pressure (214). These effects are possibly due to reduced activity of the sympathetic nerve terminals (214). Parasympathetic input is not affected in these mice (214).

Expression of $Ca_v2.3$ isoforms in the mouse heart has been reported in atrial tissue by in situ hybridization (332), and in the heart at the protein level (293). Enhanced sympathetic tonus, ventricular arrhythmias, and dysfunction in ventricular conduction have been found in mice lacking $Ca_v2.3$ channels (293, 516). Disturbances of atrial activation and alterations of the QRS complex are ob-

Downloaded from physrev.physiology.org on October 4, 2011

served even after administration of atropine and propranolol (516). Overexpression of $Ca_v3.1$ mRNA has been reported in adult $Ca_v2.3^{-/-}$ hearts (516), but direct evidence supporting functional expression of $Ca_v2.3$ channels in the mouse SAN and conduction system is lacking.

H. Role of I_{Na} in Automaticity

Primary pacemaker cells are characterized by a relatively slow action potential upstroke. The concept that the action potential of pacemaker cells is mainly driven by Ca^{2+} rather than Na^+ channels is still valid, although new studies on the rabbit SAN have indicated that a distinction has to be made between small pacemaker cells from the SAN center and larger cells from the periphery of the node. Two different I_{Na} components have been functionally identified in SAN, a TTX-sensitive "neuronal" I_{Na} predominantly coded by the $Na_v1.1$ (24, 25, 279, 304) isoform, and a TTX-resistant I_{Na}, coded by the $Na_v1.5$ isoform (276, 279). TTX-sensitive I_{Na} contributes to pacemaking in newborn rabbits (24) (Fig. 17*A*) and in the adult mouse (279, 304). $Na_v1.5$-mediated TTX-resistant I_{Na} is involved in SAN intranodal conduction (276) (Fig. 17, *B* and *C*).

The contribution of TTX-sensitive I_{Na} to automaticity has been studied in neonatal rabbit SAN by Baruscotti et al. (24). In newborn SAN cells, application of 3 μM TTX slows pacemaker activity by 63%. Baruscotti et al. (24) have reported slowing by TTX of the late phase of the diastolic depolarization, reduction of the action potential threshold, and overshoot. These observations indicate that TTX-sensitive I_{Na} contributes to SAN pacemaking essentially by quickening the late diastolic depolarization phase and by shifting the action potential threshold negatively to that of VDCCs. The mechanism of contribution of TTX-sensitive I_{Na} to the diastolic depolarization in neonatal rabbit SAN cells has also been investigated by these authors in two distinct studies (23, 24). In the first study (24), they reported the presence of a significant I_{Na} "window" component that declines with increasing age of the animal. In a follow-up (23) study, these authors have shown that the amount of TTX-sensitive current recorded by applying ramp depolarizations mainly depends on the ramp slope. This observation suggests that incomplete inactivation of TTX-sensitive I_{Na} during the upstroke phase underlies persistent I_{Na} during the diastolic depolarization (23). The expression of the $Na_v1.1$ isoform is downregulated in the adult (Fig. 17*A*) (23). The physiological significance of the expression of $Na_v1.1$-mediated I_{Na} in newborn SAN has not been completely elucidated, but it is likely that TTX-sensitive I_{Na} constitutes a mech-

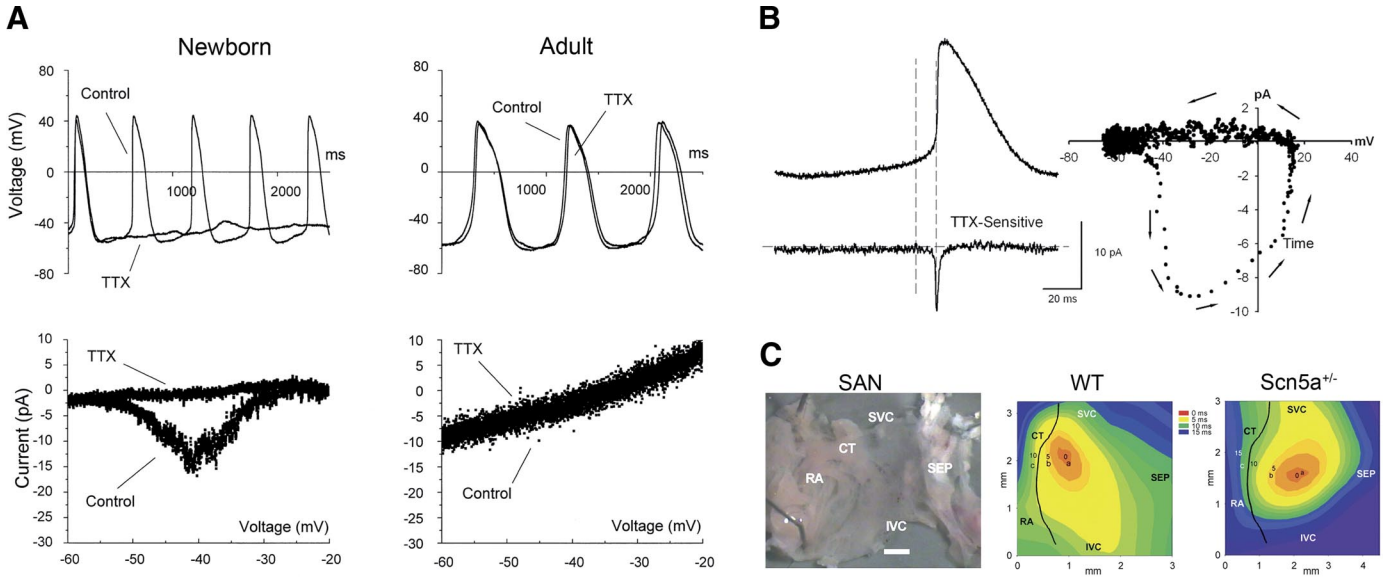

FIG. 17. *A*: differential effect of TTX on pacemaker activity in SAN pacemaker cells from newborn (*top*, *left*) and adult (*top*, *right*) rabbits. Inhibition of I_{Na} by TTX blocks pacemaking in newborn cells, while it has no effect on automaticity of adult cells. A voltage-clamp ramp protocol shows the presence of a TTX-sensitive current component in pacemaker cells from newborn rabbits (*bottom*, *left*). Such a component is not recorded in cells from adult rabbits, indicating a developmental regulation of the expression of TTX-sensitive I_{Na}. [From Baruscotti et al. (23).] *B*: a TTX-sensitive I_{Na} contributes to the exponential phase of the diastolic depolarization in the mouse SAN. The figure depicts an "action potential clamp experiment" in which a mouse SAN cell has been clamped with its own action potential (*top*, *left*) so that the net clamp current equals zero. The cell has then been exposed to TTX and the current necessary to maintain the membrane voltage recorded. This net TTX-sensitive I_{Na} is plotted versus the time (*bottom*, *left*) and versus the membrane voltage (*right*). From this experiment, it is apparent that TTX-sensitive I_{Na} activates in the exponential phase of the diastolic depolarization between −45 and −40 mV, quickly reaches its peak at −20 mV, and switches off at about +20 mV. [From Lei et al. (279).] *C*: electrical mapping of SAN intranodal conduction in WT and $Scn5a^{+/-}$ mice. The change in the SAN activation sequence in $Scn5a^{+/-}$ mice indicates that TTX-resistant Scn5a-mediated I_{Na} is important in impulse conduction within the SAN and from the SAN to the right atrium. [From Lei et al. (276), with permission from Wiley-Blackwell.]

Downloaded from physrev.physiology.org on October 4, 2011

anism for increasing the basal heart rate in newborn animals (24).

During the last years, it has become apparent that I_{Na} significantly contributes to mouse pacemaking. Pharmacological inhibition of I_{Na} by lidocaine reduces the heart rate of adult mice (268). The pacing rate of Laghendorff-perfused mouse hearts is slowed by low doses of TTX (50–100 nM) (304). Adult mouse pacemaker cells show constitutive expression of I_{Na} (86, 312). Both TTX-sensitive and -resistant I_{Na} have been functionally identified in mouse SAN cells (279). Similar to newborn rabbits, expression of $Na_v1.1$ α-subunit has been reported in SAN sections from adult mice (279, 304). These in vivo and in vitro experiments have demonstrated the involvement of TTX-sensitive, neuronal I_{Na} in mouse cardiac pacemaking. The action of TTX on cellular pacemaking has been directly investigated in spontaneously beating mouse SAN cells by Lei et al. (279). These authors have combined voltage-clamp recordings of I_{Na} with staining of SAN tissue with antibodies directed against Na_v subunits. TTX-sensitive and TTX-resistant I_{Na} have been recorded. TTX-sensitive I_{Na} is associated with expression of the $Na_v1.1$ α-subunit, while TTX-resistant I_{Na} is associated with $Na_v1.5$ expression. Block of TTX-sensitive I_{Na} by 50 nM TTX slows automaticity of intact SAN and isolated pacemaker cells (279). TTX-sensitive I_{Na} has been recorded in action potential clamp experiments and shown to be present during the late phase of the diastolic depolarization and upstroke (Fig. 17*B*) (279). $Na_v1.5$ channels underlie TTX-resistant I_{Na} (276, 279). The role of $Na_v1.5$ channels in SAN pacemaking has been described in heterozygous $Scn5a^{+/-}$ mice (276). $Scn5a^{+/-}$ mice display major age-dependent dysfunction in atrioventricular conduction and a moderate reduction of the mean heart rate (381). Intact atrial-SAN preparations from $Scn5a^{+/-}$ mice have shown normal pacemaking in the SAN center, but demonstrated slower intranodal SAN conduction and exit block (276) (Fig. 17*C*). Pacemaking in small leading SAN cells from $Scn5a^{+/-}$ mice is not different from that recorded in wild-type mice. In conclusion, available evidence indicates that $Na_v1.5$-mediated I_{Na} does not participate in the generation of automaticity per se (in the central SAN), but can influence heart rate by contributing to impulse propagation within the SAN and from the SAN to the atrium. (276).

I. Role of I_{st} in Automaticity

Limited knowledge exists on the role of I_{st} in the generation of cardiac automaticity. Indeed, we presently lack selective pharmacological agents targeting the I_{st} current. Genetic manipulation of st-channels is also impossible, since their molecular basis is still unknown. Consequently, it is difficult to directly investigate the significance of I_{st} in pacemaking. A significant contribution of I_{st} in controlling the rate of the diastolic depolarization has been proposed by Shinagawa et al. (457) on the basis of numerical simulations of pacemaking in the rat SAN. Modeling suggests the possibility that I_{st} contributes to pacemaking by virtue of its low threshold of activation and slow inactivation rate. These properties would allow I_{st} to be present throughout the pacemaker cycle (457). The potential contribution of I_{st} compared with that of other currents involved in pacemaking has also been investigated by Zhang et al. (544). This study suggests that I_{st} will affect pacemaking depending on its relative size compared with other currents contributing to pacemaking such as I_f or I_{Na}. Consequently, in rabbit central SAN pacemaker cells, a significant contribution of I_{st} to pacemaking is predicted. According to Zhang et al. (544), pacemaking at the periphery of the SAN would be less sensitive to I_{st}, because of the larger density of I_{Na} and I_f (544). Elucidation of the molecular nature of I_{st} is needed to gain new insights into the physiological role of this current.

L. SR Ca^{2+} Release and Automaticity

Two studies by Rubenstein and Lipsius (428) and Li et al. (285) supplied initial evidence that Ca^{2+} release and I_{NCX} were involved in the generation of pacemaker activity. Rubenstein and Lipsius (428) observed that ryanodine slowed automaticity in atrial subsidiary pacemaker cells by reducing the slope of the late diastolic depolarization (the exponential phase), while Cs^+ (presumably by blocking I_f) reduced the first fraction of the diastolic depolarization. They concluded that multiple mechanisms were involved in automaticity of subsidiary cells and that Ca^{2+} release from the SR was important in the generation of the late phase of the diastolic depolarization (428). Slowing of automaticity by ryanodine was also reported by Rigg and Terrar in guinea pig SAN preparations (417) and by Li et al. (285) in cultured rabbit SAN cells. The latter report also described a reduction of intracellular Ca^{2+} transients (417) and abolition of I_{NCX} by ryanodine and BAPTA-AM (285). These studies were indicative of a role of intracellular Ca^{2+} signaling in maintaining automaticity, yet they did not establish a link between a specific Ca^{2+} signal and pacemaking. Particularly, we can wonder if spontaneously active cells posses an intracellular Ca^{2+} signal coupled to the diastolic depolarization phase. Ju and Allen (226) have described distinct types of Ca^{2+} signals in toad sinus venosus cells: a cytosolic transient (predominantly driven by the action potential), a delayed Ca^{2+} signal linked to a change in nuclear Ca^{2+} content, and a third signal possibly due to subsarcolemmal local Ca^{2+}-induced Ca^{2+} release (LCICR).

Downloaded from physrev.physiology.org on October 4, 2011

During the last five years, the group led by E. Lakatta has extensively investigated the cellular mechanism generating LCICR and emphasized its relevance in determining the chronotropic state of rabbit SAN cells. Bogdanov et al. (44) have studied intracellular Ca^{2+} release in beating SAN cells and documented "preaction potential" Ca^{2+} signals due to LCICR. These signals precede the Ca^{2+} transient evoked by the action potential upstroke phase (Fig. 18, *A–C*). These signals are initiated at the cell edge and are due to Ca^{2+} release from the SR, since they are abolished by ryanodine (Fig. 18*D*). During spontaneous activity, preaction potential signals are generated by LCICR. LCICR stimulates I_{NCX} activity (44). Using ramp protocols mimicking the diastolic depolarization, Bogdanov et al. (44) have estimated LCICR-mediated I_{NCX} density to be ~1.7 pA/pF (Fig. 18*F*). The size of I_{NCX} would thus be sufficient to quicken the exponential fraction of the diastolic depolarization. LCICRs observed in rabbit SAN cells are similar to diastolic Ca^{2+} release described in cat latent pacemaker cells (211). Vinogradova et al. (510) have supplied evidence indicating that LCICRs in rabbit primary SAN can be generated in the absence of a change in the membrane voltage. Indeed, LCICRs can still be observed in quiescent permeabilized SAN cells. LCICR size depends on extracellular Ca^{2+} concentration. (Fig. 19, *A* and *B*). Furthermore, if spontaneously beating SAN cells are arrested by voltage clamping at the maximum diastolic potential or at a positive voltage (−10 mV), LCICRs do not disappear, but persist for some seconds in the absence of action potentials (Fig. 19*C*) (510). Under these conditions, LCICRs display stochastic "roughly periodical" (510) behavior and maintain similar periodicity as during spontaneous activity. These results support the view that LCICRs are not directly linked to the activity of membrane ion channels but reflect the existence of an independent intracellular "Ca^{2+} clock" mediated by spontaneous Ca^{2+} release from SR. LCICRs eventually disappear in arrested cells possibly after SR depletion. We can expect that during pacemaking, Ca^{2+} stores of the SR are cyclically refilled by opening of VDCCs (510) or by store-operated Ca^{2+} influx as described by Ju et al. (229).

Cellular mechanisms underlying this internal "Ca^{2+} clock" are not understood, but Vinogradova et al. (508) have recently shown that LCICRs are abolished by inhibition of PKA activity and stimulated by cAMP (Figs. 20 and 21). They also reported that basal PKA activity is almost 10 times higher in SAN cells than in atrial and ventricular myocytes and that high PKA activity seems to be a prerequisite for pacemaking. Indeed, PKA inhibitors can stop cellular automaticity (Fig. 20) (508).

In conclusion, SR-mediated LCICR is involved in the generation of the exponential fraction of the diastolic depolarization. The two key elements of this mechanism are pre-action potential RyR-mediated LCICR and NCX,

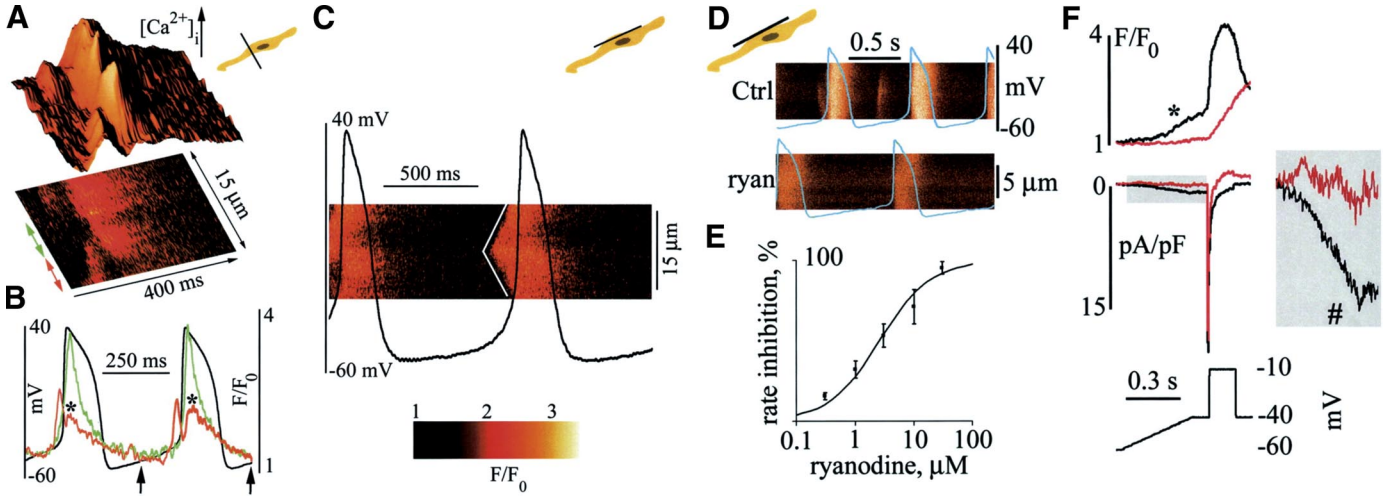

FIG. 18. Characteristics of LCICR in rabbit SAN pacemaker cells. *A*: line scan image of Ca^{2+} release (*bottom panel*) and corresponding normalized fluorescence (*top panel*) as a function of time and position within the scan line. The scan line lays perpendicularly to the cell long axis (inset cell drawing). Colored arrows indicate areas where fluorescence is averaged. *B*: pacemaker activity (black line) and normalized fluorescence at the cell edge (red line) and middle (green line). Arrows indicate the time interval corresponding to the 3-dimensional plot in *A*. Asterisks indicate a peak of Ca^{2+} release at the cell edge. This Ca^{2+} release occurs locally, during the exponential part of the diastolic depolarization. *C*: here, the line scan image is oriented parallel to long cell axis and visualizes the cell edge where LCICR is triggered. White lines indicate the propagation of the $[Ca^{2+}]_i$ wave. *D*: 3 μM ryanodine (ryan) slows pacemaker activity and abolishes preaction potential LCICR in rabbit SAN cells. *E*: dose-response curve of pacemaker activity inhibition by ryanodine. *F*: Ca^{2+} release (*top panel*) and total membrane current (*middle panel*) during voltage clamping of a SAN cell with a waveform simulating the SAN pacemaker cycle (*bottom panel*). In each panel, the black line indicates recording in control conditions, and the red line is plotted after application of 3 μM ryanodine. Ryanodine blocks diastolic LCICR and reduces the inward current recorded during the simulated diastolic depolarization (see enlarged *middle inset*). Asterisks indicate LCICR; the symbol (#) indicates the residual inward current in presence of ryanodine. [From Bogdanov et al. (44).]

Downloaded from physrev.physiology.org on October 4, 2011

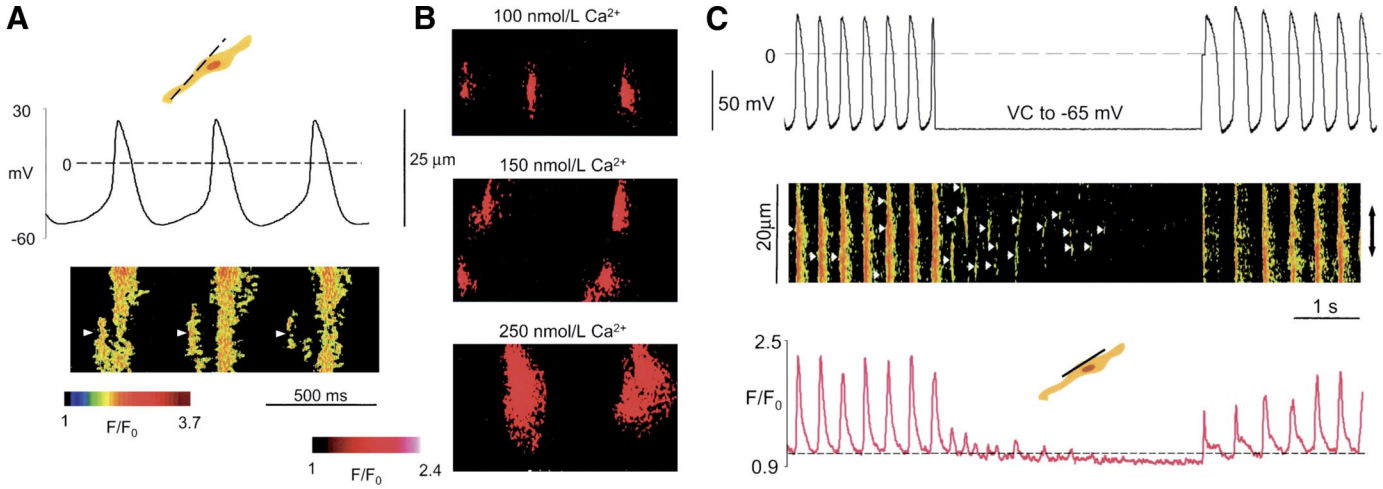

FIG. 19. LCICR in intact (*A*) and permeabilized (*B*) rabbit SAN pacemaker cells. *A*: simultaneous recordings of pacemaker activity and confocal line scan images of LCICR as in Fig. 18*C*. *B*: images of Ca^{2+} release in a quiescent permebilized SAN cell under different extracellular Ca^{2+} concentrations as indicated. LCICR is present even in quiescent SAN cells, and its amplitude is a function of extracellular Ca^{2+} concentration. *C*: voltage clamping to the cell maximum diastolic potential does not immediately block LCICR in SAN cells. Note LCICR events (wither arrows) in the absence of changes in membrane voltage. Membrane voltage oscillations, possibly due to I_{NCX} activated by LCICR, are recorded. These observations indicate LCICR are a spontaneous voltage-independent phenomenon. [From Vinogradova et al. (510).]

which converts subsarcolemmal Ca^{2+} release to an inward current contributing to diastolic depolarization. In a recent work, Lyashkov et al. (299) have reported colocalization of NCX and RyRs in rabbit SAN cells and proposed that the proximity between NCX and RyRs permits quick conversion of LCICR into oscillations of the membrane voltage.

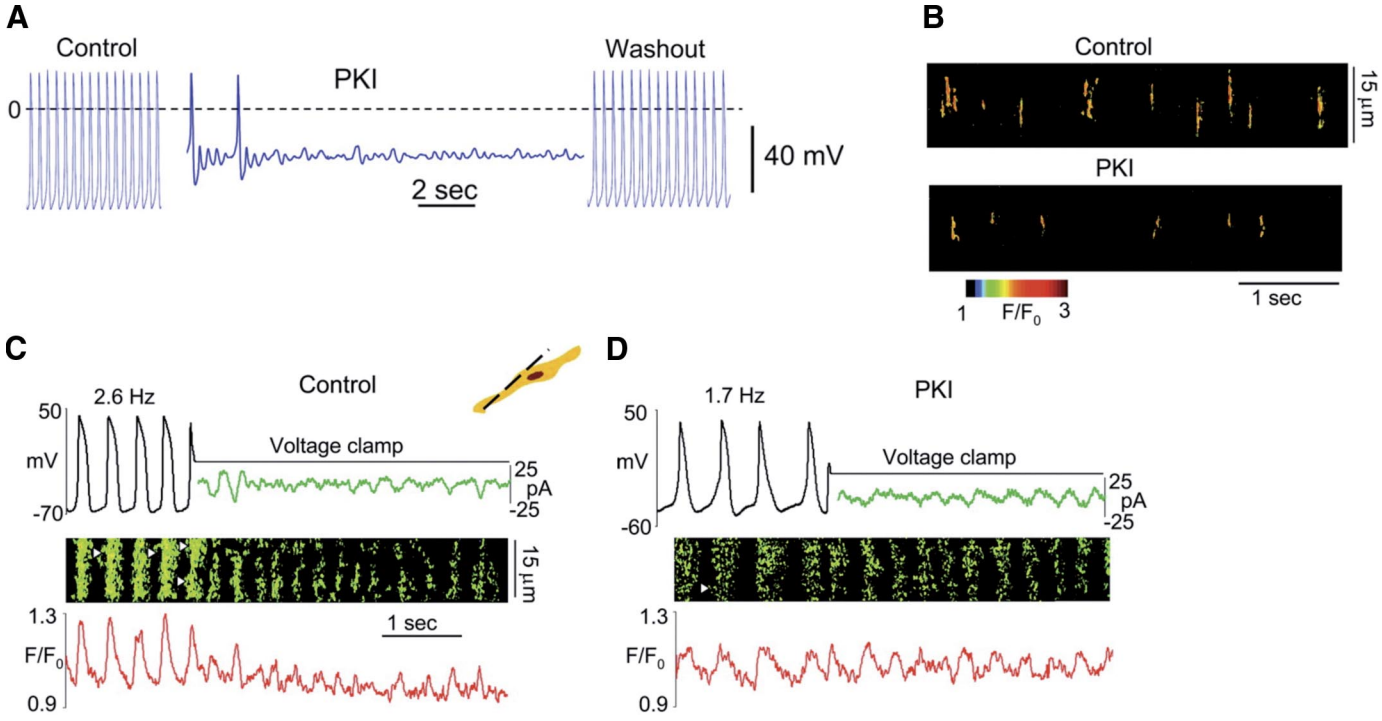

FIG. 20. Basal PKA-dependent phosphorylation is necessary for maintaining pacemaker activity in rabbit SAN pacemaker cells. *A*: superfusion with 15 μM of protein kinase inhibitor (PKI) reversibly suppresses pacemaking. *B*: a line scan image shows strong reduction of spontaneous LCICR by PKI in permebilized SAN cells. *C* and *D*: simultaneous recordings of pacemaker activity (*top panel*), line scan images (*middle panel*), and normalized Ca^{2+} release averaged over the line scan image (*bottom panel*). In *C*, control conditions are established by voltage clamping a spontaneously beating SAN cell to −30 mV to record spontaneous Ca^{2+} release. In *D*, note the reduction in both frequency and size of spontaneous Ca^{2+} release by PKI. [From Vinogradova et al. (510).]

Downloaded from physrev.physiology.org on October 4, 2011

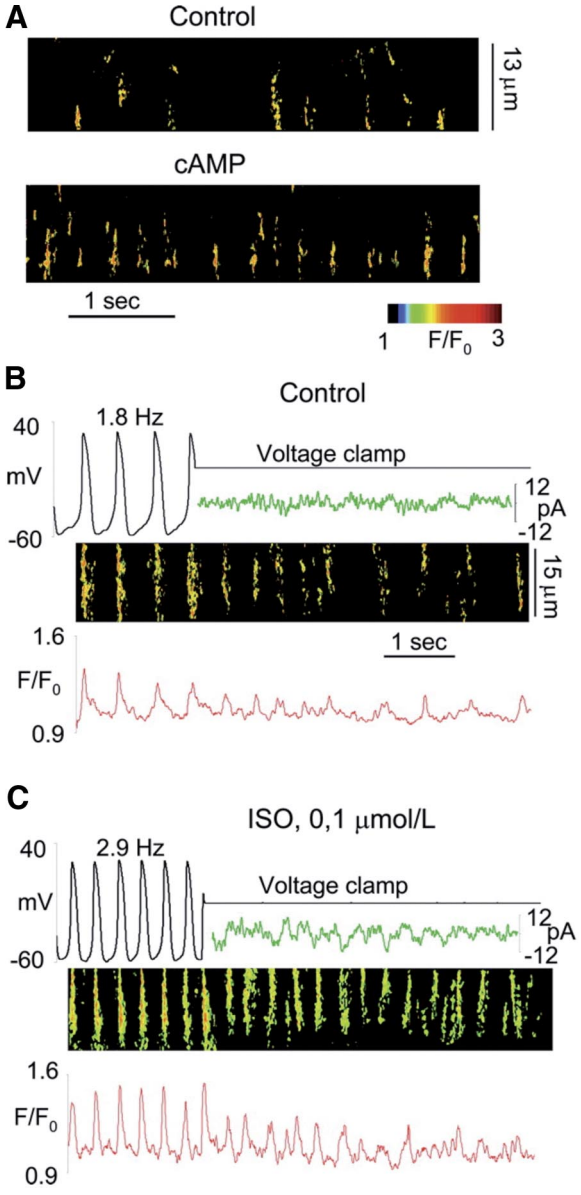

FIG. 21. Stimulation of the PKA-dependent signaling pathway by cAMP or 0.1 μM isoproterenol (ISO) stimulates intracellular Ca^{2+} release. *A*: this line scan image shows the increase in the frequency of Ca^{2+} release in a permebilized rabbit SAN cell superfused with 10 μM cAMP. *B*: recordings of pacemaker activity (*top panel*) line scan image (*middle panel*) and fluorescence (*bottom panel*, same protocol as in Fig. 20) in control conditions (*B*) and during superfusion with ISO (*C*). [From Vinogradova et al. (510).]

VII. AUTONOMIC REGULATION OF PACEMAKER ACTIVITY

A. Principles

In this section, we review the current knowledge on the cellular mechanisms underlying the autonomic regulation of cardiac automaticity.

The autonomic nervous system is the major extracardiac determinant of the heart rate. Sympathovagal control of cardiac automaticity is a complex phenomenon. Multiple interactions occur between sympathetic and parasympathetic centers in the central nervous system, and presynaptic peripheral interactions exist also (223, 284, 375). In the adult heart, the sympathetic branch of the autonomic nervous system accelerates heart rate, while the parasympathetic branch slows it. Exceptions to this general rule can be observed experimentally, but a detailed discussion of these mechanisms is beyond the scope of this review. The terminal part of the cardiac autonomic nervous system is constituted by the intrinsic cardiac neuronal plexus (ICNP), which plays a pivotal role in regulating the heart rate, conduction, and contractile force (15). Autonomic fiber projections to the heart rhythmogenic centers are abundant. The canine SAN is densely innervated by postganglionic fibers of the ICNP, which is formed by nerve fibers entering the epicardium and forming ~400 ganglia around the junction between the right atrium and the superior vena cava (384). Pauza et al. (384) have estimated that the canine SAN can be innervated by more than 54,000 intracardiac neurons residing in the INP. A similar organization of SAN innervation by the INP has been found in humans (385). The rat AVN and common bundle are innervated by a dense network of thin fibers projecting from a neuronal cluster adjacent to the interatrial septum and the right pulmonary sinus (26). The distribution of sympathetic and parasympathetic fibers in the SAN is heterogeneous (375) and can slightly vary between individuals (385), as well as on an age-dependent way (26, 385). Vagal and sympathetic activation induce a shift of the leading pacemaker site (54). Compared with the atrial myocardium, the SAN is enriched in adrenergic and muscarinic receptors (29). Similar to SAN ion channels, adrenergic and muscarinic receptor densities vary regionally and may contribute to pacemaker shift during autonomic stimulation (300, 375). SAN nerves contain between 5 and 15 axons and terminate as naked terminals with varicosities containing the neurotransmitter release site (419). Adrenergic and nonadrenergic release sites are in close vicinity to each other (375, 419). Choate et al. (88) reported that synaptic varicosities at cholinergic terminals in the guinea pig SAN are in close proximity with the membranes of SAN myocytes. According to Hirst et al. (200), cholinergic terminals form specialized "neuromuscular" junctions with SAN myocytes.

Autonomic control of pacemaker activity in vivo is based on concomitant input from sympathetic and parasympathetic limbs. However, the ratio between vagal and sympathetic input varies in a species-dependent way (375). The impact of sympathovagal balance on the heart rate can be appreciated by comparing basal rates in different mammalian species in the presence and in the absence of autonomic input. In mammals, basal heart rates are inversely correlated with the body weight. Smaller mammals such as mice and bats have fast heart

Downloaded from physrev.physiology.org on October 4, 2011

rate, ranging from ~500 beats/min in mice during daytime (157) to 800–1,000 beats/min in flying bats (269). In contrast, the heart rate in medium-sized and larger mammals can vary between 60 and 70 beats/min in humans and ~20 beats/min in whales (see Ref. 375 for review). Isolated hearts and SAN pacemaker cells also show a wide range of basal rates and maintain the same rate-to-animal weight ratio as in the presence of an autonomic input (375). The intrinsic properties of pacemaker cells in different species are one of the bases of the variability of heart rate in mammals. However, the species-dependent balance between sympathetic and parasympathetic input also contributes to this wide range of pacemaking frequencies (375). The two branches of the autonomic nervous system interact to generate an adaptable equilibrium so that SAN automaticity can be under dominance of the sympathetic or parasympathetic limb. Sympathovagal dominance is generally assessed in vivo by pharmacological inhibition of the autonomic input by combined injection of atropine and propranolol. Even if propranolol does not block α-adrenergic receptors, the heart rate measured under these conditions constitutes a reliable estimate of the intrinsic pacing rate of a "denervated" heart (29).

In animals, the beating frequency of the isolated SAN is also an index of the intrinsic heart rate. In the mouse, the intrinsic SAN rate is significantly lower than the in vivo heart rate, indicating the existence of a significant sympathetic tone in this species (157). In contrast, it can be shown that dogs and humans are under prominent vagal tone, since pharmacological block of the autonomic input significantly accelerates the basal heart rate (223, 375). However, adrenergic dominance does not demonstrate the absence of a vagal tone. For example, the presence of vagal tone in small rodents can be easily demonstrated by injection of atropine in freely moving mice (157).

The effect of parasympathetic input on pacemaking is greater when the SAN is under sympathetic tone. This phenomenon has been named "accentuated antagonism" by Levy (284). At the organ level, presynaptic regulation of catecholaminergic terminals by the vagus nerve and pacemaker shift contribute to accentuated antagonism (300). In this respect, the functional inhomogeneity of SAN tissue can be an important factor underlying accentuated antagonisms (300). In SAN and AVN cells of the rabbit, accentuated antagonism has been explained by the regulation of cAMP levels by nitric oxide (NO) (see below). Beside the basal regulation of the heart rate exerted by the autonomic balance, cardiac automaticity is modulated on a beat-by-beat basis so that pacemaking is quickly adapted to the physiological state of the organism. In this respect, the high-frequency (HF) and low-frequency (LF) spectra of the heart rate variability (HRV) have been used to study the dynamic regulation of pacemaking (157). However, it is becoming clear that intrinsic factors are also involved in the beat-by-beat regulation of heart rate. Indeed, it has been shown that "nonautonomic mechanisms" may contribute to HF spectra of HRV in some physiological conditions (34, 76, 463). Bernardi et al. (34) reported that, at peak exercise, in both healthy human subjects and transplanted patients the HF spectra of the HRV is almost completely generated by a "nonautonomic" mechanism that is synchronized with ventilation. These results were then confirmed by Casadei et al. (76), who reported that under exercise, the "nonneuronal" component of heart rate regulation increases by ~35%. Slovut et al. (463) have suggested that this phenomenon is due to SAN stretch during diastolic atrial filling (see sect. IX*D*).

B. Sympathetic Regulation of Pacemaker Activity

Activation of the β-adrenergic receptor underlies the positive chronotropic effect induced by catecholamines on automaticity. Catecholamines enhance the activity of ion channels as well as intracellular Ca^{2+} release. The relative importance of sarcolemmal ion channels and LCICR in the β-adrenergic regulation of pacemaker activity is still debated. In this section, we will present and compare evidence linking these mechanisms to stimulation of pacemaker activity by catecholamines.

I_f and $I_{Ca,L}$ have been proposed to constitute important mechanisms in heart rate acceleration by catecholamines (64, 67, 120, 364). The open probability of f-channels increases even for a small augmentation of intracellular cAMP. A rise in cAMP positively shifts the I_f activation curve, thereby supplying more inward current during the linear part of diastolic depolarization (120) (Fig. 22). DiFrancesco (120) has proposed that I_f is the predominant mechanism for increasing the slope of the diastolic depolarization at low adrenergic tone. This is based on the observation that low doses of the β-adrenergic agonist isoproterenol (which is supposed to mimic weak adrenergic activity) increase the slope of the diastolic depolarization without affecting the action potential waveform (120). Remarkably, specific regulation of the diastolic depolarization slope is a common property of low doses of autonomic agonists and selective I_f blockers (21). Another strong line of experimental evidence for the capability of f-channels to stimulate pacemaker activity is the acceleration by cAMP analogs of pacing rate in SAN cells. Bucchi et al. (67) have shown that isoproterenol and *R*p-cAMP similarly increase the diastolic depolarization slope in rabbit SAN cells. Stieber et al. (466) also gave strong evidence for the ability of f-channels to accelerate embryonic heart rate. These authors have shown that cAMP cannot accelerate the heartbeat of $HCN4^{-/-}$ embryos. Overall, different lines of direct and indirect evidence are in favor of an important contribution of f-channels in sympathetic regulation of pacemaker activity.

Downloaded from physrev.physiology.org on October 4, 2011

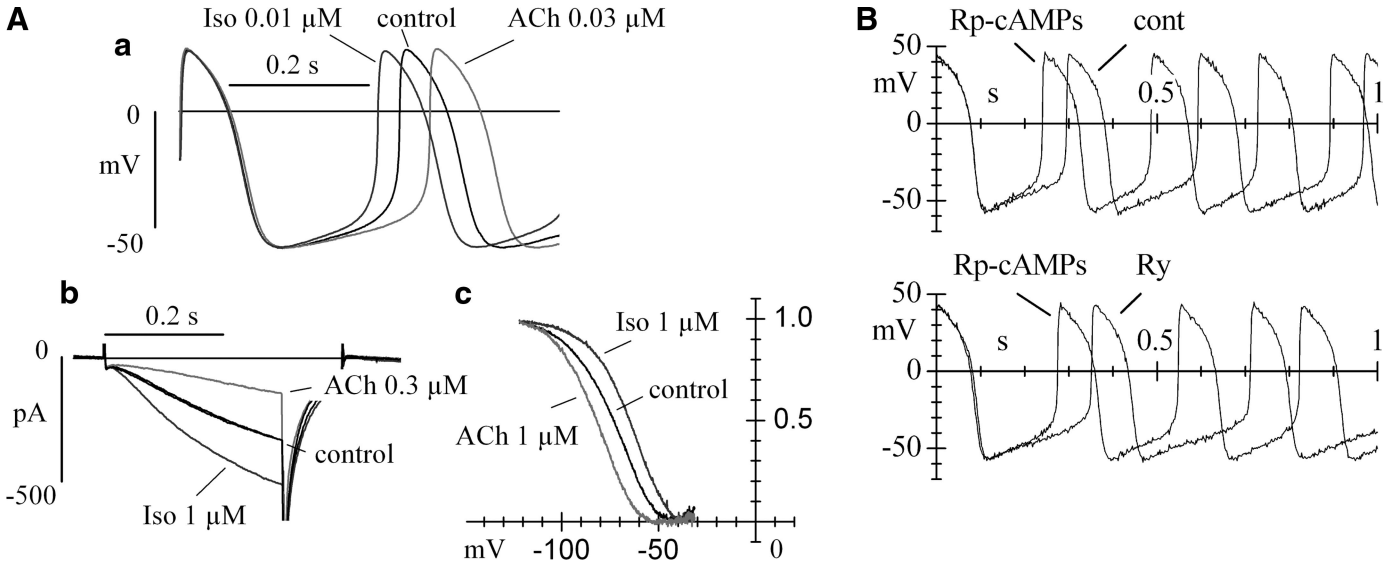

FIG. 22. *A*: low doses of isoproterenol and ACh selectively modulate the slope of the diastolic depolarization in rabbit SAN cells (*a*) and shift the I_f voltage dependence (*b*, *c*). These experiments have led DiFrancesco (see Ref. 121 and sect. VII for discussion) to propose that the predominant mechanism by which the autonomic nervous system controls the heart rate is I_f. [*a* from DiFrancesco (120), with permission from the Annual Review of Physiology; *b* and *c* are from Accili and DiFrancesco (4).] *B*: a cAMP analog (R_p-cAMPs) stimulates pacemaker activity by increasing the slope of the diastolic depolarization under control conditions and in the presence of ryanodine (Ry). This observation suggests that impairment of Ca^{2+} release from the SR does not prevent regulation of pacemaker activity by direct binding of cAMP analogs to f-channels. [From Bucchi et al. (67), with permission from Elsevier.]

The functional role of $I_{Ca,L}$ in adrenergic regulation of heart rate is still unresolved. Three lines of indirect evidence are suggestive of a role of $I_{Ca,L}$ in the sympathetic regulation of heart rate. First, catecholamines robustly enhance $I_{Ca,L}$ in the same concentration range as pacemaker activity (542). Zaza et al. (542) have shown that I_f and $I_{Ca,L}$ have similar sensitivity to isoproterenol in rabbit SAN cells. Second, Choate and Feldman (87) have reported that DHPs reduce the positive chronotropic response of mouse atria to stimulation of the stellate ganglion. Third, the contribution of $Ca_v1.3$ channels in the generation of the diastolic depolarization in mouse SAN cells suggests that $I_{Ca,L}$ can constitute an important mechanism for accelerating the diastolic depolarization slope upon activation of β-adrenergic receptors (309, 310). Consistent with this hypothesis, the positive chronotropic response to isoproterenol of isolated $Ca_v1.3^{-/-}$ hearts is moderately reduced (321). However, the in vivo heart rate of mice lacking $Ca_v1.3$ channels is comparable to that of wild-type mice (393). The maximal heart rates of wild-type and $Ca_v1.3^{-/-}$ mice are significantly reduced by selective I_f block by ivabradine (Mangoni et al., unpublished observations). Taken together, these observations are suggestive of a distinct role of f-channels and $Ca_v1.3$ channels in the autonomic regulation of heart rate (see also Ref. 196).

The relevance of TTX-sensitive and TTX-resistant I_{Na} in the sympathetic regulation of heart rate is of interest, yet no reports have specifically studied the autonomic regulation of I_{Na} in the SAN. The cardiac TTX-resistant Scn5A-mediated I_{Na} is sensitive to phosphorylation by PKA and PKC (286, 407). Taking into consideration the relevance of Scn5A channels in SAN conduction, we can speculate that sympathetic stimulation of TTX-resistant I_{Na} can accelerate heart rate by accelerating impulse conduction within the SAN as well as from the SAN to the atrium. In contrast, the effects of autonomic agonists on TTX-sensitive I_{Na} are not easily predictable. Maier et al. (304) have hypothesized that TTX-sensitive Na^+ channels can be negatively regulated by the sympathetic nervous system as in neurons. If this hypothesis is valid, the contribution of TTX-sensitive I_{Na} to the diastolic depolarization may be higher in basal conditions than under strong adrenergic activation.

In pacemaker cells of amphibians (227) and mammals, β-adrenergic receptor activation stimulates SR Ca^{2+} release and NCX activity (415, 506). In spontaneously active rabbit SAN cells, isoproterenol robustly enhances the amplitude and frequency of RyR-dependent LCICR (415, 506). Vinogradova et al. (506) have reported that ryanodine abolishes the augmentation of subsarcolemmal Ca^{2+} release and LCICRs. This effect is accompanied by a strong reduction in the isoproterenol-induced positive chronotropic effect, particularly at low agonist doses. Vinogradova et al. (506) have thus proposed that SR Ca^{2+} release is the major effector of the positive chronotropic effect of the β-adrenergic receptor pathway. Partial inhibition of the isoproterenol chronotropic effect in rabbit SAN has been qualitatively confirmed by other authors (67, 267, 415), although it shows quantitative variability.

Downloaded from physrev.physiology.org on October 4, 2011

Indeed, in a previous study using intact SAN, ryanodine reduced β-adrenergic stimulation of pacemaking by ~40% (415). Pacemaking in the intact SAN is also less sensitive to ryanodine than in isolated pacemaker cells. Musa et al. (349) have indicated that such a difference can be due to heterogeneous expression of proteins regulating Ca^{2+} handling in the center versus the periphery of the SAN. Functionally, the central leading pacemaking site is less sensitive to inhibition of SR Ca^{2+} release (267). However, Lyashkov et al. (299) have reported that, in isolated rabbit SAN cells, the effects of ryanodine, BAPTA, and Li^+ on pacemaker activity are similar irrespective of the cell size. Discrepancy between results obtained in intact SAN tissue and isolated cells may be attributed to the network organization of pacemaker cells in the SAN.

In Figure 23, we attempt to summarize the downstream targets of the β-adrenergic receptor-dependent signaling pathway in SAN pacemaker cells. This model is based on evidence from rabbit SAN cells and is complemented by recent insights from genetically modified mouse strains. For our discussion, we can distinguish two distinct pacemaker mechanisms: an "ion channel clock" formed by voltage-dependent ion channels and the intracellular SR-dependent "Ca^{2+} clock" (307). Activation of β-adrenergic receptors stimulates adenylyl cyclase (AC) activity, which converts ATP in cAMP. Elevated cAMP promotes voltage-dependent opening of f-channels and activates PKA (126). The catalytic subunit of PKA enhances the activity of different ion channels of the membrane-delimited pacemaker mechanism by channel phosphorylation. These include $Ca_v1.3$, $Ca_v1.2$ channels (309), as well as st-channel complexes (334). Vinogradova et al. (508) have reported that basal PKA activity is higher in rabbit SAN cells than in working myocytes. High phosphorylation of PLB and RyRs generates periodical LCICR causing I_{NCX}-mediated membrane voltage oscillations, which contribute to the control of the chronotropic state of the cell (43, 508). β-Adrenergic receptor activation further elevates PKA activity, thereby increasing the frequency and number of LCICRs and stimulating I_{NCX}.

The "I_f-based" pacemaker mechanism (121) and that of the spontaneous SR-dependent "Ca^{2+} clock" (307) have been placed as opposed to each other. However, they can be qualitatively reconciled in a general framework. Both models have a common major messenger that is cAMP. cAMP can control the chronotropic state of the cell by at least three distinct effectors: *1*) f-channels by direct channel opening, *2*) $Ca_v1.3$ channels, and *3*) RyRs by channel

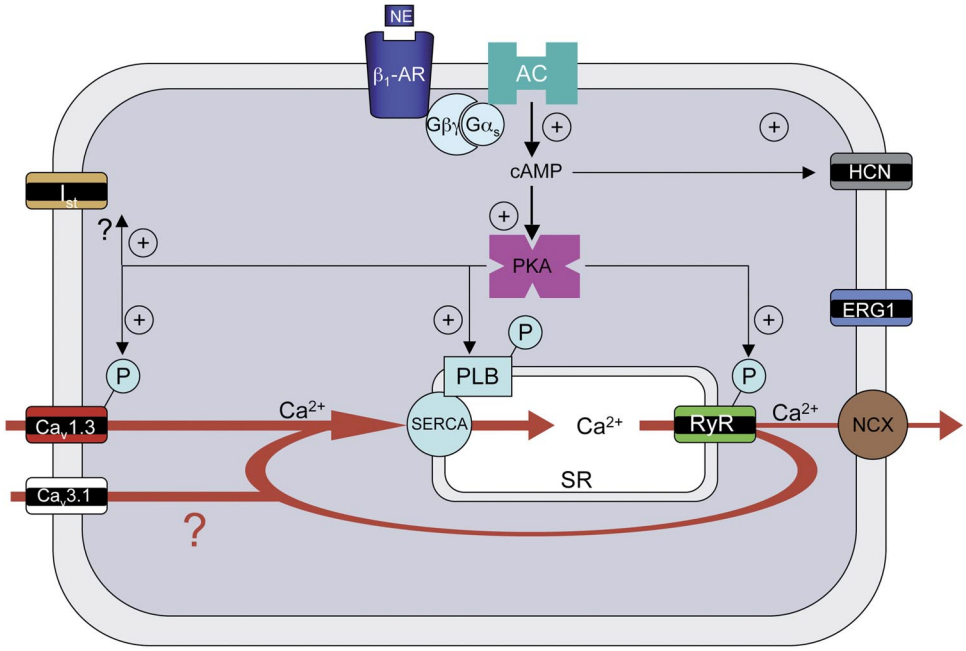

FIG. 23. This cartoon summarizes the ionic mechanisms contributing to the diastolic depolarization in a SAN pacemaker cell. Voltage-dependent ion channels as well as the proposed "Ca^{2+} clock" (307) are represented together. Possible interactions between these mechanisms are indicated. In pacemaker cells, high basal cAMP-mediated PKA-dependent phosphorylation stimulates a perpetual "free running" Ca^{2+} cycling by pumping Ca^{2+} into the SR via SERCA2 and LCICR via RyRs. PKA also stimulates Ca^{2+} entry through $Ca_v1.3$-mediated $I_{Ca,L}$. The thick red line indicates the persistent spontaneous Ca^{2+} cycling. The possibility that $Ca_v3.1$-mediated $I_{Ca,T}$ can contribute to replenishment of SR Ca^{2+} stores is suggested. Spontaneous LCICR from SR is linked to the diastolic depolarization via Ca^{2+} activation of inward I_{NCX} current. Direct cAMP-dependent activation of HCN channels or cAMP-mediated, PKA-dependent phosphorylation of $Ca_v1.3$ channels and I_{st} (dashed lines) strongly stimulates the pacemaker cycle driven by the "membrane ion channels clock" (MCC). It is conceivable that the MCC can entrain the intracellular Ca^{2+} clock because of the dependency of SR Ca^{2+} content from VDCCs. On the other hand, the Ca^{2+} clock may trigger oscillations of the membrane voltage and initiate normal pacemaking via the MCC. It is thus likely that under physiological conditions the MCC and the Ca^{2+} clock mutually entrain one another. [Adapted from Vinogradova et al. (508).]

Downloaded from physrev.physiology.org on October 4, 2011

phosphorylation. Experimentally, maneuvers altering intracellular cAMP levels will affect the activity of all these effectors. One may wonder why the "ion channels clock" and the "free-running Ca^{2+} clock" (307) share a common messenger. The answer probably resides in the necessity to synchronize the replenishment of SR Ca^{2+} stores to Ca^{2+} release in the late phase of the diastolic depolarization. Spontaneous LCICR ceases in arrested cells, since $Ca_v1.3$ channels are probably the predominant source of Ca^{2+} entry during the action potential. Consequently, as much as the "Ca^{2+} clock" accelerates under the action of catecholamines, the sarcolemmal pacemaker mechanism mediated by f- and $Ca_v1.3$ channels will also speed up and shorten diastolic depolarization.

However, as highlighted by Maltsev et al. (307), the "Ca^{2+} clock" hypothesis of the genesis of SAN automaticity assumes that spontaneous LCICR is the predominant mechanism that controls the chronotropic state of SAN cells in both basal conditions and under β-adrenergic receptor stimulation. These authors have proposed that I_f plays only a minor role in mediating the effect of catecholamines on heart rate. This view is contradicted by a substantial set of experimental results, such as the observation that ryanodine does not prevent acceleration of pacemaker activity in rabbit SAN cells by cAMP analogs (67, 68) and that specific f-channel inhibition by ivabradine can reduce the heart rate of freely moving mice by up to 26% (Mangoni et al., unpublished observations). Furthermore, the importance of f-channels in the autonomic regulation of heart rate is strongly supported by inherited dysfunction of pacemaking in humans harboring mutations in the HCN4 gene (see sect. x*A*) and related murine models (see sect. vi*D*).

C. Parasympathetic Regulation of Pacemaking

The parasympathetic regulation of cardiac automaticity is mediated by the activation of muscarinic receptors following release of acetylcholine (ACh) from vagal nerve endings. Cholinergic agonists induce a potent negative chronotropic effect on cardiac automaticity and atrioventricular conduction in vivo as well as in isolated heart preparations (215, 325). Signaling and ionic mechanisms underlying the muscarinic regulation of heart rate have been studied for more than 30 years, yet it is not completely understood which mechanisms determine responses in heart rate under various physiological conditions, such as high sympathetic tone or parasympathetic discharge.

Hutter and Trautwein (212) observed that vagal stimulation stops pacemaking in the frog sinus venosus. As suppression of automaticity was due to an increase in membrane K^+ conductance, Hutter and Trautwein (212, 213) concluded that the vagal control of the heart rate was due to activation of a K^+ current. Early observations by Hutter and Trautwein are now accounted for by the activation of I_{KACh} channels via vagally released ACh (432). However, other authors have failed to observe hyperpolarization of the membrane potential after vagal stimulation. For instance, studies by Toda and West (481, 519) reported that vagal stimulation slowed automaticity by reducing the slope of diastolic depolarization in atrial and AVN preparations. This has been confirmed by Shibata et al. (453) on isolated rabbit SAN preparations. Both hyperpolarization of the maximum diastolic potential and a decrease in the slope of diastolic depolarization are observed when the muscarinic regulation of pacemaker activity is studied using isolated spontaneously active cells. Indeed, in isolated rabbit SAN cells, high ACh doses (1 μM) hyperpolarize the maximum diastolic potential and eventually stop pacemaking due to maximal I_{KACh} activation (124, 507). In contrast, low ACh doses (1–10 nM) slow pacemaker activity by decreasing the slope of diastolic depolarization in the absence of other changes in action potential parameters and maximum diastolic potential (Fig. 22*A*). This is because binding of ACh to muscarinic receptors activates different signaling pathways in pacemaker cells. These pathways involve direct activation of I_{KACh} channels, negative regulation of cAMP production, and positive regulation of cAMP hydrolysis.

The muscarinic M_2 receptor activates the inhibitory G protein α-subunit (α_i) which negatively couples to AC activity (283, 440). Downregulation of cAMP can affect the activity of voltage-dependent ion channels involved in pacemaker activity and reverse the signaling processes involved in sympathetic stimulation of heart rate (Fig. 24). Moreover, βγ-subunits of α_i directly open K_{ACh} channels (520, 523). The role of I_{KACh}, I_f, and $I_{Ca,L}$ in mediating the negative chronotropic effect of ACh has been studied in isolated SAN pacemaker cells. Recently, insight into the importance of I_{KACh} in the regulation of heart rate has been obtained using genetically modified mice lacking $K_{ir}3.4$ channels (522). Wickmann et al. (522) have shown that $K_{ir}3.4^{-/-}$ mice lack I_{KACh} in the atrium and show prominent reduction autonomic regulation of heart rate in the HF and LF spectrum of the HRV. Consistent with these observations, Gehrmann et al. (158) have shown that transgenic mice expressing low amounts of βγ have a reduced negative chronotropic response to cholinergic agonists.

DiFrancesco et al. (124) have studied the relative sensitivity to ACh of I_f and I_{KACh} in rabbit SAN cells. These authors have compared the ACh dose dependency of the shift in the I_f activation curve, the I_{KACh} density, and the slowing of pacemaker activity. In this study, low ACh doses significantly shifted the I_f activation curve in the negative direction and slowed pacemaking in a concentration range that did not activate I_{KACh}. Using a similar approach, Zaza et al. (542) have compared the sensi-

Downloaded from physrev.physiology.org on October 4, 2011

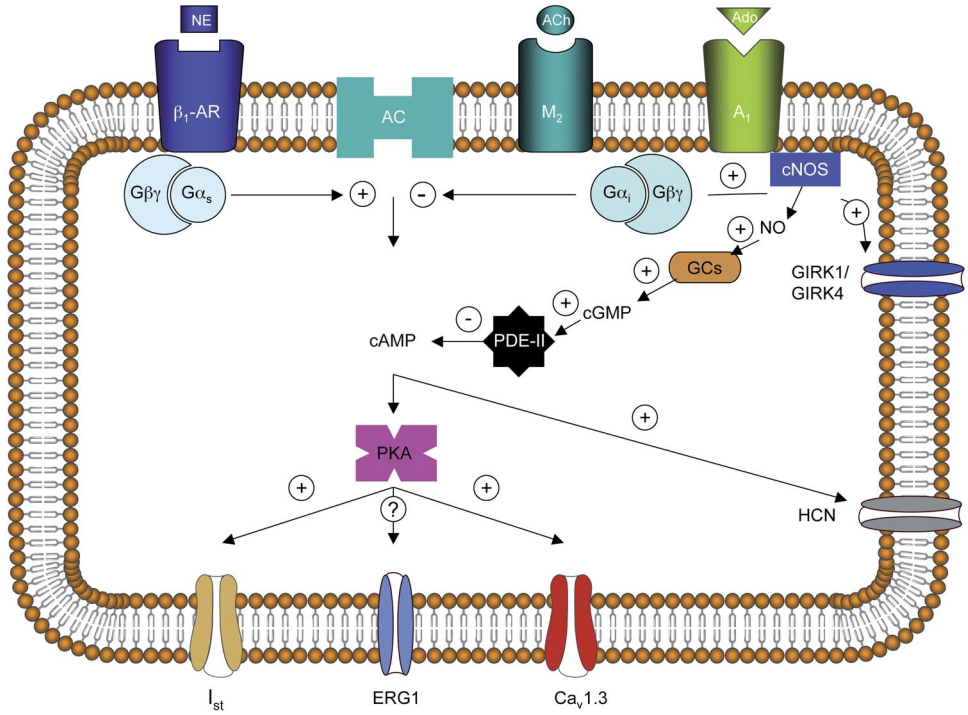

FIG. 24. Summary of the signaling pathways involved in the muscarinic regulation of pacemaker activity. In the SAN and AVN, ACh and Ado share the same pathways for signal transduction. ACh binds to the muscarinic M_2 receptor, which is coupled to a "direct" G protein-dependent pathway activating Kir3.1/Kir3.4 (GIRK1/GIRK4) channel complexes. Beside this direct pathway, two other "indirect" channel regulation pathways lead to downregulation of intracellular cAMP. In the first cascade of events, the αG_i protein subunit inhibits AC activity, thereby reducing the synthesis of cAMP. Inhibition of AC synthesis is viewed as the predominant pathway by which ACh regulates the voltage dependence of f-channels (HCN). The second muscarinic pathway is initiated by the stimulation of the NOS activity and production of NO. NOS activates the enzyme guanylate cyclase (GC), which converts GTP in cGMP. Elevation of cGMP concentration stimulates PDE II-dependent hydrolysis of cAMP, thereby reducing PKA activity. This NOS-dependent pathway for regulation of PKA activity has been proposed to be the major pathway for the muscarinic regulation of $I_{Ca,L}$ during pacemaking. In the figure, negative NOS-dependent regulation of $Ca_v1.3$-mediated $I_{Ca,L}$ and I_{st} is suggested. It is not known if the SAN I_{Kr} can also be negatively regulated by the NOS-dependent pathway.

tivity of $I_{Ca,L}$ and I_f to ACh. In this study, I_f inhibition was observed at lower doses of ACh than that required to inhibit "basal" $I_{Ca,L}$ (542). These results have led DiFrancesco (119) to propose that I_f is the predominant ion channel which underlies the muscarinic control of heart rate at low vagal tone. This view is consistent with recent evidence obtained by Yamada in isolated beating mouse hearts (530). In these experiments, heart rate reduction induced by low ACh doses was reported to be insensitive to I_{KACh} inhibition by tertiapin. Caution should be used when transposing in vitro observations from isolated pacemaker cells and denervated hearts to in situ heart rate regulation. Due to the accentuated antagonism phenomenon, different ionic mechanisms can participate to muscarinic regulation of pacemaker activity, according to their relative sensitivity in cholinergic agonists as well as to intracellular levels of cAMP. The cardiac $I_{Ca,L}$ has been reported to be remarkably "insensitive" to muscarinic regulation in basal conditions, because relatively high ACh doses are required to inhibit this current (190, 323). However, Petit-Jacques et al. (390) have shown that muscarinic regulation of SAN $I_{Ca,L}$ depends on the previous β-adrenergic stimulation and cAMP levels. Indeed, moderate doses of ACh can significantly inhibit $I_{Ca,L}$ if previously stimulated by β-adrenergic agonists (390). PKA inhibition or cell dialysis with a nonhydrolyzable cAMP analog abolishes $I_{Ca,L}$ regulation by ACh (390). ACh can thus act as an "antiadrenergic" agent. Interestingly, accentuated antagonism of ACh after β-adrenergic receptor activation has been observed also on I_f in canine Purkinje fibers (81). It is thus important to distinguish between "direct" and "indirect" cholinergic regulation of $I_{Ca,L}$, to distinguish between basal current inhibition and that observed after adrenergic stimulation. Thus it cannot be excluded that indirect (or antiadrenergic) inhibition of $I_{Ca,L}$ can be relevant in vagal regulation of heart rate in conditions of tonic sympathetic activation, when the accentuated antagonism phenomenon is present. The regulation of $Ca_v1.3$ channels by ACh has not yet been investigated. In this respect, the relatively positive holding potentials (about −30 mV) employed thus far to study the regulation of $I_{Ca,L}$ by autonomic agonists (186, 542) would inactivate most of $Ca_v1.3$ channels (309).

Han et al. (186) have demonstrated that an NO signaling pathway is involved in the muscarinic regulation of $I_{Ca,L}$ in conditions of accentuated antagonism, when in-

Downloaded from physrev.physiology.org on October 4, 2011

tracellular cAMP is increased by stimulation of β-adrenergic receptors. In cardiac myocytes, muscarinic receptor activation is coupled to NO synthesis, which stimulates guanylyl cyclase activity. Elevated cGMP production promotes phosphodiesterase activity that inhibits $I_{Ca,L}$ by cAMP breakdown (323). Han et al. (186) have provided evidence that the NO signaling pathway plays an obligatory role in the muscarinic regulation of rabbit SAN $I_{Ca,L}$ (186). In these cells, block of NO synthesis prevents $I_{Ca,L}$ inhibition by cholinergic agonists such as carbamylcholine (185). This signaling pathway regulating $I_{Ca,L}$ is present also in the AVN (170). The NO signaling pathway in rabbit SAN seems to be primarily mediated by a constitutive endothelial NO oxide synthase (eNOS) isoform (182). Also, specific pharmacological inhibition of posphodiesterase II (PDEII) blocks NO-dependent inhibition of $I_{Ca,L}$, indicating that this PDE isoform plays a dominant role in downstream regulation of cAMP level (182). In contrast, the role of intracellular $[Ca^{2+}]_i$ in mediating NO-dependent inhibition of $I_{Ca,L}$ would need further investigation. Han et al. (186) have shown that buffering $[Ca^{2+}]_i$ with BAPTA blocks eNOS activity. However, in the same study, depletion of SR Ca^{2+} stores by ryanodine and thapsigargin did not affect regulation of $I_{Ca,L}$, suggesting that Ca^{2+} involved in modulation of eNOS activity comes from an independent intracellular compartment. The relevance of the eNOS/PDEII signaling pathway in mediating accentuated antagonism in the canine heart has been shown by Sasaki et al. (437). These authors have also shown that NO can partially modulate accentuated antagonism but does not play an important role in the absence of previous β-adrenergic receptor stimulation.

Beside the eNOS/PDEII signaling pathway, protein phosphatases can also regulate the activity of ion channels under basal conditions or under the action of autonomic agonists. Ke et al. (235) have reported that the p21-activated protein kinase (Pak1) is functionally expressed in guinea pig SAN cells. In pacemaker cells, when cellular Pak1 activity is enhanced by expressing a constitutively active form of the protein, $I_{Ca,L}$ and I_K densities are reduced and the positive chronotropic response of cells to isoproterenol is blunted. The regulatory role of active Pak1 on $I_{Ca,L}$ and I_K is likely attributable to increased activity of the protein phosphatase PP2A (235). It remains to be established if Pak1 can be functionally associated with the vagal regulation of heart rate.

The importance of NO signaling pathway in the vagal regulation of heart rate in mice has not been clearly demonstrated. Mice lacking eNOS or the $G\alpha_o$ protein isoforms lack muscarinic regulation of $I_{Ca,L}$ (183, 487). However, Vandecasteele et al. (494) failed to observe reduction of both adrenergic and muscarinic regulation of $I_{Ca,L}$ in another eNOS-deficient mouse line. Consistent with these results, Mori et al. (343) have reported that inhibition of eNOS does not change accentuated antagonism in isolated mouse atria.

VIII. CARDIAC AUTOMATICITY AS AN INTEGRATED MECHANISM: NUMERICAL MODELING OF PACEMAKER ACTIVITY

A. General Models of Automaticity

Modeling of cardiac automaticity integrates the behavior of channels and ionic homeostasis in a calculating environment to predict pacemaking under different conditions. Numerical models are used to gain insight into the roles of ion channels and/or Ca^{2+} handling proteins, when biophysical or pharmacological approaches are limited or impossible. The growing knowledge on the cardiac pacemaker mechanism is reflected by the increasing complexity of numerical models of automaticity. A detailed comparison of all the numerical models of automaticity that have been developed in the past is beyond the scope of this review. For further discussion on the historical and technical aspects of this topic, the reader can consult the recently published manuscript by Wilders (525). Here, we will discuss some predictions of numerical models on the importance of ion channels and Ca^{2+} signaling in the generation and regulation of automaticity.

Recent cellular models of SAN automaticity have been developed from the DiFrancesco and Noble model of Purkinje fibers automaticity (127). In this model, automaticity is based on I_f. Suppression of I_f abolishes automaticity (127). The DiFrancesco and Noble model included calculations of intracellular systolic Ca^{2+} transients and I_{NCX} activity. Noble and Noble (360) have adapted the DiFrancesco and Noble model to the central and peripheral SAN automaticity, by scaling current densities to approximate that of SAN cells. Noble et al. (359) have used this model to predict the possible roles of I_f and that of Na^+ background current $[I_{b(Na)}]$ and proposed that I_f is a major mechanism for stabilizing automaticity and to protect SAN pacemaking from hyperpolarizations. Wilders et al. (526) have also assessed the role of I_f and $I_{b(Na)}$ in the generation of the diastolic depolarization. These authors have predicted that the association of I_f and $I_{b(Na)}$ is necessary for pacemaking of isolated rabbit SAN cells, since joint abolition of both currents stops automaticity (526). Block of I_f slows pacemaking by specifically reducing the slope of the diastolic depolarization (526). Wilders et al. have suggested that their modeling results are consistent with the experimental work by Denyer et al. who proposed that I_b can sustain pacemaking under I_f block (113, 526) (see sect. VI*D*). Demir et al. (111) have developed a model of automaticity of peripheral SAN cells, by associating voltage-dependent ion channels activity with intracellular Ca^{2+} release and handling

Downloaded from physrev.physiology.org on October 4, 2011

by intracellular Ca^{2+} buffers. In this model, different ionic currents contribute to the generation of the diastolic depolarization. Particularly, block of I_f and $I_{Ca,T}$ almost equally slow pacemaker activity, while inhibition of $I_{Ca,L}$ mainly affects the late diastolic depolarization and action potential upstroke (111). Predictions obtained by the Demir et al. model are generally consistent with many physiological and pharmacological results on several ionic currents involved in automaticity, including $I_{Ca,T}$, $I_{Ca,L}$, I_{Kr}, and I_f (111). The Demir et al. model can successfully reproduce certain aspects of the parasympathetic regulation of pacemaker activity. Particularly, the negative regulation of pacemaking by specific reduction of the slope of the diastolic depolarization, and the phase-resetting SAN response upon bursts of vagal activity can be computed by this model (110). More generally, predictions obtained by the Wilders et al. and Demir et al. models are qualitatively consistent with experimental results in rabbit SAN cells. However, they have some limitations when inferring the role of $I_{Ca,L}$ and intracellular Ca^{2+} release. These limitations are justified as far as these models have been developed when experimental data on $Ca_v1.3$ channels and LCICR were not available. Kurata et al. (262) have been the first to develop a model of SAN automaticity in which the subsarcolemmal Ca^{2+} ($[Ca^{2+}]_{sub}$) and the SR Ca^{2+} content were included in calculations. Furthermore, buffering of $[Ca^{2+}]_i$ by troponin, calsequestrin, and calmodulin were also included (262). The Kurata et al. model (262) thus aims to combine the advantages of calculating Ca^{2+} buffering and Ca^{2+} exchange between the subsarcolemmal space and the SR. Subsarcolemmal Ca^{2+} controls Ca^{2+}-dependent inactivation of $I_{Ca,L}$ (262). In the Kurata et al. model, block of SR Ca^{2+} release has only minor effects on pacemaking, essentially because Ca^{2+} release is limited to the action potential upstroke phase.

B. Dedicated Models of Automaticity

Recently developed models of SAN pacemaking consider specific SAN properties, such as the regional variations of ion channel expression (545), regulation of automaticity by LCICR (306), and automaticity in genetically modified mice (314). These models will be referred to here as "dedicated."

Zhang et al. (545) have modeled pacemaker activity in the periphery and center of the SAN. This model is based on experimental results on the heterogeneity of cell size and ionic current densities observed in the rabbit SAN (58) (see sects. II and III). Numerical simulations by Zhang et al. (545) show that it is possible to reproduce the slower pacemaker activity, action potential upstroke velocity, and the more positive maximum diastolic potential in the SAN center by setting lower densities of $I_{Ca,L}$, I_f, I_{Kr}, and I_{Na} in the central than in the peripheral SAN model. In the central model, I_{Na} is set to zero so that the action potential upstroke phase is entirely controlled by $I_{Ca,L}$. In the peripheral model, the diastolic depolarization is carried by $I_{Ca,T}$ and I_f, while in the central model $I_{Ca,T}$ predominates on I_f. The model predicts the higher effect of I_f blockers on automaticity in the SAN periphery versus the center. Suppression of $I_{Ca,L}$ in the Zhang et al. model stops pacemaking in the center and sets the membrane potential to −35 mV (545). In the peripheral model, block of $I_{Ca,L}$ moderately accelerates automaticity possibly because of the shortening of the action potential duration. I_{Kr} suppression stops automaticity in both the peripheral and central SAN model. However, it is possible to set a 20% block of I_{Kr} without stopping pacemaking. According to Zhang et al. (545), the moderate slowing of pacemaking induced by partial inhibition of I_{Kr} is consistent with what is observed in peripheral SAN tissue balls (249). In the peripheral SAN model, I_{to} has higher density than in the central model. Consistent with experimental results (60), suppression of I_{to} in the peripheral model prolongs the action potential duration, while has limited effects on the central SAN model (545). Garny et al. (152) have adapted the Zhang et al. model in an attempt to reproduce atriosinus interactions and calculate the predicted position of the SAN leading pacemaker site in the presence and absence of the sorrounding atrium (Fig. 25). In this model, a gradual transition between cells matched with the central and the peripheral model was established via a distribution function. A variable ratio of intercellular conductivity was also implemented (see legend of Fig. 25). This cellular array was connected to cells matched with a rabbit (197) or human (368) atrial model. The position of the leading pacemaker site settled in the SAN center when a greater intercellular coupling between cells in the SAN periphery than in the center was established. The leading pacemaker site shifted to the periphery when intercellular conduction was uniform in the SAN center and periphery. Finally, the leading pacemaker site was located in the periphery when the SAN cellular array was electrically disconneted from the atrium (Fig. 25). In conclusion, this atriosinus model successfully reproduced the electrotonic inhibition of atrial cells on SAN pacemaking. Garny et al. (152) have interpreted the electrotonic suppression of pacemaking in the SAN periphery in terms of an "opposing depolarization," rather than a simple hyperpolarizing inhibition (152).

In its first version, the model by Zhang et al. did not include calculations of intracellular Ca^{2+} handling. Similarly $[Na^+]_i$ and $[K^+]_i$ were kept constant (58). In a follow up manuscript, these authors have included calculations of Ca^{2+} handling in both the central and peripheral SAN model (56). Available experimental data on Ca^{2+}-dependent effects on $I_{Ca,T}$, $I_{Ca,L}$, I_{Kr}, and I_f were included. Boyett et al. (56) have then compared the effects of

Downloaded from physrev.physiology.org on October 4, 2011

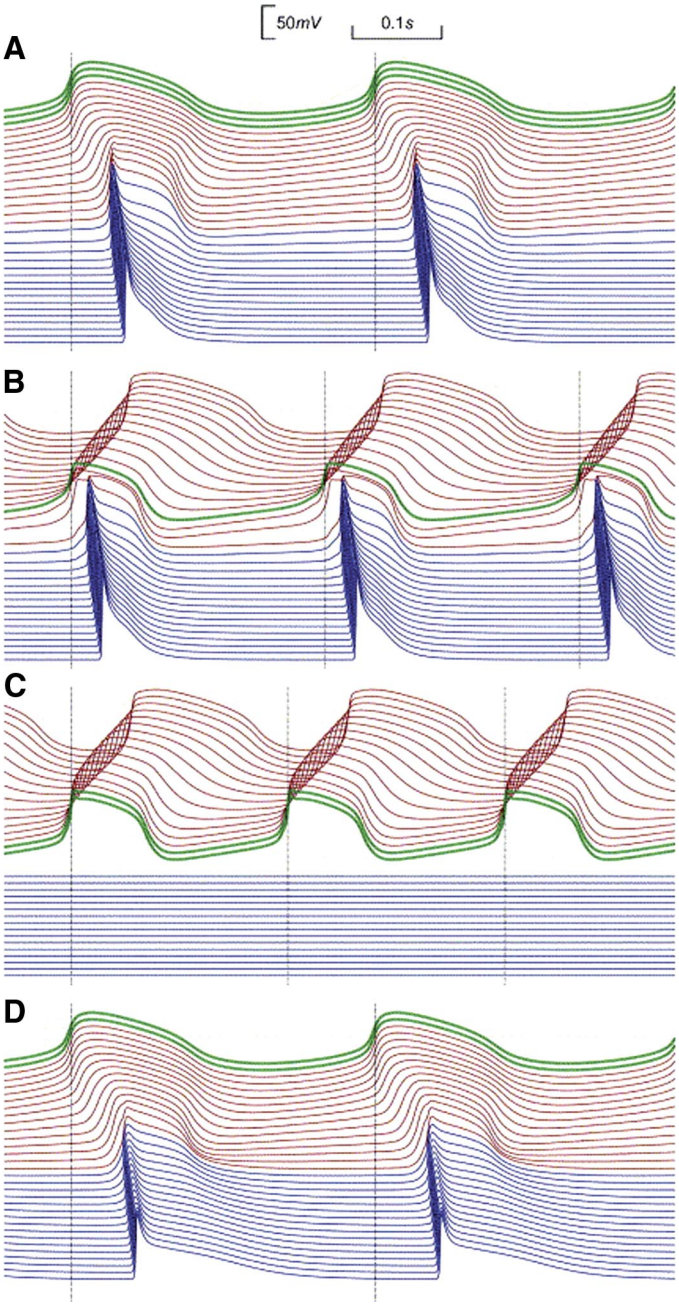

FIG. 25. Numerical modeling of SAN-atrium interactions using a modified version of the Zhang et al. model of rabbit central and peripheral SAN automaticity (152). The membrane voltage of the leading pacemaker site is depicted in green, the "follower" SAN membrane voltage in red, and the atrial membrane voltage is depicted in blue. In *A*, the central SAN coupling conductance is set 10 times lower than the peripheral conductance (37.5 vs. 375 nS, see Ref. 152). Note that the leading pacemaker site locates in the SAN center. In *B*, a uniformly low coupling conductance has been set throughout the SAN model (37.5 nS). In these conditions, the leading pacemaker site shifts to the SAN periphery. *C*: when the SAN and atrium are disconnected (no SAN-driven action potential in the atrium), the leading pacemaker site shifts to the SAN periphery, where the intrinsic cell beating rate is faster than in the SAN center. *D*: simulation parameters has been set as in *A*, but a numerical model of a human atrial cell has been employed. [From Garny et al. (153), with permission from Elsevier.]

blocking Ca^{2+} transients in this model and that by Noble and Noble (360), Wilders et al. (526), and Demir et al. (111). In all models tested, abolition of Ca^{2+} transients variably slowed pacemaking, from a minimum of 9% in the Wilders et al. model and a maximum of 41% in the Demir et al. model. Calculations by Boyett et al. suggested that this slowing of automaticity was predominantly due to changes in the Ca^{2+}-dependent activity of ion channels rather then I_{NCX}. These calculations are very useful for interpreting the possible physiological consequences of the Ca^{2+} dependency of ion channel activities, but do not include LCICR and its functional coupling with I_{NCX} (see sect. VI*L*).

Maltsev et al. (306) have modified the Kurata et al. (262) model to include spontaneous preaction potential LCICR and activation of I_{NCX}. These authors have interpreted spontaneous LCICR in terms of a periodical global cellular release phenomenon of a variable phase (and amplitude), occurring during the diastolic interval. In this model, a global LCICR eventually induces the exponential part of the diastolic depolarization. Shortening of the interval between successive LCICRs is predicted to augment the frequency of pacemaking of rabbit SAN cells, by accelerating the onset of the exponential late phase of the diastolic depolarization. Vinogradova et al. (508) and Bogdanov et al. (43) further developed this model by dividing the global LCICR into the sum of finite release elements of which the individual phase of a given release event is set by a random generator (Fig. 26*A*). In this model, a release event can occur at any time comprised between the mean and the standard deviation of the phase of LCICRs observed experimentally. This modification allows one to take into account the "roughly periodical" nature of LCICR in basal conditions and to simulate synchronization of Ca^{2+} release units under activation of the β-adrenergic receptor (508). Bogdanov et al. (43) have used this model to calculate fluctuations of I_{NCX} under basal conditions and stimulation of pacemaking by isoproterenol (Fig. 26, *A* and *B*). In conclusion, numerical modeling predicts that subsarcolemmal Ca^{2+} sigaling may have little effect on pacemaking when only systolic SR Ca^{2+} release is considered (262). However, models including diastolic preaction potential Ca^{2+} release show that LCICR significantly accelerates pacemaking (43, 306, 508). At present, no model including both LCICR and Ca^{2+} dependency of ion channels is available.

Mangoni et al. (314) have adapted the Zhang et al. (545) central model to predict the activation of $Ca_v1.3$ and $Ca_v3.1$ channels during the diastolic depolarization in mouse SAN pacemaker cells (Fig. 26*C*). Simulations obtained using this model suggest that, in the mouse SAN, I_{Kr} controls the action potential repolarization phase and is present as a relatively large outward component throughout the diastolic depolarization (see sect. VI*C*). I_f is the first time-dependent current to be

Downloaded from physrev.physiology.org on October 4, 2011

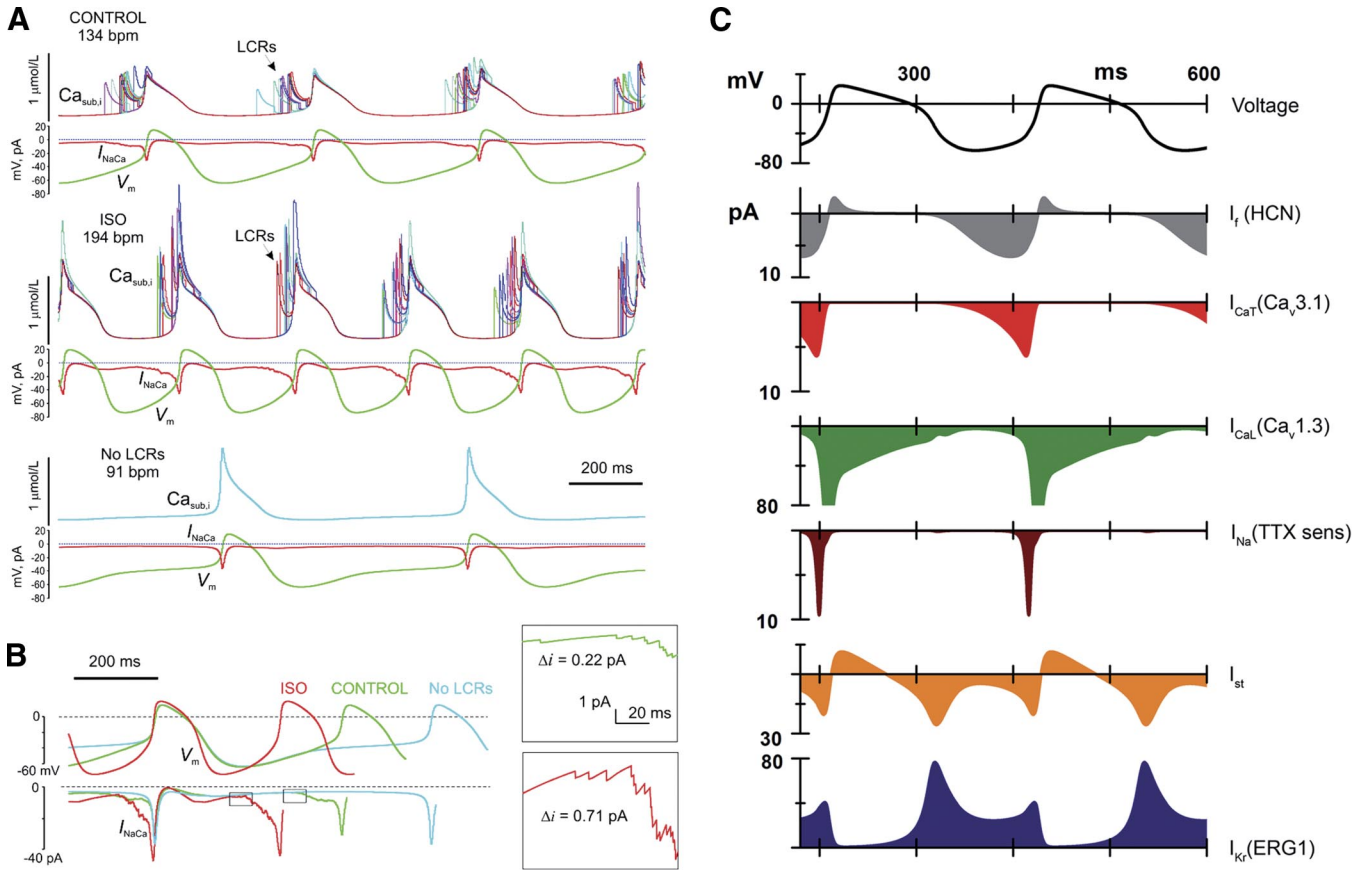

FIG. 26. *A*: simulated effects of β-adrenergic receptor activation (ISO) on I_{NCX} and membrane voltage noise during the diastolic depolarization. Families of simulated LCICR events, total I_{NCX} (I_{NaCa}), and membrane voltage (V_m) in control conditions (*top panel*), under ISO (*middle panel*), and ryanodine (no LCRs, *bottom panel*). Predicted beating rates are shown in beats per min (bpm). *B*: overlapped representative cycles from simulations as in *A*, showing changes in cycle length and I_{NCX} amplitude and fluctuations. *Inset* depicts fluctuating I_{NCX} at the initiation of the exponential phase of the diastolic depolarization (indicated as boxes). The symbol Δ_i indicates initial changes in the NCX current related to individual LCRs. [From Bogdanov et al. (43)] *C*: voltage-dependent "ion channels clock" generating automaticity is proposed here. The "clock" has been represented by using a numerical computation of the mouse SAN automaticity according to Mangoni et al. (314). For each ionic current considered, the underlying ion channel or channel gene family has been indicated. See the text (sect. VIII*B*) for further discussion.

activated at the end of the repolarization phase. $Ca_v3.1$ channels activate upon depolarization before $Ca_v1.3$ and TTX-sensitive Na^+ channels. According to this model, $Ca_v3.1$ channels can contribute to the linear part of the diastolic depolarization. $Ca_v1.3$ channels activate close to the exponential fraction of the diastolic depolarization and may constitute the predominant voltage-dependent mechanism contributing to this phase. This prediction is consistent with experimental observations indicating that DHPs mainly affect the late phase of the diastolic depolarization (319). $Ca_v1.3$ channels also contribute to the upstroke phase of the action potential. Consistent with experimental observations in mouse SAN cells (279), TTX-sensitive I_{Na} appears to contribute to the exponential fraction of the diastolic depolarization, as observed by Lei et al. (279). I_{st} is present throughout the pacemaker cycle as a sustained component.

IX. ADDITIONAL REGULATORS OF CARDIAC AUTOMATICITY

A. Neuropeptides

Neuropeptides are released with ACh or norepinephrine at autonomic nerve terminals (297, 468). The vasoactive intestinal polypeptide (VIP) is coreleased with ACh and stimulates the synthesis of cAMP (91). VIP accelerates heart rate in different species including monkeys (107), dogs (412), and rats (418). It has been proposed that VIP can contribute to postvagal tachycardia, because at the end of vagal discharge ACh will be removed faster from the synaptic space than VIP (195). Shvilkin et al. (458) have reported that in Langendorff-perfused rat hearts, vagally released VIP moderates the negative chronotropic effect induced by high-frequency vagal stimulation. A direct positive chronotropic effect of VIP has been

Downloaded from physrev.physiology.org on October 4, 2011

reported by Rigel and Lathrop in dogs (413). These authors have observed stimulation of pacemaker activity of SAN and atrioventricular junctional pacemakers (414). A positive shift of I_f activation curve by VIP (5–6 mV) has been described by Chang et al. (82) in canine Purkinje cells, and by Accili and DiFrancesco (3) in rabbit SAN cells. This shift of the I_f voltage dependence is probably the predominant mechanism of action of VIP (3, 82).

B. Adenosine

Adenosine (Ado) is a paracrine and autocrine factor regulating a plethora of cellular functions in the cardiovascular system. These include automaticity, coronary circulation, cell adhesion and migration, angiogenesis, and metabolism (346). The cardiovascular effects of Ado have been intensively studied, due to its cardioprotective effects in ischemic preconditioning and cardiac stunning (345). Three distinct Ado receptors (AAR), namely, the A1, A2, and A3AR are expressed in heart tissue (346). Transgenic mice overexpressing A1ARs have significant bradycardia and constitutive slowing of atrioventricular conduction (242). Indeed, Ado is a potent negative regulator of SAN pacemaker activity (517, 518) and AVN conduction (31). This latter property has led to the clinical use of Ado for termination of reentrant supraventricular tachycardias (32). In spontaneously active cells, AARs share the signaling pathway of muscarinic receptors (Fig. 24). Ado mimics downstream effects of muscarinic receptor activation, such as downregulation of cAMP synthesis and activation of Kir3.1/Kir3.4 channels (I_{KAdo}) (30, 543). Under conditions of accentuated antagonisms, Ado reduces automaticity in guinea pig Purkinje fibers (281) and rabbit SAN cells (30). Belardinelli et al. (30) have studied the effects of Ado on I_f and $I_{Ca,L}$ in rabbit SAN cells. They reported that Ado consistently activated I_{KAdo}, but inhibited $I_{Ca,L}$ and I_f only after stimulation by isoproterenol (30). Shimoni et al. (456) have proposed that the indirect inhibitory effect of Ado on $I_{Ca,L}$ is mediated by a NO-dependent signaling pathway (Fig. 24). However, Zaza, Rocchetti, and DiFrancesco (543) have reported that Ado and ACh can shift the activation of "basal" I_f (without previous stimulation by isoproterenol) by ~5 and 9 mV, respectively. In this study, low doses (0.03 μM) of Ado slowed automaticity of SAN cells without hyperpolarizing the maximum diastolic potential. Reasons for the discrepancy between these two studies are not known. Zaza et al. (543) have emphasized that Ado can slow the heart rate by specific regulation of I_f (543).

C. Hormones

Some hormones can influence pacemaking by regulating ion channels involved in automaticity. The SAN and AVN are enriched with ANG II receptors (430). Habuchi et al. (169) have shown that ANG II can slow pacemaker activity in rabbit SAN cells by inhibiting $I_{Ca,L}$. These authors have reported that maximal $I_{Ca,L}$ inhibition by ANG II is ~30%. Slowing of pacemaker activity is characterized by depolarization of the maximum diastolic potential and a reduction of the action potential velocity. These effects on the pacemaker cycle are consistent with inhibition by ANG II of $I_{Ca,L}$ (169). Relaxin (RLX), a reproduction hormone, accelerates heart rate in vivo in animal models. Han et al. (181) have studied the effects of RLX in rabbit SAN cells. In this study, RLX accelerated pacemaker activity of isolated cells and dose-dependently enhanced $I_{Ca,L}$ amplitude. The RLX signaling pathway is dependent on cAMP and PKA, because cAMP analogs and PKI abolished the effects of RLX (181).

Thyroid hormones (TH) are involved in many physiological processes. The TH triiodothyronine (T_3) has a major role in long-term regulation of heart rate, cardiac output, and tissue lipid content (246). Hyperthyroidism is associated with tachycardia, arrhythmias, and elevated cardiac output in animals and humans (28). In contrast, hypothyroidism is associated with reduced heart rate and cardiac output (28). THs act through nuclear hormone receptors (TRs), which are ligand-dependent transcription factors (28). Changes in the expression of cardiac ion channels have been observed in hyperthyroid and hypothyroid animals. Shimoni et al. and Guo et al. have shown that I_{to} density is robustly augmented in ventricles (455) and neonatal cardiomyocytes (167) isolated from hyperthyroid rats. Renaudon et al. (410) have studied the effects of incubation of isolated rabbit SAN cells with T_3. In this study, T_3 significantly increased the density of I_f in the absence of an effect on its current-voltage dependence. This observation suggests an augmentation of f-channels expression in the cell membrane. Renaudon et al. (410) have proposed that an increase in f-channel expression underlies the increase in heart rate in hyperthyroid states. This hypothesis is partially supported by three studies measuring the amount of mRNAs coding for HCN2 channels in the heart of hyperthyroid and hypothyroid rats and mice (161, 270, 380). Indeed, Pachucki et al. (380) have reported a fourfold increase in HCN2 mRNA when T_3 was administrated to hypothyroid rats. Le Bouter et al. (270) have found complex remodeling of ion channel gene expression patterns in ventricles of hypothyroid mice and reported a significant reduction in HCN2 mRNAs. In mammals, two genes encode for TRs, namely, the TRα and TRβ receptors with their isoforms (28). Mice lacking the TRα isoform show ~20% heart rate slowing even after stimulation by T_3. Gloss and co-workers (161, 524) have produced two distinct mouse lines lacking TRα and TRβ. TR$\alpha^{-/-}$ mice have mild bradycardia and a reduction in HCN2 and HCN4 mRNAs in the heart. These effects were mimicked by hypothyroidism. In contrast,

Downloaded from physrev.physiology.org on October 4, 2011

TR$\beta^{-/-}$ mice were euthyroid and showed no significant alterations in HCN4 and HCN2 mRNAs. Consequently, Gloss et al. (161) proposed that TRα is the target for T_3 in the heart and is responsible for the regulation of heart automaticity by TH. However, the functional expression of ion channels in SAN cells of TR$\alpha^{-/-}$ mice has not been studied. It is possible that T_3 affects the expression of proteins other than HCN in the SAN. For instance, down-regulation of NCX and concomitant augmentation of Na^+-K^+-ATPase in hypothyroid hearts has been reported (303).

Parathyroid (PTH) hormones accelerate heart rate. Hara et al. (189) have studied the effects of PTH on pacemaker activity in rabbit SAN and canine Purkinje fibers. PTH reversibly accelerated pacing rate in both preparations and augmented the I_f maximal conductance by 68% (189). The effect of PTH was due to an increase in the slope of diastolic depolarization. In isolated rabbit SAN cells, Cs^+ inhibited the effects of PTH much better than the VDCC blocker verapamil. Hara et al. (189) have thus proposed that I_f is the predominant mechanism by which PTH increases heart rate.

D. Mechanical Load and Atrial Stretch

The cardiac cycle is associated with periodical filling of the atrial chambers. Changes in the venous return thus affect the diastolic atrial dimensions. An increase in the right atrial filling stretches the atrial wall, as well as the SAN. Atrial stretch due to venous return can have a direct effect on pacemaker activity. Bainbridge (17) reported that injection of fluids into the jugular vein of anesthetized dogs elevated venous return and increased the heart rate. This phenomenon is still referred to as the "Bainbridge reflex." Other investigators repeated Bainbridge's experiments and observed a positive or negative in vivo chronotropic response under various experimental conditions (see Refs. 177, 251 for review). In vivo, this variability has been accounted for by a dependence of the Bainbridge reflex from the initial heart rate (95, 99).

Even if Bainbridge had attributed the positive chronotropic response to a reduced vagal tone upon increased venous return, there is now substantial evidence indicating that at least part of the Bainbridge reflex is due to an intrinsic control of SAN pacemaking by the mechanical load of the atrium. Indeed, it is possible to reproduce a positive chronotropic response to stretch in SAN tissue (108), and on Purkinje fibers automaticity (233). These results strongly suggest that the Bainbridge effect is, at least in part, an intracardiac phenomenon. In this respect, Wilson and Bolter have excluded that the Bainbridge reflex can be due to a stretch effect on intracardiac neurons (527). Furthermore, and consistent with early in vivo evidence (95), Cooper and Kohl (99) have reported that the direction of the chronotropic effect (positive or negative) induced by cell stretch depends on the initial cell pacing rate. At the species level, the chronotropic effect will be positive or negative depending on the mean resting cellular rate of the species considered (99).

Cooper et al. (100) have shown that pacemaker activity of SAN cells can be intrinsically mechano-modulated via activation of SACs, because application of the GsMTx-4 toxin, which blocks SACs, prevents the positive chronotropic response to stretch in guinea pig SAN tissue strips (99). The action of stretch on SAN cells can explain, in part, the differences in pacing rate of isolated pacemaker cells and in vivo heart rate, because electrophysiological experiments are generally performed on mechanically unloaded myocytes (251). Beside SACs, it is likely that the mechanosensitivity of other ion channels can also be involved in the chronotropic response to stretch of SAN cells. For example, Lin et al. (287) have reported that HCN channels are mechanosensitive. Regulation of pacemaker activity by atrial filling can be relevant for the fine beat-by-beat modulation of heart rate. Cooper et al. (99) have highlighted that regulation of the diastolic phase by mechanical load is useful for initiating a new heartbeat when the venous return is elevated (99). Somewhat conflicting evidence exists as to the physiological relevance of Bainbridge's reflex in humans. Slovut et al. (463) have proposed that stretch-induced modulation of SAN automaticity can be responsible of the respiratory sinus arrhythmia in cardiac allograft recipients (see also sect. VII*A*). This suggestion is based on the observation that in ~23% of patients studied, the heart rate oscillated with arterial pulse pressure (463). These authors have also shown that intrinsic cardiac neurons are not involved in this phenomenon so that HRV could be related to Bainbridge's reflex. On the other hand, Casadei et al. (76) have reported that, in normal subjects, the nonneuronal component of HRV is negligible at rest and that this component augments only in conditions of ganglionic block during strong exercise. It is thus possible that, in humans, Bainbridge's reflex can become relevant under particular physiological conditions (e.g., under reduced or blocked autonomic tone), while under basal conditions, the autonomic nervous system dominates the beat-by-beat regulation of heart rate.

E. Electrolytes and Temperature

By affecting SAN pacemaker activity, the extracellular ionic environment (89, 447, 448) and the body temperature can influence the heart rate.

In conditions of cardiac ischemia or intense exercise, there is a significant augmentation of the extracellular K^+

Downloaded from physrev.physiology.org on October 4, 2011

and of the sympathetic tone (75). In the SAN, an increase in the extracellular K^+ concentration shifts the leading pacemaker site (292) (Fig. 6) and depolarizes the maximum diastolic potential (240, 248). It has been proposed that increased extracellular K^+ will reduce the contribution of I_f to the diastolic depolarization (240), but such an effect would be difficult to demonstrate, because K^+ will also enhance the I_f Na^+ conductance (89). The negative chronotropism associated with increased extracellular K^+ may thus be attributed to a reduction of I_{Kr} current (240). Choate et al. (89) have reported that in intact SAN preparations, the positive chronotropic effect observed after stimulation of the sympathetic ganglion is reduced when the extracellular K^+ is raised. These authors have proposed that such a mechanism may protect the ischemic heart from deleterious effects of an excessive sympathetic input (89). Ca^{2+} and Mg^{2+} also affect SAN chronotropism and can induce pacemaker shift (373, 378). Ca^{2+} has a positive chronotropic effect, while Mg^{2+} induces negative chronotropism (378). Mg^{2+} also interferes with autonomic regulation of SAN pacemaking, possibly by preventing pacemaker shift associated with norepinephrine and ACh (378) (see Fig. 6). Acidosis of the extracellular environment induces negative chronotropism (399, 469). This mechanism can be responsible for bradycardia during parturition (469) or under ischemic conditions (164). Changes in heart rate following alterations in the ionic concetrations of blood plasma have been reported also in humans. For example, Severi and co-workers (447, 448) have shown that even moderate (within the physiological range) changes in the plasma concentration of Ca^{2+}, K^+, and H^+ induce significant changes in the heart rate of human subjects, thus highlighting the importance of plasma electrolyte composition in regulating cardiac automaticity.

The effects of temperature on pacemaking can be roughly distinguished between short-term effects (e.g., transient changes in pacing rate) or long-term effects that represent adaptation to low temperatures. In vivo, lowering the temperature induces reduction of the SAN rhythm and conduction time (247, 271). In the intact SAN, the effects of temperature on pacemaking can also be associated with pacemaker shift (271). Le Heuzey et al. (271) reported that lowering the temperature in isolated rabbit SAN preparations induces a caudal shift of the leading pacemaker site. Hof et al. (202) have shown that a drop in the temperature below the physiological range can also interfere with the chronotropic effect of extracellular Ca^{2+}, a phenomenon which seems also to be due to pacemaker shift.

It has been recently demonstrated that pacemaking can show long-term adaptation to low environmental temperatures (193). Haverinen and Vornanen (193) reported that rainbow trout bred at low water temperature have increased heart rate. These authors have shown increased I_{Kr} density in isolated sinus venous cells of low-temperature bred fish. These results demonstrate that ionic currents involved in pacemaking can be modulated on a long-term basis to adapt to environmental constraints.

SAN tissue seems also particularly resistant to long-term exposure to low temperatures. Nishi et al. (357) have shown that SAN automaticity can be recovered unscathed after several days in cold Tyrode's solution (5°C), while the surrounding atrial tissue becomes completely unexcitable. Similarly, Furuse et al. (147) reported that SAN pacemaking is resistant to cold cardioplegia. Resistance of SAN pacemaking to low temperatures has been exploited clinically for cardioprotection during heart surgery, grafting and, more generally, for clinical hypothermia (259, 382, 409). Indeed, heart rate slowing induced by low temperatures increases coronary blood flow, via an improvement of diastolic atrial filling (10). Clinical hypothermia can be very important in the treatment of ischemic heart disease, because elevated body temperature is associated with worsening of ischemia-induced myocardial necrosis (178).

Increased body temperature can directly affect the heart rate (51, 98, 188, 239). Core temperature elevation can significantly increase SAN rate during exercise (51). Fever also induces a direct positive chronotropic response (98, 188, 239). In a clinical study by Kiekkas et al. (239), it was noted that increase of core temperature during fever episodes was followed by a significant increase in heart rate and a decrease in arterial blood pressure. Alterations of heart rate and arterial blood pressure were significantly affected by magnitude of fever (239).

X. GENETIC AND ACQUIRED DISEASES OF CARDIAC AUTOMATICITY

A. Inherited Dysfunction of SAN Automaticity

Propagation of the heartbeat requires coordination between impulse generation and the spread of cardiac excitation through the conduction system, which delivers the impulse to the working myocardium. Genetic or acquired dysfunction of cardiac ion channels can lead to debilitating and life-threatening arrhythmias or heart block. Arrhythmias are generally linked to desynchronization of the sequential activation of the heart, or to defects in myocardial repolarization. Acquired arrhythmogenic diseases can be secondary to medical interventions, including cardiac surgery and/or drug administration. Furthermore, cardiac ischemia and heart failure can favor the genesis of arrhythmias and sudden death (266, 315). Several mutations in genes coding for cardiac ion channels

Downloaded from physrev.physiology.org on October 4, 2011

have been identified and shown to be linked to either inherited dysfunction of the heartbeat or enhanced susceptibility to drug-induced arrhythmias (92, 236). During the last few years, alterations in ion channels contributing to the genesis and regulation of pacemaker activity have been found, and some insight into possible physiopathological mechanisms underlying inherited dysfunction of automaticity is now available.

SAN dysfunction (SND) accounts for half of the number of patients requiring implantation of an electronic pacemaker device (266). SND is characterized by a combination of symptoms including fatigue and syncope. Bradycardia, SAN arrest, or exit block are typical features of SND (315). In some cases, alternating periods of bradycardia and tachyarrhythmias can be observed in SND patients (36). In a substantial number of cases, SND is associated with acquired cardiac conditions, such as heart failure, ischemia, cardiomyopathy, or administration of antiarrhythmic drugs. However, in a significant percentage of patients, SND is unrelated to structural abnormalities of the heart, but shows familial legacy (274, 301, 436).

To date, three mutations underlying SND have been identified in the human HCN4 gene (hHCN4) (330, 443, 486). In a recent case report, Schultze-Bahr et al. (443) have identified a hHCN4 mutation that caused sinus bradycardia with intermittent atrial fibrillation and loss of exercise-dependent increase in heart rate in a patient. This mutation named (hHCN4–573X) generates a truncation at the protein COOH terminus upstream to the channel cAMP-binding domain (CNBD). Recombinant hHCN4 and hHCN4–573X channels have similar voltage dependence. However, hHCN4–573X channels are insensitive to cAMP. Coexpression of hHCN4–573X with normal recombinant hHCN4 channels indicates that mutant channels have a dominant-negative effect so that coexpressed f-channels cannot be facilitated by cAMP. Insensitivity of hHCN4–573X channels to cAMP can explain SAN bradycardia and autonomic incompetence in patients carrying the hHCN4–573X mutation (443). It is possible that atrial fibrillation could be secondary to bradycardia. Ueda et al. (486) have searched for mutations in ion channel genes in a series of 25 unrelated patients having SND, conduction disturbances, and idiopathic ventricular fibrillation. A missense mutation in hHCN4 (hHCN4-D553N) has been identified in this survey. This mutation is located in the linker region between the transmembrane core and the intracellular COOH terminus of hHCN4. The D553N mutation seems to affect cellular trafficking of hHCN4 channels. In coexpression experiments, hHCN4-D553N channels reduced I_f current mediated by normal HCN4 channels, suggesting a dominant negative suppression of HCN4. In a patient carrying the hHCN4-D553N mutation, severe bradycardia with associated prolongation of the Q-T interval was present. Also, a long sinus pause, followed by polymorphic ventricular tachycardia, has been recorded (486).

A mutation named hHCN4-S672R has been recently identified by Milanesi et al. (330) in members of a large Italian family. Compared with the other two mutations discussed above, hHCN4-S672R is associated with congenital asymptomatic bradycardia and is inherited as an autosomal dominant allele. Affected individuals have mild bradycardia (mean heart rate is 52 beats/min) without other associated arrhythmias. The hHCN4-S672R maps in the CNBD, yet affected f-channels are normally responsive to cAMP. However, coexpressing normal hHCN4 with hHCN4-S672R channels yields currents that activate at voltages ~10 mV more negative than wild-type hHCN4-mediated currents (330). We can infer that such a negative shift in the I_f activation curve results in diminished I_f-mediated inward current in the diastolic depolarization range, leading to slowed basal heart rate. Milanesi et al. (330) have emphasized the similarity between the moderate reduction of heart rate in patients carrying hHCN4-S672R mutation and the effect of low ACh doses (10–30 nM) on pacemaking of isolated rabbit SAN cells. Another hHCN4 familial mutation, namely, G480R, has been recently identified by Nof et al. (361). The hHCN4-G480R maps in the pore domain. Affected f-channels activate at more negative voltages than wild-type counterparts and have defective regulation of intracellular trafficking. Individuals carrying hHCN4-G480R have asymptomatic bradycardia (361).

SAN bradycardia has also been shown in association with congenital heart block (CHB) (209). CHB is characterized by progressive complete atrioventricular block affecting fetuses and newborns (see Ref. 55 for review). CHB is generally detected just before or immediately after birth (512). CHB is due to production of autoantibodies against intracellular soluble ribonucleoproteins named 48 kDa SSB/La, 52 kDa SSA/Ro, and 60 kDa SSA/Ro (512). Hu et al. (209) have reported inhibition of $I_{Ca,L}$ and $I_{Ca,T}$ by IgGs isolated from mothers having CHB-affected children. It is thus tempting to speculate that downregulation of $Ca_v1.3$ and $Ca_v3.1$ channels by maternal antibodies underlies SAN bradycardia in CHB (209). This hypothesis has been recently supported by Qu et al. (406), who showed that the $Ca_v1.3$ channel protein is expressed in the human fetal heart and that anti-Ro/La antibodies can effectively inhibit $Ca_v1.3$-mediated $I_{Ca,L}$ expressed in tsA201 cells.

Mutations in $Na_v1.5$ channels can also cause SND. Benson et al. (33) have recently described two mutations in the $Na_v1.5$ gene leading to recessive disorders of cardiac conduction, characterized by bradycardia progressing to atrial unexcitability during infancy. It is unclear whether bradycardia is due to dysfunction of the impulse generation in the SAN or to partial block of intranodal conduction.

Downloaded from physrev.physiology.org on October 4, 2011

B. Automaticity in Heart Failure and Cardiac Ischemia

Heart failure (HF) is a major risk factor for life-threatening ventricular arrhythmias and sudden death. HF carries a poor prognosis; mortality rates at 5 years for untreated or poorly treated HF are close to 60% (231). ECG recordings in HF patients show decreased mean heart rate and heart rate variability (223, 375). Remodeling of intrinsic SAN function and regulation by the autonomic nervous system has been observed in HF. For example, Sanders et al. (434) have mapped SAN activation and conduction reserve in 18 HF patients. They have shown complex rearrangements of SAN excitability, including alteration of intranodal conduction, prolongation of the SAN recovery time, and a caudal shift of the leading pacemaker site. Experimental animal models of HF fairly reproduce clinical observations (see the recent review by Janse, Ref. 221). Opthof et al. (376) have investigated SAN function in a rabbit model of HF associated with sudden death. Isolated right atrial preparations of HF rabbits (376) show a decrease in the intrinsic SAN rate and an increase in the sensitivity to ACh. However, in spite of such an enhancement of negative chronotropic factors, sudden death is still observed in these animals at accelerated heart rates. Opthof et al. (376) have suggested that the reduction of intrinsic SAN rate constitutes an adaptation mechanism to counteract an augmentation in sympathetic tone and its arrhythmogenic potential, and to optimize myocardial oxygen consumption. Verkerk et al. (503) have reported that isolated SAN cells from HF rabbits have an intrinsically longer cycle length and show a 40% reduction of I_f (and 20% of I_{Ks}) compared with control cells. The slope of the diastolic depolarization appears to be specifically affected by HF. Verkerk et al. (503) have thus proposed that the intrinsically slower SAN rate observed in HF animal models (and possibly in humans) is due to I_f downregulation. Consistent with these findings, a strong reduction in HCN4 and HCN2 mRNA and protein in the SAN has been reported by Zicha et al. (548) using a canine model of congestive HF. Disease seems also to have differential effects on the SAN and the atria, since HF induced an increase in HCN4 expression in atrial tissue. It is possible that HCN upregulation can contribute to the development of supraventricular arrhythmias associated with HF (548).

Cardiac ischemia can induce SND. Bradycardia is commonly observed upon resuscitation after cardiac arrest or ventricular fibrillation (379). Severe bradycardia following cardiac ischemia is a major cause of poor survival after cardiac arrest (156, 379). SAN artery stenosis or occlusion is another factor leading to bradycardia in patients (5) and dogs (85). Heart rate slowing can be observed in Langendorff-perfused hearts upon ischemia-reperfusion (337). Considerable interest exists therefore in elucidating the mechanisms of ischemia-induced bradycardia for managing cardiac ischemic disease and cardiac arrest. The cellular basis of ischemia-dependent bradycardia is not entirely understood. Slowing of diastolic depolarization, reduction in action potential amplitude, and depolarization of the maximum diastolic potential have been consistently observed in isolated rabbit atria during hypoxia (446) or metabolic inhibition (253). Similar changes in the pacemaker cycle parameters have been recently reported in isolated rabbit SAN cells by Gryshenko et al. (164), using a low pH (6.6) "ischemic" Tyrode's solution to mimic acidosis of the extracellular environment in ischemic conditions (see Ref. 75 for review). These effects were reversible when switching back to normal Tyrode's solution. Metabolic inhibition of rabbit SAN cells attenuates $I_{Ca,L}$, I_{Kr}, and I_f (180) and activates $I_{K,ATP}$ (184). In contrast, Gryshenko et al. (164) have observed an augmentation of the instantaneous net inward current upon hyperpolarization, an effect attributed to acidosis-dependent reduction of I_{KACh} (even if the induction of an inward background current cannot be excluded). Furthermore, reduction in $I_{Ca,T}$ and I_{NCX} has been reported by Du and Nathan (133). It is a surprising finding of this work that $I_{Ca,L}$ was augmented by ischemic Tyrode's solution. However, as suggested by Du and Nathan (133), such an augmentation may not lead to a positive chronotropic effect, since the more positive maximum diastolic potential, induced by ischemic Tyrode's solution, can accentuate $I_{Ca,L}$ inactivation. From the above results, it is difficult to attribute ischemia-induced slowing of cardiac automaticity to a single ionic mechanism. Furthermore, it is possible that a given ionic current can be more or less affected depending on the experimental conditions (e.g., acidosis or direct metabolic inhibition). Future investigations will further elucidate the cellular mechanisms of ischemia-induced bradycardia and SND.

XI. HEART AUTOMATICITY AND CARDIOPROTECTION

In the preceding sections, we have discussed the mechanisms underlying automaticity and its regulation by the autonomic nervous system, hormones, and different physiopathological conditions including cardiac ischemia and HF. We will now review recent pharmacological and gene therapy approaches aiming to control pacemaker activity and heart rate in cardiac disease. These new therapeutic strategies are currently focused on f-channels and reduction in I_{K1}. Indeed, the capability of I_f to modulate the slope of the diastolic depolarization renders f-channels suitable targets for pharmacological regulation

Downloaded from physrev.physiology.org on October 4, 2011

of heart rate and for creating "biological pacemakers" in the diseased myocardium.

A. Heart Rate and Cardiac Morbidity

The mean resting heart rate is correlated with all-cause cardiovascular mortality and morbidity. The Framingham epidemiological study has highlighted the association between elevated heart rate and all-cause mortality (134, 160, 232). The mechanistic link between heart rate and mortality is still unclear. Perski et al. (389) presented evidence supporting the hypothesis that elevated heart rate contributes to the progression of atherosclerosis in postinfarct patients. In subjects with ischemic cardiac disease such as stable angina pectoris, elevated heart rate can cause an imbalance between myocardial oxygen supply and the actual physiological demand. Heart rate is inversely correlated with the degree of filling of the left ventricle with oxygen-rich blood (10). A better irrigation of the coronary system is achieved by a reduction of the heart rate (10). Andrews et al. (9) have confirmed this prediction at the clinical level by showing that lowering heart rate with propranolol effectively prevents cardiac ischemic episodes. Development of therapeutically active molecules, able to reduce heart rate, is thus of outstanding interest. Targeting of ion channels specifically involved in the regulation of diastolic depolarization rate constitutes a natural approach toward this goal. β-Blockers (201) and I_f inhibitors (123) are effective in reducing ischemic episodes and cardiac mortality by virtue of their heart rate-reducing action. Specific reduction of heart rate is now considered as a new therapeutically effective approach to manage cardiac ischemia (123, 201).

Among I_f inhibitors, the only molecule that has been clinically developed for treatment of stable angina pectoris is ivabradine (123). In animal models, ivabradine limits exercise-induced tachycardia and improves the balance between myocardial oxygen supply and demand (97). To date, no inotropic (461) or dromotropic effects (96) have been reported for ivabradine. A phase II clinical study, conducted on patients with stable angina, has confirmed specific heart rate reduction at rest and during exercise and shown the efficacy of ivabradine as an anti-ischemic and antianginal agent (52). The in vivo pharmacological properties of ivabradine are consistent with a specific action on I_f in the SAN. Compared with β-blockers, ivabradine seems more effective in preserving myocardial recovery and performance after cardiac stunning (52). The f-channel is the first ion channel underlying pacemaking to be targeted by a therapeutically active drug. It is possible that other channel classes, such as $Ca_v1.3$ and $Ca_v3.1$ channels, will constitute future pharmacological targets for the development of new molecules to regulate heart rate without negative inotropism.

B. Automaticity in Engineered "Biological Pacemakers"

1. Direct gene transfer of "pacemaker" channels in cardiac cells

Identification of ion channels involved in cardiac automaticity harbors the attractive perspective of engineering "biological" pacemakers to stimulate automaticity in defined regions of the heart (Fig. 27). Biological pacemakers have been proposed as a possible alternative to electronic devices (424), even if a biological pacemaker can also work in combination with an electronic pacemaker (421). Several up-to-date reviews have been recently published on this topic (421, 423, 424). Here, we focus on some fundamental aspects of biological pacemakers. The first gene therapy approach to increase pacemaker activity in the working myocardium came from experiments in which a cDNA encoding for the β_2-adrenergic receptor was injected in the right atrium of mouse (137) and pig (138). Overexpression of β_2-receptors increased the basal heart rate in both animal models (137, 138).

A gene therapy approach was employed by Miake et al. (327) to generate pacemaker activity in the ventricular myocardium of guinea pigs. In this work, adenoviral gene transfer of a dominant negative Kir2.1 subunit (Kir2.1AAA) has been employed (327). This construct downregulated I_{K1} by 80% in ~20% of ventricular myocytes tested (328). Depolarization of the resting potential to −60 mV generated a diastolic depolarization phase in ventricular myocytes and triggered premature ventricular beats in vivo (327). On the basis of these results, Miake et al. (327) have suggested that the working myocardium is also endowed with automaticity, but pacemaking in ventricular cells is naturally repressed by I_{K1} expression. This proposal challenges the view that automaticity depends on the expression of particular "pacemaker" ion channel. Silva and Rudy (459) and Kurata et al. (263) have studied the possible mechanisms of automaticity in ventricular cells expressing Kir2.1AAA by employing modified versions of the Luo and Rudy model of ventricular action potential (298). Numerical simulations suggest that automaticity in these cells can be generated by I_{NCX} (459), or by $I_{Ca,L}$ and I_{NCX} (263). Particularly, CICR triggered by $I_{Ca,L}$ during the action potential would stimulate I_{NCX}, which depolarizes the cell membrane to begin a new cycle (459), while $I_{Ca,L}$ can be responsible for a membrane voltage instability which promotes automaticity (263). Silva and Rudy have proposed also that β-adrenergic stimulation of the ventricular I_{NCX}-driven pacemaker mechanism could not exceed 25%. Consequently, the automaticity in Kir2.1AAA-expressing cells probably lacks the sensitivity to autonomic regulation needed to sustain everyday life. Viswanathan et al. (511) have further assessed, by numerical modeling, the problem of

Downloaded from physrev.physiology.org on October 4, 2011

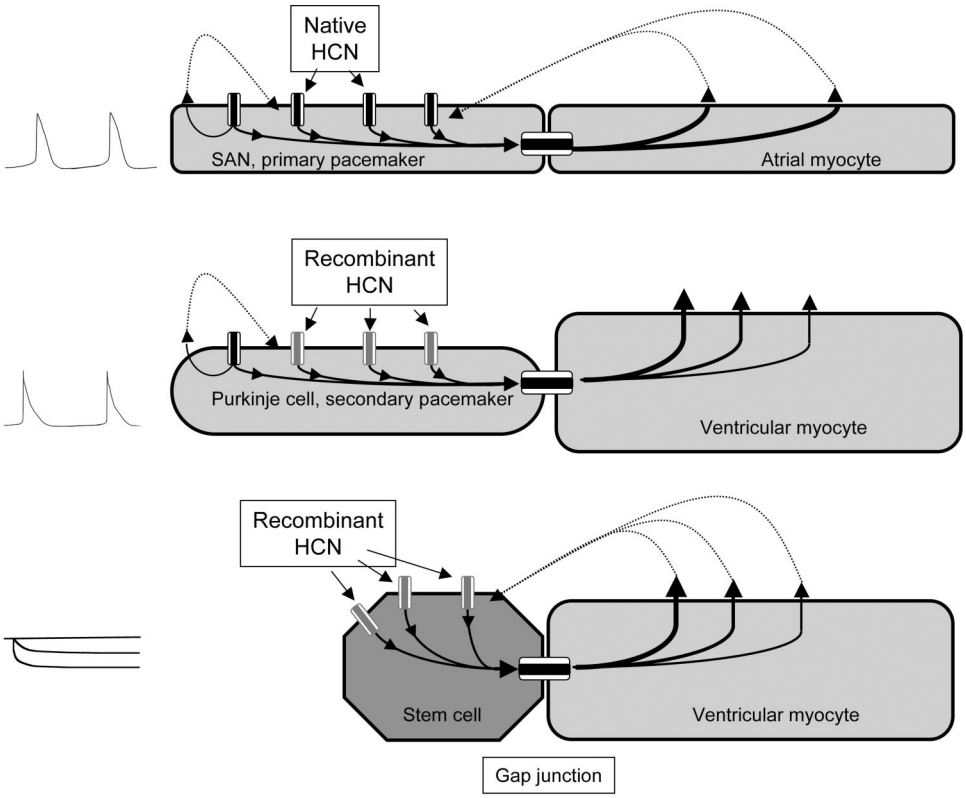

FIG. 27. The primary SAN pacemaker cell is the natural pacemaker (*top panel*). In SAN cells, high expression of native HCN channels (black channels) contributes to SAN pacemaker dominance and to the autonomic regulation of heart rate. The SAN pacemaker cycle (*top*, *left*) drives the right atrium at a physiological suitable rate. In case of SAN failure or AVN block, the intrinsic pacing rate of the Purkinje fibers network could be enhanced by gene transfer of recombinant HCN channels (gray channels) in the bundle branches. The ideal Purkinje cell (*middle panel*) will thus drive the ventricular cell at a faster frequency than under normal conditions, thereby generating a physiologically suitable ventricular basal rate. The sensitivity of HCN channels to cAMP is also potentially important for creating a ventricular pacemaker that can be regulated by the autonomic nervous system. A stem cell-derived biological pacemaker (*bottom panel*) is based on overexpression of recombinant HCN channels in unexcitable stem cells implanted in a target region of the working myocardium. Stem cells connect to ventricular cells by forming gap junctions with ventricular cells. The positive membrane potential of stem cells will cyclically drive ventricular cells to the action potential threshold. [Adapted from Robinson et al. (421).]

automaticity in directly transfected ventricular cells. These authors have suggested that to obtain stable automaticity, both downregulation of I_{K1} and expression of HCN channels are required (511).

Overexpression of HCN channels by gene transfer constitutes another strategy for creating biological pacemakers (421). This approach is based on the experimental observation that expression of HCN2 or HCN4 channels in cultured neonatal ventricular myocytes robustly improves cellular automaticity (143, 403). Expression of a dominant negative HCN2 subunit abolished automaticity (143). These observations indicate that HCN channels are able to confer automaticity to myocardial cells upon gene transfer. Qu et al. (405) took advantage of this new concept and employed gene transfer of HCN2 channels in vivo in the canine left atrium. Qu et al. (405) have shown that I_f expression in atrial myocytes generated viable atrial rhythms upon inhibition of SAN activity. Plotnikov et al. (394) have employed gene transfer of HCN2 channels to stimulate automaticity in the left bundle branch of the Purkinje fiber network (Fig. 27). In this work, adenoviral gene transfer of HCN2 channels improved the rate of ventricular rhythms observed after inhibition of SAN activity by transient vagal stimulation. To evaluate the sensitivity of these ventricular rhythms to autonomic agonists, radiofrequency ablation of the AVN was performed to dissociate the atrial rhythm from that originating from the left bundle branch (421). In these conditions, ventricular rhythms were significantly responsive to epinephrine (421).

Bucchi et al. (69) have employed gene transfer of a mutant HCN2 channel having a positively shifted activation curve midpoint (−46 versus −66 mV for wild-type HCN2 channels). Compared with rhythms generated by wild-type HCN2 channels, expression of mutant HCN2 channel significantly improved the responsiveness of ventricular rhythms to catecholamines. Expression of HCN4 channels in the ventricle also seems to create β-adrenergic modulation of ventricular escape rhythms (71). Modification of HCN voltage dependency to favor channel opening at positive voltages has been employed also by Tse et al. (483). These authors have shown that focal

Downloaded from physrev.physiology.org on October 4, 2011

expression of a mutant form of HCN1 in the left atrium reduces the dependence on electronic pacemakers of SAN-ablated pigs (483).

2. Stem-cell based gene transfer

An alternative approach for creating biological pacemakers consists in overexpressing HCN channels in unexcitable human mesenchymal stem cells (hMSCs). These cells have the natural capability of coupling to cardiac myocytes via gap junctions (400). When unexcitable hMSCs connect to myocytes, their membrane potential will become more negative due to the electrotonic influence of myocytes. Membrane hyperpolarization will activate HCN channels, thereby generating inward current that is fed back to the myocyte to trigger an action potential [Fig. 27, see Robinson et al. (421) for further discussion]. Action potential repolarization will then tend to shut off HCN channels in the hMSC before the beginning of a new cycle. Potapova et al. (400) have reported that HCN2-mediated currents expressed in hMSCs are sensitive to isoproterenol, indicating that the signaling pathway necessary for HCN channel regulation is present in hMSCs. For a more detailed discussion on the clinical and experimental problems associated with stem cell transfection and implantation in the heart, the reader is referred to the review by Rosen et al. (423). Downregulation of I_{K1} in ventricular cells could also be employed to achieve robust stem cell-mediated pacemaking (230). Gene transfer of stem cells may not constitute an exclusive approach to create biological pacemakers based on cell therapy. Indeed, it is possible that also fibroblasts can be genetically modified to express ion channels (144). Fibroblasts are spontaneously capable of connecting with cardiomyocytes in vitro and can affect conduction between myocytes (144). In cell culture, Kizana et al. (243) have obtained functional electrical coupling between myotubes differentiated from MyoD-Cx43 coexpressing fibroblasts. Interestingly, these authors have reported that coexpression of Cx43 with MyoD was critical for observing electrical coupling and uniform threshold for excitation between adjacent myotubes (243). Cx43 expression also enhances electrical coupling between neonatal cardiomyocytes and fibroblasts in cell culture (244). Expression and modulation of appropriate Cxs together with ion channels can thus be an important step for overcoming the problem of poor electrical coupling between stem cells and myocytes in situ. This potential approach is supported by a numerical modeling study by Jacquemet (219), who emphasized that fibroblasts can significantly affect myocardial conduction only if the degree of coupling between fibroblast and myocytes is sufficiently high.

In conclusion, establishment of biological pacemakers in defined regions of the heart is a fascinating perspective for the cellular therapy of the heartbeat. A biological pacemaker may also necessitate the coexpression or modification of more than one type of ion channel to reach a suitable degree of intrinsic automaticity and autonomic regulation of pacemaking (263, 511). The observation that the Tbx3 transcription factor can reprogram nonpacing atrial cells to a phenotype similar to that of automatic cells may also open new perspectives into the creation of biological pacemakers (208).

XII. CONCLUDING REMARKS

Our understanding of cardiac automaticity has progressed considerably during the last 10 years. Indeed, at the beginning of the 1990s, the study of the generation of pacemaker activity was somewhat limited to the electrophysiological description of ion currents in spontaneously active cells. Molecular cloning of gene families coding for ion channels has since allowed investigation of gene expression in cardiac tissue and the establishment of genetically engineered mouse lines that show specific dysfunctions of cardiac automaticity. These lines are now yielding precious insights into the generation and regulation of pacemaking and will probably constitute new animal models of heart rhythm pathologies. We can expect that the molecular basis of many inherited diseases of cardiac automaticity will be elucidated in the near future and that different ion channels and proteins regulating Ca^{2+} handling will be involved in such diseases.

Several questions on how the heart rhythm is generated and controlled in physiological and pathological conditions remain unanswered. It is not completely understood, for example, which ion channels are essential for generating the diastolic depolarization in the SAN, AVN, and the Purkinje fibers network, and which mechanisms play a dominant role in the autonomic regulation of automaticity in humans. The interactions between the membrane "ion channels clock" and the intracellular "Ca^{2+} clock" are not completely elucidated. Nevertheless, these interactions are of fundamental importance for understanding the integration of pacemaker mechanisms at the cellular level.

From the above discussion, it also appears that cardiac automaticity at the organ level is a very complex phenomenon and that, beside cellular mechanisms, integrative factors are involved in cardiac pacemaking. These factors include the heterogeneity of SAN and AVN tissue organization and the regulation of heart rate by mechanical load and by several humoral, environmental, and pathophysiological states.

Finally, ion channels involved in automaticity, such as f-channels, are now becoming potential new drug targets. In this respect, the development of specific heart rate-reducing agents underlines the importance of pursu-

Downloaded from physrev.physiology.org on October 4, 2011

ing the effort of obtaining further insight into the cardiac pacemaker mechanisms. The engineering of "biological pacemakers" is currently based on expression and manipulation of K_{ir} and f-channels in native myocardium or in stem cells. Other complementary approaches can be the use of fibroblasts and, possibly, manipulation of Cxs. It will also be interesting to see if future approaches will also include coexpression of other ion channels involved in "native" automaticity.

NOTE ADDED IN PROOF

After acceptance of this manuscript, Li et al. (284a) have proposed a detailed anatomical model of the rabbit AVN. Numerical simulations of impulse conduction through AVN are consistent with the hypothesis that automaticity originates in the PNE of the AVN.

Harzeim et al. (190a) have shown that abolition of cAMP sensitivity of HCN4 channels by knock-in of a point mutation in the channel CNBD prevents β-adrenergic stimulation of heart rate in mouse embryos and lethality as in HCN4 knockout embryos.

ACKNOWLEDGMENTS

We thank Patrick Atger for excellent technical skills in creating and editing the manuscript figures. We are indebted to Elodie Kupfer and Anne Cohen-Solal for breeding and managing mouse lines in our group. We thank Peter Kohl and Etienne Verheijck for helpful discussion. We also thank Halina Dobrzynski, Mark Boyett, and Dario DiFrancesco for sharing figure originals.

Address for reprint request and other correspondence: M. E. Mangoni, Institute of Functional Genomics, Dept. of Physiology CNRS UMR5203, INSERM, U661, Univ. of Montpellier I, Univ. of Montpellier II, Montpellier, F-34094 France (e-mails: matteo.mangoni@igf.cnrs.fr; joel.nargeot@igf.cnrs.fr).

GRANTS

Work in our laboratory has been supported by grants from the CNRS, the Action Concertée Incitative in Physiology and Developmental Biology of the French Ministry of Education, the INSERM National Program for Cardiovascular Diseases, the Fondation de France and the Agence Nationale pour la Recherche (ANR). We also thank the International Research Institute Sevier (IRIS) for having supported research activity in our group.

REFERENCES

1. **Abi-Gerges N, Ji GJ, Lu ZJ, Fischmeister R, Hescheler J, Fleischmann BK.** Functional expression and regulation of the hyperpolarization activated non-selective cation current in embryonic stem cell-derived cardiomyocytes. *J Physiol* 523: 377–389, 2000.
2. **Accili EA, Proenza C, Baruscotti M, DiFrancesco D.** From funny current to HCN channels: 20 years of excitation. *News Physiol Sci* 17: 32–37, 2002.
3. **Accili EA, Redaelli G, DiFrancesco D.** Activation of the hyperpolarization-activated current (i_f) in sino-atrial node myocytes of the rabbit by vasoactive intestinal peptide. *Pflügers Arch* 431: 803–805, 1996.
4. **Accili EA, Robinson RB, DiFrancesco D.** Properties and modulation of I_f in newborn versus adult cardiac SA node. *Am J Physiol Heart Circ Physiol* 272: H1549–H1552, 1997.
5. **Alboni P, Baggioni GF, Scarfo S, Cappato R, Percoco GF, Paparella N, Antonioli GE.** Role of sinus node artery disease in sick sinus syndrome in inferior wall acute myocardial infarction. *Am J Cardiol* 67: 1180–1184, 1991.
6. **Alings AM, Abbas RF, Bouman LN.** Age-related changes in structure and relative collagen content of the human and feline sinoatrial node. A comparative study. *Eur Heart J* 16: 1655–1667, 1995.
7. **Altomare C, Terragni B, Brioschi C, Milanesi R, Pagliuca C, Viscomi C, Moroni A, Baruscotti M, DiFrancesco D.** Heteromeric HCN1-HCN4 channels: a comparison with native pacemaker channels from the rabbit sinoatrial node. *J Physiol* 549: 347–359, 2003.
8. **An WF, Bowlby MR, Betty M, Cao J, Ling HP, Mendoza G, Hinson JW, Mattsson KI, Strassle BW, Trimmer JS, Rhodes KJ.** Modulation of A-type potassium channels by a family of calcium sensors. *Nature* 403: 553–556, 2000.
9. **Andrews TC, Fenton T, Toyosaki N, Glasser SP, Young PM, MacCallum G, Gibson RS, Shook TL, Stone PH.** Subsets of ambulatory myocardial ischemia based on heart rate activity. Circadian distribution and response to anti-ischemic medication The Angina and Silent Ischemia Study Group (ASIS). *Circulation* 88: 92–100, 1993.
10. **Anrep GV, Hausler H.** The coronary circulation. II. The effect of changes of temperature and of heart rate. *J Physiol* 67: 299–314, 1929.
11. **Anumonwo JM, Delmar M, Jalife J.** Electrophysiology of single heart cells from the rabbit tricuspid valve. *J Physiol* 425: 145–167, 1990.
12. **Anumonwo JM, Freeman LC, Kwok WM, Kass RS.** Delayed rectification in single cells isolated from guinea pig sinoatrial node. *Am J Physiol Heart Circ Physiol* 262: H921–H925, 1992.
13. **Anumonwo JM, Tallini YN, Vetter FJ, Jalife J.** Action potential characteristics and arrhythmogenic properties of the cardiac conduction system of the murine heart. *Circ Res* 89: 329–335, 2001.
14. **Arai A, Kodama I, Toyama J.** Roles of Cl^- channels and Ca^{2+} mobilization in stretch-induced increase of SA node pacemaker activity. *Am J Physiol Heart Circ Physiol* 270: H1726–H1735, 1996.
15. **Ardell JL.** Structure and function of mammalian intrinsic cardiac neurons. In: *Neurocardiology*, edited by Armour JA, Ardell JL. New York: Oxford Univ. Press, 1994, p. 95–114.
16. **Bahinski A, Nairn AC, Greengard P, Gadsby DC.** Chloride conductance regulated by cyclic AMP-dependent protein kinase in cardiac myocytes. *Nature* 340: 718–721, 1989.
17. **Bainbridge FA.** The influence of venous filling upon the rate of the heart. *J Physiol* 50: 65–84, 1915.
18. **Baker K, Warren KS, Yellen G, Fishman MC.** Defective "pacemaker" current (I_h) in a zebrafish mutant with a slow heart rate. *Proc Natl Acad Sci USA* 94: 4554–4559, 1997.
19. **Barbuti A, Gravante B, Riolfo M, Milanesi R, Terragni B, DiFrancesco D.** Localization of pacemaker channels in lipid rafts regulates channel kinetics. *Circ Res* 94: 1325–1331, 2004.
20. **Barbuti A, Terragni B, Brioschi C, DiFrancesco D.** Localization of f-channels to caveolae mediates specific beta2-adrenergic receptor modulation of rate in sinoatrial myocytes. *J Mol Cell Cardiol* 42: 71–78, 2007.
21. **Baruscotti M, Bucchi A, Difrancesco D.** Physiology and pharmacology of the cardiac pacemaker ("funny") current. *Pharmacol Ther* 107: 59–79, 2005.
22. **Baruscotti M, Difrancesco D.** Pacemaker channels. *Ann NY Acad Sci* 1015: 111–121, 2004.
23. **Baruscotti M, DiFrancesco D, Robinson RB.** Na^+ current contribution to the diastolic depolarization in newborn rabbit SA node cells. *Am J Physiol Heart Circ Physiol* 279: H2303–H2309, 2000.
24. **Baruscotti M, DiFrancesco D, Robinson RB.** A TTX-sensitive inward sodium current contributes to spontaneous activity in newborn rabbit sino-atrial node cells. *J Physiol* 492: 21–30, 1996.

Downloaded from physrev.physiology.org on October 4, 2011

25. **Baruscotti M, Westenbroek R, Catterall WA, DiFrancesco D, Robinson RB.** The newborn rabbit sino-atrial node expresses a neuronal type I-like Na^+ channel. *J Physiol* 498: 641–648, 1997.
26. **Batulevicius D, Pauziene N, Pauza DH.** Topographic morphology and age-related analysis of the neuronal number of the rat intracardiac nerve plexus. *Ann Anat* 185: 449–459, 2003.
27. **Baumgarten CM, Clemo HF.** Swelling-activated chloride channels in cardiac physiology and pathophysiology. *Prog Biophys Mol Biol* 82: 25–42, 2003.
28. **Baxter JD, Dillmann WH, West BL, Huber R, Furlow JD, Fletterick RJ, Webb P, Apriletti JW, Scanlan TS.** Selective modulation of thyroid hormone receptor action. *J Steroid Biochem Mol Biol* 76: 31–42, 2001.
29. **Beau SL, Hand DE, Schuessler RB, Bromberg BI, Kwon B, Boineau JP, Saffitz JE.** Relative densities of muscarinic cholinergic and beta-adrenergic receptors in the canine sinoatrial node and their relation to sites of pacemaker activity. *Circ Res* 77: 957–963, 1995.
30. **Belardinelli L, Giles WR, West A.** Ionic mechanisms of adenosine actions in pacemaker cells from rabbit heart. *J Physiol* 405: 615–633, 1988.
31. **Belardinelli L, Shryock J, West GA, Clemo HF, DiMarco JP, Berne RM.** Effects of adenosine and adenine nucleotides on the atrioventricular node of isolated guinea pig hearts. *Circulation* 70: 1083–1091, 1984.
32. **Belhassen B, Pelleg A, Shoshani D, Geva B, Laniado S.** Electrophysiologic effects of adenosine-5′-triphosphate on atrioventricular reentrant tachycardia. *Circulation* 68: 827–833, 1983.
33. **Benson DW, Wang DW, Dyment M, Knilans TK, Fish FA, Strieper MJ, Rhodes TH, George AL Jr.** Congenital sick sinus syndrome caused by recessive mutations in the cardiac sodium channel gene (SCN5A). *J Clin Invest* 112: 1019–1028, 2003.
34. **Bernardi L, Salvucci F, Suardi R, Solda PL, Calciati A, Perlini S, Falcone C, Ricciardi L.** Evidence for an intrinsic mechanism regulating heart rate variability in the transplanted and the intact heart during submaximal dynamic exercise? *Cardiovasc Res* 24: 969–981, 1990.
35. **Bers DM.** Cardiac excitation-contraction coupling. *Nature* 415: 198–205, 2002.
36. **Bertram H, Paul T, Beyer F, Kallfelz HC.** Familial idiopathic atrial fibrillation with bradyarrhythmia. *Eur J Pediatr* 155: 7–10, 1996.
37. **Bescond J, Bois P, Petit-Jacques J, Lenfant J.** Characterization of an angiotensin-II-activated chloride current in rabbit sino-atrial cells. *J Membr Biol* 140: 153–161, 1994.

37a. **Bharati S.** Anatomic-morphologic relations between AV nodal structure and function in the normal and diseased heart. In: *Atrial-AV Nodal Electrophysiology: A View From the Millenium*, edited by Mazgalev TN, Tchou PJ. Armonki Futura, 2000, p. 25–48.

38. **Billette J.** Atrioventricular nodal activation during periodic premature stimulation of the atrium. *Am J Physiol Heart Circ Physiol* 252: H163–H177, 1987.
39. **Billette J.** What is the atrioventricular node? Some clues in sorting out its structure-function relationship. *J Cardiovasc Electrophysiol* 13: 515–518, 2002.
40. **Blaschke RJ, Hahurij ND, Kuijper S, Just S, Wisse LJ, Deissler K, Maxelon T, Anastassiadis K, Spitzer J, Hardt SE, Scholer H, Feitsma H, Rottbauer W, Blum M, Meijlink F, Rappold G, Gittenberger-de Groot AC.** Targeted mutation reveals essential functions of the homeodomain transcription factor Shox2 in sinoatrial and pacemaking development. *Circulation* 115: 1830–1838, 2007.
41. **Bleeker WK, Mackaay AJ, Masson-Pevet M, Bouman LN, Becker AE.** Functional and morphological organization of the rabbit sinus node. *Circ Res* 46: 11–22, 1980.
42. **Bode F, Sachs F, Franz MR.** Tarantula peptide inhibits atrial fibrillation. *Nature* 409: 35–36, 2001.
43. **Bogdanov KY, Maltsev VA, Vinogradova TM, Lyashkov AE, Spurgeon HA, Stern MD, Lakatta EG.** Membrane potential fluctuations resulting from submembrane Ca^{2+} releases in rabbit sinoatrial nodal cells impart an exponential phase to the late diastolic depolarization that controls their chronotropic state. *Circ Res* 99: 979–987, 2006.
44. **Bogdanov KY, Vinogradova TM, Lakatta EG.** Sinoatrial nodal cell ryanodine receptor and Na(+)-Ca(2+) exchanger: molecular partners in pacemaker regulation. *Circ Res* 88: 1254–1258, 2001.
45. **Bohn G, Moosmang S, Conrad H, Ludwig A, Hofmann F, Klugbauer N.** Expression of T- and L-type calcium channel mRNA in murine sinoatrial node. *FEBS Lett* 481: 73–76, 2000.
46. **Boineau JP, Canavan TE, Schuessler RB, Cain ME, Corr PB, Cox JL.** Demonstration of a widely distributed atrial pacemaker complex in the human heart. *Circulation* 77: 1221–1237, 1988.
47. **Boineau JP, Schuessler RB, Hackel DB, Miller CB, Brockus CW, Wylds AC.** Widespread distribution and rate differentiation of the atrial pacemaker complex. *Am J Physiol Heart Circ Physiol* 239: H406–H415, 1980.
48. **Bois P, Bescond J, Renaudon B, Lenfant J.** Mode of action of bradycardic agent, S 16257, on ionic currents of rabbit sinoatrial node cells. *Br J Pharmacol* 118: 1051–1057, 1996.
49. **Bois P, Lenfant J.** Evidence for two types of calcium currents in frog cardiac sinus venosus cells. *Pflügers Arch* 417: 591–596, 1991.
50. **Bois P, Renaudon B, Baruscotti M, Lenfant J, DiFrancesco D.** Activation of f-channels by cAMP analogues in macropatches from rabbit sino-atrial node myocytes. *J Physiol* 501: 565–571, 1997.
51. **Bolter CP, Atkinson KJ.** Influence of temperature and adrenergic stimulation on rat sinoatrial frequency. *Am J Physiol Regul Integr Comp Physiol* 254: R840–R844, 1988.
52. **Borer JS, Fox K, Jaillon P, Lerebours G.** Antianginal and antiischemic effects of ivabradine, an I_f inhibitor, in stable angina: a randomized, double-blind, multicentered, placebo-controlled trial. *Circulation* 107: 817–823, 2003.
53. **BoSmith RE, Briggs I, Sturgess NC.** Inhibitory actions of ZENECA ZD7288 on whole-cell hyperpolarization activated inward current (I_f) in guinea-pig dissociated sinoatrial node cells. *Br J Pharmacol* 110: 343–349, 1993.
54. **Bouman LN, Gerlings ED, Biersteker PA, Bonke FI.** Pacemaker shift in the sino-atrial node during vagal stimulation. *Pflügers Arch* 302: 255–267, 1968.
55. **Boutjdir M.** Molecular and ionic basis of congenital complete heart block. *Trends Cardiovasc Med* 10: 114–122, 2000.
56. **Boyett M, Zhang H, Garny A, Holden AV.** Control of the pacemaker activity of the sinoatrial node by intracellular Ca^{2+}. Experiments and modelling. *Philos Trans R Soc Lond B Biol Sci* 359: 1091–1110, 2001.
57. **Boyett MR, Dobrzynski H, Lancaster MK, Jones SA, Honjo H, Kodama I.** Sophisticated architecture is required for the sinoatrial node to perform its normal pacemaker function. *J Cardiovasc Electrophysiol* 14: 104–106, 2003.
58. **Boyett MR, Honjo H, Kodama I.** The sinoatrial node, a heterogeneous pacemaker structure. *Cardiovasc Res* 47: 658–687, 2000.
59. **Boyett MR, Honjo H, Yamamoto M, Nikmaram MR, Niwa R, Kodama I.** Downward gradient in action potential duration along conduction path in and around the sinoatrial node. *Am J Physiol Heart Circ Physiol* 276: H686–H698, 1999.
60. **Boyett MR, Honjo H, Yamamoto M, Nikmaram MR, Niwa R, Kodama I.** Regional differences in effects of 4-aminopyridine within the sinoatrial node. *Am J Physiol Heart Circ Physiol* 275: H1158–H1168, 1998.
61. **Boyett MR, Inada S, Yoo S, Li J, Liu J, Tellez J, Greener ID, Honjo H, Billeter R, Lei M, Zhang H, Efimov IR, Dobrzynski H.** Connexins in the sinoatrial and atrioventricular nodes. *Adv Cardiol* 42: 175–197, 2006.
62. **Brown H, Difrancesco D.** Voltage-clamp investigations of membrane currents underlying pace-maker activity in rabbit sino-atrial node. *J Physiol* 308: 331–351, 1980.
63. **Brown HF.** Electrophysiology of the sinoatrial node. *Physiol Rev* 62: 505–530, 1982.
64. **Brown HF, DiFrancesco D, Noble SJ.** How does adrenaline accelerate the heart? *Nature* 280: 235–236, 1979.
65. **Brown HF, Kimura J, Noble D, Noble SJ, Taupignon A.** The slow inward current, i_{si}, in the rabbit sino-atrial node investigated by voltage clamp and computer simulation. *Proc R Soc Lond B Biol Sci* 222: 305–328, 1984.
66. **Bucchi A, Baruscotti M, DiFrancesco D.** Current-dependent block of rabbit sino-atrial node I_f channels by ivabradine. *J Gen Physiol* 120: 1–13, 2002.

Downloaded from physrev.physiology.org on October 4, 2011

67. **Bucchi A, Baruscotti M, Robinson RB, DiFrancesco D.** I_f-dependent modulation of pacemaker rate mediated by cAMP in the presence of ryanodine in rabbit sino-atrial node cells. *J Mol Cell Cardiol* 35: 905–913, 2003.
68. **Bucchi A, Baruscotti M, Robinson RB, Difrancesco D.** Modulation of rate by autonomic agonists in SAN cells involves changes in diastolic depolarization and the pacemaker current. *J Mol Cell Cardiol* 43: 39–48, 2007.
69. **Bucchi A, Plotnikov AN, Shlapakova I, Danilo P Jr, Kryukova Y, Qu J, Lu Z, Liu H, Pan Z, Potapova I, KenKnight B, Girouard S, Cohen IS, Brink PR, Robinson RB, Rosen MR.** Wild-type and mutant HCN channels in a tandem biological-electronic cardiac pacemaker. *Circulation* 114: 992–999, 2006.
70. **Bukauskas FF, Kreuzberg MM, Rackauskas M, Bukauskiene A, Bennett MV, Verselis VK, Willecke K.** Properties of mouse connexin 30.2 and human connexin 31 9 hemichannels: implications for atrioventricular conduction in the heart. *Proc Natl Acad Sci USA* 103: 9726–9731, 2006.
71. **Cai J, Yi FF, Li YH, Yang XC, Song J, Jiang XJ, Jiang H, Lin GS, Wang W.** Adenoviral gene transfer of HCN4 creates a genetic pacemaker in pigs with complete atrioventricular block. *Life Sci* 80: 1746–1753, 2007.
72. **Callewaert G, Carmeliet E, Vereecke J.** Single cardiac Purkinje cells: general electrophysiology and voltage-clamp analysis of the pace-maker current. *J Physiol* 349: 643–661, 1984.
73. **Camelliti P, Green CR, LeGrice I, Kohl P.** Fibroblast network in rabbit sinoatrial node: structural and functional identification of homogeneous and heterogeneous cell coupling. *Circ Res* 94: 828–835, 2004.
74. **Campbell DL, Rasmusson RL, Strauss HC.** Ionic current mechanisms generating vertebrate primary cardiac pacemaker activity at the single cell level: an integrative view. *Annu Rev Physiol* 54: 279–302, 1992.
75. **Carmeliet E.** Cardiac ionic currents and acute ischemia: from channels to arrhythmias. *Physiol Rev* 79: 917–1017, 1999.
76. **Casadei B, Moon J, Johnston J, Caiazza A, Sleight P.** Is respiratory sinus arrhythmia a good index of cardiac vagal tone in exercise? *J Appl Physiol* 81: 556–564, 1996.
77. **Catterall WA.** Structure and regulation of voltage-gated Ca^{2+} channels. *Annu Rev Cell Dev Biol* 16: 521–555, 2000.
78. **Catterall WA, Striessnig J, Snutch TP, Perez-Reyes E.** International Union of Pharmacology XL. Compendium of voltage-gated ion channels: calcium channels. *Pharmacol Rev* 55: 579–581, 2003.
79. **Cerbai E, Mugelli A.** I_f in non-pacemaker cells: role and pharmacological implications. *Pharmacol Res* 53: 416–423, 2006.
80. **Chang F, Cohen IS, DiFrancesco D, Rosen MR, Tromba C.** Effects of protein kinase inhibitors on canine Purkinje fiber pacemaker depolarization and the pacemaker current i_f. *J Physiol* 440: 367–384, 1991.
81. **Chang F, Gao J, Tromba C, Cohen I, DiFrancesco D.** Acetylcholine reverses effects of beta-agonists on pacemaker current in canine cardiac Purkinje fibers but has no direct action. A difference between primary and secondary pacemakers. *Circ Res* 66: 633–636, 1990.
82. **Chang F, Yu H, Cohen IS.** Actions of vasoactive intestinal peptide and neuropeptide Y on the pacemaker current in canine Purkinje fibers. *Circ Res* 74: 157–162, 1994.
83. **Chang SL, Chen YC, Chen YJ, Wangcharoen W, Lee SH, Lin CI, Chen SA.** Mechanoelectrical feedback regulates the arrhythmogenic activity of pulmonary veins. *Heart* 93: 82–88, 2007.
84. **Chen CC, Lamping KG, Nuno DW, Barresi R, Prouty SJ, Lavoie JL, Cribbs LL, England SK, Sigmund CD, Weiss RM, Williamson RA, Hill JA, Campbell KP.** Abnormal coronary function in mice deficient in alpha1H T-type Ca^{2+} channels. *Science* 302: 1416–1418, 2003.
85. **Chiba S, Simmons TW, Levy MN.** Chronotropic responses to experimental ischemia of the canine sino auricular node. *Arch Int Physiol Biochim* 84: 81–88, 1976.
86. **Cho HS, Takano M, Noma A.** The electrophysiological properties of spontaneously beating pacemaker cells isolated from mouse sinoatrial node. *J Physiol* 550: 169–180, 2003.
87. **Choate JK, Feldman R.** Neuronal control of heart rate in isolated mouse atria. *Am J Physiol Heart Circ Physiol* 285: H1340–H1346, 2003.
88. **Choate JK, Klemm M, Hirst GD.** Sympathetic and parasympathetic neuromuscular junctions in the guinea-pig sino-atrial node. *J Auton Nerv Syst* 44: 1–15, 1993.
89. **Choate JK, Nandhabalan M, Paterson DJ.** Raised extracellular potassium attenuates the sympathetic modulation of sino-atrial node pacemaking in the isolated guinea-pig atria. *Exp Physiol* 86: 19–25, 2001.
90. **Choi HS, Wang DY, Noble D, Lee CO.** Effect of isoprenaline, carbachol, Cs^+ on Na^+ activity and pacemaker potential in rabbit SA node cells. *Am J Physiol Heart Circ Physiol* 276: H205–H214, 1999.
91. **Christophe J, Waelbroeck M, Chatelain P, Robberecht P.** Heart receptors for VIP, PHI and secretin are able to activate adenylate cyclase and to mediate inotropic and chronotropic effects. Species variations and physiopathology. *Peptides* 5: 341–353, 1984.
92. **Clancy CE, Kass RS.** Inherited and acquired vulnerability to ventricular arrhythmias: cardiac Na^+ and K^+ channels. *Physiol Rev* 85: 33–47, 2005.
93. **Clark RB, Mangoni ME, Lueger A, Couette B, Nargeot J, Giles WR.** A rapidly activating delayed rectifier K^+ current regulates pacemaker activity in adult mouse sinoatrial node cells. *Am J Physiol Heart Circ Physiol* 286: H1757–H1766, 2004.
94. **Cohen IS, Robinson RB.** Pacemaker current and automatic rhythms: toward a molecular understanding. *Handbook Exp Pharmacol* 41–71, 2006.
95. **Coleridge JC, Linden RJ.** The effect of intravenous infusions upon the heart rate of the anaesthetized dog. *J Physiol* 128: 310–319, 1955.
96. **Colin P, Ghaleh B, Hittinger L, Monnet X, Slama M, Giudicelli JF, Berdeaux A.** Differential effects of heart rate reduction and beta-blockade on left ventricular relaxation during exercise. *Am J Physiol Heart Circ Physiol* 282: H672–H679, 2002.
97. **Colin P, Ghaleh B, Monnet X, Su J, Hittinger L, Giudicelli JF, Berdeaux A.** Contributions of heart rate and contractility to myocardial oxygen balance during exercise. *Am J Physiol Heart Circ Physiol* 284: H676–H682, 2003.
98. **Cooper KE.** Some responses of the cardiovascular system to heat and fever. *Can J Cardiol* 10: 444–448, 1994.
99. **Cooper PJ, Kohl P.** Species- and preparation-dependence of stretch effects on sino-atrial node pacemaking. *Ann NY Acad Sci* 1047: 324–335, 2005.
100. **Cooper PJ, Lei M, Cheng LX, Kohl P.** Selected contribution: axial stretch increases spontaneous pacemaker activity in rabbit isolated sinoatrial node cells. *J Appl Physiol* 89: 2099–2104, 2000.
101. **Coraboeuf E, Deroubaix E, Coulombe A.** Effect of tetrodotoxin on action potentials of the conducting system in the dog heart. *Am J Physiol Heart Circ Physiol* 236: H561–H567, 1979.
102. **Crampin EJ, Halstead M, Hunter P, Nielsen P, Noble D, Smith N, Tawhai M.** Computational physiology and the Physiome Project. *Exp Physiol* 89: 1–26, 2004.
103. **Cribbs LL, Lee JH, Yang J, Satin J, Zhang Y, Daud A, Barclay J, Williamson MP, Fox M, Rees M, Perez-Reyes E.** Cloning and characterization of alpha1H from human heart, a member of the T-type Ca^{2+} channel gene family. *Circ Res* 83: 103–109, 1998.
104. **Cribbs LL, Martin BL, Schroder EA, Keller BB, Delisle BP, Satin J.** Identification of the t-type calcium channel [Ca(v)3.1d] in developing mouse heart. *Circ Res* 88: 403–407, 2001.
105. **De Maziere AM, van Ginneken AC, Wilders R, Jongsma HJ, Bouman LN.** Spatial and functional relationship between myocytes and fibroblasts in the rabbit sinoatrial node. *J Mol Cell Cardiol* 24: 567–578, 1992.
106. **De Mello WC.** Role of chloride ions in cardiac action and pacemaker potential. *Am J Physiol* 205: 567–575, 1963.
107. **De Neef P, Robberecht P, Chatelain P, Waelbroeck M, Christophe J.** The in vitro chronotropic and inotropic effects of vasoactive intestinal peptide (VIP) on the atria and ventricular papillary muscle from Cynomolgus monkey heart. *Regul Pept* 8: 237–244, 1984.

Downloaded from physrev.physiology.org on October 4, 2011

108. **Deck KA.** Effects of stretch on the spontaneously beating, isolated sinus node. *Pflügers Arch* 280: 120–130, 1964.
109. **Demion M, Bois P, Launay P, Guinamard R.** TRPM4, a Ca^{2+}-activated nonselective cation channel in mouse sino-atrial node cells. *Cardiovasc Res* 73: 531–538, 2007.
110. **Demir SS, Clark JW, Giles WR.** Parasympathetic modulation of sinoatrial node pacemaker activity in rabbit heart: a unifying model. *Am J Physiol Heart Circ Physiol* 276: H2221–H2244, 1999.
111. **Demir SS, Clark JW, Murphey CR, Giles WR.** A mathematical model of a rabbit sinoatrial node cell. *Am J Physiol Cell Physiol* 266: C832–C852, 1994.
112. **Demolombe S, Marionneau C, Le Bouter S, Charpentier F, Escande D.** Functional genomics of cardiac ion channel genes. *Cardiovasc Res* 67: 438–447, 2005.
113. **Denyer JC, Brown HF.** Pacemaking in rabbit isolated sino-atrial node cells during Cs^+ block of the hyperpolarization-activated current i_f. *J Physiol* 429: 401–409, 1990.
114. **Denyer JC, Brown HF.** Rabbit sino-atrial node cells: isolation and electrophysiological properties. *J Physiol* 428: 405–424, 1990.
115. **DiFrancesco D.** Characterization of single pacemaker channels in cardiac sino-atrial node cells. *Nature* 324: 470–473, 1986.
116. **DiFrancesco D.** The contribution of the "pacemaker" current (i_f) to generation of spontaneous activity in rabbit sino-atrial node myocytes. *J Physiol* 434: 23–40, 1991.
117. **DiFrancesco D.** Funny channels in the control of cardiac rhythm and mode of action of selective blockers. *Pharmacol Res* 53: 399–406, 2006.
118. **DiFrancesco D.** A new interpretation of the pace-maker current in calf Purkinje fibers. *J Physiol* 314: 359–376, 1981.
119. **DiFrancesco D.** The onset and autonomic regulation of cardiac pacemaker activity: relevance of the f current. *Cardiovasc Res* 29: 449–456, 1995.
120. **DiFrancesco D.** Pacemaker mechanisms in cardiac tissue. *Annu Rev Physiol* 55: 455–472, 1993.
121. **DiFrancesco D.** Serious workings of the funny current. *Prog Biophys Mol Biol* 90: 13–25, 2006.
122. **DiFrancesco D.** A study of the ionic nature of the pace-maker current in calf Purkinje fibers. *J Physiol* 314: 377–393, 1981.
123. **DiFrancesco D, Camm JA.** Heart rate lowering by specific and selective I_f current inhibition with ivabradine: a new therapeutic perspective in cardiovascular disease. *Drugs* 64: 1757–1765, 2004.
124. **DiFrancesco D, Ducouret P, Robinson RB.** Muscarinic modulation of cardiac rate at low acetylcholine concentrations. *Science* 243: 669–671, 1989.
125. **DiFrancesco D, Ferroni A, Mazzanti M, Tromba C.** Properties of the hyperpolarizing-activated current (i_f) in cells isolated from the rabbit sino-atrial node. *J Physiol* 377: 61–88, 1986.
126. **DiFrancesco D, Mangoni M.** Modulation of single hyperpolarization-activated channels [i_f] by cAMP in the rabbit sino-atrial node. *J Physiol* 474: 473–482, 1994.
127. **DiFrancesco D, Noble D.** A model of cardiac electrical activity incorporating ionic pumps and concentration changes. *Philos Trans R Soc Lond B Biol Sci* 307: 353–398, 1985.
128. **DiFrancesco D, Tortora P.** Direct activation of cardiac pacemaker channels by intracellular cyclic AMP. *Nature* 351: 145–147, 1991.
129. **DiFrancesco D, Tromba C.** Muscarinic control of the hyperpolarization-activated current (i_f) in rabbit sino-atrial node myocytes. *J Physiol* 405: 493–510, 1988.
130. **Dobrzynski H, Li J, Tellez J, Greener ID, Nikolski VP, Wright SE, Parson SH, Jones SA, Lancaster MK, Yamamoto M, Honjo H, Takagishi Y, Kodama I, Efimov IR, Billeter R, Boyett MR.** Computer three-dimensional reconstruction of the sinoatrial node. *Circulation* 111: 846–854, 2005.
131. **Dobrzynski H, Nikolski VP, Sambelashvili AT, Greener ID, Yamamoto M, Boyett MR, Efimov IR.** Site of origin and molecular substrate of atrioventricular junctional rhythm in the rabbit heart. *Circ Res* 93: 1102–1110, 2003.
132. **Du XJ, Feng X, Gao XM, Tan TP, Kiriazis H, Dart AM.** I_f channel inhibitor ivabradine lowers heart rate in mice with enhanced sympathoadrenergic activities. *Br J Pharmacol* 142: 107–112, 2004.
133. **Du YM, Nathan RD.** Ionic basis of ischemia-induced bradycardia in the rabbit sinoatrial node. *J Mol Cell Cardiol* 42: 315–325. 2007.
134. **Dyer AR, Persky V, Stamler J, Paul O, Shekelle RB, Berkson DM, Lepper M, Schoenberger JA, Lindberg HA.** Heart rate as a prognostic factor for coronary heart disease and mortality: findings in three Chicago epidemiologic studies. *Am J Epidemiol* 112: 736–749, 1980.
135. **Dzhura I, Wu Y, Colbran RJ, Balser JR, Anderson ME.** Calmodulin kinase determines calcium-dependent facilitation of L-type calcium channels. *Nat Cell Biol* 2: 173–177, 2000.
136. **Ebert SN, Taylor DG.** Catecholamines and development of cardiac pacemaking: an intrinsically intimate relationship. *Cardiovasc Res* 72: 364–374, 2006.
137. **Edelberg JM, Aird WC, Rosenberg RD.** Enhancement of murine cardiac chronotropy by the molecular transfer of the human beta2 adrenergic receptor cDNA. *J Clin Invest* 101: 337–343, 1998.
138. **Edelberg JM, Huang DT, Josephson ME, Rosenberg RD.** Molecular enhancement of porcine cardiac chronotropy. *Heart* 86: 559–562, 2001.
139. **Efimov IR, Mazgalev TN.** High-resolution, three-dimensional fluorescent imaging reveals multilayer conduction pattern in the atrioventricular node. *Circulation* 98: 54–57, 1998.
140. **Efimov IR, Nikolski VP, Rothenberg F, Greener ID, Li J, Dobrzynski H, Boyett M.** Structure-function relationship in the AV junction. *Anat Rec* 280: 952–965, 2004.
141. **Ehrlich JR, Cha TJ, Zhang L, Chartier D, Melnyk P, Hohnloser SH, Nattel S.** Cellular electrophysiology of canine pulmonary vein cardiomyocytes: action potential and ionic current properties. *J Physiol* 551: 801–813, 2003.
142. **Eisner DA, Choi HS, Diaz ME, O'Neill SC, Trafford AW.** Integrative analysis of calcium cycling in cardiac muscle. *Circ Res* 87: 1087–1094, 2000.
143. **Er F, Larbig R, Ludwig A, Biel M, Hofmann F, Beuckelmann DJ, Hoppe UC.** Dominant-negative suppression of HCN channels markedly reduces the native pacemaker current I_f and undermines spontaneous beating of neonatal cardiomyocytes. *Circulation* 107: 485–489, 2003.
144. **Feld Y, Melamed-Frank M, Kehat I, Tal D, Marom S, Gepstein L.** Electrophysiological modulation of cardiomyocytic tissue by transfected fibroblasts expressing potassium channels: a novel strategy to manipulate excitability. *Circulation* 105: 522–529, 2002.
145. **Fermini B, Nathan RD.** Removal of sialic acid alters both T- and L-type calcium currents in cardiac myocytes. *Am J Physiol Heart Circ Physiol* 260: H735–H743, 1991.
146. **Ferron L, Capuano V, Deroubaix E, Coulombe A, Renaud JF.** Functional and molecular characterization of a T-type Ca^{2+} channel during fetal and postnatal rat heart development. *J Mol Cell Cardiol* 34: 533–546, 2002.
147. **Furuse A, Kotsuka Y, Asano K.** Sinus node potential during cold cardioplegia. *Jpn J Surg* 13: 146–151, 1983.
148. **Gaborit N, Le Bouter S, Szuts V, Varro A, Escande D, Nattel S, Demolombe S.** Regional and tissue specific transcript signatures of ion channel genes in the non-diseased human heart. *J Physiol* 582: 675–693, 2007.
149. **Gadsby DC, Cranefield PF.** Direct measurement of changes in sodium pump current in canine cardiac Purkinje fibers. *Proc Natl Acad Sci USA* 76: 1783–1787, 1979.
150. **Gadsby DC, Kimura J, Noma A.** Voltage dependence of Na/K pump current in isolated heart cells. *Nature* 315: 63–65, 1985.
151. **Gannier F, White E, Lacampagne A, Garnier D, Le Guennec JY.** Streptomycin reverses a large stretch induced increase in $[Ca^{2+}]_i$ in isolated guinea pig ventricular myocytes. *Cardiovasc Res* 28: 1193–1198, 1994.
152. **Garny A, Kohl P, Hunter PJ, Boyett MR, Noble D.** One-dimensional rabbit sinoatrial node models: benefits and limitations. *J Cardiovasc Electrophysiol* 14: S121–132, 2003.
153. **Garny A, Noble D, Kohl P.** Dimensionality in cardiac modelling. *Prog Biophys Mol Biol* 87: 47–66, 2005.
154. **Gaskell WH.** On the innervation of the heart, with special reference to the heart of the tortoise. *J Physiol* 4: 43–214, 1883.
155. **Gaskell WH.** Preliminary observations on the innervation of the heart of the tortoise. *J Physiol* 3: 369–379, 1882.

Downloaded from physrev.physiology.org on October 4, 2011

156. **Gaul GB, Gruska M, Titscher G, Blazek G, Havelec L, Marktl W, Muellner W, Kaff A.** Prediction of survival after out-of-hospital cardiac arrest: results of a community-based study in Vienna. *Resuscitation* 32: 169–176, 1996.
157. **Gehrmann J, Hammer PE, Maguire CT, Wakimoto H, Triedman JK, Berul CI.** Phenotypic screening for heart rate variability in the mouse. *Am J Physiol Heart Circ Physiol* 279: H733–H740, 2000.
158. **Gehrmann J, Meister M, Maguire CT, Martins DC, Hammer PE, Neer EJ, Berul CI, Mende U.** Impaired parasympathetic heart rate control in mice with a reduction of functional G protein betagamma-subunits. *Am J Physiol Heart Circ Physiol* 282: H445–H456, 2002.
159. **Giles W, Noble SJ.** Changes in membrane currents in bullfrog atrium produced by acetylcholine. *J Physiol* 261: 103–123, 1976.
160. **Gillman MW, Kannel WB, Belanger A, D'Agostino RB.** Influence of heart rate on mortality among persons with hypertension: the Framingham Study. *Am Heart J* 125: 1148–1154, 1993.
161. **Gloss B, Trost S, Bluhm W, Swanson E, Clark R, Winkfein R, Janzen K, Giles W, Chassande O, Samarut J, Dillmann W.** Cardiac ion channel expression and contractile function in mice with deletion of thyroid hormone receptor alpha or beta. *Endocrinology* 142: 544–550, 2001.
162. **Goethals M, Raes A, van Bogaert PP.** Use-dependent block of the pacemaker current I_f in rabbit sinoatrial node cells by zatebradine (UL-FS 49). On the mode of action of sinus node inhibitors. *Circulation* 88: 2389–2401, 1993.
163. **Grace AA, Kirschenlohr HL, Metcalfe JC, Smith GA, Weissberg PL, Cragoe EJ Jr, Vandenberg JI.** Regulation of intracellular pH in the perfused heart by external HCO_3^-- and Na^+-H^+ exchange. *Am J Physiol Heart Circ Physiol* 265: H289–H298, 1993.
164. **Gryshchenko O, Qu J, Nathan RD.** Ischemia alters the electrical activity of pacemaker cells isolated from the rabbit sinoatrial node. *Am J Physiol Heart Circ Physiol* 282: H2284–H2295, 2002.
165. **Guo J, Noma A.** Existence of a low-threshold and sustained inward current in rabbit atrio-ventricular node cells. *Jpn J Physiol* 47: 355–359, 1997.
166. **Guo J, Ono K, Noma A.** A sustained inward current activated at the diastolic potential range in rabbit sino-atrial node cells. *J Physiol* 483: 1–13, 1995.
167. **Guo W, Kamiya K, Hojo M, Kodama I, Toyama J.** Regulation of Kv4.2 and Kv1.4 K^+ channel expression by myocardial hypertrophic factors in cultured newborn rat ventricular cells. *J Mol Cell Cardiol* 30: 1449–1455, 1998.
168. **Guo W, Li H, Aimond F, Johns DC, Rhodes KJ, Trimmer JS, Nerbonne JM.** Role of heteromultimers in the generation of myocardial transient outward K^+ currents. *Circ Res* 90: 586–593, 2002.
169. **Habuchi Y, Lu LL, Morikawa J, Yoshimura M.** Angiotensin II inhibition of L-type Ca^{2+} current in sinoatrial node cells of rabbits. *Am J Physiol Heart Circ Physiol* 268: H1053–H1060, 1995.
170. **Habuchi Y, Nishio M, Tanaka H, Yamamoto T, Lu LL, Yoshimura M.** Regulation by acetylcholine of Ca^{2+} current in rabbit atrioventricular node cells. *Am J Physiol Heart Circ Physiol* 271: H2274–H2282, 1996.
171. **Hagiwara N, Irisawa H.** Modulation by intracellular Ca^{2+} of the hyperpolarization-activated inward current in rabbit single sino-atrial node cells. *J Physiol* 409: 121–141, 1989.
172. **Hagiwara N, Irisawa H, Kameyama M.** Contribution of two types of calcium currents to the pacemaker potentials of rabbit sino-atrial node cells. *J Physiol* 395: 233–253, 1988.
173. **Hagiwara N, Irisawa H, Kasanuki H, Hosoda S.** Background current in sino-atrial node cells of the rabbit heart. *J Physiol* 448: 53–72, 1992.
174. **Hagiwara N, Masuda H, Shoda M, Irisawa H.** Stretch-activated anion currents of rabbit cardiac myocytes. *J Physiol* 456: 285–302, 1992.
175. **Haissaguerre M, Jais P, Shah DC, Takahashi A, Hocini M, Quiniou G, Garrigue S, Le Mouroux A, Le Metayer P, Clementy J.** Spontaneous initiation of atrial fibrillation by ectopic beats originating in the pulmonary veins. *N Engl J Med* 339: 659–666, 1998.
176. **Haissaguerre M, Shah DC, Jais P, Shoda M, Kautzner J, Arentz T, Kalushe D, Kadish A, Griffith M, Gaita F, Yamane T, Garrigue S, Hocini M, Clementy J.** Role of Purkinje conducting system in triggering of idiopathic ventricular fibrillation. *Lancet* 359: 677–678, 2002.
177. **Hakumaki MO.** Seventy years of the Bainbridge reflex. *Acta Physiol Scand* 130: 177–185, 1987.
178. **Hale SL, Kloner RA.** Elevated body temperature during myocardial ischemia/reperfusion exacerbates necrosis and worsens no-reflow. *Coron Artery Dis* 13: 177–181, 2002.
179. **Han W, Bao W, Wang Z, Nattel S.** Comparison of ion-channel subunit expression in canine cardiac Purkinje fibers and ventricular muscle. *Circ Res* 91: 790–797, 2002.
180. **Han X, Habuchi Y, Giles WR.** Effects of metabolic inhibition on action potentials and ionic currents in cardiac pacemaking cells (Abstract). *Circulation* 90 *Suppl* I: 582, 1994.
181. **Han X, Habuchi Y, Giles WR.** Relaxin increases heart rate by modulating calcium current in cardiac pacemaker cells. *Circ Res* 74: 537–541, 1994.
182. **Han X, Kobzik L, Severson D, Shimoni Y.** Characteristics of nitric oxide-mediated cholinergic modulation of calcium current in rabbit sino-atrial node. *J Physiol* 509: 741–754, 1998.
183. **Han X, Kubota I, Feron O, Opel DJ, Arstall MA, Zhao YY, Huang P, Fishman MC, Michel T, Kelly RA.** Muscarinic cholinergic regulation of cardiac myocyte I_{CaL} is absent in mice with targeted disruption of endothelial nitric oxide synthase. *Proc Natl Acad Sci USA* 95: 6510–6515, 1998.
184. **Han X, Light PE, Giles WR, French RJ.** Identification and properties of an ATP-sensitive K^+ current in rabbit sino-atrial node pacemaker cells. *J Physiol* 490: 337–350, 1996.
185. **Han X, Shimoni Y, Giles WR.** A cellular mechanism for nitric oxide-mediated cholinergic control of mammalian heart rate. *J Gen Physiol* 106: 45–65, 1995.
186. **Han X, Shimoni Y, Giles WR.** An obligatory role for nitric oxide in autonomic control of mammalian heart rate. *J Physiol* 476: 309–314, 1994.
187. **Hancox JC, Levi AJ, Lee CO, Heap P.** A method for isolating rabbit atrioventricular node myocytes which retain normal morphology and function. *Am J Physiol Heart Circ Physiol* 265: H755–H766, 1993.
188. **Hanna CM, Greenes DS.** How much tachycardia in infants can be attributed to fever? *Ann Emerg Med* 43: 699–705, 2004.
189. **Hara M, Liu YM, Zhen L, Cohen IS, Yu H, Danilo P Jr, Ogino K, Bilezikian JP, Rosen MR.** Positive chronotropic actions of parathyroid hormone and parathyroid hormone-related peptide are associated with increases in the current, I_f, the slope of the pacemaker potential. *Circulation* 96: 3704–3709, 1997.
190. **Hartzell HC.** Regulation of cardiac ion channels by catecholamines, acetylcholine and second messenger systems. *Prog Biophys Mol Biol* 52: 165–247, 1988.
190a. **Harzheim D, Pfeiffer KH, Fabritz L, Kremmer E, Buch T, Waisman A, Kirchhof P, Kaupp UB, Seifert R.** Cardiac pacemaker function of HCN4 channels in mice is confined to embryonic development and requires cyclic AMP. *Embo J* 27: 692–703, 2008.
191. **Haufe V, Cordeiro JM, Zimmer T, Wu YS, Schiccitano S, Benndorf K, Dumaine R.** Contribution of neuronal sodium channels to the cardiac fast sodium current I_{Na} is greater in dog heart Purkinje fibers than in ventricles. *Cardiovasc Res* 65: 117–127, 2005.
192. **Hauswirth O, Noble D, Tsien RW.** Adrenaline: mechanism of action on the pacemaker potential in cardiac Purkinje fibers. *Science* 162: 916–917, 1968.
193. **Haverinen J, Vornanen M.** Temperature acclimation modifies sinoatrial pacemaker mechanism of the rainbow trout heart. *Am J Physiol Regul Integr Comp Physiol* 292: R1023–R1032, 2007.
194. **Heath BM, Terrar DA.** Protein kinase C enhances the rapidly activating delayed rectifier potassium current, I_{Kr}, through a reduction in C-type inactivation in guinea-pig ventricular myocytes. *J Physiol 522 Pt* 3: 391–402, 2000.
195. **Henning RJ.** Vagal stimulation during muscarinic and beta-adrenergic blockade increases atrial contractility and heart rate. *J Auton Nerv Syst* 40: 121–129, 1992.
196. **Herrmann S, Stieber J, Stockl G, Hofmann F, Ludwig A.** HCN4 provides a "depolarization reserve" and is not required for heart rate acceleration in mice. *EMBO J* 26: 4423–4432, 2007.

Downloaded from physrev.physiology.org on October 4, 2011

197. **Hilgemann DW, Noble D.** Excitation-contraction coupling and extracellular calcium transients in rabbit atrium: reconstruction of basic cellular mechanisms. *Proc R Soc Lond B Biol Sci* 230: 163–205, 1987.
198. **Hilgemann DW, Yaradanakul A, Wang Y, Fuster D.** Molecular control of cardiac sodium homeostasis in health and disease. *J Cardiovasc Electrophysiol* 17 *Suppl* 1: S47–S56, 2006.
199. **Hirano Y, Fozzard HA, January CT.** Characteristics of L- and T-type Ca^{2+} currents in canine cardiac Purkinje cells. *Am J Physiol Heart Circ Physiol* 256: H1478–H1492, 1989.
200. **Hirst GD, Choate JK, Cousins HM, Edwards FR, Klemm MF.** Transmission by post-ganglionic axons of the autonomic nervous system: the importance of the specialized neuroeffector junction. *Neuroscience* 73: 7–23, 1996.
201. **Hjalmarson A.** Significance of reduction in heart rate in cardiovascular disease. *Clin Cardiol* 21: II3–7, 1998.
202. **Hof TO, Mackaay AJ, Bleeker WK, Houtkooper JM, Abels R, Bouman LN.** Dependence of the chronotropic effects of calcium, magnesium and sodium on temperature and cycle length in isolated rabbit atria. *J Pharmacol Exp Ther* 212: 183–189, 1980.
203. **Hoffman BF, Cranefield PF.** *Electrophysiology of the Heart.* Mount Kisco, NY: Futura, 1976.
204. **Honjo H, Boyett MR, Kodama I, Toyama J.** Correlation between electrical activity and the size of rabbit sino-atrial node cells. *J Physiol* 496: 795–808, 1996.
205. **Honjo H, Boyett MR, Niwa R, Inada S, Yamamoto M, Mitsui K, Horiuchi T, Shibata N, Kamiya K, Kodama I.** Pacing-induced spontaneous activity in myocardial sleeves of pulmonary veins after treatment with ryanodine. *Circulation* 107: 1937–1943, 2003.
206. **Honjo H, Lei M, Boyett MR, Kodama I.** Heterogeneity of 4-aminopyridine-sensitive current in rabbit sinoatrial node cells. *Am J Physiol Heart Circ Physiol* 276: H1295–H1304, 1999.
207. **Hoogaars WM, Barnett P, Moorman AF, Christoffels VM.** T-box factors determine cardiac design. *Cell Mol Life Sci* 64: 646–660, 2007.
208. **Hoogaars WM, Engel A, Brons JF, Verkerk AO, de Lange FJ, Wong LY, Bakker ML, Clout DE, Wakker V, Barnett P, Ravesloot JH, Moorman AF, Verheijck EE, Christoffels VM.** Tbx3 controls the sinoatrial node gene program and imposes pacemaker function on the atria. *Genes Dev* 21: 1098–1112, 2007.
209. **Hu K, Qu Y, Yue Y, Boutjdir M.** Functional basis of sinus bradycardia in congenital heart block. *Circ Res* 94: e32–38, 2004.
210. **Hume JR, Duan D, Collier ML, Yamazaki J, Horowitz B.** Anion transport in heart. *Physiol Rev* 80: 31–81, 2000.
211. **Huser J, Blatter LA, Lipsius SL.** Intracellular Ca^{2+} release contributes to automaticity in cat atrial pacemaker cells. *J Physiol* 524: 415–422, 2000.
212. **Hutter OF, Trautwein W.** Effect of vagal stimulation on the sinus venosus of the frog's heart. *Nature* 176: 512–513, 1955.
213. **Hutter OF, Trautwein W.** Vagal and sympathetic effects on the pacemaker fibers in the sinus venosus of the heart. *J Gen Physiol* 39: 715–733, 1956.
214. **Ino M, Yoshinaga T, Wakamori M, Miyamoto N, Takahashi E, Sonoda J, Kagaya T, Oki T, Nagasu T, Nishizawa Y, Tanaka I, Imoto K, Aizawa S, Koch S, Schwartz A, Niidome T, Sawada K, Mori Y.** Functional disorders of the sympathetic nervous system in mice lacking the alpha 1B subunit (Cav 2.2) of N-type calcium channels. *Proc Natl Acad Sci USA* 98: 5323–5328, 2001.
215. **Irisawa H, Brown HF, Giles W.** Cardiac pacemaking in the sinoatrial node. *Physiol Rev* 73: 197–227, 1993.
216. **Isenberg G, Klockner U.** Calcium tolerant ventricular myocytes prepared by preincubation in a "KB medium". *Pflügers Arch* 395: 6–18, 1982.
217. **Ishii TM, Takano M, Xie LH, Noma A, Ohmori H.** Molecular characterization of the hyperpolarization-activated cation channel in rabbit heart sinoatrial node. *J Biol Chem* 274: 12835–12839, 1999.
218. **Ito H, Ono K.** A rapidly activating delayed rectifier K^+ channel in rabbit sinoatrial node cells. *Am J Physiol Heart Circ Physiol* 269: H443–H452, 1995.
219. **Jacquemet V.** Pacemaker activity resulting from the coupling with nonexcitable cells. *Phys Rev E Stat Nonlin Soft Matter Phys* 74: 011908, 2006.
220. **James TN.** Structure and function of the sinus node, AV node and his bundle of the human heart: part II–function. *Prog Cardiovasc Dis* 45: 327–360, 2003.
221. **Janse MJ.** Electrophysiological changes in heart failure and their relationship to arrhythmogenesis. *Cardiovasc Res* 61: 208–217, 2004.
222. **Jones SA, Boyett MR, Lancaster MK.** Declining into failure: the age-dependent loss of the L-type calcium channel within the sinoatrial node. *Circulation* 115: 1183–1190, 2007.
223. **Jose AD, Collison D.** The normal range and determinants of the intrinsic heart rate in man. *Cardiovasc Res* 4: 160–167, 1970.
224. **Joyner RW, Kumar R, Golod DA, Wilders R, Jongsma HJ, Verheijck EE, Bouman L, Goolsby WN, Van Ginneken AC.** Electrical interactions between a rabbit atrial cell and a nodal cell model. *Am J Physiol Heart Circ Physiol* 274: H2152–H2162, 1998.
225. **Joyner RW, van Capelle FJ.** Propagation through electrically coupled cells. How a small SA node drives a large atrium. *Biophys J* 50: 1157–1164, 1986.
226. **Ju YK, Allen DG.** The distribution of calcium in toad cardiac pacemaker cells during spontaneous firing. *Pflügers Arch* 441: 219–227, 2000.
227. **Ju YK, Allen DG.** How does beta-adrenergic stimulation increase the heart rate? The role of intracellular Ca^{2+} release in amphibian pacemaker cells. *J Physiol* 516: 793–804, 1999.
228. **Ju YK, Allen DG.** Intracellular calcium and Na^+-Ca^{2+} exchange current in isolated toad pacemaker cells. *J Physiol* 508: 153–166, 1998.
229. **Ju YK, Chu Y, Chaulet H, Lai D, Gervasio OL, Graham RM, Cannell MB, Allen DG.** Store-operated Ca^{2+} influx and expression of TRPC genes in mouse sinoatrial node. *Circ Res* 100: 1605–1614, 2007.
230. **Kanani S, Pumir A, Krinski V.** Genetically engineered cardiac pacemaker: stem cells transfected with HCN2 gene and a myocyte–a model. *Physics Letters A.* In press.
231. **Kannel WB, Ho K, Thom T.** Changing epidemiological features of cardiac failure. *Br Heart J* 72: S3–9, 1994.
232. **Kannel WB, Kannel C, Paffenbarger RS Jr, Cupples LA.** Heart rate and cardiovascular mortality: the Framingham Study. *Am Heart J* 113: 1489–1494, 1987.
233. **Kaufmann R, Theophile U.** [Autonomously promoted extension effect in Purkinje fibers, papillary muscles and trabeculae carneae of rhesus monkeys]. *Pflügers Arch* 297: 174–189, 1967.
234. **Kaupp UB, Seifert R.** Molecular diversity of pacemaker ion channels. *Annu Rev Physiol* 63: 235–257, 2001.
235. **Ke Y, Lei M, Collins TP, Rakovic S, Mattick PA, Yamasaki M, Brodie MS, Terrar DA, Solaro RJ.** Regulation of L-type calcium channel and delayed rectifier potassium channel activity by p21-activated kinase-1 in guinea pig sinoatrial node pacemaker cells. *Circ Res* 100: 1317–1327, 2007.
236. **Keating MT, Sanguinetti MC.** Molecular and cellular mechanisms of cardiac arrhythmias. *Cell* 104: 569–580, 2001.
237. **Keith A, Flack M.** The form and nature of the muscular connections between the primary divisions of the vertebrate heart. *J Anat Physiol* 41: 172–189, 1907.
238. **Kennedy ME, Nemec J, Corey S, Wickman K, Clapham DE.** GIRK4 confers appropriate processing and cell surface localization to G-protein-gated potassium channels. *J Biol Chem* 274: 2571–2582, 1999.
239. **Kiekkas P, Brokalaki H, Manolis E, Askotiri P, Karga M, Baltopoulos GI.** Fever and standard monitoring parameters of ICU patients: a descriptive study. *Intensive Crit Care Nurs* 23: 281–288, 2007.
240. **Kim EM, Choy Y, Vassalle M.** Mechanisms of suppression and initiation of pacemaker activity in guinea-pig sino-atrial node superfused in high $[K^+]_o$. *J Mol Cell Cardiol* 29: 1433–1445, 1997.
241. **Kirchhof CJ, Bonke FI, Allessie MA, Lammers WJ.** The influence of the atrial myocardium on impulse formation in the rabbit sinus node. *Pflügers Arch* 410: 198–203, 1987.
242. **Kirchhof P, Fabritz L, Fortmuller L, Matherne GP, Lankford A, Baba HA, Schmitz W, Breithardt G, Neumann J, Boknik P.** Altered sinus nodal and atrioventricular nodal function in freely moving mice overexpressing the A1 adenosine receptor. *Am J Physiol Heart Circ Physiol* 285: H145–H153, 2003.

Downloaded from physrev.physiology.org on October 4, 2011

243. **Kizana E, Ginn SL, Allen DG, Ross DL, Alexander IE.** Fibroblasts can be genetically modified to produce excitable cells capable of electrical coupling. *Circulation* 111: 394–398, 2005.
244. **Kizana E, Ginn SL, Smyth CM, Boyd A, Thomas SP, Allen DG, Ross DL, Alexander IE.** Fibroblasts modulate cardiomyocyte excitability: implications for cardiac gene therapy. *Gene Ther* 13: 1611–1615, 2006.
245. **Kleber AG, Rudy Y.** Basic mechanisms of cardiac impulse propagation and associated arrhythmias. *Physiol Rev* 84: 431–488, 2004.
246. **Klein I.** Thyroid hormone and the cardiovascular system. *Am J Med* 88: 631–637, 1990.
247. **Kobayashi M, Godin D, Nadeau R.** Sinus node responses to perfusion pressure changes, ischaemia and hypothermia in the isolated blood-perfused dog atrium. *Cardiovasc Res* 19: 20–26, 1985.
248. **Kodama I, Boyett MR.** Regional differences in the electrical activity of the rabbit sinus node. *Pflügers Arch* 404: 214–226, 1985.
249. **Kodama I, Boyett MR, Nikmaram MR, Yamamoto M, Honjo H, Niwa R.** Regional differences in effects of E-4031 within the sino-atrial node. *Am J Physiol Heart Circ Physiol* 276: H793–H802, 1999.
250. **Kodama I, Nikmaram MR, Boyett MR, Suzuki R, Honjo H, Owen JM.** Regional differences in the role of the Ca^{2+} and Na^{+} currents in pacemaker activity in the sinoatrial node. *Am J Physiol Heart Circ Physiol* 272: H2793–H2806, 1997.
251. **Kohl P, Bollensdorff C, Garny A.** Effects of mechanosensitive ion channels on ventricular electrophysiology: experimental and theoretical models. *Exp Physiol* 91: 307–321, 2006.
252. **Kohl P, Kamkin AG, Kiseleva IS, Noble D.** Mechanosensitive fibroblasts in the sino-atrial node region of rat heart: interaction with cardiomyocytes and possible role. *Exp Physiol* 79: 943–956, 1994.
253. **Kohlhardt M, Mnich Z, Maier G.** Alterations of the excitation process of the sinoatrial pacemaker cell in the presence of anoxia and metabolic inhibitors. *J Mol Cell Cardiol* 9: 477–488, 1977.
254. **Koschak A, Reimer D, Huber I, Grabner M, Glossmann H, Engel J, Striessnig J.** Alpha 1D (Cav1.3) subunits can form L-type Ca^{2+} channels activating at negative voltages. *J Biol Chem* 276: 22100–22106, 2001.
255. **Kreitner D.** Electrophysiological study of the two main pacemaker mechanisms in the rabbit sinus node. *Cardiovasc Res* 19: 304–318, 1985.
256. **Kreuzberg MM, Schrickel JW, Ghanem A, Kim JS, Degen J, Janssen-Bienhold U, Lewalter T, Tiemann K, Willecke K.** Connexin 30.2 containing gap junction channels decelerate impulse propagation through the atrioventricular node. *Proc Natl Acad Sci USA* 103: 5959–5964, 2006.
257. **Kreuzberg MM, Sohl G, Kim JS, Verselis VK, Willecke K, Bukauskas FF.** Functional properties of mouse connexin30.2 expressed in the conduction system of the heart. *Circ Res* 96: 1169–1177, 2005.
258. **Kreuzberg MM, Willecke K, Bukauskas FF.** Connexin-mediated cardiac impulse propagation: connexin 30.2 slows atrioventricular conduction in mouse heart. *Trends Cardiovasc Med* 16: 266–272, 2006.
259. **Kuniyoshi Y, Koja K, Miyagi K, Mistuyoshi S, Uezu T, Arakaki K, Yamashiro S, Mabuni K, Haneji S.** Management of the heart rate during coronary artery bypass grafting on the beating heart: newly devised methods of decreasing heart rate–a preliminary report. *Ann Thorac Cardiovasc Surg* 7: 358–367, 2001.
260. **Kuo HC, Cheng CF, Clark RB, Lin JJ, Lin JL, Hoshijima M, Nguyen-Tran VT, Gu Y, Ikeda Y, Chu PH, Ross J, Giles WR, Chien KR.** A defect in the Kv channel-interacting protein 2 (KChIP2) gene leads to a complete loss of I_{to} and confers susceptibility to ventricular tachycardia. *Cell* 107: 801–813, 2001.
261. **Kurachi Y, Noma A, Irisawa H.** Electrogenic sodium pump in rabbit atrio-ventricular node cell. *Pflügers Arch* 391: 261–266, 1981.
262. **Kurata Y, Hisatome I, Imanishi S, Shibamoto T.** Dynamical description of sinoatrial node pacemaking: improved mathematical model for primary pacemaker cell. *Am J Physiol Heart Circ Physiol* 283: H2074–H2101, 2002.
263. **Kurata Y, Hisatome I, Matsuda H, Shibamoto T.** Dynamical mechanisms of pacemaker generation in I_{K1}-downregulated human ventricular myocytes: insights from bifurcation analyses of a mathematical model. *Biophys J* 89: 2865–2887, 2005.
264. **Kurata Y, Matsuda H, Hisatome I, Shibamoto T.** Effects of pacemaker currents on creation and modulation of human ventricular pacemaker: theoretical study with application to biological pacemaker engineering. *Am J Physiol Heart Circ Physiol* 292: H701–H718, 2007.
265. **Lacinova L, Klugbauer N, Hofmann F.** Regulation of the calcium channel alpha(1G) subunit by divalent cations and organic blockers. *Neuropharmacology* 39: 1254–1266, 2000.
266. **Lamas GA, Lee K, Sweeney M, Leon A, Yee R, Ellenbogen K, Greer S, Wilber D, Silverman R, Marinchak R, Bernstein R, Mittleman RS, Lieberman EH, Sullivan C, Zorn L, Flaker G, Schron E, Orav EJ, Goldman L.** The mode selection trial (MOST) in sinus node dysfunction: design, rationale, baseline characteristics of the first 1000 patients. *Am Heart J* 140: 541–551, 2000.
267. **Lancaster MK, Jones SA, Harrison SM, Boyett MR.** Intracellular Ca^{2+} and pacemaking within the rabbit sinoatrial node: heterogeneity of role and control. *J Physiol* 556: 481–494, 2004.
268. **Lande G, Demolombe S, Bammert A, Moorman A, Charpentier F, Escande D.** Transgenic mice overexpressing human Kv-LQT1 dominant-negative isoform. Part II: Pharmacological profile. *Cardiovasc Res* 50: 328–334, 2001.
269. **Laskowski MB, D'Agrosa LS.** The ultrastructure of the sinu-atrial node of the bat. *Acta Anat* 117: 85–101, 1983.
270. **Le Bouter S, Demolombe S, Chambellan A, Bellocq C, Aimond F, Toumaniantz G, Lande G, Siavoshian S, Baro I, Pond AL, Nerbonne JM, Leger JJ, Escande D, Charpentier F.** Microarray analysis reveals complex remodeling of cardiac ion channel expression with altered thyroid status: relation to cellular and integrated electrophysiology. *Circ Res* 92: 234–242, 2003.
271. **Le Heuzey JY, Guize L, Valty J, Moutet JP, Kouz S, Lavergne T, Boutjdir M, Peronneau P.** Intracellular and extracellular recordings of sinus node activity: comparison with estimated sinoatrial conduction times during pacemaker shifts in rabbit heart. *Cardiovasc Res* 20: 81–88, 1986.
272. **Lees-Miller JP, Guo J, Somers JR, Roach DE, Sheldon RS, Rancourt DE, Duff HJ.** Selective knockout of mouse ERG1 B potassium channel eliminates *I*(Kr) in adult ventricular myocytes and elicits episodes of abrupt sinus bradycardia. *Mol Cell Biol* 23: 1856–1862, 2003.
273. **Lees-Miller JP, Kondo C, Wang L, Duff HJ.** Electrophysiological characterization of an alternatively processed ERG K^{+} channel in mouse and human hearts. *Circ Res* 81: 719–726, 1997.
274. **Lehmann H, Klein UE.** Familial sinus node dysfunction with autosomal dominant inheritance. *Br Heart J* 40: 1314–1316, 1978.
275. **Lei M, Cooper PJ, Camelliti P, Kohl P.** Role of the 293b-sensitive, slowly activating delayed rectifier potassium current, *i*(Ks), in pacemaker activity of rabbit isolated sino-atrial node cells. *Cardiovasc Res* 53: 68–79, 2002.
276. **Lei M, Goddard C, Liu J, Leoni AL, Royer A, Fung SS, Xiao G, Ma A, Zhang H, Charpentier F, Vandenberg JI, Colledge WH, Grace AA, Huang CL.** Sinus node dysfunction following targeted disruption of the murine cardiac sodium channel gene Scn5a. *J Physiol* 567: 387–400, 2005.
277. **Lei M, Honjo H, Kodama I, Boyett MR.** Characterisation of the transient outward K^{+} current in rabbit sinoatrial node cells. *Cardiovasc Res* 46: 433–441, 2000.
278. **Lei M, Honjo H, Kodama I, Boyett MR.** Heterogeneous expression of the delayed-rectifier K^{+} currents *i*(K,r) and *i*(K,s) in rabbit sinoatrial node cells. *J Physiol* 535: 703–714, 2001.
279. **Lei M, Jones SA, Liu J, Lancaster MK, Fung SS, Dobrzynski H, Camelliti P, Maier SK, Noble D, Boyett MR.** Requirement of neuronal- and cardiac-type sodium channels for murine sinoatrial node pacemaking. *J Physiol* 559: 835–848, 2004.
280. **Leoni AL, Marionneau C, Demolombe S, Le Bouter S, Mangoni ME, Escande D, Charpentier F.** Chronic heart rate reduction remodels ion channel transcripts in the mouse sinoatrial node but not in the ventricle. *Physiol Genomics* 24: 4–12, 2005.
281. **Lerman BB, Wesley RC Jr, DiMarco JP, Haines DE, Belardinelli L.** Antiadrenergic effects of adenosine on His-Purkinje automaticity. Evidence for accentuated antagonism. *J Clin Invest* 82: 2127–2135, 1988.

Downloaded from physrev.physiology.org on October 4, 2011

282. **Leuranguer V, Monteil A, Bourinet E, Dayanithi G, Nargeot J.** T-type calcium currents in rat cardiomyocytes during postnatal development: contribution to hormone secretion. *Am J Physiol Heart Circ Physiol* 279: H2540–H2548, 2000.
283. **Levitzki A.** Beta-adrenergic receptors and their mode of coupling to adenylate cyclase. *Physiol Rev* 66: 819–854, 1986.
284. **Levy MN.** Sympathetic-parasympathetic interactions in the heart. *Circ Res* 29: 437–445, 1971.
284a. **Li J, Greener ID, Inada S, Nikolski VP, Yamamoto M, Hancox JC, Zhang H, Billeter R, Efimov IR, Dobrzynski H, Boyett MR.** Computer three-dimensional reconstruction of the atrioventricular node. *Circ Res*. In press.
285. **Li J, Qu J, Nathan RD.** Ionic basis of ryanodine's negative chronotropic effect on pacemaker cells isolated from the sinoatrial node. *Am J Physiol Heart Circ Physiol* 273: H2481–H2489, 1997.
286. **Li M, West JW, Numann R, Murphy BJ, Scheuer T, Catterall WA.** Convergent regulation of sodium channels by protein kinase C and cAMP-dependent protein kinase. *Science* 261: 1439–1442, 1993.
287. **Lin W, Laitko U, Juranka PF, Morris CE.** Dual stretch responses of mHCN2 pacemaker channels: accelerated activation, accelerated deactivation. *Biophys J* 92: 1559–1572, 2007.
288. **Lipsius SL, Huser J, Blatter LA.** Intracellular Ca^{2+} release sparks atrial pacemaker activity. *News Physiol Sci* 16: 101–106, 2001.
289. **Liu J, Dobrzynski H, Yanni J, Boyett MR, Lei M.** Organisation of the mouse sinoatrial node: structure and expression of HCN channels. *Cardiovasc Res* 73: 729–738, 2007.
290. **London B, Guo W, Pan X, Lee JS, Shusterman V, Rocco CJ, Logothetis DA, Nerbonne JM, Hill JA.** Targeted replacement of KV1.5 in the mouse leads to loss of the 4-aminopyridine-sensitive component of *I*(K,slow) and resistance to drug-induced qt prolongation. *Circ Res* 88: 940–946, 2001.
291. **London B, Wang DW, Hill JA, Bennett PB.** The transient outward current in mice lacking the potassium channel gene Kv1.4. *J Physiol* 509: 171–182, 1998.
292. **Lu HH.** Shifts in pacemaker dominance within the sinoatrial region of cat and rabbit hearts resulting from increase of extracellular potassium. *Circ Res* 26: 339–346, 1970.
293. **Lu ZJ, Pereverzev A, Liu HL, Weiergraber M, Henry M, Krieger A, Smyth N, Hescheler J, Schneider T.** Arrhythmia in isolated prenatal hearts after ablation of the Cav2.3 (alpha1E) subunit of voltage-gated Ca^{2+} channels. *Cell Physiol Biochem* 14: 11–22, 2004.
294. **Ludwig A, Budde T, Stieber J, Moosmang S, Wahl C, Holthoff K, Langebartels A, Wotjak C, Munsch T, Zong X, Feil S, Feil R, Lancel M, Chien KR, Konnerth A, Pape HC, Biel M, Hofmann F.** Absence epilepsy and sinus dysrhythmia in mice lacking the pacemaker channel HCN2. *EMBO J* 22: 216–224, 2003.
295. **Ludwig A, Zong X, Hofmann F, Biel M.** Structure and function of cardiac pacemaker channels. *Cell Physiol Biochem* 9: 179–186, 1999.
296. **Ludwig A, Zong X, Stieber J, Hullin R, Hofmann F, Biel M.** Two pacemaker channels from human heart with profoundly different activation kinetics. *EMBO J* 18: 2323–2329, 1999.
297. **Lundberg JM, Hokfelt T.** Multiple co-existence of peptides and classical transmitters in peripheral autonomic and sensory neurons–functional and pharmacological implications. *Prog Brain Res* 68: 241–262, 1986.
298. **Luo CH, Rudy Y.** A dynamic model of the cardiac ventricular action potential. I. Simulations of ionic currents and concentration changes. *Circ Res* 74: 1071–1096, 1994.
299. **Lyashkov AE, Juhaszova M, Dobrzynski H, Vinogradova TM, Maltsev VA, Juhasz O, Spurgeon HA, Sollott SJ, Lakatta EG.** Calcium cycling protein density and functional importance to automaticity of isolated sinoatrial nodal cells are independent of cell size. *Circ Res* 100: 1723–1731, 2007.
300. **Mackaay AJ, Op't Hof T, Bleeker WK, Jongsma HJ, Bouman LN.** Interaction of adrenaline and acetylcholine on cardiac pacemaker function. Functional inhomogeneity of the rabbit sinus node. *J Pharmacol Exp Ther* 214: 417–422, 1980.
301. **Mackintosh AF, Chamberlain DA.** Sinus node disease affecting both parents and both children. *Eur J Cardiol* 10: 117–122, 1979.
302. **Macri V, Proenza C, Agranovich E, Angoli D, Accili EA.** Separable gating mechanisms in a Mammalian pacemaker channel. *J Biol Chem* 277: 35939–35946, 2002.
303. **Magyar CE, Wang J, Azuma KK, McDonough AA.** Reciprocal regulation of cardiac Na-K-ATPase and Na/Ca exchanger: hypertension, thyroid hormone, and development. *Am J Physiol Cell Physiol* 269: C675–C682, 1995.
304. **Maier SK, Westenbroek RE, Yamanushi TT, Dobrzynski H, Boyett MR, Catterall WA, Scheuer T.** An unexpected requirement for brain-type sodium channels for control of heart rate in the mouse sinoatrial node. *Proc Natl Acad Sci USA* 100: 3507–3512, 2003.
305. **Malo ME, Fliegel L.** Physiological role and regulation of the Na^+/H^+ exchanger. *Can J Physiol Pharmacol* 84: 1081–1095, 2006.
306. **Maltsev VA, Vinogradova TM, Bogdanov KY, Lakatta EG, Stern MD.** Diastolic calcium release controls the beating rate of rabbit sinoatrial node cells: numerical modeling of the coupling process. *Biophys J* 86: 2596–2605, 2004.
307. **Maltsev VA, Vinogradova TM, Lakatta EG.** The emergence of a general theory of the initiation and strength of the heartbeat. *J Pharmacol Sci* 100: 338–369, 2006.
308. **Maltsev VA, Wobus AM, Rohwedel J, Bader M, Hescheler J.** Cardiomyocytes differentiated in vitro from embryonic stem cells developmentally express cardiac-specific genes and ionic currents. *Circ Res* 75: 233–244, 1994.
309. **Mangoni ME, Couette B, Bourinet E, Platzer J, Reimer D, Striessnig J, Nargeot J.** Functional role of L-type Cav1.3 Ca^{2+} channels in cardiac pacemaker activity. *Proc Natl Acad Sci USA* 100: 5543–5548, 2003.
310. **Mangoni ME, Couette B, Marger L, Bourinet E, Striessnig J, Nargeot J.** Voltage-dependent calcium channels and cardiac pacemaker activity: from ionic currents to genes. *Prog Biophys Mol Biol* 90: 38–63, 2006.
311. **Mangoni ME, Fontanaud P, Noble PJ, Noble D, Benkemoun H, Nargeot J, Richard S.** Facilitation of the L-type calcium current in rabbit sino-atrial cells: effect on cardiac automaticity. *Cardiovasc Res* 48: 375–392, 2000.
312. **Mangoni ME, Nargeot J.** Properties of the hyperpolarization-activated current [I_f] in isolated mouse sino-atrial cells. *Cardiovasc Res* 52: 51–64, 2001.
313. **Mangoni ME, Striessnig J, Platzer J, Nargeot J.** Pacemaker currents in mouse pacemaker cells. *Circulation* 104: R1047, 2001.
314. **Mangoni ME, Traboulsie A, Leoni AL, Couette B, Marger L, Le Quang K, Kupfer E, Cohen-Solal A, Vilar J, Shin HS, Escande D, Charpentier F, Nargeot J, Lory P.** Bradycardia and slowing of the atrioventricular conduction in mice lacking CaV3.1/alpha1G T-type calcium channels. *Circ Res* 98: 1422–1430, 2006.
315. **Mangrum JM, DiMarco JP.** The evaluation and management of bradycardia. *N Engl J Med* 342: 703–709, 2000.
316. **Marger L, Bouly M, Malhberg-Gaudin F, Cohen-Solal A, Leoni A, Kupfer E, Striessnig J, Nargeot J, Mangoni ME.** Physiological effects of I_f inhibition by ivabradine in mice lacking L-type Cav1.3 calcium channels: a differential role for for HCN and Cav1.3 channels in the genesis and regulation of heart rate. *European Society of Cardiology Conference Vienna 2007*, p. P1412.
317. **Marionneau C, Couette B, Liu J, Li H, Mangoni ME, Nargeot J, Lei M, Escande D, Demolombe S.** Specific pattern of ionic channel gene expression associated with pacemaker activity in the mouse heart. *J Physiol* 562: 223–234, 2005.
318. **Marshall PW, Rouse W, Briggs I, Hargreaves RB, Mills SD, McLoughlin BJ.** ICI D7288, a novel sinoatrial node modulator. *J Cardiovasc Pharmacol* 21: 902–906, 1993.
319. **Masumiya H, Tanaka H, Shigenobu K.** Effects of Ca^{2+} channel antagonists on sinus node: prolongation of late phase 4 depolarization by efonidipine. *Eur J Pharmacol* 335: 15–21, 1997.
320. **Matsuura H, Ehara T, Ding WG, Omatsu-Kanbe M, Isono T.** Rapidly and slowly activating components of delayed rectifier K^+ current in guinea-pig sino-atrial node pacemaker cells. *J Physiol* 540: 815–830, 2002.
321. **Matthes J, Huber I, Haaf O, Antepohl W, Striessnig J, Herzig S.** Pharmacodynamic interaction between mibefradil and other calcium channel blockers. *Naunyn-Schmiedebergs Arch Pharmacol* 361: 578–583, 2000.

Downloaded from physrev.physiology.org on October 4, 2011

322. **Matthes J, Yildirim L, Wietzorrek G, Reimer D, Striessnig J, Herzig S.** Disturbed atrio-ventricular conduction and normal contractile function in isolated hearts from Cav1.3-knockout mice. *Naunyn-Schmiedebergs Arch Pharmacol* 369: 554–562, 2004.
323. **McDonald TF, Pelzer S, Trautwein W, Pelzer DJ.** Regulation and modulation of calcium channels in cardiac, skeletal, smooth muscle cells. *Physiol Rev* 74: 365–507, 1994.
324. **McRory JE, Hamid J, Doering CJ, Garcia E, Parker R, Hamming K, Chen L, Hildebrand M, Beedle AM, Feldcamp L, Zamponi GW, Snutch TP.** The CACNA1F gene encodes an L-type calcium channel with unique biophysical properties and tissue distribution. *J Neurosci* 24: 1707–1718, 2004.
325. **Meijler FL, Janse MJ.** Morphology and electrophysiology of the mammalian atrioventricular node. *Physiol Rev* 68: 608–647, 1988.
326. **Mery A, Aimond F, Menard C, Mikoshiba K, Michalak M, Puceat M.** Initiation of embryonic cardiac pacemaker activity by inositol 1,4,5-trisphosphate-dependent calcium signaling. *Mol Biol Cell* 16: 2414–2423, 2005.
327. **Miake J, Marban E, Nuss HB.** Biological pacemaker created by gene transfer. *Nature* 419: 132–133, 2002.
328. **Miake J, Marban E, Nuss HB.** Functional role of inward rectifier current in heart probed by Kir2.1 overexpression and dominant-negative suppression. *J Clin Invest* 111: 1529–1536, 2003.
329. **Milan DJ, Peterson TA, Ruskin JN, Peterson RT, MacRae CA.** Drugs that induce repolarization abnormalities cause bradycardia in zebrafish. *Circulation* 107: 1355–1358, 2003.
330. **Milanesi R, Baruscotti M, Gnecchi-Ruscone T, DiFrancesco D.** Familial sinus bradycardia associated with a mutation in the cardiac pacemaker channel. *N Engl J Med* 354: 151–157, 2006.
331. **Miquerol L, Meysen S, Mangoni M, Bois P, van Rijen HV, Abran P, Jongsma H, Nargeot J, Gros D.** Architectural and functional asymmetry of the His-Purkinje system of the murine heart. *Cardiovasc Res* 63: 77–86, 2004.
332. **Mitchell JW, Larsen JK, Best PM.** Identification of the calcium channel alpha 1E [Ca(v)2.3] isoform expressed in atrial myocytes. *Biochim Biophys Acta* 1577: 17–26, 2002.
333. **Mitsuiye T, Guo J, Noma A.** Nicardipine-sensitive Na^+-mediated single channel currents in guinea-pig sinoatrial node pacemaker cells. *J Physiol* 521: 69–79, 1999.
334. **Mitsuiye T, Shinagawa Y, Noma A.** Sustained inward current during pacemaker depolarization in mammalian sinoatrial node cells. *Circ Res* 87: 88–91, 2000.
335. **Mobley BA, Page E.** The surface area of sheep cardiac Purkinje fibers. *J Physiol* 220: 547–563, 1972.
336. **Moe GK, Preston JB, Burlington H.** Physiologic evidence for a dual A-V transmission system. *Circ Res* 4: 357–375, 1956.
337. **Moffat MP.** Concentration-dependent effects of prostacyclin on the response of the isolated guinea pig heart to ischemia and reperfusion: possible involvement of the slow inward current. *J Pharmacol Exp Ther* 242: 292–299, 1987.
338. **Mommersteeg MT, Hoogaars WM, Prall OW, de Gier-de Vries C, Wiese C, Clout DE, Papaioannou VE, Brown NA, Harvey RP, Moorman AF, Christoffels VM.** Molecular pathway for the localized formation of the sinoatrial node. *Circ Res* 100: 354–362, 2007.
339. **Monteil A, Chemin J, Bourinet E, Mennessier G, Lory P, Nargeot J.** Molecular and functional properties of the human alpha(1G) subunit that forms T-type calcium channels. *J Biol Chem* 275: 6090–6100, 2000.
340. **Monteil A, Chemin J, Leuranguer V, Altier C, Mennessier G, Bourinet E, Lory P, Nargeot J.** Specific properties of T-type calcium channels generated by the human alpha 1I subunit. *J Biol Chem* 275: 16530–16535, 2000.
341. **Moorman AF, Christoffels VM.** Cardiac chamber formation: development, genes, evolution. *Physiol Rev* 83: 1223–1267, 2003.
342. **Moosmang S, Biel M, Hofmann F, Ludwig A.** Differential distribution of four hyperpolarization-activated cation channels in mouse brain. *Biol Chem* 380: 975–980, 1999.
343. **Mori T, Hashimoto A, Takase H, Kambe T.** Nitric oxide (NO) is not involved in accentuated antagonism for chronotropy in the isolated mouse atrium. *Naunyn-Schmiedebergs Arch Pharmacol* 369: 363–366, 2004.
344. **Moroni A, Gorza L, Beltrame M, Gravante B, Vaccari T, Bianchi ME, Altomare C, Longhi R, Heurteaux C, Vitadello M, Malgaroli A, DiFrancesco D.** Hyperpolarization-activated cyclic nucleotide-gated channel 1 is a molecular determinant of the cardiac pacemaker current I_f. *J Biol Chem* 276: 29233–29241, 2001.
345. **Mubagwa K, Flameng W.** Adenosine, adenosine receptors and myocardial protection: an updated overview. *Cardiovasc Res* 52: 25–39, 2001.
346. **Mubagwa K, Mullane K, Flameng W.** Role of adenosine in the heart and circulation. *Cardiovasc Res* 32: 797–813, 1996.
347. **Munk AA, Adjemian RA, Zhao J, Ogbaghebriel A, Shrier A.** Electrophysiological properties of morphologically distinct cells isolated from the rabbit atrioventricular node. *J Physiol* 493: 801–818, 1996.
348. **Muramatsu H, Zou AR, Berkowitz GA, Nathan RD.** Characterization of a TTX-sensitive Na^+ current in pacemaker cells isolated from rabbit sinoatrial node. *Am J Physiol Heart Circ Physiol* 270: H2108–H2119, 1996.
349. **Musa H, Lei M, Honjo H, Jones SA, Dobrzynski H, Lancaster MK, Takagishi Y, Henderson Z, Kodama I, Boyett MR.** Heterogeneous expression of Ca(2+) handling proteins in rabbit sinoatrial node. *J Histochem Cytochem* 50: 311–324, 2002.
350. **Nakayama T, Kurachi Y, Noma A, Irisawa H.** Action potential and membrane currents of single pacemaker cells of the rabbit heart. *Pflügers Arch* 402: 248–257, 1984.
351. **Nathan RD.** Two electrophysiologically distinct types of cultured pacemaker cells from rabbit sinoatrial node. *Am J Physiol Heart Circ Physiol* 250: H325–H329, 1986.
352. **Nerbonne JM.** Molecular basis of functional voltage-gated K^+ channel diversity in the mammalian myocardium. *J Physiol* 525: 285–298, 2000.
353. **Nerbonne JM, Kass RS.** Molecular physiology of cardiac repolarization. *Physiol Rev* 85: 1205–1253, 2005.
354. **Nerbonne JM, Nichols CG, Schwarz TL, Escande D.** Genetic manipulation of cardiac K^+ channel function in mice: what have we learned, and where do we go from here? *Circ Res* 89: 944–956, 2001.
355. **Nikmaram MR, Boyett MR, Kodama I, Suzuki R, Honjo H.** Variation in effects of Cs^+, UL-FS-49, ZD-7288 within sinoatrial node. *Am J Physiol Heart Circ Physiol* 272: H2782–H2792, 1997.
356. **Nikolski V, Efimov I.** Fluorescent imaging of a dual-pathway atrioventricular-nodal conduction system. *Circ Res* 88: E23–30, 2001.
357. **Nishi K, Yoshikawa Y, Takenaka F, Akaike N.** Electrical activity of sinoatrial node cells of the rabbit surviving a long exposure to cold Tyrode's solution. *Circ Res* 41: 242–247, 1977.
358. **Niwa N, Yasui K, Opthof T, Takemura H, Shimizu A, Horiba M, Lee JK, Honjo H, Kamiya K, Kodama I.** Cav 3.2 subunit underlies the functional T-type Ca^{2+} channel in murine hearts during the embryonic period. *Am J Physiol Heart Circ Physiol* 286: H2257–H2263, 2004.
359. **Noble D, Denyer JC, Brown HF, DiFrancesco D.** Reciprocal role of the inward currents ib, Na and i_f in controlling and stabilizing pacemaker frequency of rabbit sino-atrial node cells. *Proc R Soc Lond B Biol Sci* 250: 199–207, 1992.
360. **Noble D, Noble SJ.** A model of sino-atrial node electrical activity based on a modification of the DiFrancesco-Noble (1984) equations. *Proc R Soc Lond B Biol Sci* 222: 295–304, 1984.
361. **Nof E, Luria D, Brass D, Marek D, Lahat H, Reznik-Wolf H, Pras E, Dascal N, Eldar M, Glikson M.** Point mutation in the HCN4 cardiac ion channel pore affecting synthesis, trafficking, functional expression is associated with familial asymptomatic sinus bradycardia. *Circulation* 116: 463–470, 2007.
362. **Noma A, Irisawa H.** Contribution of an electrogenic sodium pump to the membrane potential in rabbit sinoatrial node cells. *Pflügers Arch* 358: 289–301, 1975.
363. **Noma A, Irisawa H, Kokobun S, Kotake H, Nishimura M, Watanabe Y.** Slow current systems in the A-V node of the rabbit heart. *Nature* 285: 228–229, 1980.
364. **Noma A, Kotake H, Irisawa H.** Slow inward current and its role mediating the chronotropic effect of epinephrine in the rabbit sinoatrial node. *Pflügers Arch* 388: 1–9, 1980.

Downloaded from physrev.physiology.org on October 4, 2011

365. **Noma A, Morad M, Irisawa H.** Does the "pacemaker current" generate the diastolic depolarization in the rabbit SA node cells? *Pflügers Arch* 397: 190–194, 1983.
366. **Noma A, Nakayama T, Kurachi Y, Irisawa H.** Resting K conductances in pacemaker and non-pacemaker heart cells of the rabbit. *Jpn J Physiol* 34: 245–254, 1984.
367. **Noma A, Trautwein W.** Relaxation of the ACh-induced potassium current in the rabbit sinoatrial node cell. *Pflügers Arch* 377: 193–200, 1978.
368. **Nygren A, Fiset C, Firek L, Clark JW, Lindblad DS, Clark RB, Giles WR.** Mathematical model of an adult human atrial cell: the role of K^+ currents in repolarization. *Circ Res* 82: 63–81, 1998.
369. **Oehmen CS, Giles WR, Demir SS.** Mathematical model of the rapidly activating delayed rectifier potassium current *I*(Kr) in rabbit sinoatrial node. *J Cardiovasc Electrophysiol* 13: 1131–1140, 2002.
370. **Oei HI, Van Ginneken AC, Jongsma HJ, Bouman LN.** Mechanisms of impulse generation in isolated cells from the rabbit sinoatrial node. *J Mol Cell Cardiol* 21: 1137–1149, 1989.
371. **Ono K, I_{to} H.** Role of rapidly activating delayed rectifier K^+ current in sinoatrial node pacemaker activity. *Am J Physiol Heart Circ Physiol* 269: H453–H462, 1995.
372. **Ono K, Shibata S, Iijima T.** Properties of the delayed rectifier potassium current in porcine sino-atrial node cells. *J Physiol* 524: 51–62, 2000.
373. **Op't Hof T, Mackaay AJ, Bleeker WK, Jongsma HJ, Bouman LN.** Differences between rabbit sinoatrial pacemakers in their response to Mg, Ca and temperature. *Cardiovasc Res* 17: 526–532, 1983.
374. **Opthof T.** The mammalian sinoatrial node. *Cardiovasc Drugs Ther* 1: 573–597, 1988.
375. **Opthof T.** The normal range and determinants of the intrinsic heart rate in man. *Cardiovasc Res* 45: 177–184, 2000.
376. **Opthof T, Coronel R, Rademaker HM, Vermeulen JT, Wilms-Schopman FJ, Janse MJ.** Changes in sinus node function in a rabbit model of heart failure with ventricular arrhythmias and sudden death. *Circulation* 101: 2975–2980, 2000.
377. **Opthof T, de Jonge B, Jongsma HJ, Bouman LN.** Functional morphology of the mammalian sinuatrial node. *Eur Heart J* 8: 1249–1259, 1987.
378. **Opthof T, de Jonge B, Schade B, Jongsma HJ, Bouman LN.** Cycle length dependence of the chronotropic effects of adrenaline, acetylcholine, Ca^{2+} and Mg^{2+} in the guinea-pig sinoatrial node. *J Auton Nerv Syst* 11: 349–366, 1984.
379. **Ornato JP, Peberdy MA.** The mystery of bradyasystole during cardiac arrest. *Ann Emerg Med* 27: 576–587, 1996.
380. **Pachucki J, Burmeister LA, Larsen PR.** Thyroid hormone regulates hyperpolarization-activated cyclic nucleotide-gated channel (HCN2) mRNA in the rat heart. *Circ Res* 85: 498–503, 1999.
381. **Papadatos GA, Wallerstein PM, Head CE, Ratcliff R, Brady PA, Benndorf K, Saumarez RC, Trezise AE, Huang CL, Vandenberg JI, Colledge WH, Grace AA.** Slowed conduction and ventricular tachycardia after targeted disruption of the cardiac sodium channel gene Scn5a. *Proc Natl Acad Sci USA* 99: 6210–6215, 2002.
382. **Parsonnet V, Driller J, Hudson P, Villanueva A, Rough W, Dick L.** An experimental method for thermal control of heart rate: work in progress. *Pacing Clin Electrophysiol* 3: 562–567, 1980.
383. **Pascarel C, Hongo K, Cazorla O, White E, Le Guennec JY.** Different effects of gadolinium on *I*(KR), *I*(KS) and *I*(K1) in guinea-pig isolated ventricular myocytes. *Br J Pharmacol* 124: 356–360, 1998.
384. **Pauza DH, Skripka V, Pauziene N, Stropus R.** Anatomical study of the neural ganglionated plexus in the canine right atrium: implications for selective denervation and electrophysiology of the sinoatrial node in dog. *Anat Rec* 255: 271–294, 1999.
385. **Pauza DH, Skripka V, Pauziene N, Stropus R.** Morphology, distribution, variability of the epicardiac neural ganglionated subplexuses in the human heart. *Anat Rec* 259: 353–382, 2000.
386. **Pennisi DJ, Rentschler S, Gourdie RG, Fishman GI, Mikawa T.** Induction and patterning of the cardiac conduction system. *Int J Dev Biol* 46: 765–775, 2002.
387. **Perez-Reyes E.** Molecular characterization of a novel family of low voltage-activated, T-type, calcium channels. *J Bioenerg Biomembr* 30: 313–318, 1998.
388. **Perez-Reyes E.** Molecular physiology of low-voltage-activated T-type calcium channels. *Physiol Rev* 83: 117–161, 2003.
389. **Perski A, Olsson G, Landou C, de Faire U, Theorell T, Hamsten A.** Minimum heart rate and coronary atherosclerosis: independent relations to global severity and rate of progression of angiographic lesions in men with myocardial infarction at a young age. *Am Heart J* 123: 609–616, 1992.
390. **Petit-Jacques J, Bois P, Bescond J, Lenfant J.** Mechanism of muscarinic control of the high-threshold calcium current in rabbit sino-atrial node myocytes. *Pflügers Arch* 423: 21–27, 1993.
391. **Petrecca K, Amellal F, Laird DW, Cohen SA, Shrier A.** Sodium channel distribution within the rabbit atrioventricular node as analysed by confocal microscopy. *J Physiol* 501: 263–274, 1997.
392. **Pian P, Bucchi A, Robinson RB, Siegelbaum SA.** Regulation of gating and rundown of HCN hyperpolarization-activated channels by exogenous and endogenous PIP_2. *J Gen Physiol* 128: 593–604, 2006.
393. **Platzer J, Engel J, Schrott-Fischer A, Stephan K, Bova S, Chen H, Zheng H, Striessnig J.** Congenital deafness and sinoatrial node dysfunction in mice lacking class D L-type Ca^{2+} channels. *Cell* 102: 89–97, 2000.
394. **Plotnikov AN, Sosunov EA, Qu J, Shlapakova IN, Anyukhovsky EP, Liu L, Janse MJ, Brink PR, Cohen IS, Robinson RB, Danilo P Jr, Rosen MR.** Biological pacemaker implanted in canine left bundle branch provides ventricular escape rhythms that have physiologically acceptable rates. *Circulation* 109: 506–512, 2004.
395. **Pollack GH.** Cardiac pacemaking. *Science* 199: 1234, 1978.
396. **Pollack GH.** Cardiac pacemaking: an obligatory role of catecholamines? *Science* 196: 731–738, 1977.
397. **Pond AL, Scheve BK, Benedict AT, Petrecca K, Van Wagoner DR, Shrier A, Nerbonne JM.** Expression of distinct ERG proteins in rat, mouse, human heart. Relation to functional I_{Kr} channels. *J Biol Chem* 275: 5997–6006, 2000.
398. **Pond AL, Scheve BK, Benedict AT, Petrecca K, Van Wagoner DR, Shrier A, Nerbonne JM.** Expression of Distinct ERG Proteins in Rat, Mouse, Human Heart. Relation to functional I_{Kr} channels. *J Biol Chem* 275: 5997–6006, 2000.
399. **Posner P, Baker SP, Epstein ML, MacIntosh BR, Buss DD.** Effects of chronic hypoxia during maturation on the negative chronotropic effect of $[H^+]$ on the rabbit sino-atrial node. *Biol Neonate* 59: 109–113, 1991.
400. **Potapova I, Plotnikov A, Lu Z, Danilo P Jr, Valiunas V, Qu J, Doronin S, Zuckerman J, Shlapakova IN, Gao J, Pan Z, Herron AJ, Robinson RB, Brink PR, Rosen MR, Cohen IS.** Human mesenchymal stem cells as a gene delivery system to create cardiac pacemakers. *Circ Res* 94: 952–959, 2004.
401. **Protas L, DiFrancesco D, Robinson RB.** L-type but not T-type calcium current changes during postnatal development in rabbit sinoatrial node. *Am J Physiol Heart Circ Physiol* 281: H1252–H1259, 2001.
402. **Qu J, Altomare C, Bucchi A, DiFrancesco D, Robinson RB.** Functional comparison of HCN isoforms expressed in ventricular and HEK 293 cells. *Pflügers Arch* 444: 597–601, 2002.
403. **Qu J, Barbuti A, Protas L, Santoro B, Cohen IS, Robinson RB.** HCN2 overexpression in newborn and adult ventricular myocytes: distinct effects on gating and excitability. *Circ Res* 89: E8–14, 2001.
404. **Qu J, Kryukova Y, Potapova IA, Doronin SV, Larsen M, Krishnamurthy G, Cohen IS, Robinson RB.** MiRP1 modulates HCN2 channel expression and gating in cardiac myocytes. *J Biol Chem* 279: 43497–43502, 2004.
405. **Qu J, Plotnikov AN, Danilo P Jr, Shlapakova I, Cohen IS, Robinson RB, Rosen MR.** Expression and function of a biological pacemaker in canine heart. *Circulation* 107: 1106–1109, 2003.
406. **Qu Y, Baroudi G, Yue Y, Boutjdir M.** Novel molecular mechanism involving alpha1D (Cav1.3) L-type calcium channel in autoimmune-associated sinus bradycardia. *Circulation* 111: 3034–3041, 2005.
407. **Qu Y, Rogers J, Tanada T, Scheuer T, Catterall WA.** Modulation of cardiac Na^+ channels expressed in a mammalian cell line

Downloaded from physrev.physiology.org on October 4, 2011

and in ventricular myocytes by protein kinase C. *Proc Natl Acad Sci USA* 91: 3289–3293, 1994.
408. **Randall WC, Jones SB, Lipsius SL, Rozanski GJ.** Subsidiary atrial pace-makers and their neuronal control. In: *Nervous Control of Cardiovascular Function*, edited by Randall WC. New York: Oxford Univ. Press, 1984, p. 199–224.
409. **Rastan AJ, Eckenstein JI, Hentschel B, Funkat AK, Gummert JF, Doll N, Walther T, Falk V, Mohr FW.** Emergency coronary artery bypass graft surgery for acute coronary syndrome: beating heart versus conventional cardioplegic cardiac arrest strategies. *Circulation* 114: I477–485, 2006.
410. **Renaudon B, Lenfant J, Decressac S, Bois P.** Thyroid hormone increases the conductance density of f-channels in rabbit sino-atrial node cells. *Receptors Channels* 7: 1–8, 2000.
411. **Rentschler S, Vaidya DM, Tamaddon H, Degenhardt K, Sassoon D, Morley GE, Jalife J, Fishman GI.** Visualization and functional characterization of the developing murine cardiac conduction system. *Development* 128: 1785–1792, 2001.
412. **Rigel DF.** Effects of neuropeptides on heart rate in dogs: comparison of VIP, PHI, NPY, CGRP, NT. *Am J Physiol Heart Circ Physiol* 255: H311–H317, 1988.
413. **Rigel DF, Lathrop DA.** Vasoactive intestinal polypeptide enhances automaticity of supraventricular pacemakers in anesthetized dogs. *Am J Physiol Heart Circ Physiol* 261: H463–H468, 1991.
414. **Rigel DF, Lathrop DA.** Vasoactive intestinal polypeptide facilitates atrioventricular nodal conduction and shortens atrial and ventricular refractory periods in conscious and anesthetized dogs. *Circ Res* 67: 1323–1333, 1990.
415. **Rigg L, Heath BM, Cui Y, Terrar DA.** Localisation and functional significance of ryanodine receptors during beta-adrenoceptor stimulation in the guinea-pig sino-atrial node. *Cardiovasc Res* 48: 254–264, 2000.
416. **Rigg L, Mattick PA, Heath BM, Terrar DA.** Modulation of the hyperpolarization-activated current [I_f] by calcium and calmodulin in the guinea-pig sino-atrial node. *Cardiovasc Res* 57: 497–504, 2003.
417. **Rigg L, Terrar DA.** Possible role of calcium release from the sarcoplasmic reticulum in pacemaking in guinea-pig sino-atrial node. *Exp Physiol* 81: 877–880, 1996.
418. **Robberecht P, Gillet L, Chatelain P, De Neef P, Camus JC, Vincent M, Sassard J, Christophe J.** Specific decrease of secretin/VIP-stimulated adenylate cyclase in the heart from the Lyon strain of hypertensive rats. *Peptides* 5: 355–358, 1984.
419. **Roberts LA, Slocum GR, Riley DA.** Morphological study of the innervation pattern of the rabbit sinoatrial node. *Am J Anat* 185: 74–88, 1989.
420. **Robinson RB, Baruscotti M, DiFrancesco D.** Autonomic modulation of heart rate: pitfalls of nonselective channel blockade. *Am J Physiol Heart Circ Physiol* 285: H2865, 2003.
421. **Robinson RB, Brink PR, Cohen IS, Rosen MR.** I_f and the biological pacemaker. *Pharmacol Res* 53: 407–415, 2006.
422. **Roden DM, Balser JR, George AL Jr, Anderson ME.** Cardiac ion channels. *Annu Rev Physiol* 64: 431–475, 2002.
423. **Rosen MR, Brink PR, Cohen IS, Robinson RB.** Genes, stem cells and biological pacemakers. *Cardiovasc Res* 64: 12–23, 2004.
424. **Rosen MR, Robinson RB, Brink P, Cohen IS.** Recreating the biological pacemaker. *Anat Rec A Discov Mol Cell Evol Biol* 280: 1046–1052, 2004.
425. **Rottbauer W, Baker K, Wo ZG, Mohideen MA, Cantiello HF, Fishman MC.** Growth and function of the embryonic heart depend upon the cardiac-specific L-type calcium channel alpha1 subunit. *Dev Cell* 1: 265–275, 2001.
426. **Rozanski GJ, Lipsius SL.** Electrophysiology of functional subsidiary pacemakers in canine right atrium. *Am J Physiol Heart Circ Physiol* 249: H594–H603, 1985.
427. **Rozanski GJ, Lipsius SL, Randall WC, Jones SB.** Alterations in subsidiary pacemaker function after prolonged subsidiary pacemaker dominance in the canine right atrium. *J Am Coll Cardiol* 4: 535–542, 1984.
428. **Rubenstein DS, Lipsius SL.** Mechanisms of automaticity in subsidiary pacemakers from cat right atrium. *Circ Res* 64: 648–657, 1989.
429. **Saikawa T, Carmeliet E.** Slow recovery of the maximal rate of rise (V_{max}) of the action potential in sheep cardiac Purkinje fibers. *Pflügers Arch* 394: 90–93, 1982.
430. **Saito K, Gutkind JS, Saavedra JM.** Angiotensin II binding sites in the conduction system of rat hearts. *Am J Physiol Heart Circ Physiol* 253: H1618–H1622, 1987.
431. **Sakai R, Hagiwara N, Matsuda N, Kassanuki H, Hosoda S.** Sodium-potassium pump current in rabbit sino-atrial node cells. *J Physiol* 490: 51–62, 1996.
432. **Sakmann B, Noma A, Trautwein W.** Acetylcholine activation of single muscarinic K^+ channels in isolated pacemaker cells of the mammalian heart. *Nature* 303: 250–253, 1983.
433. **Sanders L, Rakovic S, Lowe M, Mattick PA, Terrar DA.** Fundamental importance of Na^+-Ca^{2+} exchange for the pacemaking mechanism in guinea-pig sino-atrial node. *J Physiol* 571: 639–649, 2006.
434. **Sanders P, Kistler PM, Morton JB, Spence SJ, Kalman JM.** Remodeling of sinus node function in patients with congestive heart failure: reduction in sinus node reserve. *Circulation* 110: 897–903, 2004.
435. **Santoro B, Liu DT, Yao H, Bartsch D, Kandel ER, Siegelbaum SA, Tibbs GR.** Identification of a gene encoding a hyperpolarization-activated pacemaker channel of brain. *Cell* 93: 717–729, 1998.
436. **Sarachek NS, Leonard JL.** Familial heart block and sinus bradycardia. Classification and natural history. *Am J Cardiol* 29: 451–458, 1972.
437. **Sasaki S, Daitoku K, Iwasa A, Motomura S.** NO is involved in MCh-induced accentuated antagonism via type II PDE in the canine blood-perfused SA node. *Am J Physiol Heart Circ Physiol* 279: H2509–H2518, 2000.
438. **Satin J, Cribbs LL.** Identification of a T-type Ca^{2+} channel isoform in murine atrial myocytes (AT-1 cells). *Circ Res* 86: 636–642, 2000.
439. **Satoh H.** Role of T-type Ca^{2+} channel inhibitors in the pacemaker depolarization in rabbit sino-atrial nodal cells. *Gen Pharmacol* 26: 581–587, 1995.
440. **Schimerlik MI.** Structure and regulation of muscarinic receptors. *Annu Rev Physiol* 51: 217–227, 1989.
441. **Schram G, Pourrier M, Melnyk P, Nattel S.** Differential distribution of cardiac ion channel expression as a basis for regional specialization in electrical function. *Circ Res* 90: 939–950, 2002.
442. **Schuessler RB, Boineau JP, Bromberg BI.** Origin of the sinus impulse. *J Cardiovasc Electrophysiol* 7: 263–274, 1996.
443. **Schulze-Bahr E, Neu A, Friederich P, Kaupp UB, Breithardt G, Pongs O, Isbrandt D.** Pacemaker channel dysfunction in a patient with sinus node disease. *J Clin Invest* 111: 1537–1545, 2003.
444. **Seifert R, Scholten A, Gauss R, Mincheva A, Lichter P, Kaupp UB.** Molecular characterization of a slowly gating human hyperpolarization-activated channel predominantly expressed in thalamus, heart, testis. *Proc Natl Acad Sci USA* 96: 9391–9396, 1999.
445. **Seisenberger C, Specht V, Welling A, Platzer J, Pfeifer A, Kuhbandner S, Striessnig J, Klugbauer N, Feil R, Hofmann F.** Functional embryonic cardiomyocytes after disruption of the L-type alpha1C (Cav1.2) calcium channel gene in the mouse. *J Biol Chem* 275: 39193–39199, 2000.
446. **Senges J, Mizutani T, Pelzer D, Brachmann J, Sonnhof U, Kubler W.** Effect of hypoxia on the sinoatrial node, atrium, atrioventricular node in the rabbit heart. *Circ Res* 44: 856–863, 1979.
447. **Severi S, Cavalcanti S.** Electrolyte and pH dependence of heart rate during hemodialysis: a computer model analysis. *Artif Organs* 24: 245–260, 2000.
448. **Severi S, Cavalcanti S, Mancini E, Santoro A.** Effect of electrolyte and pH changes on the sinus node pacemaking in humans. *J Electrocardiol* 35: 115–124, 2002.
449. **Seyama I.** Characteristics of the anion channel in the sino-atrial node cell of the rabbit. *J Physiol* 294: 447–460, 1979.
450. **Shi W, Wymore R, Yu H, Wu J, Wymore RT, Pan Z, Robinson RB, Dixon JE, McKinnon D, Cohen IS.** Distribution and prevalence of hyperpolarization-activated cation channel (HCN) mRNA expression in cardiac tissues. *Circ Res* 85: e1–6, 1999.
451. **Shibasaki T.** Conductance and kinetics of delayed rectifier potassium channels in nodal cells of the rabbit heart. *J Physiol* 387: 227–250, 1987.

Downloaded from physrev.physiology.org on October 4, 2011

452. **Shibasaki T.** Conductance and kinetics of delayed rectifier potassium channels in nodal cells of the rabbit heart. *J Physiol* 387: 227–250, 1987.
453. **Shibata EF, Giles W, Pollack GH.** Threshold effects of acetylcholine on primary pacemaker cells of the rabbit sino-atrial node. *Proc R Soc Lond B Biol Sci* 223: 355–378, 1985.
454. **Shigekawa M, Iwamoto T.** Cardiac Na^+-Ca^{2+} exchange: molecular and pharmacological aspects. *Circ Res* 88: 864–876, 2001.
455. **Shimoni Y, Fiset C, Clark RB, Dixon JE, McKinnon D, Giles WR.** Thyroid hormone regulates postnatal expression of transient K^+ channel isoforms in rat ventricle. *J Physiol* 500: 65–73, 1997.
456. **Shimoni Y, Han X, Severson D, Giles WR.** Mediation by nitric oxide of the indirect effects of adenosine on calcium current in rabbit heart pacemaker cells. *Br J Pharmacol* 119: 1463–1469, 1996.
457. **Shinagawa Y, Satoh H, Noma A.** The sustained inward current and inward rectifier K^+ current in pacemaker cells dissociated from rat sinoatrial node. *J Physiol* 523: 593–605, 2000.
458. **Shvilkin A, Danilo P Jr, Chevalier P, Chang F, Cohen IS, Rosen MR.** Vagal release of vasoactive intestinal peptide can promote vagotonic tachycardia in the isolated innervated rat heart. *Cardiovasc Res* 28: 1769–1773, 1994.
459. **Silva J, Rudy Y.** Mechanism of pacemaking in I_{K1}-downregulated myocytes. *Circ Res* 92: 261–263, 2003.
460. **Silverman ME, Grove D, Upshaw CB Jr.** Why does the heart beat? The discovery of the electrical system of the heart. *Circulation* 113: 2775–2781, 2006.
461. **Simon L, Ghaleh B, Puybasset L, Giudicelli JF, Berdeaux A.** Coronary and hemodynamic effects of S 16257, a new bradycardic agent, in resting and exercising conscious dogs. *J Pharmacol Exp Ther* 275: 659–666, 1995.
462. **Sinnegger-Brauns MJ, Hetzenauer A, Huber IG, Renstrom E, Wietzorrek G, Berjukov S, Cavalli M, Walter D, Koschak A, Waldschutz R, Hering S, Bova S, Rorsman P, Pongs O, Singewald N, Striessnig JJ.** Isoform-specific regulation of mood behavior and pancreatic beta cell and cardiovascular function by L-type Ca^{2+} channels. *J Clin Invest* 113: 1430–1439, 2004.
463. **Slovut DP, Wenstrom JC, Moeckel RB, Wilson RF, Osborn JW, Abrams JH.** Respiratory sinus dysrhythmia persists in transplanted human hearts following autonomic blockade. *Clin Exp Pharmacol Physiol* 25: 322–330, 1998.
464. **Sorota S, Du XY.** Delayed activation of cardiac swelling-induced chloride current after step changes in cell size. *J Cardiovasc Electrophysiol* 9: 825–831, 1998.
465. **Soufan AT, Ruijter JM, van den Hoff MJ, de Boer PA, Hagoort J, Moorman AF.** Three-dimensional reconstruction of gene expression patterns during cardiac development. *Physiol Genomics* 13: 187–195, 2003.
466. **Stieber J, Herrmann S, Feil S, Loster J, Feil R, Biel M, Hofmann F, Ludwig A.** The hyperpolarization-activated channel HCN4 is required for the generation of pacemaker action potentials in the embryonic heart. *Proc Natl Acad Sci USA* 100: 15235–15240, 2003.
467. **Stieber J, Hofmann F, Ludwig A.** Pacemaker channels and sinus node arrhythmia. *Trends Cardiovasc Med* 14: 23–28, 2004.
468. **Stjarne L, Lundberg JM.** On the possible roles of noradrenaline, adenosine 5′-triphosphate and neuropeptide Y as sympathetic cotransmitters in the mouse vas deferens. *Prog Brain Res* 68: 263–278, 1986.
469. **Stowe DF, Bosnjak ZJ, Kampine JP.** Effects of hypoxia on adult and neonatal pacemaker rates. *Obstet Gynecol* 66: 649–656, 1985.
470. **Striessnig J.** Pharmacology, structure and function of cardiac L-type Ca^{2+} channels. *Cell Physiol Biochem* 9: 242–269, 1999.
471. **Takano M, Noma A.** Distribution of the isoprenaline-induced chloride current in rabbit heart. *Pflügers Arch* 420: 223–226, 1992.
472. **Takimoto K, Li D, Nerbonne JM, Levitan ES.** Distribution, splicing and glucocorticoid-induced expression of cardiac alpha 1C and alpha 1D voltage-gated Ca^{2+} channel mRNAs. *J Mol Cell Cardiol* 29: 3035–3042, 1997.
473. **Tamargo J, Caballero R, Gomez R, Valenzuela C, Delpon E.** Pharmacology of cardiac potassium channels. *Cardiovasc Res* 62: 9–33, 2004.
474. **Tanabe T, Beam KG, Powell JA, Numa S.** Restoration of excitation-contraction coupling and slow calcium current in dysgenic muscle by dihydropyridine receptor complementary DNA. *Nature* 336: 134–139, 1988.
475. **Tanabe T, Mikami A, Numa S, Beam KG.** Cardiac-type excitation-contraction coupling in dysgenic skeletal muscle injected with cardiac dihydropyridine receptor cDNA. *Nature* 344: 451–453, 1990.
476. **Tawara S.** *Das Reizleitungssystem des Saiigethierherzens. Jena*: Gustav Fischer, 1906.
477. **Tellez JO, Dobrzynski H, Greener ID, Graham GM, Laing E, Honjo H, Hubbard SJ, Boyett MR, Billeter R.** Differential expression of ion channel transcripts in atrial muscle and sinoatrial node in rabbit. *Circ Res* 99: 1384–1393, 2006.
478. **Temple J, Frias P, Rottman J, Yang T, Wu Y, Verheijck EE, Zhang W, Siprachanh C, Kanki H, Atkinson JB, King P, Anderson ME, Kupershmidt S, Roden DM.** Atrial fibrillation in KCNE1-null mice. *Circ Res* 97: 62–69, 2005.
479. **Thollon C, Bidouard JP, Cambarrat C, Lesage L, Reure H, Delescluse I, Vian J, Peglion JL, Vilaine JP.** Stereospecific in vitro and in vivo effects of the new sinus node inhibitor (+)-S 16257. *Eur J Pharmacol* 339: 43–51, 1997.
480. **Thollon C, Cambarrat C, Vian J, Prost JF, Peglion JL, Vilaine JP.** Electrophysiological effects of S 16257, a novel sino-atrial node modulator, on rabbit and guinea-pig cardiac preparations: comparison with UL-FS 49. *Br J Pharmacol* 112: 37–42, 1994.
481. **Toda N, West TC.** The influence of ouabain on cholinergic responses in the sinoatrial node. *J Pharmacol Exp Ther* 153: 104–113, 1966.
482. **Toyama J, Boyett MR, Watanabe E, Honjo H, Anno T, Kodama I.** Computer simulation of the electrotonic modulation of pacemaker activity in the sinoatrial node by atrial muscle. *J Electrocardiol* 28 *Suppl*: 212–215, 1995.
483. **Tse HF, Xue T, Lau CP, Siu CW, Wang K, Zhang QY, Tomaselli GF, Akar FG, Li RA.** Bioartificial sinus node constructed via in vivo gene transfer of an engineered pacemaker HCN channel reduces the dependence on electronic pacemaker in a sick-sinus syndrome model. *Circulation* 114: 1000–1011, 2006.
484. **Tseng GN, Boyden PA.** Multiple types of Ca^{2+} currents in single canine Purkinje cells. *Circ Res* 65: 1735–1750, 1989.
485. **Tsien RW, Carpenter DO.** Ionic mechanisms of pacemaker activity in cardiac Purkinje fibers. *Federation Proc* 37: 2127–2131, 1978.
486. **Ueda K, Nakamura K, Hayashi T, Inagaki N, Takahashi M, Arimura T, Morita H, Higashiuesato Y, Hirano Y, Yasunami M, Takishita S, Yamashina A, Ohe T, Sunamori M, Hiraoka M, Kimura A.** Functional characterization of a trafficking-defective HCN4 mutation, D553N, associated with cardiac arrhythmia. *J Biol Chem* 279: 27194–27198, 2004.
487. **Valenzuela D, Han X, Mende U, Fankhauser C, Mashimo H, Huang P, Pfeffer J, Neer EJ, Fishman MC.** G alpha(o) is necessary for muscarinic regulation of Ca^{2+} channels in mouse heart. *Proc Natl Acad Sci USA* 94: 1727–1732, 1997.
488. **Van Bogaert PP, Goethals M.** Pharmacological influence of specific bradycardic agents on the pacemaker current of sheep cardiac Purkinje fibers. *A* comparison between three different molecules. *Eur Heart J* 8 *Suppl* L: 35–42, 1987.
489. **Van Bogaert PP, Goethals M, Simoens C.** Use- and frequency-dependent blockade by UL-FS 49 of the if pacemaker current in sheep cardiac Purkinje fibers. *Eur J Pharmacol* 187: 241–256, 1990.
490. **Van Bogaert PP, Pittoors F.** Use-dependent blockade of cardiac pacemaker current (I_f) by cilobradine and zatebradine. *Eur J Pharmacol* 478: 161–171, 2003.
491. **Van der Heyden MA, Wijnhoven TJ, Opthof T.** Molecular aspects of adrenergic modulation of cardiac L-type Ca^{2+} channels. *Cardiovasc Res* 65: 28–39, 2005.
492. **Van Ginneken AC, Giles W.** Voltage clamp measurements of the hyperpolarization-activated inward current I_f in single cells from rabbit sino-atrial node. *J Physiol* 434: 57–83, 1991.
493. **Van Wagoner DR.** Mechanosensitive gating of atrial ATP-sensitive potassium channels. *Circ Res* 72: 973–983, 1993.
494. **Vandecasteele G, Eschenhagen T, Scholz H, Stein B, Verde I, Fischmeister R.** Muscarinic and beta-adrenergic regulation of heart rate, force of contraction and calcium current is preserved in

Downloaded from physrev.physiology.org on October 4, 2011

mice lacking endothelial nitric oxide synthase. *Nat Med* 5: 331–334, 1999.
495. **Vassalle M.** Analysis of cardiac pacemaker potential using a "voltage clamp" technique. *Am J Physiol* 210: 1335–1341, 1966.
496. **Verheijck EE, van Ginneken AC, Bourier J, Bouman LN.** Effects of delayed rectifier current blockade by E-4031 on impulse generation in single sinoatrial nodal myocytes of the rabbit. *Circ Res* 76: 607–615, 1995.
497. **Verheijck EE, van Ginneken AC, Wilders R, Bouman LN.** Contribution of L-type Ca^{2+} current to electrical activity in sinoatrial nodal myocytes of rabbits. *Am J Physiol Heart Circ Physiol* 276: H1064–1077, 1999.
498. **Verheijck EE, van Kempen MJ, Veereschild M, Lurvink J, Jongsma HJ, Bouman LN.** Electrophysiological features of the mouse sinoatrial node in relation to connexin distribution. *Cardiovasc Res* 52: 40–50, 2001.
499. **Verheijck EE, Wessels A, van Ginneken AC, Bourier J, Markman MW, Vermeulen JL, de Bakker JM, Lamers WH, Opthof T, Bouman LN.** Distribution of atrial and nodal cells within the rabbit sinoatrial node: models of sinoatrial transition. *Circulation* 97: 1623–1631, 1998.
500. **Verheijck EE, Wilders R, Bouman LN.** Atrio-sinus interaction demonstrated by blockade of the rapid delayed rectifier current. *Circulation* 105: 880–885, 2002.
501. **Verkerk AO, Veldkamp MW, Abbate F, Antoons G, Bouman LN, Ravesloot JH, van Ginneken AC.** Two types of action potential configuration in single cardiac Purkinje cells of sheep. *Am J Physiol Heart Circ Physiol* 277: H1299–H1310, 1999.
502. **Verkerk AO, Veldkamp MW, Bouman LN, van Ginneken AC.** Calcium-activated Cl^- current contributes to delayed afterdepolarizations in single Purkinje and ventricular myocytes. *Circulation* 101: 2639–2644, 2000.
503. **Verkerk AO, Wilders R, Coronel R, Ravesloot JH, Verheijck EE.** Ionic remodeling of sinoatrial node cells by heart failure. *Circulation* 108: 760–766, 2003.
504. **Verkerk AO, Wilders R, Zegers JG, van Borren MM, Ravesloot JH, Verheijck EE.** Ca^{2+}-activated Cl^- current in rabbit sinoatrial node cells. *J Physiol* 540: 105–117, 2002.
505. **Viatchenko-Karpinski S, Fleischmann BK, Liu Q, Sauer H, Gryshchenko O, Ji GJ, Hescheler J.** Intracellular Ca^{2+} oscillations drive spontaneous contractions in cardiomyocytes during early development. *Proc Natl Acad Sci USA* 96: 8259–8264, 1999.
506. **Vinogradova TM, Bogdanov KY, Lakatta EG.** beta-Adrenergic stimulation modulates ryanodine receptor Ca^{2+} release during diastolic depolarization to accelerate pacemaker activity in rabbit sinoatrial nodal cells. *Circ Res* 90: 73–79, 2002.
507. **Vinogradova TM, Fedorov VV, Yuzyuk TN, Zaitsev AV, Rosenshtraukh LV.** Local cholinergic suppression of pacemaker activity in the rabbit sinoatrial node. *J Cardiovasc Pharmacol* 32: 413–424, 1998.
508. **Vinogradova TM, Lyashkov AE, Zhu W, Ruknudin AM, Sirenko S, Yang D, Deo S, Barlow M, Johnson S, Caffrey JL, Zhou YY, Xiao RP, Cheng H, Stern MD, Maltsev VA, Lakatta EG.** High basal protein kinase A-dependent phosphorylation drives rhythmic internal Ca^{2+} store oscillations and spontaneous beating of cardiac pacemaker cells. *Circ Res* 98: 505–514, 2006.
509. **Vinogradova TM, Zhou YY, Bogdanov KY, Yang D, Kuschel M, Cheng H, Xiao RP.** Sinoatrial node pacemaker activity requires Ca^{2+}/calmodulin-dependent protein kinase II activation. *Circ Res* 87: 760–767, 2000.
510. **Vinogradova TM, Zhou YY, Maltsev V, Lyashkov A, Stern M, Lakatta EG.** Rhythmic ryanodine receptor Ca^{2+} releases during diastolic depolarization of sinoatrial pacemaker cells do not require membrane depolarization. *Circ Res* 94: 802–809, 2004.
511. **Viswanathan PC, Coles JA Jr, Sharma V, Sigg DC.** Recreating an artificial biological pacemaker: insights from a theoretical model. *Heart Rhythm* 3: 824–831, 2006.
512. **Waltuck J, Buyon JP.** Autoantibody-associated congenital heart block: outcome in mothers and children. *Ann Intern Med* 120: 544–551, 1994.
513. **Warren KS, Baker K, Fishman MC.** The slow mo mutation reduces pacemaker current and heart rate in adult zebrafish. *Am J Physiol Heart Circ Physiol* 281: H1711–H1719, 2001.
514. **Watanabe EI, Honjo H, Anno T, Boyett MR, Kodama I, Toyama J.** Modulation of pacemaker activity of sinoatrial node cells by electrical load imposed by an atrial cell model. *Am J Physiol Heart Circ Physiol* 269: H1735–H1742, 1995.
515. **Watanabe Y, Dreifus LS.** Sites of impulse formation within the atrioventricular junction of the rabbit. *Circ Res* 22: 717–727, 1968.
516. **Weiergraber M, Henry M, Sudkamp M, de Vivie ER, Hescheler J, Schneider T.** Ablation of $Ca_v2.3$ / E-type voltage-gated calcium channel results in cardiac arrhythmia and altered autonomic control within the murine cardiovascular system. *Basic Res Cardiol* 100: 1–13, 2005.
517. **West GA, Belardinelli L.** Correlation of sinus slowing and hyperpolarization caused by adenosine in sinus node. *Pflügers Arch* 403: 75–81, 1985.
518. **West GA, Belardinelli L.** Sinus slowing and pacemaker shift caused by adenosine in rabbit SA node. *Pflügers Arch* 403: 66–74, 1985.
519. **West TC, Toda N.** Response of the A-V node of the rabbit to stimulation of intracardiac cholinergic nerves. *Circ Res* 20: 18–31, 1967.
520. **Wickman K, Clapham DE.** Ion channel regulation by G proteins. *Physiol Rev* 75: 865–885, 1995.
521. **Wickman K, Krapivinsky G, Corey S, Kennedy M, Nemec J, Medina I, Clapham DE.** Structure, G protein activation, functional relevance of the cardiac G protein-gated K^+ channel, I_{KACh}. *Ann NY Acad Sci* 868: 386–398, 1999.
522. **Wickman K, Nemec J, Gendler SJ, Clapham DE.** Abnormal heart rate regulation in GIRK4 knockout mice. *Neuron* 20: 103–114, 1998.
523. **Wickman KD, Iniguez-Lluhl JA, Davenport PA, Taussig R, Krapivinsky GB, Linder ME, Gilman AG, Clapham DE.** Recombinant G-protein beta gamma-subunits activate the muscarinic-gated atrial potassium channel. *Nature* 368: 255–257, 1994.
524. **Wikstrom L, Johansson C, Salto C, Barlow C, Campos Barros A, Baas F, Forrest D, Thoren P, Vennstrom B.** Abnormal heart rate and body temperature in mice lacking thyroid hormone receptor alpha 1. *EMBO J* 17: 455–461, 1998.
525. **Wilders R.** Computer modelling of the sinoatrial node. *Med Biol Eng Comput* 45: 189–207, 2007.
526. **Wilders R, Jongsma HJ, van Ginneken AC.** Pacemaker activity of the rabbit sinoatrial node. A comparison of mathematical models. *Biophys J* 60: 1202–1216, 1991.
527. **Wilson SJ and Bolter CP.** Do cardiac neurons play a role in the intrinsic control of heart rate in the rat? *Exp Physiol* 87: 675–682, 2002.
528. **Xiao RP, Cheng H, Lederer WJ, Suzuki T, Lakatta EG.** Dual regulation of Ca^{2+}/calmodulin-dependent kinase II activity by membrane voltage and by calcium influx. *Proc Natl Acad Sci USA* 91: 9659–9663, 1994.
529. **Xu M, Welling A, Paparisto S, Hofmann F, Klugbauer N.** Enhanced expression of L-type Cav1.3 calcium channels in murine embryonic hearts from Cav1 2-deficient mice. *J Biol Chem* 278: 40837–40841, 2003.
530. **Yamada M.** The role of muscarinic K^+ channels in the negative chronotropic effect of a muscarinic agonist. *J Pharmacol Exp Ther* 300: 681–687, 2002.
531. **Yamamoto M, Dobrzynski H, Tellez J, Niwa R, Billeter R, Honjo H, Kodama I, Boyett MR.** Extended atrial conduction system characterised by the expression of the HCN4 channel and connexin45. *Cardiovasc Res* 72: 271–281, 2006.
532. **Yamane T, Shah DC, Jais P, Haissaguerre M.** Pseudo sinus rhythm originating from the left superior pulmonary vein in a patient with paroxysmal atrial fibrillation. *J Cardiovasc Electrophysiol* 12: 1190–1191, 2001.
533. **Yanagihara K, Noma A, Irisawa H.** Reconstruction of sino-atrial node pacemaker potential based on the voltage clamp experiments. *Jpn J Physiol* 30: 841–857, 1980.
534. **Yu FH, Catterall WA.** Overview of the voltage-gated sodium channel family. *Genome Biol* 4: 207, 2003.
535. **Yu H, Chang F, Cohen IS.** Pacemaker current exists in ventricular myocytes. *Circ Res* 72: 232–236, 1993.
536. **Yu H, Wu J, Potapova I, Wymore RT, Holmes B, Zuckerman J, Pan Z, Wang H, Shi W, Robinson RB, El-Maghrabi MR, Ben-**

Downloaded from physrev.physiology.org on October 4, 2011

jamin W, Dixon J, McKinnon D, Cohen IS, Wymore R. MinK-related peptide 1: a beta subunit for the HCN ion channel subunit family enhances expression and speeds activation. *Circ Res* 88: E84–87, 2001.

537. **Yu X, Chen XW, Zhou P, Yao L, Liu T, Zhang B, Li Y, Zheng H, Zheng LH, Zhang CX, Bruce I, Ge JB, Wang SQ, Hu ZA, Yu HG, Zhou Z.** Calcium influx through I_f channels in rat ventricular myocytes. *Am J Physiol Cell Physiol* 292: C1147–C1155, 2007.
538. **Yu X, Duan KL, Shang CF, Yu HG, Zhou Z.** Calcium influx through hyperpolarization-activated cation channels [I_h channels] contributes to activity-evoked neuronal secretion. *Proc Natl Acad Sci USA* 101: 1051–1056, 2004.
539. **Yuill KH, Hancox JC.** Characteristics of single cells isolated from the atrioventricular node of the adult guinea-pig heart. *Pflügers Arch* 445: 311–320, 2002.
540. **Zaza A, Maccaferri G, Mangoni M, DiFrancesco D.** Intracellular calcium does not directly modulate cardiac pacemaker (i_f) channels. *Pflügers Arch* 419: 662–664, 1991.
541. **Zaza A, Micheletti M, Brioschi A, Rocchetti M.** Ionic currents during sustained pacemaker activity in rabbit sino-atrial myocytes. *J Physiol* 505: 677–688, 1997.
542. **Zaza A, Robinson RB, DiFrancesco D.** Basal responses of the L-type Ca^{2+} and hyperpolarization-activated currents to autonomic agonists in the rabbit sino-atrial node. *J Physiol* 491: 347–355, 1996.
543. **Zaza A, Rocchetti M, DiFrancesco D.** Modulation of the hyperpolarization-activated current [I_f] by adenosine in rabbit sinoatrial myocytes. *Circulation* 94: 734–741, 1996.
544. **Zhang H, Holden AV, Boyett MR.** Sustained inward current and pacemaker activity of mammalian sinoatrial node. *J Cardiovasc Electrophysiol* 13: 809–812, 2002.
545. **Zhang H, Holden AV, Kodama I, Honjo H, Lei M, Varghese T, Boyett MR.** Mathematical models of action potentials in the periphery and center of the rabbit sinoatrial node. *Am J Physiol Heart Circ Physiol* 279: H397–H421, 2000.
546. **Zhang Z, Xu Y, Song H, Rodriguez J, Tuteja D, Namkung Y, Shin HS, Chiamvimonvat N.** Functional roles of Ca(v)1.3 [alpha(1D)] calcium channel in sinoatrial nodes: insight gained using gene-targeted null mutant mice. *Circ Res* 90: 981–987., 2002.
547. **Zhou Z, Lipsius SL.** Na^+-Ca^{2+} exchange current in latent pacemaker cells isolated from cat right atrium. *J Physiol* 466: 263–285, 1993.
548. **Zicha S, Fernandez-Velasco M, Lonardo G, L'Heureux N, Nattel S.** Sinus node dysfunction and hyperpolarization-activated (HCN) channel subunit remodeling in a canine heart failure model. *Cardiovasc Res* 66: 472–481, 2005.

Downloaded from physrev.physiology.org on October 4, 2011

Genesis and Regulation of the Heart Automaticity

Matteo E. Mangoni and Joël Nargeot

Physiol Rev 88:919-982, 2008. doi:10.1152/physrev.00018.2007

You might find this additional info useful...

This article cites 541 articles, 326 of which can be accessed free at:
http://physrev.physiology.org/content/88/3/919.full.html#ref-list-1

This article has been cited by 31 other HighWire hosted articles, the first 5 are:

Endoplasmic Reticulum Ca^{2+} Handling in Excitable Cells in Health and Disease
Grace E. Stutzmann and Mark P. Mattson
Pharmacol Rev, September , 2011; 63 (3): 700-727.
[Abstract] [Full Text] [PDF]

A mathematical model of action potentials of mouse sinoatrial node cells with molecular bases
Sanjay Kharche, Jian Yu, Ming Lei and Henggui Zhang
Am J Physiol Heart Circ Physiol, September , 2011; 301 (3): H945-H963.
[Abstract] [Full Text] [PDF]

Molecular Analysis of Patterning of Conduction Tissues in the Developing Human Heart
Aleksander Sizarov, Harsha D. Devalla, Robert H. Anderson, Robert Passier, Vincent M. Christoffels and Antoon F.M. Moorman
Circ Arrhythm Electrophysiol, August , 2011; 4 (4): 532-542.
[Abstract] [Full Text] [PDF]

Changes in Ion Channel Gene Expression Underlying Heart Failure-Induced Sinoatrial Node Dysfunction
Joseph Yanni, James O. Tellez, Michal Maczewski, Urszula Mackiewicz, Andrzej Beresewicz, Rudi Billeter, Halina Dobrzynski and M.R. Boyett
Circ Heart Fail, July , 2011; 4 (4): 496-508.
[Abstract] [Full Text] [PDF]

Postinfarction healing dynamics in the mechanically unloaded rat left ventricle
Xin Zhou, Ji-Li Yun, Zhi-Qi Han, Fei Gao, He Li, Tie-Min Jiang and Yu-Ming Li
Am J Physiol Heart Circ Physiol, May , 2011; 300 (5): H1863-H1874.
[Abstract] [Full Text] [PDF]

Updated information and services including high resolution figures, can be found at:
http://physrev.physiology.org/content/88/3/919.full.html

Additional material and information about ***Physiological Reviews*** can be found at:
http://www.the-aps.org/publications/prv

This infomation is current as of October 4, 2011.

Physiological Reviews provides state of the art coverage of timely issues in the physiological and biomedical sciences. It is published quarterly in January, April, July, and October by the American Physiological Society, 9650 Rockville Pike, Bethesda MD 20814-3991. Copyright © 2008 by the American Physiological Society. ISSN: 0031-9333, ESSN: 1522-1210. Visit our website at http://www.the-aps.org/.

Downloaded from physrev.physiology.org on October 4, 2011